Inaugural – Dissertation

zur

Erlangung der Doktorwürde

der

Gesamtfakultät für Mathematik, Ingenieur- und Naturwissenschaften

der

Ruprecht – Karls – Universität

Heidelberg

vorgelegt von

Reichert, Maurice, M.Sc.
aus Heidelberg

Tag der mündlichen Prüfung: ____________

Geometric Invariants and Asymptotics of Translation Surfaces

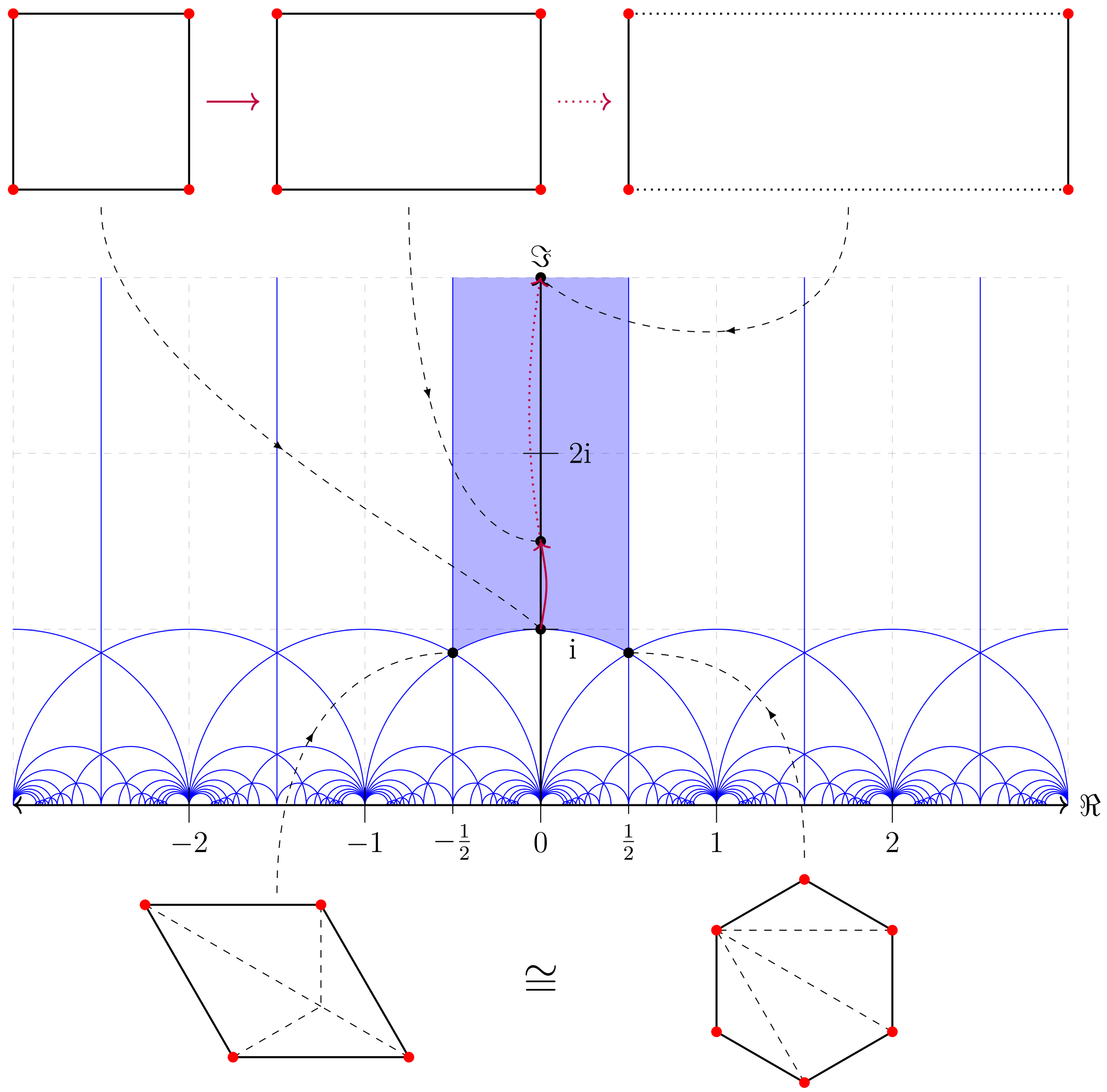

Advisor: Dr. Anja Randecker

Abstract

By gluing together polygons along parallel edges in a well-defined matter, we obtain translation surfaces, which are two-dimensional manifolds with rich geometric structures.

This thesis examines the geometry of translation surfaces with a focus on understanding the properties of random translation surfaces of high genus in order to gain a broader understanding of the moduli space of translation surfaces.

One of the primary challenges in this field is bridging the gap between finite and infinite translation surfaces corresponding to the compact and non-compact cases. We address this challenge by examining the convergence of sequences of finite translation surfaces from different strata and approximating infinite translation surfaces with them.

We use different methods to achieve this approximation. On the one hand, we use some sense of convergence in the underlying Veech group to approach infinite translation surfaces; on the other hand, we want to understand geometric invariants for translation surfaces of large genus. In particular, we explore the behavior of the Cheeger constant, a measure of the inverse of bottleneckedness.

By advancing existing constructions, introducing new perspectives, and analyzing key geometric invariants, this thesis enhances our understanding of translation surfaces for future research.

Zusammenfassung

Indem man Polygone auf wohldefinierte Weise entlang paralleler Kanten zusammenfügt, erhält man Translationsflächen, die zweidimensionale Mannigfaltigkeiten mit reichen geometrischen Strukturen sind.

Diese Arbeit untersucht die Geometrie auf Translationsflächen mit dem Fokus, die Eigenschaften zufälliger Translationsflächen mit hohem Geschlecht zu verstehen, um den Modulraum der Translationsflächen allgemeiner zu begreifen.

Eine der Hauptherausforderungen in diesem Bereich besteht darin, die Lücke zwischen endlichen und unendlichen Translationsflächen zu überbrücken, die dem kompakten und nicht-kompakten Fall entsprechen. Wir gehen diese Herausforderung an, indem wir die Konvergenz von Folgen endlicher Translationsflächen aus verschiedenen Strata untersuchen und unendliche Translationsflächen mit ihnen approximieren.

Wir verwenden verschiedene Methoden, um diese Approximation zu erreichen. Einerseits nutzen wir eine Form von Konvergenz in der zugrundeliegenden Veech-Gruppe, um uns unendlichen Translationsflächen zu nähern; andererseits möchten wir geometrische Invarianten für Translationsflächen mit hohem Geschlecht verstehen. Hierzu erforschen wir das Verhalten der Cheeger-Konstante, ein Maß für das Inverse der Größe der Engstelle auf einer Fläche.

Durch die Weiterentwicklung bestehender Konstruktionen, die Einführung neuer Perspektiven und die Analyse zentraler geometrischer Invarianten erweitert diese Arbeit unser Verständnis von Translationsflächen für zukünftige Forschungen.

Acknowledgments

Looking back on my doctoral journey, I am incredibly grateful to all the individuals and institutions that have been important in my academic career. My thesis has been a collective effort, I owe a great deal to everyone who has supported and guided me along the way.

Primarily, I want to express my highest gratitude to my supervisor, Anja Randecker. Being your first Ph.D. student has been an incredible honor and I am immensely thankful for the mentorship and wisdom you have shared with me. Your dedication to fostering intellectual curiosity and collaboration has been a cornerstone of my academic experience. The countless hours we spent discussing ideas, refining methodologies, and overcoming research challenges have left a lasting impact on my journey. Your mentorship has been a beacon guiding me through the complexities of academia and for that I am truly thankful.

I also want to extend my gratitude to my master's thesis supervisors, Stefan Kühnlein and Frank Herrlich. Your guidance, encouragement, and scholarly insight during my undergraduate years laid a sturdy foundation for my academic interests. I am especially thankful for your support in recommending me to my current supervisor, which made for a smooth transition from master's to doctoral studies.

In the final stages of this academic journey, I owe a special thanks to my roommate, Erick Gordillo. Your unwavering support, camaraderie, and positive energy during the intense final phases of my research were highly appreciated.

I am grateful to the members of the research station for the collaborative spirit and scholarly community we have built together. The exchange of ideas and discussions have been integral to my research journey.

A special thanks to Jayadev Athreya for his warm welcome and support during my visit to the Jean-Morlet chair. This period of collaboration and exchange of ideas has been immensely valuable in shaping the direction of my research. Jayadev, your insights, expertise, and collaborative spirit have enriched my academic experience. Regarding my visit to the Jean-Morlet chair, I cannot forget to thank Nicolas Bédaride and Julien Cassaigne for their constructive mathematical discussions. Thank you all for the opportunity to collaborate with you and benefit from your guidance in Marseille.

The unconditional support of my parents during the challenging moments of the past few years was limitless. Their encouragement and belief in me have been invaluable and I owe them everything.

I also want to thank the people helping me to proofread everything: Lina Deschamps, Erick Gordillo, Klaus Koblmiller, Jasmin Mencin, Anja Randecker, and Amelie Reichert.

To everyone who has contributed to this chapter of my life, whether within the academic community or outside, I extend my gratitude.

This work is funded by the Deutsche Forschungsgemeinschaft (DFG, German Research Foundation) - 281869850;313840899 under the Schwerpunktprogramm SPP 2026: „Geometrie im Unendlichen“ (Priority programme SPP 2026: “Geometry at Infinity”).

Additionally, the Graduiertenkolleg GRK 2229: „Asymptotische Invarianten und Limiten von Gruppen und Räumen“ (Research Training Group RTG 2229: “Asymptotic Invariants and Limits of Groups and Spaces”), also funded by the DFG, supported my research over the past five months, providing a bridge to the completion of this work. The seminars, lectures, recurring colloquium talks, and all the additional opportunities provided by the Research Training Group were truly outstanding.

As I close this chapter, I look forward with gratitude and anticipation to the next phase of my life. This journey has been made meaningful through the relationships and collaborations formed along the way and for that I am very thankful.

Contents

1 Introduction

Translation surfaces are interesting objects at the intersection of complex analysis, geometry, topology, and dynamical systems. The current theory of translation surfaces traces its origins back to [Vee89]. However, earlier works have historical connections with translation surfaces, though they may have been expressed using different terminology. Nevertheless, Veech's introduction of the Veech group in [Vee89] is widely regarded as the beginning of the theory of translation surfaces in its own right. Subsequently, this theory has undergone substantial evolution, expanding its influence into various domains including dynamical systems.

A translation surface can be visualized as a collection of polygons in the Euclidean plane, glued together along parallel edges as in Figure 1.1. They are glued together in such a way that except for some singular points corresponding to corners of the polygons, every point locally looks like the plane.

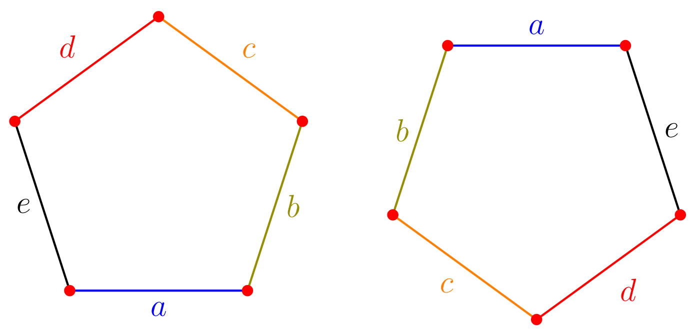

Figure 1.1: Translation surface obtained by gluing together two pentagons

So, this construction endows the surface with a flat metric, except at a finite set of singularities, where the total angle around the point is an integer multiple of 2π in the well-behaved cases and the direction is well-defined. These singularities are critical to understanding the surface's geometry and dynamics, as they introduce “points of curvature” that significantly influence structural properties.

The study of translation surfaces is deeply connected to various fields. In dynamical systems, translation surfaces provide models for the behavior of billiard trajectories in polygonal tables. Half-translation surfaces, which are closely related to translation surfaces, appear naturally in Teichmüller theory as the cotangent bundle of the Teichmüller space.

The classical origin of translation surfaces can be considered to be in dynamics, such as the study of billiard paths in polygons with rational angles. An important historical approach to understanding such systems was developed in [FK36], where one of the first translation surfaces arose from unfolding billiard paths to straight line trajectories. However, the first use of the notion translation surface can be found in the unpublished lecture notes of Thurston [Thu78].

From a topological perspective, the space of translation surfaces is particularly interesting. This moduli space, which parameterizes translation surfaces of a fixed topological type, can be stratified according to the combinatorial data of the singularities, leading to strata that correspond to translation surfaces with a specified configuration of singularities. Within each stratum, one can study various geometric and dynamical properties, such as the distribution of closed geodesics, the behavior of the straight-line flow, and the structure of the Veech group.

The Veech group, which captures the symmetries of a translation surface, plays a crucial role in understanding the dynamics on these surfaces. It remains an open question whether every group can be realized as a Veech group of some finite translation surface, though this is already known for all countable subgroups of $\mathrm{GL}_2^+(\mathbb{R})$ for infinite translation surfaces with infinite area. For a more detailed description and classification based on the underlying surface, see the preprint of [Art+23]. Finite translation surfaces, for comparison, are better understood in terms of their stratification.

One of the primary challenges in the study of translation surfaces is bridging the understanding between finite and infinite translation surfaces. Despite substantial progress in understanding translation surfaces of finite and infinite type, much is still unknown about the generic properties of these surfaces as the genus increases. Specifically, the geometrical properties of a random large-genus translation surface are not well understood. Recent progress in this area has been made by [Del+22], focusing on the combinatorial geometry of a random closed multicurve on a surface of large genus and of a random square-tiled surface of large genus.

The classical immersive topology [Hoo18; Hoo13b] is often considered too coarse, as the convergence of sequences of translation surfaces in this topology is quite weak. It derives its name from being defined by immersions, specifically continuous maps between subsets of translation surfaces that respect both basepoints and translation structures, particularly for the space of translation structures on the open disk. This limitation is a primary motivation for this research. By looking into the structure and behavior of high-genus translation surfaces, we aim to uncover new insights and develop a more comprehensive understanding of their properties.

The current state of research in translation surfaces is thus marked by a rich interplay between geometry, dynamics, and combinatorics, with significant contributions from various groundbreaking studies that continue to shape our understanding of these fascinating mathematical objects.

This thesis explores several fundamental questions about translation surfaces, particularly focusing on the asymptotic behavior of surfaces in the large-genus limit, the stratification of moduli spaces, and the computation of key geometric invariants. Our goal is to contribute to the broader understanding of these surfaces, offering new perspectives and tools for future research.

The results presented in this thesis are divided into several interconnected themes, each addressing a specific aspect of translation surfaces and their moduli spaces. Our primary contributions include extensions of existing constructions, new insights into connected components of the phase space of cutting sequences on the octagon, and some progress on an important geometric invariant.

In the following three sections, we provide an overview to the key concepts and results necessary for understanding the work presented in Parts II to IV.

1.1 An asymptotic construction

One of the central objects associated with a translation surface is its Veech group, which is a subgroup of $\mathrm{GL}_2^+(\mathbb{R})$. The Veech group encodes the symmetries of the surface, specifically the derivatives of orientation-preserving affine automorphisms that preserve the translation structure.

Significant advancements over the past decades have been made in the construction of infinite translation surfaces with large Veech groups, particularly through the development of Hooper–Thurston–Veech surfaces.

Hooper–Thurston–Veech surfaces form a special class of translation surfaces that exhibit particularly rich dynamical and geometric properties. These surfaces admit two cylinder decompositions in noncollinear directions, where all cylinders in a given decomposition share the same modulus $\frac{1}{\lambda}$, which is given by the ratio of circumference to height. This symmetry allows their Veech groups for $\lambda \geq 2$ to contain large, freely generated subgroups, conjugated to

$$G_\lambda = \left\langle \begin{pmatrix} 1 & \lambda \\ 0 & 1 \end{pmatrix}, \begin{pmatrix} 1 & 0 \\ \lambda & 1 \end{pmatrix} \right\rangle,$$

which makes them a nice object of study.

Building on the idea of constructing the double n–gon from [Vee89], this method was further generalized in the work of [BM10]. In [Hoo13a], this construction was extended to produce the Thurston–Veech construction for finite translation surfaces, before being adapted to infinite translation surfaces in [Hoo15], now referred to as the Hooper–Thurston–Veech construction. The upcoming book [DHV24] offers a comprehensive overview and further expands on this topic.

A multicurve on a topological surface is a disjoint union of simple closed curves that are essential, meaning they do not bound a disk or a punctured disk. When two multicurves α and β are in minimal position, their count of intersection points is minimized and the resulting intersection pattern can be encoded as a graph. The two multicurves α and β fill a surface X if every connected component of $X \setminus (\alpha \cup \beta)$ is an at most once-punctured disk.

The configuration graph $\mathcal{G}(\alpha \cup \beta)$ of two multicurves α and β is a bipartite graph that encodes how the curves intersect, see Figure 1.2. The vertices of the graph correspond

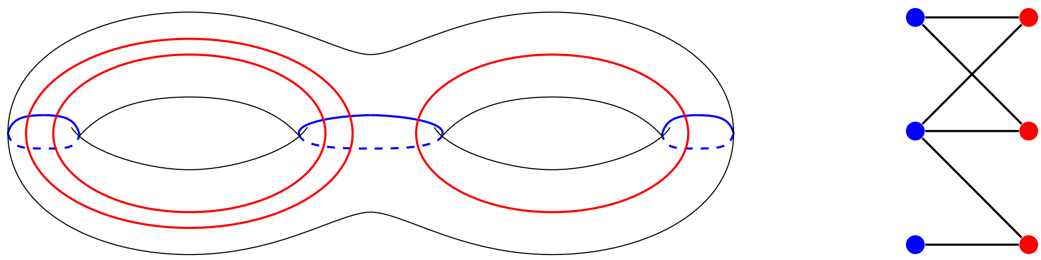

(a) Multicurves in minimal position and filling S_2

(b) Corresponding configuration graph

Figure 1.2: Hooper–Thurston–Veech surface on a double torus S_2

to the components of each multicurve and edges are drawn between vertices when the corresponding curves intersect.

In [Hoo15], the Hooper–Thurston–Veech construction for infinite translation surfaces was shown:

Theorem 4.2.5 (Hooper–Thurston–Veech construction — Hooper)
Let X be a topological surface, $\alpha = \bigcup_{i \in I} \alpha_i$ and $\beta = \bigcup_{j \in J} \beta_i$ two multicurves in minimal position that fill X. Let $h : \mathcal{G}(\alpha \cup \beta) \to \mathbb{R}_{>0}$ be a positive λ–harmonic function with $\lambda > 1$. Furthermore, the following conditions hold:

(a) The configuration graph $\mathcal{G}(\alpha \cup \beta)$ has finite degree, that is to say, there is an upper bound on the degree of the vertices in $\mathcal{G}(\alpha \cup \beta)$.

(b) For every component D of the complement of $\alpha \cup \beta$ in X, its boundary ∂D in X is connected.

(c) For every component D of the complement of $\alpha \cup \beta$ for which ∂D intersects infinitely many curves in $\alpha \cup \beta$, D is a disk without punctures.

Then, there exists a translation structure ω on X such that $M(\alpha, \beta, h) \coloneqq (X^*, \omega)$ is a Hooper–Thurston–Veech surface of modulus $\frac{1}{\lambda}$ whose horizontal cylinders have core curves $\{\alpha_i\}_{i \in I}$ and vertical cylinders have core curves $\{\beta_j\}_{j \in J}$.

This construction relies on associating a positive λ–harmonic function to the configuration graph, which is an eigenvector of the graph's adjacency operator with eigenvalue λ. For finite translation surfaces this adjacency operator is the adjacency matrix.

Given a bipartite configuration graph $\mathcal{G}$, the Hooper–Thurston–Veech surface $M(\mathcal{G}, h)$ is the translation surface obtained by assigning cylinders to the vertices of the graph and gluing them together according to the edges. The function h governs the sizes of the cylinders and the surface inherits the combinatorial structure of the graph. The modulus of the surface is related to the eigenvalue λ of the harmonic function.

The construction of finite Hooper–Thurston–Veech surfaces from graphs provides a natural way to approximate infinite surfaces. Starting with an infinite configuration graph $\mathcal{G}$, we can consider a sequence of growing subgraphs $\mathcal{G}_i$, where each subgraph is a finite induced subgraph of $\mathcal{G}$ that contains more vertices than the previous one. The corresponding sequence of finite Hooper–Thurston–Veech surfaces $M(\mathcal{G}_i, h_i)$ forms a growing Hooper–Thurston–Veech sequence.

The sequence of surfaces in the growing Hooper–Thurston–Veech sequence can be used to approximate the original infinite surface in various respects. In particular, the moduli of the finite surfaces in the sequence converge to the modulus of the original infinite surface and the Veech groups of the finite surfaces contain subgroups that approximate the Veech group of the infinite surface. This leads to the following Theorem, which provides a precise formulation of this approximation process.

Theorem 4.3.3 (Hooper–Thurston–Veech sequence convergence)
Let (X, ω) be an infinite Hooper–Thurston–Veech surface with configuration operator $\mathcal{A}$ and $(C(\mathcal{G}_i))_{i\in\mathbb{N}}$ be a growing Hooper–Thurston–Veech sequence of (X, ω). If $\|\mathcal{A}\| < \infty$ and $\bigcup_{i\in\mathbb{N}} \mathcal{G}_i = \mathcal{G}$, then the sequence of moduli $(\lambda_i)_{i\in\mathbb{N}}$ of the Hooper–Thurston–Veech surfaces coming from $(C(\mathcal{G}_i))_{i\in\mathbb{N}}$ converges to the modulus λ of the original Hooper–Thurston–Veech surface $M(\mathcal{G}, h)$. This yields a sequence of finite translation surfaces (X_i, ω_i) whose Veech groups contain a conjugate of G_{λ_i} with $\lambda_i \to \lambda$.

The proof establishes that the operator $\mathcal{A}_k$, corresponding to the restriction of $\mathcal{A}$ to a sequence of nested spaces $V_1 \subseteq V_2 \subseteq \ldots$, converges to the Hooper–Thurston–Veech operator $\mathcal{A}$ of the original surface in the spectral norm. This convergence implies that the maximal eigenvalues of $\mathcal{A}_k$ converge to the maximal eigenvalue of the original surface. The Veech group of each finite translation surface $C(\mathcal{G}_i)$ will contain a conjugate of G_{λ_i} by construction.

We apply this theorem to construct a new example of an infinite translation surface with finite area, featuring a large Veech group, which we refer to as the (un-)lucky clover surface, see Figure 1.3.

By examining a sequence of finite translation surfaces across different examples, we observe some interesting numerical properties in computational programs. The corresponding SageMath code is provided in [Rei24a; Rei24b; Rei24d] for the reader.

1.2 Cutting sequences

In addition to extending known constructions on the space of translation surfaces that respect the dynamical properties of the Veech group, we are also interested in exploring further related dynamical properties.

Consider mathematical billiards, in which a point "mass" moves with unit speed inside a polygon $P \subsetneq \mathbb{R}^2$ and reflects instantaneously at the boundary ∂P with the rule "the angle of incidence is equal to the angle of reflection". By adding a mirrored copy of a polygon along each edge instead of instantaneous reflection at the boundary, we can

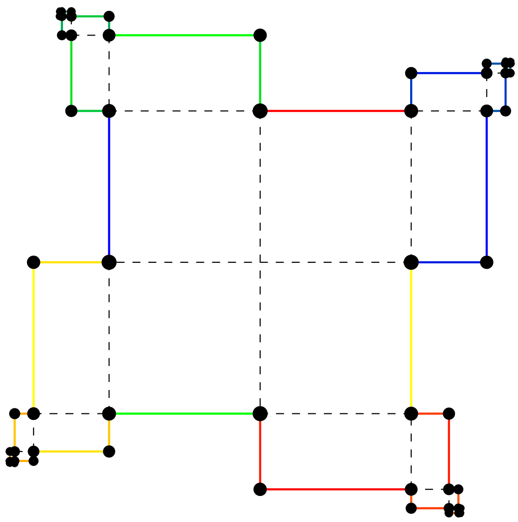

Figure 1.3: (Un-)lucky clover surface

understand a billiard path by continuing in some straight line flow on copies of different polygons [ZK75]. This gives rise to a translation surface and even a finite translation surface if all angles of P are rational.

Symbolic dynamics on translation surfaces is another crucial area of research that has been extensively studied in the context of word dynamics and substitutions.

Let (X, ω) be a finite translation surface. A geodesic flow on (X, ω) in a direction θ is an additive action of $\mathbb{R}$ on $\overline{X}$ over some time parameter t, preserving the initial surface for $t = 0$. The trajectory of a point $x \in X$ under this flow, denoted by $\tau_{x,\theta}$, is well-defined until it hits a singularity, see Figure 1.4.

To study the behavior of trajectories, we encode their paths using cutting sequences. A cutting sequence tracks the sides of a polygonal decomposition of (X, ω) crossed by a geodesic trajectory by labeling the edges with some finite alphabet $\mathcal{A}$. The collection of all cutting sequences corresponding to different trajectories forms a language.

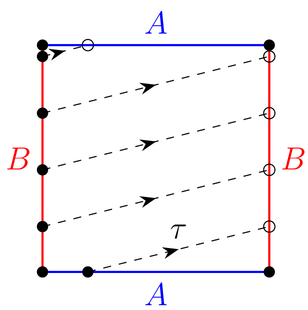

Figure 1.4: Square torus with sides labeled A and B, illustrating the cutting sequences $c(\tau) = ABBBB\ldots$

The question which arises naturally is on the complexity of this billiard game, or how many possible, truly distinct paths there are. We can formalize this using a complexity function that captures the rate of this growth.

Consider an infinite word $w \in \mathcal{A}^{\mathbb{N}}$, where $\mathcal{A}$ is a finite alphabet. We define the complexity function p_s of the infinite word w as

$$p_w(n) = |\mathcal{L}_n(s)|,$$

where $\mathcal{L}_n(w)$ represents the set of all distinct subwords, also called factors, of length n that appear in the infinite word w.

A comprehensive introduction can be found in [Fog02], which is fundamental for understanding the complexities of word dynamics, particularly on regular polygons like the octagon.

The behavior of geodesics and their cutting sequences can be captured by transition diagrams. These are directed graphs where the vertices represent different letters from the alphabet $\mathcal{A}$ and edges indicate possible transitions between letters that correspond to valid geodesic paths on the surface. The directed edge (s, t) exists if and only if the pair of sides labeled by s and t can be crossed consecutively by a geodesic.

Not every word with letters from $\mathcal{A}$ is a valid cutting sequence. The transition diagrams help filter out invalid words, leaving us with a description of the cutting sequences corresponding to actual geodesic trajectories.

The complexity of the billiard game, that is, the number of distinct possible paths, can be measured by counting certain types of geodesics known as generalized diagonals. A generalized diagonal is a geodesic trajectory that begins and ends at vertices of the polygon without passing through any other vertices. In the setting of translation surfaces, they are referred to as saddle connections.

We are interested in counting such diagonals based on their geometric length (the Euclidean distance between the endpoints) or combinatorial length (the number of edges crossed by the diagonal). These counts are denoted by $N_g(t)$ and $N_c(n)$ for the geometric and combinatorial cases, respectively.

The set of saddle connections on (X, ω) up to a given length l is denoted by $V_{\mathrm{sc}}(X, l)$. A famous result for the asymptotic count of saddle connection states is given by [EM01], which will be also especially useful for Part IV.

Theorem 6.1.4 (Quadratic saddle connection length count — Eskin and Masur)
Let (X, ω) be a finite translation surface, then

$$\lim_{t \to \infty} \frac{|V_{\mathrm{sc}}(X, t)|}{t^2} \in \mathbb{R}_{>0},$$

where $V_{\mathrm{sc}}(X, t)$ is the set of saddle connections on (X, ω) with length smaller than t.

The complexity function of a billiard game on a polygon is related to the combinatorial count of generalized diagonals as shown in [CHT02].

Theorem 6.1.7 (Complexity combinatorics — Cassaigne, Hubert, and Troubetzkoy)
Let P be a polygon, p_P be the complexity function coming from billiards in P and N_c the

combinational count of generalized diagonals for P. Then the following equality holds:

$$p_P(n) = \sum_{k=0}^{n-1} N_c(k).$$

Based on Theorems 6.1.4 and 6.1.7, the complexity function exhibits cubic growth, so there exist $C, C' \in \mathbb{R}_{>0}$, such that

$$C \leq \frac{p_P(n)}{n^3} \leq C'$$

for all $n \in \mathbb{N}^+$. The complexity has cubic growth due to the interplay between the quadratic growth of saddle connections and the linear growth of Sturmian words, which are a special class of infinite words with linear complexity growth, to which our cutting sequences belong.

While the general growth rate of the complexity function is known for all convex polygon, calculating the explicit form of this growth for specific polygons remains a challenge. In the case of billiards in a square S we know that $\frac{p_S(n)}{n^3} \to \frac{2}{3\pi^2}$ for $n \to \infty$ by [CHT02]. Analogous results are known for the complexity function on an isosceles right triangle and the equilateral triangle [CHT02].

Cutting sequences on the regular octagon have been extensively studied and are quite well understood, particularly due to the work of Smillie–Ulcigrai [SU11]. In collaboration with Athreya, Bédaride, and Cassaigne, we aim to expand the list of polygons whose complexity is explicitly known by the regular octagon.

Various methods can be used for this purpose, including algorithms based on substitution rules established by [SU11] and the count of saddle connections. These methods provide crucial insights into the structure of cutting sequences.

Building on this, we prove how to explicitly count the connected components in the phase space of cutting sequences on the octagon, such that the count depends solely on the word encoding the component. This is a key step towards computing the complexity function with Theorem 6.1.7 for cutting sequences arising from geodesic trajectories on the regular octagon, a task we have not yet accomplished.

Let $\Sigma := \{A, B, C, D\}$ be the letters encoding the four edges of the regular octagon O after opposite edges are identified as in Figure 1.5 to obtain a translation surface (O, ω_O).

Let $\mathcal{L}_n \subseteq \Sigma^n$ denote the set of all cutting sequences of length n obtainable via straight line trajectories on (O, ω_O) and $\mathcal{L} = \bigcup_{n=0}^{\infty} \mathcal{L}_n$. Let $\mathcal{L}^\star$ be the sublanguage of $\mathcal{L}$, whose words have a factor AA, BB, CC or DD.

The phase space is a parameterization of all possible geodesic trajectories based on their starting points and directions. For each word w in the language $\mathcal{L}_n$, the corresponding part of the phase space, denoted $\mathcal{P}(w)$, consists of the trajectories that generate the word w. We now seek to explicitly count the number of connected components, $|CC(\mathcal{P}(w))|$, in these sets, which consist of convex polygons.

We realized as the length n of the cutting sequences increases, that the number of connected components of the phase space corresponding to a given word $ws \in \mathcal{L}_{n+1}$

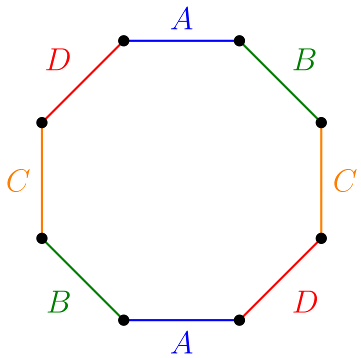

Figure 1.5: Octagon with labeled sides

did not increase compared to $w \in \mathcal{L}_n$. We also realized how symmetries of the octagon naturally correspond to symmetries in the phase space. For example if a cutting sequence exists in a direction θ, then it also exists in direction $\theta + \pi$. The corresponding trajectory can be obtained by rotating the old trajectory around the center of the octagon. These and more arguments were combined to give as the following theorem.

Theorem 6.3.20 (Double letter encodes case — Athreya, Bédaride, Cassaigne, and R.) For every word $w \in \mathcal{L}$:

$$|CC(\mathcal{P}(w))| = \begin{cases} 2, & \text{if } w \in \mathcal{L}^\star \cup \mathcal{L}_1 \\ 4, & \text{otherwise.} \end{cases}$$

The central idea of the proof is to handle the cases where $w \in \mathcal{L}^\star$ separately from those where $w \notin \mathcal{L}^\star$. For both cases we show sharp lower and upper bounds. For the lower bounds, the transition diagrams are a useful tool to exclude some directions for a word to appear in. In combination with the symmetry arguments this forces different connected components. By demonstrating that there are always at least two connected components, we can use induction on word length, leveraging the non-increasing property of word continuations. For $w \in \mathcal{L}_n \setminus \mathcal{L}^\star$, this approach shows that $|CC(\mathcal{P}(w))| = 2$. The base case is handled by explicitly calculating the phase space, see Section 1.2. For $w \in \mathcal{L}^\star$ more symmetry arguments and the work of [SU11] is needed.

The images of the corresponding phase spaces for small word lengths are generated using Python. The Python code used for this purpose is also provided in [Rei24c] for the reader.

1.3 Geometric invariants

In the final part, the focus is on calculating the volume of strata of translation surfaces to estimate bounds for the Cheeger constant. This part delves into the most detailed and intricate aspects of this thesis. The first ideas on how to calculate volumes were independently suggested by [EM01] and [KZ03].

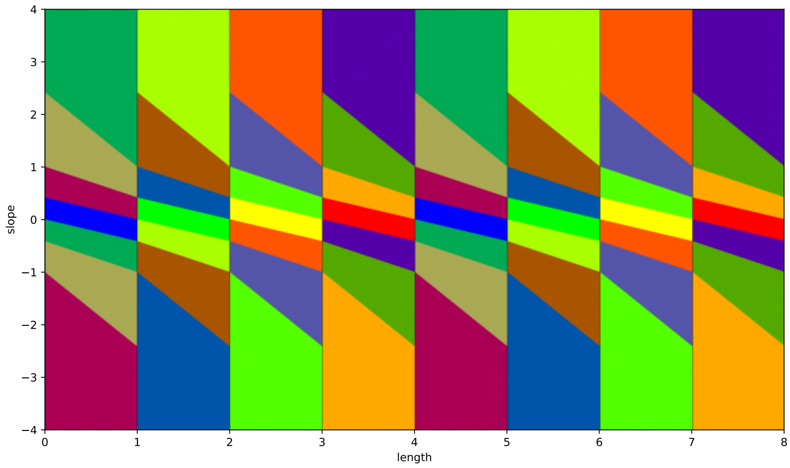

Figure 1.6: Phase space picture of $\mathcal{P}_2$, each color represents another word, $\mathcal{P}_2$ contains all 16 different words and colors

To construct a volume form in the space of translation surfaces, consider the set of holonomy vectors H_{sc} on a translation surface (X, ω) with singularities Σ. For every saddle connection, we get a holonomy vector in $\mathbb{C}$ via the translation structure ω on $\overline{X}$ as an element of the first relative cohomology group $H^1(X, \Sigma; \mathbb{C})$. Similar to the Fenchel–Nielsen coordinates for hyperbolic structures on manifolds, we obtain local coordinates for translation surface structures. In particular, these so-called period coordinates describe locally

$$H^1(X, \Sigma; \mathbb{C}) \cong \mathbb{R}^{4g+2l-2},$$

around (X, ω), where l is the count of essential singularities on (X, ω).

This moduli space can be stratified according to the combinatorial data of the singularities $\kappa = (k_1, \ldots, k_l)$ corresponding to the degree of the singularities $\Sigma = \{\sigma_1, \ldots, \sigma_l\}$, leading to strata $\mathcal{H}(\kappa)$ that correspond to space of translation surfaces with the specified degrees of singularities.

The cohomology group with complex coefficients contains a lattice $H^1(X, \Sigma; \mathbb{Z} \oplus \mathrm{i}\mathbb{Z})$ within $H^1(X, \Sigma; \mathbb{C})$. The translation surfaces corresponding to this lattice consist of surfaces that contain only squares as polygons, known as square-tiled surfaces.

We can now define a volume element in $H^1(X, \Sigma; \mathbb{C})$ and normalize it with the natural choice, such that the volume of a unit cube is one. The Masur–Veech volume ν on a stratum $\mathcal{H}(\kappa)$ can be defined locally on each neighborhood U as the pullback of the Lebesgue measure from $\mathbb{R}^{4g+2l-2}$ to U. This yields a global form of the same name on $\mathcal{H}(\kappa)$.

Scaling arguments allow to extend this definition and the volume element induces a volume element on the hyperboloid $\mathcal{H}_1(\kappa)$ of translation surfaces with area 1. We focus exclusively on translation surfaces of area 1, as any other area can be obtained by scaling. This scaling does not affect the fundamental structure of the surfaces, such as the Veech group or the trajectories from a flow, provided that the time variable is adjusted accordingly.

In this part, we will construct translation surfaces by separating them along separating curves related to the Cheeger constant. This process will result in disconnected surfaces. When a surface is separated into disconnected surfaces, we get a point in a stratum of disconnected surfaces $\mathcal{H}(\kappa') = \prod_{i=1}^{p} \mathcal{H}(\kappa_i')$. Up to some combinatorics we obtain the volume element as the product of the volume forms of the spaces $\mathcal{H}(\kappa_i')$.

A first algorithm for computing the volume of unit area strata involves using square-tiled surfaces and combinatorial methods, as detailed by [Zor02]. It was shown that:

Theorem 7.1.9 (Finite volume of $\mathcal{H}_1(\kappa)$ — Masur; Veech)
The Masur–Veech volume of $\mathcal{H}_1(\kappa)$ is finite for all κ.

One way to estimate the volume of a set $V \subsetneq \mathbb{R}^n$ is to count how many points of a lattice Λ are inside of V. An estimate for the volume of V is then just this count multiplied by the volume of the fundamental domain of the lattice. To approximate the volume, we can scale V by some factor $r > 1$ to get $V(r)$ and divide by r^n for normalization. This strategy can be extended to calculate the volume of a moduli space of translation surfaces by counting the square-tiled surfaces in this space.

For this counting problem, Eskin and Okounkov [EO01] proposed a general algorithm that determines the volume of the stratum $\nu\left(\mathcal{H}_1(\kappa)\right)$ for every κ. The algorithm in particular allows for the calculation of these volumes with the aid of computer implementations. Although this algorithm did not yield closed-form identities, Eskin–Okounkov successfully employed it to establish interesting properties of these volumes. For example, they demonstrated that $\nu\left(\mathcal{H}_1(\kappa)\right)$ is a rational multiple of π^{2g} for any κ of $2g-2$.

A natural question is how these volumes behave as the genus g tends to infinity. In the similar context of Weil–Petersson volumes, such questions were extensively and successfully explored by Mirzakhani and Zograf in [Mir13; MZ15].

Eskin was able to implement the Eskin–Okounkov algorithm as a computer program to evaluate the volumes $\nu\left(\mathcal{H}_1(\kappa)\right)$, if the genus g was limited by $g \leq 10$. Based on the numerical data from this program, Eskin and Zorich predicted in 2003, that

$$\nu\left(\mathcal{H}_1(\kappa)\right) = \frac{4}{\prod_{i=1}^{l}(k_i+1)} \left(1 + \mathcal{O}\left(\frac{1}{g^{1/2}}\right)\right).$$

This was shown to be true in [CMZ18] for the principal $\mathcal{H}_1(1^{2g-2})$ and in [Sau18] for the minimal strata $\mathcal{H}_1(2g-2)$, respectively. The conjecture was finally proven in [Agg20] for all strata:

Theorem 7.1.10 (Large-genus volume asymptotics — Aggarwal)
Let $g \geq 2$ and $\kappa = (k_1, \ldots, k_l)$ be a partition of $2g-2$. Then,

$$\frac{4}{\prod_{i=1}^{l}(k_i+1)} \left(1 - \frac{2^{2^{200}}}{g}\right) \leq \nu\left(\mathcal{H}_1(\kappa)\right) \leq \frac{4}{\prod_{i=1}^{l}(k_i+1)} \left(1 + \frac{2^{2^{200}}}{g}\right).$$

For our results on the Cheeger constant, we employ a divide-and-conquer strategy. In which we differentiate between the thick part and the thin part of $\mathcal{H}_1\left(\kappa\right)$. The thick part $\mathcal{H}_1^{\varepsilon,\text{thick}}(\kappa)$ of our stratum contains those translation surfaces, which have only saddle connections of at least length ε. The thin part $\mathcal{H}_1^{\varepsilon,\text{thin}}(\kappa)$ contains at least one saddle connection with length smaller than ε.

A method for explicitly calculating the volume of such more complicated strata was developed by Eskin, Masur, and Zorich in [EMZ03]. Their approach focused on establishing relations via Siegel–Veech formulas. Using these formulas, they constructed a recursive method for calculating the volumes of more complicated strata. This method involves expressing the volume of a given stratum in terms of simpler strata, multiplied by combinatorial constants derived from the Siegel–Veech formulas.

To understand these Siegel-type formulas, we need to encode some data on the configurations of saddle connections. For the purpose of computing the volume, it is sufficient to consider generic translation surfaces that contribute to a full measure set. We limit ourselves to translation surfaces that do not contain non-homologous saddle connections with the same holonomy as they are generic. Two saddle connections β and γ are homologous, if $\beta\gamma^{-1}$ separates the surface $\overline{X}$ into different components. We define the multiplicity of a holonomy vector v to be the number p of distinct saddle connections $\gamma_1, \ldots, \gamma_p$ that have v as their holonomy vector. Higher multiplicity is quite common on generic surfaces. We encode all this data as the configuration data $\mathcal{C}$. It contains information on the multiplicity and the order of the singularities.

Given a translation surface (X, ω) and a configuration $\mathcal{C}$, let $H_{\mathcal{C}}(X) \subset H_{\text{sc}}(X)$ denote the set of all holonomy vectors of saddle connections satisfying the configuration data $\mathcal{C}$. We can count them with [EM01]:

Theorem 7.2.9 (Asymptotics of saddle connection count — Eskin and Masur)
Given a configuration $\mathcal{C}$ and a connected component $\mathcal{H}$ of $\mathcal{H}_1(\kappa)$, there exists a constant $c = c(\kappa, \mathcal{C})$ such that for almost all $(X, \omega) \in \mathcal{H}$, it holds

$$\lim_{l\to\infty} \frac{|V_{\mathcal{C}}(X, l)|}{\pi l^2} = c(\kappa, \mathcal{C}).$$

The constant $c(\kappa, \mathcal{C})$ depends only on the connected component of the stratum and on the configuration $\mathcal{C}$.

All of these different configurations can be used in Siegel–Veech type formulas:

Proposition 7.2.10 (Siegel–Veech formula)
Let $\mathcal{C}$ be a configuration and κ be a partition of $2g-2$. Then there exists a constant $\tilde{c}(\kappa, \mathcal{C})$ such that for any $f \in \mathcal{C}_0^\infty(\mathbb{R}^2)$ the *Siegel–Veech formula*

$$\frac{1}{\nu(\mathcal{H}_1(\kappa))} \int_{\mathcal{H}_1(\kappa)} \hat{f}(X)\,\mathrm{d}\nu(X, \omega) = \tilde{c}(\kappa, \mathcal{C}) \int_{\mathbb{R}^2} f(x, y)\,\mathrm{d}x\,\mathrm{d}y$$

holds. The constant $\tilde{c}(\kappa, \mathcal{C})$ is called the *Siegel–Veech constant* of the stratum $\mathcal{H}_1(\kappa)$ and configuration $\mathcal{C}$.

The work of [EMZ03] unveils a profound connection between the calculation of volumes of strata of translation surfaces containing saddle connection in some configuration and the Siegel–Veech constant of the same configuration. Their recursive approach, which uses combinatorial constants derived from these formulas, has proven to be an effective tool in studying more difficult strata. For these calculations, they introduce and describe some surgeries to obtain a volume preserving map between $\mathcal{H}_1(\kappa') \times \overline{B}_\varepsilon(0)$ and $\mathcal{H}_1(\kappa)$ of some degree encoded by $\mathcal{C}$ and κ. A lot of work is allocated to the explicit calculation of this degree. In the end they obtained formulas that calculated the Masur–Veech volume of $\mathcal{H}_1^{\varepsilon,\text{thin}}(\kappa)$ by combinatorial data depending on $\mathcal{C}, \varepsilon$, and κ.

We can now finally shift our focus back to the Cheeger constant. The Cheeger constant is an invariant that captures how well a surface can be cut into two parts of roughly equal size with a minimal cut and therefore measuring connectivity in some sense. Let $\mathcal{A}$ be the set of all closed separating curves on (X, ω). For a separating curve $A \in \mathcal{A}$, we denote the two components of $\overline{X} \setminus A$ by X_1 and X_2.

The geometric Cheeger constant $h(X)$ is then calculated by

$$h(X) = \inf_{A \in \mathcal{A}} \frac{\text{length}(A)}{\min\{\text{area}(X_1), \text{area}(X_2)\}}.$$

In this thesis, we aim to understand the upper bounds on the growth of the Cheeger constant. It can be shown that the Cheeger constant can be arbitrarily large in value in every stratum, but this only occurs when there are short saddle connections. The expected value of the Cheeger constant is controllable on the thick part by geometric arguments. Thus, one of the goals of the thesis is to find such an upper bound, depending on the genus.

In fact, we can show that for the minimal strata $\mathcal{H}_1(2g-2)$.

Theorem 8.2.10 (Upper bound on the expected value of the geometric Cheeger constant in the minimal stratum)
There exists $\hat{g} \in \mathbb{N}^+$ and a constant $C > 0$, such that an upper bound for the expected value of the geometric Cheeger constant h in the minimal stratum for $g \geq \hat{g}$ is given by

$$\mathbb{E}_{\mathcal{H}_1(2g-2)}(h) \leq C g^{\frac{3}{2}}.$$

The main idea of the proof is to use a divide-and-conquer strategy. On the thick part, geometric arguments show that we can always embed a relatively large disk, whose boundary can be used as the separating curve. The thin part is split into progressively smaller thick parts. For each of these parts, we apply the strategy used for the thick part. In the end, we obtain the expected value as the weighted sum of these parts. Since this process is conducted infinitely many times, we end up with an convergent series.

Expanding this theorem to other strata is quite hard, but we can show a similar statement for a geotopological variant of the Cheeger constant which we need to formulate in the right language, so we can use the work of [EMZ03].

This difficulty arises because the principal stratum contains the most generic surfaces of any stratum. Since we fix the area to 1, the density of singularities and topological holes increases arbitrarily high with growing genus. Separating curves, which are generically large and rare, make the calculation of the geometric Cheeger constant quite complex.

To develop this variant, we deviate from the conventional approach of dividing by the minimum surface area on either side of a separating curve. Instead, we employ the concept of separating complexity, focusing on splitting the surface based on its genus. So for $m \in \{1, \ldots, g-1\}$, let $\mathcal{B}_m$ be the set of all closed curves connecting two distinct singularities consisting of two homologous saddle connections separating $\overline{X}$. The length of separating curves is minimized for all possible genus separations. For $m \in \{1, \ldots, g-1\}$, let

$$h_m^{\top}(X) \coloneqq \inf_{\gamma \in \mathcal{B}_m} \frac{\operatorname{length}(\gamma)}{\frac{\min\{m, g-m\}}{g}},$$

then the geotopological Cheeger constant is calculated by

$$h^{\top}(X) \coloneqq \min_{m \in \{1, \ldots, g-1\}} h_m^{\top}(X).$$

With this modified version of the Cheeger constant we show:

Theorem 9.3.1 (Upper bound on the expected value of the geotopological Cheeger constant in the principal stratum)
For any $\delta > 0$, there exists $\hat{g} \in \mathbb{N}^+$, such that an upper bound for the expected value of the geotopological Cheeger constant $h^{\top}$ in the principal stratum for $g \geq \hat{g}$ is given by

$$\mathbb{E}_{\mathcal{H}_1(1^{2g-2})}(h^{\top}) \leq 2^{16} \cdot g^{2+\delta}.$$

The main proof idea stays the same: Divide-and-conquer the stratum to obtain thick parts, use geometric arguments for the thick parts, and get a convergent series. The geometric idea here will be to approximate the separating curves with a chain of saddle connections and show some maximal length, instead of embedding a large disk. Also the estimates for the sum are harder since there are a lot of edge cases when calculating the volumes in the thin part.

All of these results collectively enhance our understanding of translation surfaces, particularly in the context of large-genus asymptotics. By providing new tools and perspectives, this research aims to lay some groundwork for further exploration and discoveries in the field.

1.4 Organization

This thesis is organized into several chapters, each addressing various aspects of translation surfaces and their properties. The structure of the thesis is designed to guide the reader from foundational concepts to advanced results, ensuring a comprehensive understanding of the subject. One of the main goals of this thesis is to be almost self-contained.

In Part I, we begin with an introduction to translation surfaces in Chapter 2, providing an overview of their definition, construction, and fundamental properties. This sets the stage for a deeper exploration of specific topics, such as finite and infinite translation surfaces corresponding to compact and non-compact surfaces.

Following the first half of the introduction, we delve into the structure of translation surfaces in Chapter 3, examining singularities, saddle connections, Veech groups, and the dynamics of the straight-line flow. This exploration provides an understanding of the geometric and dynamical features that characterize translation surfaces and their moduli spaces.

In Part II of the thesis, we present a new perspective on the Hooper–Thurston–Veech construction. This section includes a detailed description of the new asymptotic construction, along with an analysis of the resulting surfaces as well as geometric properties. The construction is illustrated with explicit examples.

Subsequently in Part III, we explore the concept of cutting sequences, which encode the combinatorial data of geodesic trajectories on translation surfaces. This part includes an investigation of word dynamics, complexity, and substitutions, offering new insights into the behavior of geodesics and their associated symbolic representations.

We then turn to the study of geometric invariants in Part IV, focusing on the volume calculation of strata and the Cheeger constant. In Chapter 7, we explain how to calculate volumes for different strata of translation surfaces. The investigation of the Cheeger constant in Chapter 8 yields the upper bound in the minimal strata.

The final Chapter 9 of the thesis introduces a topological version of the geometric Cheeger constant for the principal stratum.

Overall, this thesis aims to advance the understanding of translation surfaces; by extending existing constructions, introducing new perspectives, and investigating key geometric invariants, we contribute to the broader knowledge for future research.

Part I

Background

2 Translation surfaces

We start by defining and providing examples of our main objects of interest. Most of this chapter and partially the next chapter is rooted in the German and unpublished lecture notes of [Her21]. These notes are closely related to the also German and unpublished lecture notes of [Ran12] which are available online.

Definition 2.0.1 (Translation surface)
A *translation surface* $(X, \mathcal{T})$ is a connected surface X, equipped with a translation structure $\mathcal{T}$.

For this definition we fix a common definition for surfaces:

Definition 2.0.2 (Surface)
A *surface* X is a two-dimensional manifold.

So, the more interesting part lies within the translation structure part of the translation surface definition.

Definition 2.0.3 (Translation structure)
A *translation structure* $\mathcal{T}$ is a maximal atlas $\{(U_i, \phi_i)\}$ on an n–dimensional manifold M such that the transition maps are *translations*, this means that for each connected component U of $U_i \cap U_j$, there exists a $c \in \mathbb{R}^n$ such that

$$\phi_i \circ \phi_j^{-1}(x) = x + c$$

for all $x \in \phi_j(U)$ holds.

This definition encapsulates the local structure of our main object of interest and is the reason for its name. It provides a locally rigid geometric structure. However, as we will see later this still allows for topologically rich spaces.

Remark 2.0.4 (On translation surfaces)
This definition embraces the inclusion of infinite translation surfaces. However, in the literature, the convention often leans towards equating translation surfaces with finite translation surfaces. For the latter, three similar but contextually nuanced definitions exist, each proving more practical in different situations. We will introduce them later, after a few examples.

To study geometry on translation surfaces, a metric is required.

Definition 2.0.5 (Flat metric I)
Let x, y be points of a translation surface $(X, \mathcal{T})$. We define the metric d_X as follows:

$$d_X(x,y) \coloneqq \inf \sum_{i=0}^{n-1} \operatorname{length}\left(\phi_i\left(\gamma\mid_{[t_i,t_{i+1}]}\right)\right),$$

where the infimum is taken over all decompositions $0 = t_0 < t_1 < \ldots < t_n = 1$ and all paths $\gamma\colon [0,1] \to X$ from x to y, such that there exist translation charts (U_i, ϕ_i) satisfying $\phi_i([t_i, t_{i+1}]) \subseteq U_i$ and $(\phi_i \circ \gamma)\mid_{[t_i,t_{i+1}]}$ is rectifiable. Here, length$(\cdot)$ is the length of a path in the Euclidean metric in $\mathbb{R}^2$. The map d_X is referred to as the *flat metric* on $(X, \mathcal{T})$.

So, we define distances by the inherited distance obtained from the underlying Euclidean metric. This inheritance from the underlying structure will be a common theme for this chapter.

Proposition 2.0.6 (Metric is well-defined)
The map $d_X\colon X \times X \to \mathbb{R}$ is a metric on X.

Proof. Let $x, y, z \in X$.

- *Definiteness*: Let $x \neq y$. Since X is a manifold, it fulfills the Hausdorff property: there exist translation charts (U_x, ϕ_x) and (U_y, ϕ_y) separating x and y. Choose a ball of radius $\varepsilon > 0$ such that

  $$V'_x \coloneqq B_\varepsilon(\phi_x(x)) \subseteq \phi_x(U_x)$$

  and define $U'_x \coloneqq \phi_x^{-1}(V'_x)$. Any path in X from x to y intersects $\partial U'_x$ and as path length remains unchanged under chart transition, this path has a length of at least ε. In particular, $d_X(x,y) \neq 0$.

- *Positivity*: The distance $d_X(x,y) \geq 0$ since length$(\cdot) \geq 0$ for all paths.

- *Symmetry*: The equation $d_X(x,y) = d_X(y,x)$ holds since length$(\gamma) =$ length(γ^{-1}) for the path γ^{-1} traversed in the opposite direction from y to x.

- *Triangle inequality*: Let $\gamma_1\colon [0,1] \to X$ be a rectifiable path from x to y and analogously $\gamma_2\colon [0,1] \to X$ a rectifiable path from y to z. Then, the composite path

  $$\gamma\colon [0,1] \to X, \quad t \mapsto \begin{cases} \gamma_1(2t), & \text{if } 0 \leq t \leq \frac{1}{2}, \\ \gamma_2(2t), & \text{if } \frac{1}{2} < t \leq 1 \end{cases}$$

  is a rectifiable path from x to z and it satisfies

  $$\operatorname{length}(\gamma_1) + \operatorname{length}(\gamma_2) = \operatorname{length}(\gamma) \geq d_X(x,z).$$

  Since this inequality holds for all γ_1 and γ_2, it follows that

  $$d_X(x,y) + d_X(y,z) \geq d_X(x,z). \qquad \square$$

After fixing a metric, we can formalize geodesics, segments, rays as subsets of geodesics, and more.

Definition 2.0.7 (Geodesic)
A continuous map $\gamma\colon I \to X$ from a connected subset I of $\mathbb{R}$ into a metric space X is called *geodesic*, if for every $t \in I$ there exists a neighborhood (t_1, t_2) of t such that $\gamma|_{(t_1,t_2)}$ is isometric onto its image.

Convention 2.0.8 (Image & map)
The image of γ is also called a *geodesic*.

Our broad definition of translation surface includes non-compact spaces.

Remark 2.0.9 (Non-compactness)
A translation surface $(X, \mathcal{T})$ is generally not metrically complete and therefore generally not compact. In particular, in the definition of a geodesic path, there are paths allowed, which are defined on an open interval, which cannot be extended to the corresponding closed interval.

Even though we do sometimes have non-compact translation surfaces, we can still metrically complete these spaces classically.

Definition 2.0.10 (Metric completion)
We can complete a translation surface X like any metric space by replacing X with the space of Cauchy sequences in X modulo the subset of null sequences. We denote this *metric completion* of X as $\overline{X}$.

These newly added points are particularly important for various aspects of $\overline{X}$ and therefore are given their own name.

Definition 2.0.11 (Singularity)
We refer to the elements of $\Sigma \coloneqq \Sigma(X) \coloneqq \overline{X} \setminus X$ as *singularities* of the translation surface $(X, \mathcal{T})$.

The etymology of singularities will be clearer later, once we introduce other perspectives on these surfaces. Let us finally look at a considerably basic example of a translation surface.

Example 2.0.12 (Euclidean plane)
The *Euclidean plane* $\mathbb{R}^2$ is a translation surface. Let $\tilde{\mathcal{T}}$ be a translation atlas for $\mathbb{R}^2$, given by the identity and maps of the form

$$U \to U + c, \quad x \mapsto x + c$$

for all $c \in \mathbb{R}^2$ and open sets $U \subsetneq \mathbb{R}^2$. Taking the union of all charts compatible with $\tilde{\mathcal{T}}$ yields a maximal atlas $\mathcal{T}$, whose charts are translations, giving rise to the translation surface $(\mathbb{R}^2, \mathcal{T})$.

Convention 2.0.13 (Natural choice)
We will sometimes denote X as a translation surface instead of $(X, \mathcal{T})$ like in the previous example. In these cases, the underlying translation structure will be clear from the context and, in a sense, represents the natural choice.

Convention 2.0.14 (Euclidean and complex plane identification)
It is quite common to identify $\mathbb{C}$ with $\mathbb{R}^2$, in which case points $x \in \mathbb{R}^2$ are usually denoted as $z = x_1 + \mathrm{i}x_2$.

The Euclidean plane is often not considered to be a translation surface by other authors, who restrict themselves to finite translation surfaces, which we want to define next. Beforehand, let us define one of the most important family of examples we will use repeatedly as a toy model in this thesis.

Example 2.0.15 (Flat torus family)
A *flat torus* $\mathbb{T}_\tau$ is a translation surface defined as the quotient space of $\mathbb{R}^2 \cong \mathbb{C}$ by the action of a full rank lattice $\Lambda = \mathbb{Z} \oplus \tau\mathbb{Z}$, where $\tau \in \mathbb{H}$ is a complex number with positive imaginary part. The translation structure is induced by the translation action of Λ on $\mathbb{R}^2$ by edge identification of opposite sides of the fundamental domain of Λ.

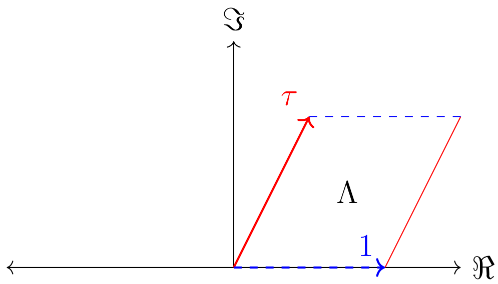

Figure 2.1: Flat torus parametrization with $\tau \in \mathbb{H}$

Convention 2.0.16 (Gluing)
Identifying edges is a process we refer to as *gluing* . This process is visualized in Figure 2.2 in the case of the torus.

The flat torus $\mathbb{T}_\mathrm{i}$ is an example of a translation surface almost everybody includes in their definition for translation surfaces. Notice that $\mathbb{T}_\mathrm{i}$ does not contain singularities, setting it apart from many other examples.

2.1 Finite translation surfaces

In the literature, it is a common convention to only consider finite translation surfaces when discussing translation surfaces. Finite and infinite translation surfaces are understood differently well in various aspects. Questions regarding the constructability of Veech

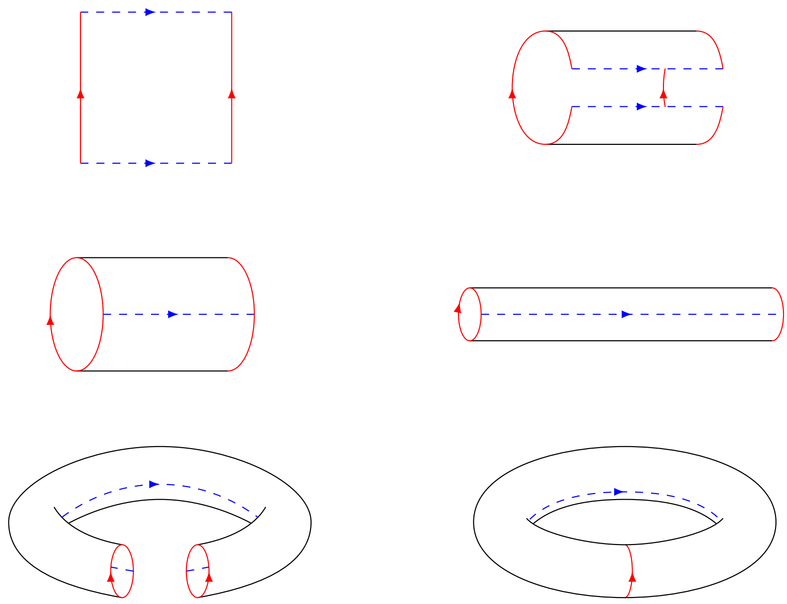

Figure 2.2: Gluing together the torus $\mathbb{T}_i$ using homeomorphisms for deformations

groups, introduced in Section 3.3, containing specific elements are better understood for infinite translation surfaces. While the question of the classification of finite translation surfaces can be approached through stratification, as we will see in Section 3.5, there is no analogous systematic description for infinite ones. The main goal of this section is to define finite translation surfaces in three different ways and showing the equivalence of these definitions. This will be helpful for this thesis since each definition gives us another insight to translations surfaces. The different viewpoints will allow us to study translation surfaces from different perspectives.

Definition 2.1.1 (Finite translation surface I)
A *finite translation surface* $(X, \mathcal{T})$ is a translation surface $(X, \mathcal{T})$, whose metric completion $\overline{X}$ is a compact surface and such that the cardinality of the set of singularities $\Sigma = \overline{X} \setminus X$ is finite.

Example 2.1.2 (Finite translation surface)
The tori from Example 2.0.15 are finite translation surfaces, the underlying compact connected two-dimensional manifold is homeomorphic to the torus as seen in Figure 2.2, it is already metrically complete. The translation structure is inherited from the Euclidean plane.

However, it is quite common and useful to fix some point on our torus.

Remark 2.1.3 (Alternative view)
Alternatively, we can consider the tori from Example 2.0.15 and exclude its corner point in the lattice, the underlying compact connected two-dimensional manifold is then homeomorphic to the punctured torus as seen in Figure 2.2, its metric completion is the regular torus.

This alternative presentation is better compatible and the toy model for the following alternative Definition.

Definition 2.1.4 (Finite translation surface II)
Let $P_1, \dots, P_n$ be finitely many disjoint polygons in the plane $\mathbb{R}^2 \cong \mathbb{C}$. Let $P_i^\star$ denote the polygon P_i without its vertices Σ_i. Consider an orientation of the plane and therefore an orientation for each polygon. For all edges of $E := \bigcup_{i=1}^n \partial P_i^\star$, let $G\colon E \to E$ be an identification, in other words a gluing, such that

(1) the edges are pairwise identified,

(2) the edges are identified by maps which are restrictions of translations and

(3) when two sides are identified, the outward pointing normals (coming from the orientation of the polygons) point in opposite directions.

Define a surface X by
$$X := \bigcup_{i=1}^n P_i^\star \big/ G .$$
If X is connected, we call $(X, \mathcal{G})$ a *finite translation surface*, where $\mathcal{G}$ is the atlas defined by embedding the polygons in $\mathbb{R}^2$ and identifying the edges via G.

This definition is the most visual one and usually referred to when describing translation surfaces to a broader audience.

Remark 2.1.5 (Flat metric II)
The *flat metric* on $(X, \mathcal{G})$ is derived as the quotient metric from the Euclidean metric on $\mathbb{R}^2$:
$$d_X(x, y) = \inf \left(d_{\mathbb{R}^2}(x, x_1) + \sum_{i=1}^{m-1} d_{\mathbb{R}^2}(G(x_i), x_{i+1}) + d_{\mathbb{R}^2}(G(x_m), y) \right),$$
where the infimum is taken over all sets $\{x_1, \dots, x_m\}$ of points on the boundary of the polygons $E \cup \Sigma$, where $\Sigma = \bigcup_{i=1}^n \Sigma_i$.

A typical example constructed with this view in mind is Veech's double n–gon.

Example 2.1.6 (Veech's double n–gon)
Let $n \geq 3$ and take two regular n–gons in the plane, such that the second n–gon can be obtained from the first n–gon by a rotation of π. Glue each side of the first n–gon with the only side of the second n–gon fulfilling (3) of Definition 2.1.4. See Figure 2.3 for the case $n = 5$. The corresponding translation surface from Definition 2.1.4 is called *Veech's double n–gon* $\mathbb{V}_n$.

We want to show that the object described in Definitions 2.1.1 and 2.1.4 are the same. For that it would be particularly useful if translation surfaces are triangulable. This is the case; we can inherit it from Riemann surfaces.

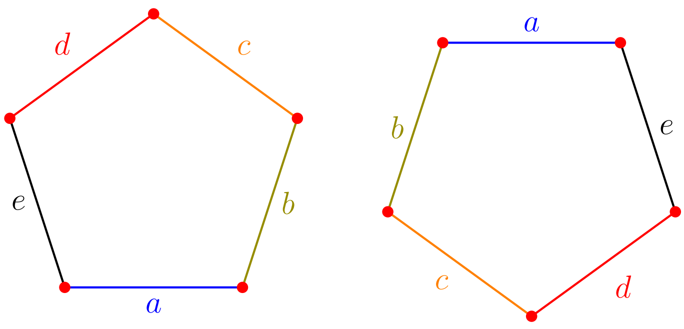

Figure 2.3: Veech's double pentagon

Definition 2.1.7 (Riemann surface)
A *Riemann surface* is a one-dimensional complex manifold, that is, a topological space X with a (maximal) atlas $\{(U_i, \phi_i) \mid i \in I\}$ for some index set I of complex charts

$$\phi_i : U_i \to \tilde{U}_i \subseteq \mathbb{C},$$

where $\tilde{U}_i$ are open. These charts satisfy the following conditions:

- the surface X is the union of the neighborhoods: $\bigcup_{i \in I} U_i = X$,
- the map ϕ_i is a homeomorphism for all $i \in I$ and
- the transition functions

$$\phi_i \circ \phi_j^{-1} : \tilde{U}_j \supset \phi_j(U_i \cap U_j) \to \phi_i(U_i \cap U_j) \subseteq \tilde{U}_i$$

  are holomorphic for all $i, j \in I$.

Remark 2.1.8 (Translation surfaces are Riemann surfaces)
Given that translations are biholomorphic, a translation surface can always be regarded as a Riemann surface.

So, we can easily inherit the property of being triangulable as Riemann surfaces are generally triangulable.

Remark 2.1.9 (Triangulable)
Translation surfaces are *triangulable* as they are Riemann surfaces.

We can show our equivalence:

Lemma 2.1.10 (Equivalence of I & II)
The objects described in Definitions 2.1.1 and 2.1.4 are the same.

Proof. We show each direction of I $\Leftrightarrow$ II separately.

"⇒": Let $(X, \mathcal{T})$ be a translation surface as defined in Definition 2.1.1. There exists a finite triangulation of $\overline{X}$ such that each $\sigma \in \Sigma$ is a vertex of a triangle and each triangle is a Euclidean triangle and geodesic with respect to the flat metric on X. These triangles constitute our polygons P_i and the gluings are determined by the shared edges in X.

"⇐": Let $(X, \mathcal{G})$ be a translation surface as defined in Definition 2.1.4. Let Σ be the set of vertices of the polygons $\{P_i\}$ after gluing.

The translation surface (X, ω) is locally homeomorphic to a Euclidean plane. Every open neighborhood can be embedded in $\mathbb{R}^2$. Since sides with opposite normals are glued, this also holds for points incident to the interior of edges of these polygons. As each side is glued and there are only finitely many polygons, $X \sqcup \Sigma$ is compact. Naturally, X is also two-dimensional, as the non-degenerate polygons are. Due to the choice of charts induced by the Euclidean metric, all chart transitions are translations and we obtain a translation structure on X.

From each of the polygons that constitute X, the flat metric is locally the Euclidean metric. Therefore, through the process of compactification, precisely the vertices of the polygons are added and $X \sqcup \Sigma$ is the metric completion of X. It remains to show that the surface structure can be extended to Σ:

Each $\sigma \in \Sigma$ arises through gluing finitely many vertices $\sigma_1, \ldots, \sigma_n$ of the polygons. Let k and l be, without loss of generality, the edges adjacent to σ_1 in the polygon P_1, such that $k = k_1$ is glued to an edge k'_1 in the polygon P_2 at the vertex σ_2. The other edge k_2 at the vertex σ_2 is glued to k'_2 and so on (see Figure 2.4).

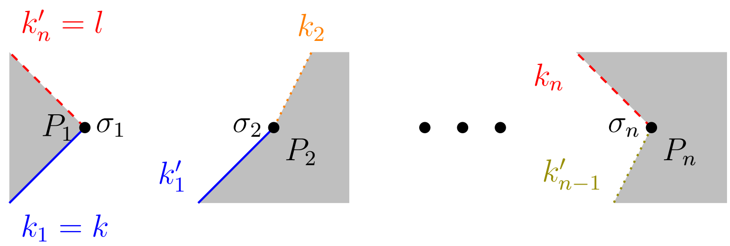

Figure 2.4: Gluing pattern around the singularity σ

After finitely many such steps, k_n is glued to $k'_n = l$. Since each k_i is parallel to k'_i, the total angle is a multiple of 2π. Let k_σ be defined such that the total angle around σ is $k_\sigma 2\pi$. The neighborhood of σ is homeomorphic to a *disk* $\mathbb{D} := \overline{B}_\varepsilon$ in $\mathbb{R}^2$ of radius ε. For small enough $\varepsilon > 0$, this can be done explicitly through the map $z \mapsto z^{k_\sigma}$. □

For the third definition of a translation surface, we need to acquire additional background knowledge in differential geometry. Since this one differs more significantly from the others, it provides us with additional methods of describing finite translation surfaces and explains the etymology of singularities.

First, we want to define derivatives to obtain 1–forms. We start by introducing different notions of holomorphic.

Definition 2.1.11 (Holomorphic)
A map $f\colon X \to Y$ between Riemann surfaces X and Y is called *holomorphic* if the composition with the charts $\psi_j \circ f \circ \phi_i^{-1}\colon \phi_i(\mathbb{C}) \to \mathbb{C}$ is holomorphic for every chart (U_i, ϕ_i) of X and every chart (V_j, ψ_j) of Y.

Definition 2.1.12 (Holomorphic function)
Let (U, ϕ) be a chart of X. A *holomorphic function* on U is a map $f\colon U \to \mathbb{C}$ such that

$$f \circ \phi^{-1}\colon \mathbb{C} \to \mathbb{C}$$

is holomorphic. We denote the *space of holomorphic functions* on U as $\mathcal{O}_X(U)$.

Holomorphic functions from $\mathbb{C}$ to $\mathbb{C}$ are smooth automatically, for a general Riemann surface we use the following definition.

Definition 2.1.13 (Smooth function)
Let X be a Riemann surface and (U, ϕ) be a chart of X. A *smooth function* on U is a map $f\colon U \to \mathbb{R}$ such that $f \circ \phi^{-1}$ is smooth, meaning it is infinitely differentiable in $\mathbb{R}$.

$$\begin{tikzcd} U \arrow[r, "f"] \arrow[d, "\phi"] & \mathbb{R} \\ \mathbb{C} \arrow[ur, "f\circ\phi^{-1}"'] & \end{tikzcd}$$

We refer to the *space of smooth functions* on U as $\mathcal{C}^\infty(U)$.

With this, partial derivatives can be defined as follows.

Definition 2.1.14 (Partial derivative)
The *partial derivative* of a smooth function f on a chart (U, ϕ) is defined by

$$\frac{\partial}{\partial_\phi x}\colon \mathcal{C}^\infty(U) \to \mathcal{C}^\infty(U), \quad f \mapsto \frac{\partial}{\partial x}(f \circ \phi^{-1}) \circ \phi.$$

Analogously for $\frac{\partial}{\partial_\phi y}$.

However, we must pay attention to the choice of basis in this definition.

Remark 2.1.15 (Partial derivatives depend on basis)
Differentiating on another chart (V, ψ) is generally not consistent with differentiating on (U, ϕ). That is, $\frac{\partial}{\partial_\phi x} f \neq \frac{\partial}{\partial_\psi x} f$ for a general $f \in \mathcal{C}^\infty(U \cap V)$. However, it can be shown that $\frac{\partial}{\partial_\psi x}$ can be expressed as a $\mathcal{C}^\infty(U \cap V)$–linear combination of $\frac{\partial}{\partial_\phi x}$ and $\frac{\partial}{\partial_\phi y}$:

$$\frac{\partial}{\partial_\psi x} = a\frac{\partial}{\partial_\phi x} + b\frac{\partial}{\partial_\phi y}$$

for some $a, b \in \mathcal{C}^\infty(U \cap V)$.

It therefore makes more sense to consider the module of derivations on U rather than the partial derivatives themselves for a chart (U, ϕ), making it base independent.

Definition 2.1.16 (Module of derivations)
Let (U, ϕ) be a chart of X. The *module of derivations* $\tilde{\Omega}_X(U)$ is defined by

$$\tilde{\Omega}_X(U) \coloneqq \left\{ f \cdot \frac{\partial}{\partial_\phi x} + g \cdot \frac{\partial}{\partial_\phi y} \;\middle|\; f, g \in \mathcal{C}^\infty(U) \right\}.$$

Evaluating an element of $\tilde{\Omega}_X(U)$ in a point is not dependent on the basis and therefore this allows us to well-define the derivative at a point.

Definition 2.1.17 (Partial derivative at p)
The *partial derivative* at $p \in U$ of a smooth function f on X is defined by

$$\left.\frac{\partial}{\partial_\phi x}\right|_p : \mathcal{C}^\infty(U) \to \mathbb{R}, \quad f \mapsto \left(\frac{\partial}{\partial_\phi x} f \right)(p).$$

Analogously for $\left.\frac{\partial}{\partial_\phi y}\right|_p$.

After defining derivatives, our next goal is to define 1–forms. For that, we define the tangent and cotangent space.

Definition 2.1.18 (Tangent space at p)
The *tangent space* $T_p(U)$ at $p \in U$ is defined by

$$T_p(U) \coloneqq \left\{ f(p) \cdot \left.\frac{\partial}{\partial_\phi x}\right|_p + g(p) \cdot \left.\frac{\partial}{\partial_\phi y}\right|_p \;\middle|\; f, g \in \mathcal{C}^\infty(U) \right\}.$$

Definition 2.1.19 (Cotangent space at p)
The *cotangent space* $T_p^*(U)$ at $p \in U$ is defined by

$$T_p^*(U) \coloneqq \{t \colon T_p(U) \to \mathbb{R} \mid t \text{ linear}\} = \{f(p) \cdot \mathrm{d}_\phi x + g(p) \cdot \mathrm{d}_\phi y \mid f, g \in \mathcal{C}^\infty(U)\},$$

where $\mathrm{d}_\phi x \coloneqq \left(\left.\frac{\partial}{\partial_\phi x}\right|_p \right)^*$ and $\mathrm{d}_\phi y \coloneqq \left(\left.\frac{\partial}{\partial_\phi y}\right|_p \right)^*$ are the dual basis elements to the basis elements $\left.\frac{\partial}{\partial_\phi x}\right|_p$ and $\left.\frac{\partial}{\partial_\phi y}\right|_p$ of $T_p(U)$.

With these objects, we can finally define 1–forms:

Definition 2.1.20 (Space of 1–forms)
For an open set $U \subseteq X$, we define the *space of differential forms* or the *space of* 1*–forms* on U by

$$\begin{aligned} \Omega'_X(U) = \Bigg\{ \omega \colon U \to \bigsqcup_{p \in U} T_p^*(U) \;\Bigg|\; & \text{for all } p \in U \colon \omega(p) \in T_p^*(U), \\ & \text{there exists a chart } (U_p, \phi_p) \text{ with } p \in U_p \subseteq U \\ & \text{and } f, g \in \mathcal{C}^\infty(U_p) \text{ such that } \omega = f \cdot \mathrm{d}_{\phi_p} x + g \cdot \mathrm{d}_{\phi_p} y \text{ on } U_p \Bigg\}. \end{aligned}$$

We can extend these definitions to complex numbers. The complex tangent space is then $T_p(U) \otimes_{\mathbb{R}} \mathbb{C}$ and the complex cotangent space is $T_p^\star(U) \otimes_{\mathbb{R}} \mathbb{C}$.

For a chart (U, z) of X with $z = x + \mathrm{i} \cdot y$, we can define the differential forms

$$\begin{aligned} \mathrm{d}z &:= \frac{1}{2}(\mathrm{d}_z x \otimes_{\mathbb{R}} 1 + \mathrm{i} \cdot \mathrm{d}_z y \otimes_{\mathbb{R}} 1), \\ \mathrm{d}\bar{z} &:= \frac{1}{2}(\mathrm{d}_z x \otimes_{\mathbb{R}} 1 - \mathrm{i} \cdot \mathrm{d}_z y \otimes_{\mathbb{R}} 1). \end{aligned}$$

Then, like $\mathrm{d}_z x \otimes_{\mathbb{R}} 1$ and $\mathrm{d}_z y \otimes_{\mathbb{R}} 1$, $\mathrm{d}z$ and $\mathrm{d}\bar{z}$ form a complex basis for the cotangent space $T_p^*(U) \otimes_{\mathbb{R}} \mathbb{C}$.

Actually, we want even more than 1–forms, we want them to be holomorphic.

Definition 2.1.21 (Holomorphic 1–form)
If a differential form $\omega \in \Omega'_X(U)$ can be locally expressed as $\omega = f \cdot \mathrm{d}z$ with $f \in \mathcal{O}(U')$ for suitable U', then ω is called a *holomorphic* 1*–form* on U.

We denote the corresponding *space of holomorphic* 1*–forms* on U by $\Omega_X(U)$, and for the space of holomorphic 1-forms on X, we use the abbreviation $\Omega(X) := \Omega_X(X)$.

Again, we inherited the order of a holomorphic 1–form from the order of $f \in \mathcal{O}(U')$.

Definition 2.1.22 (Order of a holomorphic 1–form)
Let X be a Riemann surface, $\omega = f \cdot \mathrm{d}z$ a holomorphic 1–form on X, and $p \in X$. Then, the *order* of ω at p is defined and denoted by

$$\mathrm{ord}_p(\omega) := \mathrm{ord}_p(f).$$

Let us look at an interesting example for the Alexandroff or one-point compactification of $\mathbb{C}$:

Example 2.1.23 (Riemann sphere)
Consider the *Riemann sphere* $X = \hat{\mathbb{C}} := \mathbb{C} \sqcup \{\infty\}$. On $\mathbb{C}$, z is a holomorphic function and $\mathrm{d}z$ is a holomorphic differential. In a neighborhood of ∞, $(\hat{\mathbb{C}} \setminus \{0\}, \frac{1}{z})$ is an admissible chart. Thus, we can express $\mathrm{d}z$ as a multiple of $\mathrm{d}(\frac{1}{z})$. It holds, that

$$\frac{\mathrm{d}(\frac{1}{z})}{\mathrm{d}z} = -\frac{1}{z^2},$$

so $\mathrm{d}z = -z^2\,\mathrm{d}(\frac{1}{z})$. Therefore, $\mathrm{d}z$ has a pole of order two at ∞.

Let us finally give the last definition for finite transaction surfaces we want to introduce.

Definition 2.1.24 (Finite translation surface III)
Let X be a compact connected Riemann surface and $\omega \in \Omega(X)$, $\omega \neq 0$ a holomorphic 1–form. Let Z be the set of zeros of ω and $X^* := X \setminus Z$. Then, X^* and ω define a *finite translation surface* (X^*, ω).

As before, our goal is to show that the new Definition 2.1.24 is equivalent to the previous Definitions 2.1.1 and 2.1.4.

Lemma 2.1.25 (Equivalence of I, II & III)
The objects described in Definitions 2.1.1, 2.1.4 and 2.1.24 are the same.

Proof. In Lemma 2.1.10, we already showed that the first two definitions are equivalent. We prove the remaining statement by showing (a) "II $\Rightarrow$ III" and (b) "III $\Rightarrow$ I" separately.

(a) Let $(X, \mathcal{G})$ be a finite translation surface as in Definition 2.1.4. The metric completion $\overline{X}$ is a compact connected Riemann surface because of Lemma 2.1.10.

There exists a differential form $\mathrm{d}z$, given by the variable z in the plane as well as inside the polygons $P_1, \ldots P_n$. This can be extended to a holomorphic differential form $\omega \in \Omega(X)$ on the Riemann surface defined by X. This is possible because $\mathrm{d}z$ is invariant under translations and therefore compatible with the edge gluings.

We now need to extend the holomorphic 1–form ω from X to $\overline{X}$.

For each vertex σ with an angle of $2\pi k_\sigma$, we have a neighborhood U_σ and a map $\omega = \omega_\sigma$, which, outside of σ, is given by

$$z = \omega^{k_\sigma}, \quad \mathrm{d}z = k_\sigma \omega^{k_\sigma - 1}\,\mathrm{d}\omega.$$

For each vertex σ of $\overline{X}$, $\mathrm{ord}_\sigma(\mathrm{d}z) = \mathrm{ord}_\sigma(\omega^{k_\sigma - 1}) = k_\sigma - 1$.

In this way, ω can be extended to a holomorphic 1–form $\overline{\omega}$ on $\overline{X}$.

If $\overline{\omega}$ has no zeros in the points of $\overline{X} \setminus X$ in which case $k_\sigma = 1$, we consider these points as removable singularities of $(X, \overline{\omega})$ and then obtain a finite translation surface according to Definition 2.1.24.

(b) Let (X^*, ω) be a finite translation surface as in Definition 2.1.24, where $X = X^* \cup Z$ is a compact Riemann surface. We now define new translation charts:

Since X is compact, ω has only finitely many zeros $\omega_1, \ldots, \omega_n$. On a chart (U, z) with $\omega = f\,\mathrm{d}z$ for U, the zeros of ω are the zeros of f, that is to say

$$Z = \{\omega_1, \ldots, \omega_n\}.$$

This is a discrete set according to the identity theorem for holomorphic functions.

Now, cover $X^* = X \setminus Z$ with simply connected open sets U_i. Choose $P_i \in U_i$ and define

$$\phi_i : U_i \to \mathbb{C}, \quad P \mapsto \int_{P_i}^{P} \omega = \int_{\gamma_i} f(\gamma_i(t))\gamma_i'(t)\,\mathrm{d}t.$$

Here, γ_i is a path in U_i from P_i to P. Since U_i is simply connected, $\phi_i(P)$ does not depend on γ_i. If $P \in U_i \cap U_j$, then

$$\phi_i(P) - \phi_j(P) = \int_{\gamma_{i,j}} \omega$$

for a fixed chosen path $\gamma_{i,j}$ from P_i to P_j. Hence, the functions ϕ_i and ϕ_j differ only by a translation. Completing these charts to a maximal atlas, we obtain a translation structure $\mathcal{T}$ on X^*. Thus $(X^*, \mathcal{T})$ is a finite translation surface according to Definition 2.1.1. $\square$

In the proof of Lemma 2.1.25, we saw that the singularities coincide with the zeroes of the 1–form. This explains the etymology of singularities.

All these definitions are made up by a tuple containing a surface X and some extra structure. The classification of the compactification $\overline{X}$ will be part of the next section. To bring order into the second entry of the tuple, let us use the following convention:

Convention 2.1.26 (Abuse of notation for ω)
For finite translation surfaces, the notation (X, ω) has become the most common notation. In this thesis, a certain abuse of notation is employed, speaking interchangeably about the translation structure ω, the atlas of gluing structure ω, and the holomorphic 1–form ω. The precise meaning will be clear from the context and according to Lemma 2.1.25, these can be transformed into each other anyway.

2.2 Compact surfaces

After defining translation surfaces, the question arises of how to distinguish and classify them. There has been a topological classification for two-dimensional manifolds since 1923 [Ker23]. Singularities will prove to be a crucial classification tool for the translation structure especially on finite translation surfaces, where a stratification, which will see in Section 3.5, is possible. In this chapter, we lay the groundwork necessary for this classification.

Let us start this section by reducing different notions of curves to a common denominator.

Definition 2.2.1 (Vocabulary for curves & paths)
Let X be a topological space.

- A *curve* in X is a continuous map $c : I \to X$ for some interval $I \subseteq \mathbb{R}$.
- A *path* in X is a curve in X, whose domain is closed.
- A *closed curve* c in X is a continuous map $p \colon S^1 \to X$.
- A *simple curve* c is an injective curve.
- A closed curve c in X is called *nontrivial* if it is not homotopic to a constant curve.
- A simple closed curve $c \colon S^1 \to X$ in a connected space X is called *separating* if $X \setminus c(I)$ is not connected.
- A simple closed curve $c \colon S^1 \to X$ in X is called *essential* if it is not homotopic to a point, a puncture, or a boundary component.

After fixing these basic concepts, let us continue with topological notions.

Definition 2.2.2 (Genus)
Let X be a connected topological space. The *genus* of X is the maximum number of nontrivial, disjoint, simple closed curves in X, such that X remains connected when removing the images of these paths.

Convention 2.2.3 (Genus)
Let X be a topological space. We write $g(X)$ for the genus of X.

The first topologically shape that comes to mind is the sphere.

Example 2.2.4 (Genus of the sphere)
A *2–sphere* $\{x \in \mathbb{R}^3 \mid \|x\| = 1\}$ which is homeomorphic to the Riemann sphere has genus 0 since there are no nontrivial, simple, and non-separating curves in the 2-sphere.

However, this surface cannot be the underlying compact space of a translation surfaces as we will see later. The first compact surface of interest for translation surfaces is as we have already seen the torus.

Example 2.2.5 (Genus of the torus)
A torus has genus 1 because, for every nontrivial, simple, closed, and non-separating curve, the torus without the image of this curve is homeomorphic to an open annulus in $\mathbb{R}^2$ and in this annulus, there are no nontrivial, simple, closed, and non-separating curves.

See Figure 2.5 for illustrations of several small-genus examples. Cell complexes provide an aid to calculate the genus of a topological space, these cell complexes are closed manifolds with an additional rigid structure.

Definition 2.2.6 (Closed manifold)
A *closed manifold* is a compact manifold with empty boundary.

Definition 2.2.7 (Cell complexes & more)
Let X be a closed n–dimensional manifold.

- A *k–cell* in X is a closed subset C of X that is homeomorphic to the unit ball
$$B_1^k(0) := \Big\{x \in \mathbb{R}^k \colon \ \|x\| \leq 1\Big\}.$$
Here, $k = \dim(C)$ denotes the *dimension* of the cell.
- If $C \subseteq X$ is a k–cell and $f \colon B_1^k(0) \to C$ the corresponding homeomorphism, then $f\left(\operatorname{int}\left(B_1^k(0)\right)\right)$ is called the *relative interior* of C.
- A *cellular decomposition* of X consists of cells $\{C_i\}_{i\in I}$ such that
  (a) the manifold X is the union of the cells: $X = \bigcup_{i\in I} C_i$,
  (b) the relative interiors of any two cells are disjoint,

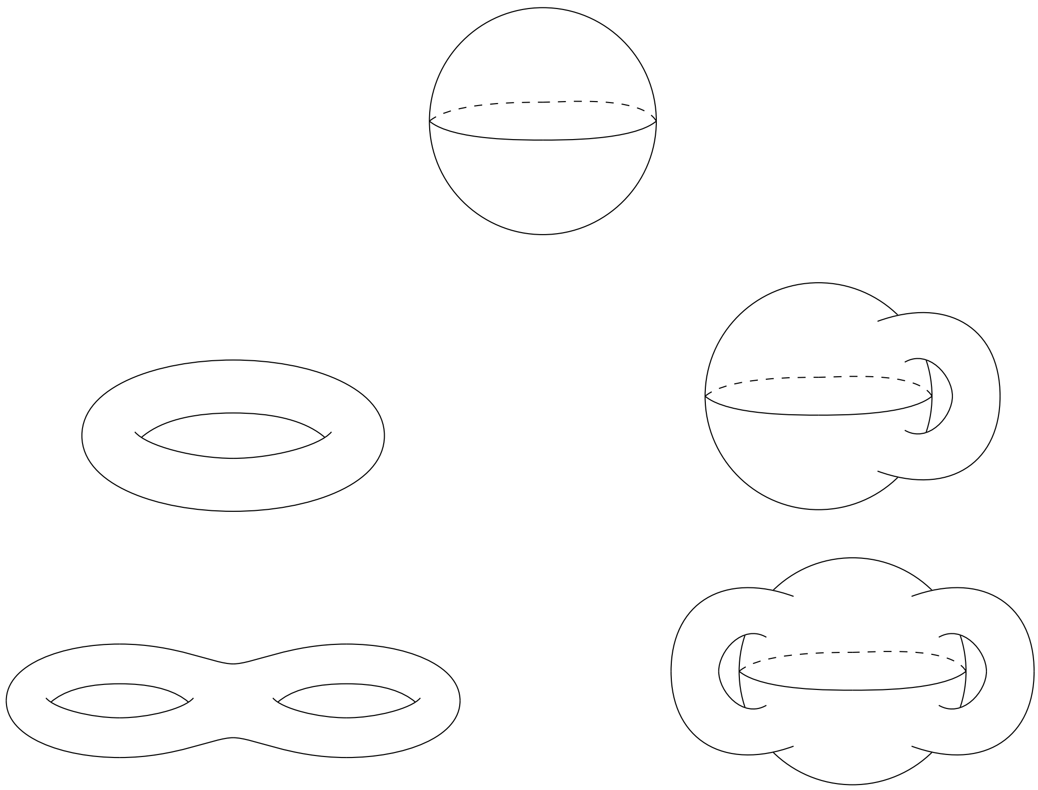

Figure 2.5: Examples of small genus surfaces with hole constructions (left) and handle constructions (right) for genus $0, 1, 2$ (corresponding to each row)

(c) the intersection of any two k–cells is the union of finitely many cells of dimension at most $k-1$.

- A cellular decomposition is *finite* if it consists of finitely many cells.
- A *cell complex* is a pair $(X, \mathcal{D})$ where $\mathcal{D}$ is a cellular decomposition of X.

These cell complexes already describe compact manifolds topologically.

Lemma 2.2.8 (Cellular decomposition for compact manifolds)
A compact manifold is homotopically equivalent to a cell complex.

Proof. This is Corollary A.12 in the Appendix of [Hat02]. □

In particular, all finite translation surfaces can be metrically completed, becoming closed and therefore compact manifolds and admit henceforth a cellular decomposition. Another topological invariant which is also closely related to the genus is the Euler characteristics.

Definition 2.2.9 (Euler characteristic)
Let X be a closed surface with a finite cellular decomposition $\{C_i\}_{i=1}^n$. Then we denote

the *Euler characteristic* of X by

$$\chi(X) = \sum_{i=1}^{n} (-1)^{\dim(C_i)}.$$

Remark 2.2.10 (Well-definedness of the Euler characteristic)
Let X be a compact surface, it therefore admits a cellular decomposition $\{C_i\}_{i=1}^n$. If X has another finite cellular decomposition $\left\{\tilde{C}_j\right\}_{j\in J}$, then for $\{C_i\}_{i\in I}$ and $\left\{\tilde{C}_j\right\}_{j\in J}$, we can find a common refinement. To demonstrate the well-definedness, one can show that each refinement step of a cellular decomposition of X does not change the Euler characteristic of X. This is also shown more generally in Theorem 2.44 of [Hat02].

Since the Euler characteristic is topologically invariant it can be a useful tool to classify compact spaces.

Remark 2.2.11 (Euler–Poincaré formula)
Let X be a closed surface with a triangulation $\triangle$. We can perceive $\triangle$ as cellular decomposition $\{C_i\}_{i=1}^n$. Then we have $V_\triangle$ cells of dimension 0 corresponding to vertices, $E_\triangle$ cells of dimension 1 corresponding to edges and $F_\triangle$ cells of dimension 2 corresponding to faces. In this case, the Euler characteristic of X can be expressed by the *Euler–Poincaré formula*

$$\chi(X) = V_\triangle - E_\triangle + F_\triangle.$$

When we set our goal to classify compact spaces, we set our goal too high. What we actually only need to classify are orientable compact spaces.

Definition 2.2.12 (Orientable surface)
Let X be a surface. Then X is called *orientable* if there exists an atlas in which the Jacobian determinants of the transition maps between charts are all positive. This means that, as one moves from one chart to another, the orientation of the local coordinate system does not change signature.

Remark 2.2.13 (On orientable)
An orientable surface is a type of surface for which it is possible to consistently assign a direction or orientation to the tangent plane at each point.

Translation surfaces are always orientable and the orientation is already determined by specifying the translation structure.

We want to classify compact orientable surfaces, as they constitute the underlying topological space for our translation surfaces. For that, we define some form of normalized way to represent surfaces.

Definition 2.2.14 (Normal form and symbol)
Consider a regular polygon with $4g$ sides. We can read off the gluing instructions of the sides anticlockwise along the boundary, obtaining a string called the *symbol*. For orientation, we fix a direction compatible for both glued edges and denote reversed sides

with inverse elements. We call the regular polygon with $4g$ sides the *fundamental polygon* of genus g, if we have the symbol

$$a_1 b_1 a_1^{-1} b_1^{-1} \dots a_g b_g a_g^{-1} b_g^{-1}$$

for the edge gluings, which can be seen in Figure 2.6.

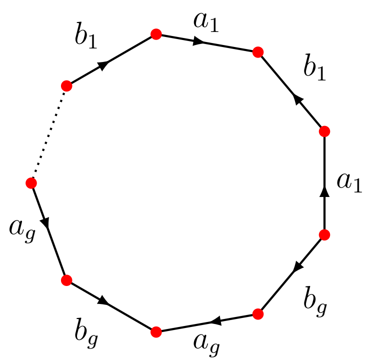

Figure 2.6: Fundamental polygon of S_g

Lemma 2.2.15 (Normal form of the g–holed torus)
The *g–holed torus* $S_g = \underbrace{T^2 \# \dots \# T^2}_{g}$ is homeomorphic to the fundamental polygon of g for $g \geq 1$.

Proof. We show this by induction. It is true for the base case, since $S_1 = T^2 \cong \mathbb{T}_\mathrm{i}$, which is a surface obtained with the symbol $a_1 b_1 a_1^{-1} b_1^{-1}$ by Example 2.0.15.

Since $S_{g+1} = S_g \# T^2$, we can take for S_g and T^2 each a fundamental polygon with a disk removed. The boundary of this disk is a closed path labeled d, we chose such that it intersect the corner in between a_1 and b_g^{-1} for the fundamental polygon of S_g and the corner in between a_{g+1} and b_{g+1}^{-1} for the fundamental polygon of T^2 with symbol $b_{g+1} a_{g+1}^{-1} b_{g+1}^{-1} a_{g+1}$. We form the connected sum, by gluing the two objects together along d as seen in Figure 2.7.

This produces again a fundamental polygon with symbol

$$a_1 b_1 a_1^{-1} b_1^{-1} \dots a_{g+1} b_{g+1} a_{g+1}^{-1} b_{g+1}^{-1}. \qquad \square$$

With this construction of the fundamental polygon in mind, we can show the classification of compact orientable surfaces. A rigorous proof was first provided by Dehn and Heegaard in [DH07], relying the triangulability of the surfaces. Combining this with Radó's result from [Rad25], which establishes that all surfaces are triangulable, we obtain a classification of compact orientable surfaces. For further details on the history of this classification, see Appendix D in [GX13].

Theorem 2.2.16 (Classification of compact orientable surfaces — Kerékjártó)
Two connected, closed, and orientable surfaces are homeomorphic to each other if and only if they have the same genus.

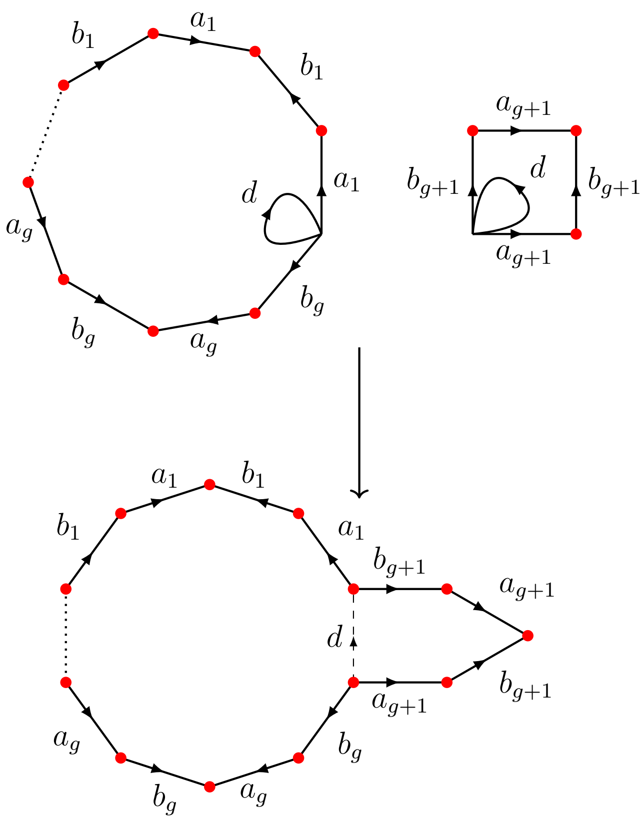

Figure 2.7: Gluing together the fundamental polygon of S_{g+1}

Proof. We show the statement by showing that $X \cong S_g$ for some $g \in \mathbb{N}_0$. Let X be a connected, closed, and orientable surface. First, for all connected, closed, and orientable surfaces, we can construct a cellular decomposition of X. This cellular decomposition can be further subdivided into a triangulation $\triangle$ of X with $V_\triangle$ vertices, $E_\triangle$ edges and $F_\triangle$ faces. Choose a maximal tree T in the graph obtained from the triangulation $\triangle$ with $V_T = V_\triangle$ vertices and $E_T \leq E_\triangle$ edges.

Let $\tilde{T}$ be the dual graph of T with $V_{\tilde{T}} = F_\triangle$ vertices and $E_{\tilde{T}} = E_\triangle - E_T$ edges, where vertices correspond to the triangles and two vertices are connected if the corresponding triangles share a common side which is not in T. Embed $\tilde{T}$ in X accordingly. The graph $\tilde{T}$ is connected, since T contains every vertex of $\triangle$ and does not disconnect X. We know that

$$\chi(X) = V_\triangle - E_\triangle + F_\triangle = V_T - E_T + V_{\tilde{T}} - E_{\tilde{T}} = \chi(T) + \chi(\tilde{T}).$$

The graph T is a tree with $V_T = E_T + 1$, so

$$\chi(X) = 1 + \chi(\tilde{T}) \leq 2,$$

since $V_{\tilde{T}} \leq E_{\tilde{T}} + 1$.

We prove the theorem by induction over $\chi(X)$.

The base case $\chi(X) = 2$ holds if and only if $\tilde{T}$ is a tree, this however implies the existence of two disjoint closed regular neighborhoods U and $\tilde{U}$ of T and $\tilde{T}$. Increasing these neighborhoods until they touch in a circle, shows that X is homeomorphic to two disks glued by its boundary, which is homeomorphic to the 2–sphere S_0.

For $\chi(X) < 2$, we know that $V_{\tilde{T}} < E_{\tilde{T}} + 1$, so $\tilde{T}$ is not a tree. Therefore, there exists a cycle $C \subseteq \tilde{T} \subsetneq X$, which does not separate X:

Let $x, y \in X \setminus C$, then there exists a path p starting in x going to a vertex x' of T in $X \setminus \tilde{T}$ and a path q starting in y going to a vertex y' of T in $X \setminus \tilde{T}$. Let t be the path connecting x' to y' in T. Then the path $p + t + q$ connects x to y in $X \setminus C$

Since X is orientable, C has two distinct sides, so cutting X along C yields a connected surface with two boundary components. Removing the boundary yields a surface X' with $\chi(X') = \chi(X) + 2$. By our induction hypothesis $X' \cong S_{g-1}$ for some $g \geq 1$, so

$$X = X' \# T^2 \cong S_{g-1} \# T^2 = S_g.$$

Finally, we need to show that $S_g \ncong S_{g'}$ for $g \neq g'$. We can triangulate the fundamental polygon of genus g into $4g - 2$ triangles (or faces) with $4g - 3$ inner edges and $2g$ outer edges after the identification of the outer edges. Following this identification, we have only one vertex, resulting in an Euler characteristic of

$$\chi(S_g) = 1 - (4g - 3) - 2g + (4g - 2) = 2 - 2g.$$

Since the Euler characteristic is a topological invariant, it follows that $S_g \ncong S_{g'}$ for $g \neq g'$. □

We already mentioned that the Euler characteristic and the genus of a surface are closely related. Using the classification, we can indeed show that:

Corollary 2.2.17 (Genus and Euler characteristic)
For a connected, closed, and orientable surface X, the Euler characteristic is given by

$$\chi(X) = 2 - 2g(X).$$

Proof. In the proof of Theorem 2.2.16, the fundamental polygon for a surface of genus g is a $4g$–gon, that is a single 2–cell, where every edge is identified with exactly one other edge, so there are $\frac{4g}{2} = 2g$ 1–cells and all vertices are identified with each other, so one 0–cell and

$$\chi(X) = \sum_{i=1}^{2g+2} (-1)^{\dim(C_i)} = 1 - 2g + 1 = 2 - 2g.$$ □

Remark 2.2.18 (Genus trick)
In the case where X is a connected orientable surface, the genus corresponds to the number of "holes" or the number of "handles" described on this surface, see also Figure 2.5. This allows the trick to quickly determine the genus by counting the "holes" or "handles" of a connected orientable surface.

Certainly, one must be careful here. Particularly, there is sometimes the notion of k–dimensional “holes”, corresponding to the dimension of the k–th homotopy group. In this case, a connected, orientable surface of genus g has precisely one zero-dimensional “hole”, corresponding to the number of connected components, $2g$ one-dimensional “holes”, representing the g “handles”, and one two-dimensional “hole”, encoding the separation of the interior and exterior due to orientability.

After seeing the connection between genus and Euler characteristic for oriented compact surfaces, there is even a deeper connection to all of that given by the singularities we want to uncover. However, this will be part of Section 3.1. Until then, we want to extend our examples of finite translation surfaces by an especially important class of translation surfaces, namely square-tiled surfaces. These surfaces play a crucial role in calculating the volumes of spaces of translation surfaces as we will see in Chapter 7.

2.3 Square-tiled surfaces

A special and useful subset of finite translation surfaces will be explored in this section. A lot of interesting continuous geometric properties on translation surfaces can be understood by square-tiled surfaces since these surfaces lie dense in the moduli space of translation surface, which we will see later.

Definition 2.3.1 (Square-tiled surfaces)
We call a finite translation surface (X, ω) a *square-tiled surface* or *origami*, if it is constructed like in Definition 2.1.4 from $d \in \mathbb{N}$ unit squares with edges in horizontal and vertical directions.

Example 2.3.2 (Flat torus)
Our flat torus family $\mathbb{T}_\tau$ contains for $\tau = i$ the smallest square-tiled surface according to the count of unit squares.

The reason this class of translation surfaces is so important will be partially explained in Chapter 7. The main idea is that the set of square-tiled surfaces is dense in the moduli space of translation surfaces. So, we can understand statements that depend continuously on translation surfaces just by understanding them on this dense subset. Furthermore, square-tiled surfaces are even more rigid than finite translation surfaces, so we can derive a lot of nice formulas for them and understand them as a key toy case.

Example 2.3.3 (L-shape as a square-tiled surface)
Consider three unit squares glued together as illustrated in Figure 2.8. This forms a square-tiled surface $L_{2,2}$ as a 3–fold covering of the punctured torus, that we call the *L-shape origami* with a single singularity σ having a total angle of 6π around the singularity. Thus, it is a compact surface of genus 2 with a differential form having a zero of order $k_\sigma = 3$.

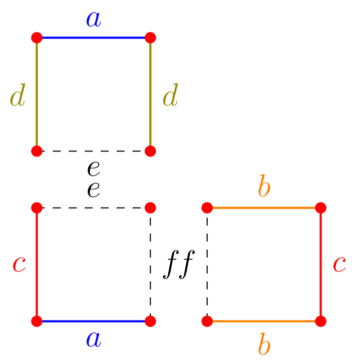

Figure 2.8: L-shape origami

Convention 2.3.4 (Gluing)
When illustrating translation surfaces, the images can quickly become confusing due to the many specified gluings. Therefore, we introduce the following *gluing convention*:

1. Polygons directly attached to each other are automatically glued for this side, which does not need to be labeled.

2. If an edge allows only one gluing with another edge that is admissible according to Definition 2.1.4, these edges are glued and do not need to be labeled.

3. If an edge has an admissible partner edge on the opposite side, for example the side labeled a, b, c and d in Figure 2.8, these edges are glued and do not need to be labeled.

Example 2.3.5 (Gluing convention)
This gluing convention simplifies the illustrations of the double pentagon from Figure 2.3 and the L-shape from Figure 2.8 as seen in Figure 2.9.

(a) Double pentagon (b) L-shape origami

Figure 2.9: Convention 2.3.4 applied to the double pentagon and L-shape origami

Another way to characterize square-tiled surfaces is given as follows.

Remark 2.3.6 (Pairs of permutations)
Let (X, ω) be a finite square-tiled surface consisting of $d \in \mathbb{N}$ unit squares. We can

identify each square with an element from an index set I, for example, $I = \{1, \dots, d\}$. The gluing instructions in the horizontal direction $R\colon I \to I$ to the right then correspond to an element of the symmetric group on I, that is to say, $R \in \mathrm{Sym}(I)$. Since this works analogously for the gluing $U \in \mathrm{Sym}(I)$ in the vertical direction upward, we can characterize a square-tiled surface with $(R, U) \in \mathrm{Sym}(I) \times \mathrm{Sym}(I)$ with $|I| = d$.

These permutations allow us to fix square-tiled surfaces with very few data. This is in particular useful for computers. Instead of fixing a complicated space with a 1–form or polygons, two permutations already uniquely describe our surface.

Example 2.3.7 (L-shape permutations)
By labeling the lower left square 1, the lower right square 2 and the upper left square 3 in our L-shape origami $L_{2,2}$, we get the element

$$(R, U) = ((1\ 2)(3), (1\ 3)(2)) \in \mathrm{Sym}(I) \times \mathrm{Sym}(I)$$

for $I = \{1, 2, 3\}$.

A community favorite square-tiled surface is the Eierlegende Wollmilchsau.

Example 2.3.8 (Eierlegende Wollmilchsau)
Let us take the units of the quaternions $Q_8 := \{1, -1, \mathrm{i}, -\mathrm{i}, \mathrm{j}, -\mathrm{j}, \mathrm{k}, -\mathrm{k}\}$, also called the *quaternion group*, and the gluings $R, U \in \mathrm{Sym}(Q_8)$ defined by:

$$\begin{aligned} R\colon Q_8 &\to Q_8, \quad q \mapsto q \cdot \mathrm{i}, \\ U\colon Q_8 &\to Q_8, \quad q \mapsto q \cdot \mathrm{j}. \end{aligned}$$

The corresponding square-tiled surface obtained by (R, U), see Figure 2.10, is called the *Eierlegende Wollmilchsau*.

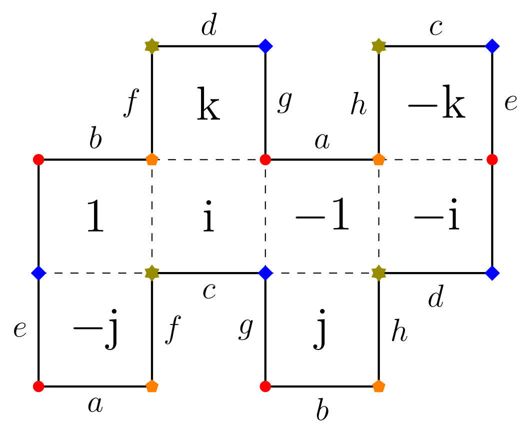

Figure 2.10: Eierlegende Wollmilchsau

Remark 2.3.9 (Etymology of Eierlegende Wollmilchsau)
The German term *Eierlegende Wollmilchsau* is an informal expression used to describe something that seemingly satisfies all needs but is unreal. The idiom illustrates this ideal concept through an imaginary utility animal that, as a hybrid creature, combines the benefits of various animal species, namely a chicken (laying eggs, German: "eierlegend"), sheep (providing wool, German: "Wolle"), cow (giving milk, German: "Milch"), and female pig (German: "Sau", providing meat).

The *Eierlegende Wollmilchsau* is a translation surface that serves as a positive example for many interesting properties of translation surfaces, since it is a very homogeneous translation surface combining various features within itself, as can be seen in Example 3.3.10. That is why it carries this name.

2.4 Infinite translation surfaces

After exploring finite translation surfaces, the question arises whether these are a true special case of translation surfaces or if almost all translation surfaces are finite. We also do not yet know precisely what must be finite in the case of finite translation surfaces. While the area must at least be finite, since the metric completion is compact, this alone is not sufficient. An example of a non-finite translation surface with finite area is the baker's map surface, but first, let us revisit our first example of a translation surface:

Example 2.4.1 (Infinite translation surfaces)
The Euclidean plane from Example 2.0.12 is not a finite translation surface, since $\mathbb{R}^2$ is not compact.

Remark 2.4.2 (Finiteness)
The difference between finite and infinite translation surfaces in Definition 2.0.1 lies in the compactness of the metric completion of the manifold as well as the finiteness of the set Σ, which corresponds to $\overline{X} \setminus X$.

Let us now define the most important example of an infinite translation surface for this thesis.

Definition 2.4.3 (Baker's map surfaces)
Let $\alpha \in (0, 1)$. We define the translation surface B_α, known as *the baker's map surface* with parameter α. These surfaces are also known as *Chamanara surfaces* and they are defined the following way:

Consider a square $abcd$ with side length $\frac{\alpha}{1-\alpha}$. This length is chosen because of the following calculations.

For each $i \in \mathbb{N}^+$ define $a_i \in ab$, $b_i \in bc$, $c_i \in cd$ and $d_i \in ad$, such that

$$d\left(a_i, b\right) = \frac{\alpha^{i+1}}{1-\alpha} = d\left(b_i, b\right), \quad d\left(c_i, d\right) = \frac{\alpha^{i+1}}{1-\alpha} = d\left(d_i, d\right).$$

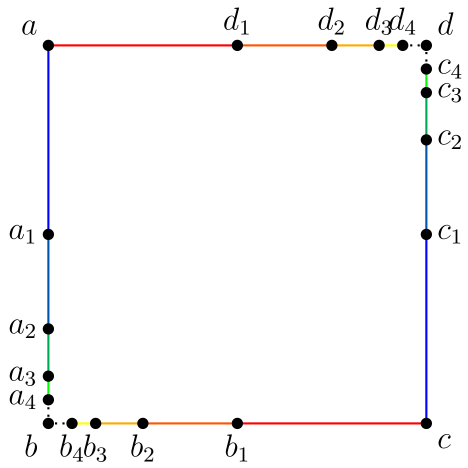

Figure 2.11: The baker's map surface construction with $\alpha = \frac{1}{2}$

With $a_0 = d_0 = a$ and $b_0 = c_0 = c$, we get a partition of each side into the segments

$$\{[a_i, a_{i+1}] \mid i \in \mathbb{N}_0\}.$$

Analogously for $[b_i, b_{i+1}]$, $[c_i, c_{i+1}]$ and $[d_i, d_{i+1}]$ each with length α^{i+1}, so that the sum of segment lengths for each edge adds up to the total edge length of our original square in Figure 2.11

$$\sum_{i=0}^{\infty} \alpha^{i+1} = \alpha \sum_{i=0}^{\infty} \alpha^i = \frac{\alpha}{1-\alpha} < \infty.$$

For the translation structure, we now glue the vertical sides $[a_i, a_{i+1}]$ with $[c_i, c_{i+1}]$ and the horizontal sides $[b_i, b_{i+1}]$ with $[d_i, d_{i+1}]$ for each $i \in \mathbb{N}_0$.

Remark 2.4.4 (On baker's map surfaces)
These surfaces are translation surfaces with inherited translation structures as squares outside of the singularities. The areas of baker's map surfaces can be calculated as the areas of the underlying squares, which is

$$\operatorname{area}(B_\alpha) = \left(\frac{\alpha}{1-\alpha}\right)^2 < \infty.$$

For $\alpha = \frac{1}{2}$, we get a translation surface with an area of 1. This special surface is also referred to as the baker's map surface or Chamanara surface if α is omitted.

Even though the area is easily understood to be finite, the reason we still have an infinite translation surface lies in the non-compactness of the metric completion, since the singularities are much more complicated.

Remark 2.4.5 (On the baker's map surface singularities)
In B_α, the singularities are the vertices of the square and the two points on the edge of each such segment. In the unglued square, these points accumulate in the bottom-left

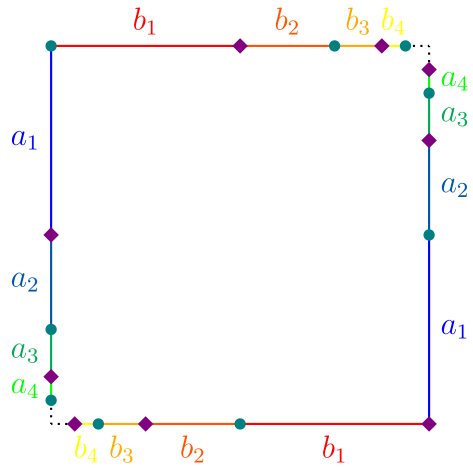

Figure 2.12: Singularities identified on the baker's map surface with $\alpha = \frac{1}{2}$

and top-right corners. By looking at the local neighborhood of these points using the gluings, it becomes clear in Figure 2.12 that every second point (on each of the four sides) is identified with each other.

To show that these are also identified with the accumulation points, one determines in B_α the distance from the top-right corner to one of the two sets of identified points: this is the infimum over the length of all horizontal or vertical geodesics connecting points from this set to the bottom-right corner. Since the length of these geodesics can become arbitrarily small, the distance is 0. This works analogously for the bottom-left corner.

Thus in B_α, all points in the set of all segment end points and the accumulation points in the corners are the same point. Overall, all considered points in B_α are thus identified and there is exactly one singularity σ.

How does this singularity destroy the compactness of the metric completion?

Remark 2.4.6 (The baker's map surface is an infinite translation surface)
Charts compatible with the translation structure can be easily defined around each point on $B_\alpha = (X, \omega)$. However, the metric completion $\overline{X}$ is not a manifold. The singularity σ lies as the only singularity discretely in the metric completion $\overline{X} = X \sqcup \{\sigma\}$. Since there is no neighborhood of σ that is homeomorphic to a subset of $\mathbb{R}^2$, this surface is not a finite translation surface and therefore an example of an infinite translation surface with finite area.

Remark 2.4.7 (Etymology of Chamanara and the baker's map surface)
The baker's map surface B_α was extensively described by Reza Chamanara in [Cha04]. His name is therefore associated with this family of infinite translation surfaces.

The baker's map surface can also be defined using the baker's map. In the theory of dynamical systems, the baker's map emerges as a chaotic transformation from the unit square onto itself. It derives its name from the familiar kneading operation employed by bakers on dough: a process wherein the dough is neatly halved, stacked upon itself, and then compressed.

It is worth noting that this translation surface can also be obtained through a limit construction from finite translation surfaces. This holds true for other examples as well, such as the Arnoux-Yoccoz surfaces described in [Bow13]. Therefore, statements regarding how certain properties of a sequence of finite translation surfaces transfer to the corresponding limit surface are interesting. We will give a construction for a special type of surfaces obtained in this way in Chapter 4.

2.5 Non-compact surfaces

The underlying topological surfaces in the case of infinite translation surfaces are generally non-compact surfaces. Besides the genus, there are many other aspects relevant to their classification, such as the various topologically distinct ways to move to infinity, or how the genus is distributed among them. To achieve a classification nevertheless, we need the concept of the space of ends.

Definition 2.5.1 (Ends, space of ends)
Let X be a topological space.

- An *admissible descending chain* in X is a chain $U_1 \supseteq U_2 \supseteq \ldots$, such that
  (a) every U_i is a connected, open, and unbounded subset of X,
  (b) every ∂U_i is compact and
  (c) for every compact set $C \subseteq X$, only finitely many U_i intersect C.
- Two admissible descending chains $U_1 \supseteq U_2 \supseteq \ldots$ and $V_1 \supseteq V_2 \supseteq \ldots$ are *equivalent* if for every $n \in \mathbb{N}^+$, there exists $N \in \mathbb{N}^+$ such that $U_N \subseteq V_n$ and $V_N \subseteq U_n$.
- The equivalence class of an admissible descending chain is called an *end* of X.
- The *space of ends* of X contains all equivalence classes of admissible descending chains in X and is denoted by $\mathrm{Ends}(X)$.

This definition is a desirable choice since the equivalence relation is well-defined.

Proposition 2.5.2 (Equivalence relation is well-defined)
The relation on the set of admissible descending chains, defined in Definition 2.5.1, is an equivalence relation.

Proof. Let $U_1 \supseteq U_2 \supseteq \ldots$, $V_1 \supseteq V_2 \supseteq \ldots$ and $W_1 \supseteq W_2 \supseteq \ldots$ be admissible descending chains.

- The reflexivity is fulfilled for the choice $N = n$.
- Symmetry follows immediately by the symmetry of the statement

$$\forall n\ \exists N \colon U_N \subseteq V_n \text{ and } V_N \subseteq U_n.$$

- Let $U_1 \supseteq U_2 \supseteq \ldots$ be equivalent to $V_1 \supseteq V_2 \supseteq \ldots$, so for every $n \in \mathbb{N}^+$, there exists an $N_{U,V}(n) \in \mathbb{N}^+$, such that $U_{N_{U,V}(n)} \subseteq V_n$ and $V_{N_{U,V}(n)} \subseteq U_n$.

  Let $V_1 \supseteq V_2 \supseteq \ldots$ and $W_1 \supseteq W_2 \supseteq \ldots$ be equivalent with $N_{V,W}(n) \in \mathbb{N}^+$ for every $n \in \mathbb{N}^+$. Then for

  $$N_{U,W}(n) = \max \{N_{U,V}\left(N_{V,W}(n)\right), N_{V,W}\left(N_{U,V}(n)\right)\},$$

  we get $U_{N_{U,W}(n)} \subseteq V_{N_{V,W}(n)}$, since $N_{U,W}(n) > N_{U,V}\left(N_{V,W}(n)\right)$ and $V_{N_{V,W}(n)} \subseteq W_n$ by choice.

  The reverse inclusion is true analogously and we get transitivity. □

After defining ends, the questions arise, what space can occur as a space of ends? How does these ends look like topologically? To partially answer the first question, consider the following examples.

Example 2.5.3 (Ends of compact spaces, $\mathbb{R}$ and $\mathbb{R}^2$)
Let us look at a few examples and determine their space of ends.

- For any compact topological space X, we have $\mathrm{Ends}(X) = \emptyset$ since there are no admissible descending chains in compact spaces.

- The line $\mathbb{R}$ has two ends, because

  $$U_1 \supseteq U_2 \supseteq \ldots \text{ with } U_i := (i, \infty) \text{ and}$$
  $$V_1 \supseteq V_2 \supseteq \ldots \text{ with } V_i := (-\infty, -i)$$

  are two admissible descending chains that do not define the same end.

  If $W_1 \supseteq W_2 \supseteq \ldots$ is another admissible descending chain, then this chain has only finitely many elements which intersect the compact set $C_n = [-n, n] \subsetneq \mathbb{R}$ for every $n \in \mathbb{N}^+$. In particular, there exists an $N_1(n) \in \mathbb{N}^+$, such that

  $$W_{N_1(n)} \subseteq (n, \infty] = U_n \text{ or } W_{N_1(n)} \subseteq (-\infty, -n] = V_n.$$

  Since W_j must be unbounded for all $j \in \mathbb{N}^+$, it must contain $U_{N_2(n)}$ or $V_{N_2(n)}$ for some $N_2(n) \in \mathbb{N}^+$ and with $N := \max\{N_1(n), N_2(n)\} \in \mathbb{N}^+$, we get equivalence with either $U_1 \supseteq U_2 \supseteq \ldots$ or $V_1 \supseteq V_2 \supseteq \ldots$ and there are exactly two ends

  $$\mathrm{Ends}(\mathbb{R}) = \{[U_1 \supseteq U_2 \supseteq \ldots], [V_1 \supseteq V_2 \supseteq \ldots]\}.$$

- The plane $\mathbb{R}^2$ has one end, because: The admissible descending chain

  $$U_1 \supseteq U_2 \supseteq \ldots \text{ with } U_i := \mathbb{R}^2 \setminus \overline{B}_i(0)$$

  defines one end. Any other admissible descending chain is equivalent to it, since only finitely many chain elements can intersect the compact set $C := \overline{B}_n(0)$, for every $n \in \mathbb{N}^+$ and analogously to the previous example we can construct both inclusions, yielding equivalence to $U_1 \supseteq U_2 \supseteq \ldots$ and $\mathrm{Ends}(\mathbb{R}^2) = \{[U_1 \supseteq U_2 \supseteq \ldots]\}$.

So, how do these ends look like topologically?

Remark 2.5.4 (Punctures are ends)
From a topological perspective, not every end is a puncture. However, every puncture on a surface X is already an end, because for every compact set $C \subseteq X$, there exists $\varepsilon > 0$ such that the ε–neighborhood of the puncture in X is disjoint from C. Thus, an admissible descending chain can be defined with ever smaller ε–neighborhoods of the puncture.

If $\overline{X}$ is a compact surface as in the case for finite translation surfaces, then the punctures on $\overline{X} \setminus X$ are discrete and for any two punctures, there exists a compact set $K \subseteq X$ such that these punctures lie in different connected components of $X \setminus K$. Therefore, the corresponding admissible descending chains also define different ends.

As it turns out, the set of ends and the genus is not enough to fully classify orientable surfaces. The last ingredient we need is the set of planar ends and defining a topology on both of these sets of ends to obtain spaces of ends.

Definition 2.5.5 (Planar end)
An end is *planar* if there exists an admissible descending chain $U_1 \supseteq U_2 \supseteq \ldots$ as a representative, such that U_1 has genus 0. The subset of non-planar ends in $\mathrm{Ends}(X)$ is denoted by $\mathrm{Ends}_\infty(X)$.

We can define a topology on the space of ends and planar ends with the compact-open topology:

Definition 2.5.6 (Compact-open topology on the space of ends)
Let X be a surface, $U \subseteq X$ be open with ∂U compact. Define

$$U^* := \{[U_1 \supseteq U_2 \supseteq \ldots] \mid \exists n > 0 \text{ such that } U_n \subseteq U\}.$$

With the basis $\{U^*\colon U \subseteq X \text{ open}, \partial U \text{ compact}\}$ for the topology on $\mathrm{Ends}(X)$, we get a topological space. Analogously for $\mathrm{Ends}_\infty(X)$ as a subset of $\mathrm{Ends}(X)$.

This finally yields a classification for orientable surfaces.

Theorem 2.5.7 (Classification of orientable surfaces — Kerékjártó)
Two connected and orientable surfaces are homeomorphic if and only if they have the same genus and the pairs consisting of the space of ends and the space of non-planar ends are homeomorphic.

Proof. "⇒": Genus is a topological invariant. The space of ends as well since we use only topologically invariant objects in Definition 2.5.1 for admissible descending chains.

"⇐": The original proof in German dates back to 1923 by Kerékjártó [Ker23]. A modern proof is provided in [Ric63]. □

Remark 2.5.8 (Classification of translation surfaces)
Since for compact surfaces the space of ends is always empty, Theorem 2.2.16 is a special case of Theorem 2.5.7.

Finite translation surfaces can be classified using Theorem 2.2.16 by considering their metric completions. However, since these completions are generally not compact for non-finite translation surfaces, Theorem 2.5.7 must be used for their classification. It is important to note that this alone is not sufficient to capture all useful information about a translation surface. For example, specifying the genus and the ends does not determine which singularities a translation surface can have.

An alternative approach to the question of classification can be found, for example, through the definition of strata introduced in Section 3.5. However, even in this case, this classification is generally very coarse.

Before we continue to the next chapter, let us look at some examples of what such an oriented and non-compact surface can look like, to see some first impressions on the vastness of spaces there exist. Each of them can be modeled by some infinite translation surface.

Example 2.5.9 (Surfaces of infinite type)
This is a classical and by no means exhaustive collection of important examples of surfaces of infinite type.

(a) A surface of genus 0 with one end is homeomorphic to $\mathbb{R}^2$.

(b) A surface of infinite genus with one end (which is necessarily non-planar) is called a *Loch Ness Monster*.

(c) A surface of genus 0 with two ends is homeomorphic to an infinitely long or open cylinder.

(d) A surface of infinite genus with two ends, both of which are non-planar, is called *Jacob's ladder*.

(e) A surface of genus 0 with uncountably many ends as shown in Figure 2.13 is called a *Cantor tree*.

(f) A surface of infinite genus with uncountably many ends, all of which are non-planar, as shown in Figure 2.13 is called a *blooming Cantor tree*.

We already know one of these examples:

Remark 2.5.10 (Classification of the baker's map surface)
The baker's map surface from Definition 2.4.3 is a Loch Ness Monster.

Besides the different underlying Riemann surfaces, there are also more possibilities for what singularities can look like on infinite translation surfaces. We also hinted in Section 2.2 to a connection between the genus and the singularities we want to uncover.

(a) Plane $\mathbb{R}^2$

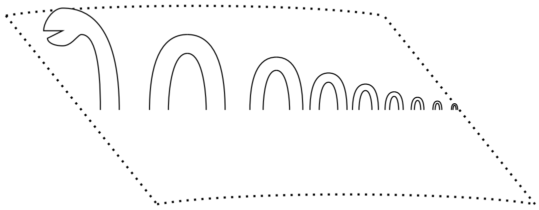

(b) Loch Ness Monster

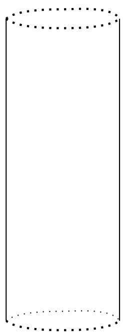

(c) Infinite cylinder

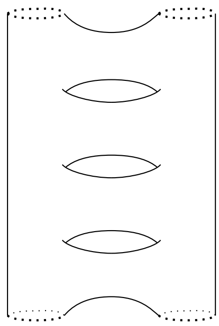

(d) Jacob's Ladder

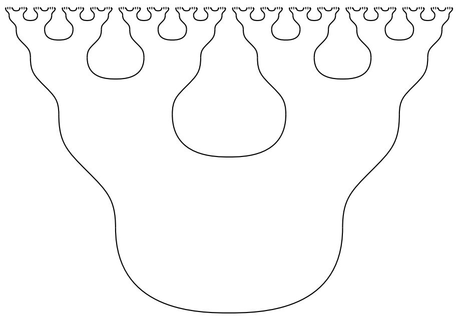

(e) Cantor tree

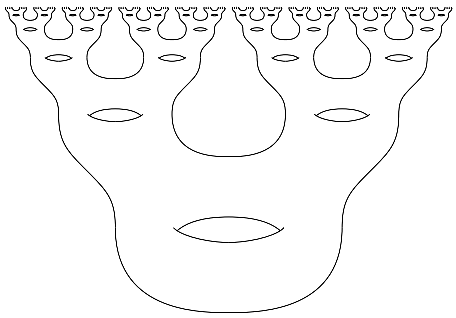

(f) Blooming Cantor tree

Figure 2.13: Examples of surfaces of infinite type

3 Structure on translation surfaces

The goal of this chapter is to introduce useful objects associated to translation surfaces themselves or spaces of translation surfaces. The first section is all about singularities and how to understand them locally as coverings. In the second section, we connect these singularities and thereby obtain saddle connections which can also be broadened to cylinders. Trying to understand the flow of translation surfaces in the moduli space, we will uncover the Veech group as a stabilizer, before also considering dynamics on the translation surfaces themselves again. All of this will help us to understand how to stratify the moduli space in the last section.

3.1 Singularities

As seen in the end of Section 2.4, the types of singularities can vary a lot even when the underlying space of translation surfaces stays the same. Before we can actually try to classify translation surfaces by singularities, we first have to differentiate between the different kind of singularities and classify them. For that, let us talk about coverings in a more general setting.

Definition 3.1.1 (Topological covering)
Let X and Y be topological spaces and $f\colon X \to Y$ be a surjective continuous map. Then, f is called a topological *covering* of Y, if for every $y \in Y$, there exists a neighborhood $U_y \subseteq Y$ such that $\pi^{-1}(U_y)$ consists of the union of pairwise disjoint sets $V_i \subseteq X$:

$$\pi^{-1}(U_y) = \bigsqcup_{i\in I} V_i$$

and $\pi|_{V_i}\colon V_i \to U_y$ is a homeomorphism for every i of some index set I.

The open sets V_i are called *sheets*, which are uniquely determined up to homeomorphism if U_y is connected. For each $y \in Y$, the discrete set $\pi^{-1}(y)$ is called the *fiber* of y.

These coverings appear naturally in our setting for surjective holomorphic maps between compact Riemann surfaces.

Proposition 3.1.2 (Branched coverings)
Let $f\colon X \to Y$ be a surjective holomorphic map between compact Riemann surfaces. Furthermore let

$$\Sigma \coloneqq \Sigma_f \coloneqq \left\{ y \in Y \;\middle|\; \exists x \in f^{-1}(y) \text{ with } \mathrm{ord}_x(f) > 1 \right\}$$

be the *branching locus*.

- The restriction
$$f^*\colon X^* = X \setminus f^{-1}(\Sigma) \to Y^* = Y \setminus \Sigma$$
is a topological covering.

- Let $y \in Y$ and $f^{-1}(y) = \{x_1, \ldots, x_n\}$. Let V_y be an open neighborhood of y, isomorphic to a disk, such that $V_y \setminus \{y\}$ contains no branching points. Then
$$f^{-1}(V_y) = \bigsqcup_{i \in I} U_i$$
is a disjoint union of disks with $x_i \in U_i$ and $f|_{U_i}$ is of the form $z \mapsto z^{\mathrm{ord}_{x_i}(f)}$.

- The number
$$P = \sum_{\substack{x \in X \\ f(x)=y}} \mathrm{ord}_x(f)$$
is independent of the choice of $y \in Y$.

Proof. Let X and Y be compact Riemann surfaces and let $f\colon X \to Y$ be a surjective holomorphic map.

- It is clear that the holomorphic map f^* is a local homeomorphism. Let $y \in Y^*$ be arbitrary and $f^{-1}(y) = \{x_1, \ldots, x_d\}$. Let V and U_i be neighborhoods of y and x_i, respectively, such that $f|_{U_i}\colon U_i \to V$ is a homeomorphism. We need to show that V can be chosen small enough so that $f^{-1}(V)$ is a disjoint union of the U_i. We do this by contradiction. Assume $y_n \in V$ is a sequence converging to y such that $f^{-1}(y_n)$ contains a point $z_n \notin \bigcup_{i \in I} U_i$. Let x be an accumulation point of this sequence. Since f is continuous, $f(x) = y$ and hence $x = x_i$ for some i. However, for n sufficiently large, $z_n \in U_i$, a contradiction.

- Let y and V_y be as stated in this proposition. Decompose $f^{-1}(V_y)$ into disjoint connected subsets U_i. With the notation $V_y^* = V_y \setminus \{y\}$ and $U_i^* = U_i \setminus \{f^{-1}(y)\}$, we have
$$f^{-1}(V_y^*) = \bigcup_{j=1}^{n} U_j^*.$$
Each restriction $f^*\colon U_i^* \to V_y^*$ is itself a covering and thus of the form
$$\mathbb{D}^* \to \mathbb{D}^*, \quad z \mapsto z^{k_i},$$
these are coverings of the *punctured disk* $\mathbb{D}^* := \overline{B}_r(0) \setminus \{0\}$.

  It follows that $U_i^* = U_i \setminus \{x_i\}$ for some $x_i \in f^{-1}(y)$. Riemann's theorem on removable singularities ensures that the isomorphism $U_i^* \cong \mathbb{D}^*$ has an extension $U_i \cong \mathbb{D}$, proving the claim.

- Let y be arbitrary and $f^{-1}(y) = \{x_1, \dots, x_n\}$. With the notation from the previous part, the order of f at the point x_i is precisely k_i. Furthermore, U_i contains exactly k_i of the d preimages of each point $y' \in V_y^*$. In particular,

$$\sum_i k_i = d$$

is independent of the choice of y. □

We can use this to express the genus of one compact Riemann surface with the genus of another compact Riemann surface coming from a covering between them.

Proposition 3.1.3 (Riemann–Hurwitz formula)
Let $f\colon X \to Y$ be a covering map of Y of degree d between two compact Riemann surfaces of genus $g(X)$ and $g(Y)$. Then the *Riemann–Hurwitz formula* holds:

$$2g(X) - 2 = d(2g(Y) - 2) + \sum_{x \in X} (\operatorname{ord}_x(f) - 1)$$

Proof. To compare the Euler characteristics of X and Y, we note that since f is a local homeomorphism outside the branching points $x_1, \dots, x_n$, there exists a triangulation $\mathcal{T} = \bigcup T_j$ on Y, such that the points $f(x_i)$ belong to the set of vertices of $\mathcal{T}$ and $X = \bigcup f^{-1}(T_j)$ generates a triangulation on X. Let V_X, E_X, F_X, and V_Y, E_Y, F_Y be the number of vertices, edges, and faces of the triangulation on X and Y, respectively. Then,

$$2 - 2g(X) = V_X - E_X + F_X, \quad 2 - 2g(Y) = V_Y - E_Y + F_Y.$$

By construction, it is obvious that $E_X = dE_Y$ and $F_X = dF_Y$. For the vertices, we need to understand f. Around a branching point x, f can be written in local coordinates with charts (U, ϕ) of X and (V, ϕ') of Y as

$$(\phi' \circ f \circ \phi^{-1})(z) = \sum_{j=m}^{\infty} a_j z^j = \psi(z)^m,$$

where $\psi(z) := z \sqrt[m]{\sum_{j=0}^{\infty} a_{m+j} z^j}$ is a bijection near the origin. In particular, in a small enough neighborhood of x, the function f takes the value $f(x)$ once and all other values m times. Therefore, each triangle T_j with vertex $f(x)$ is the image of m triangles containing the node x. The formula for the number of nodes is thus

$$V_X = dV_Y - \sum_{x \in X} (\operatorname{ord}_x(f) - 1)$$

and the Riemann–Hurwitz formula follows by simple substitution:

$$\begin{aligned} 2g(X) - 2 &= -V_X + E_X - F_X \\ &= -dV_Y + \sum_{x \in X} (\operatorname{ord}_x(f) - 1) + dE_Y - dF_Y \\ &= d\,(-V_Y + E_Y - F_Y) + \sum_{x \in X} (\operatorname{ord}_x(f) - 1) \\ &= d\,(2g(Y) - 2) + \sum_{x \in X} (\operatorname{ord}_x(f) - 1) \end{aligned}$$ □

Let us return to the case of translation surfaces.

Definition 3.1.4 (Translation covering)
Let (X, ω) and (Y, ζ) be two translation surfaces and $p\colon X \to Y$ be a covering that can be continuously extended to a map $\overline{X} \to \overline{Y}$. Then, p is called a *translation covering* if for every point $x \in X$, there exist charts $(U, \phi) \in \omega$ and $(V, \psi) \in \zeta$ with $x \in U$ and $p(U) \subseteq V$, such that for every $z \in \phi(U) \subseteq \mathbb{R}^2$

$$\left(\psi \circ p \circ \phi^{-1}\right)(z) = z + t$$

holds for some fixed $t \in \mathbb{R}^2$.

One of the most used cases of translation coverings are square-tiled surfaces. They consist of n squares and can therefore be understood as an n–fold branched covering of the square or punctured square. Let us now classify singularities with our newly obtained knowledge on translation coverings.

Definition 3.1.5 (Conical singularity)
A singularity $\sigma \in \Sigma$ of a translation surface (X, ω) is called *conical*, if there exist $k_\sigma \in \mathbb{N}_{\geq 2}$ and a neighborhood U of σ in $\overline{X}$, such that there is a k_σ–fold translation covering from $U \setminus \sigma$ to the punctured disk $\mathbb{D}^* = \overline{B}_\varepsilon(0) \setminus \{0\} \subseteq \mathbb{R}^2$, see Figure 3.1.

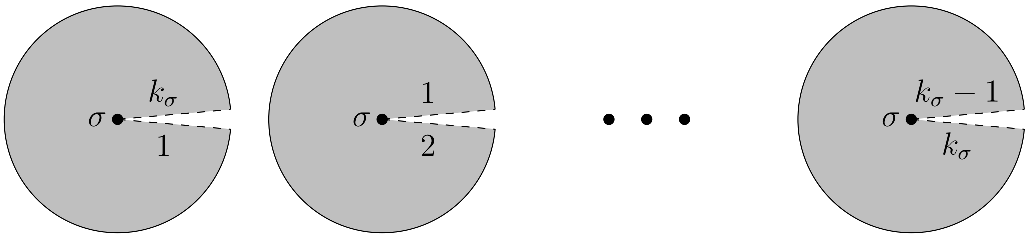

Figure 3.1: Neighborhood of σ by gluing together k_σ disks

A conical singularity is also referred to as a *cone angle singularity*. The number k_σ is called the *multiplicity* of the singularity.

Remark 3.1.6 (On conical singularities)
Let (X, ω) be a translation surface with conical singularity $\sigma \in \Sigma$ of multiplicity k_σ.

- The angle around σ is equal to $2\pi k_\sigma$.
- The neighborhood is homeomorphic to a disk via $z \mapsto z^{k_\sigma}$.
- The differential ω has a zero of order $k_\sigma - 1$ in σ.

Definition 3.1.7 (Essential and removable singularity)
A singularity $\sigma \in \Sigma$ of a translation surface (X, ω) is called *removable*, if there exists a chart (U, ϕ) of $X \cup \{\sigma\}$ with $\sigma \in U$ that is compatible with the translation atlas ω. A removable singularity is also referred to as a *flat point* or *marked point*. Non-removable singularities are referred to as *essential*.

Remark 3.1.8 (On removable singularities)
Let (X, ω) be a translation surface with removable singularity $\sigma \in \Sigma$.

- The rotation angle around σ is equal to 2π.
- If we extend the notion of a zero of a differential ω to a marked point, we find that ω has a zero of order 0 in σ.

These two types of singularities are already all there is for finite translation surfaces.

Proposition 3.1.9 (Finite translation surface singularities are conical or removable)
Every singularity of a finite translation surface is either conical or removable.

Proof. This immediately follows from Definition 2.1.4. For every singularity σ, there exists a neighborhood U, such that there is a k_σ–fold covering with $k_\sigma \geq 1$ from $U \setminus \sigma$ to a punctured disk by gluing together the polygons around σ. If $k_\sigma = 1$, then σ is removable, else it is conical. □

We can use this fact to give a nice connection between the singularities and the genus, which was already hinted at in the last chapter:

Proposition 3.1.10 (Gauß–Bonnet formula)
For a finite translation surface (X, ω) of genus g with n conical singularities with multiplicities $\{k_1, \dots k_n\}$, the *Gauß–Bonnet formula*

$$2g - 2 = \sum_{i=1}^{n} (k_i - 1)$$

holds.

Proof. We consider a finite triangulation $\mathcal{T}$ of $\overline{X}$ where each singularity $\sigma_1, \dots, \sigma_n$ corresponds to a vertex. Let V be the number of vertices, E the number of edges, and F the number of faces. It follows from the Euler–Poincaré formula for $\mathcal{T}$

$$2 - 2g = \chi(X) = V - E + F.$$

Double counting the set of pairs $\{(e, f)\}$ for edges e and faces f yields $2E = 3F$, so

$$2 - 2g = V - \frac{F}{2}.$$

Now, let us examine the sum of interior angles of the triangles of $\mathcal{T}$. Since there are $V - n$ vertices that are removable singularities, we have

$$F \cdot \pi = \sum_{i=1}^{n} k_i \cdot 2\pi + (V - n) \cdot 2\pi.$$

This implies $F = 2 \sum_{i=1}^{n} k_i + 2(V - n)$ and thus

$$2 - 2g = V - \sum_{i=1}^{n} k_i - (V - n) = -\sum_{i=1}^{n} (k_i - 1).$$

Multiplying with -1 gives us the statement we want to show. □

Remark 3.1.11 (Etymology of Gauß–Bonnet formula)
Usually, the *classical Gauß–Bonnet formula* is defined more generally for a compact two-dimensional Riemannian manifold M with boundary ∂M. If K is the Gaussian curvature of M and k_g is the geodesic curvature of ∂M, then

$$\int_M K \,\mathrm{d}A + \int_{\partial M} k_g \,\mathrm{d}s = 2\pi\chi(M),$$

where $\mathrm{d}A$ is the element of area of the surface and $\mathrm{d}s$ is the line element along the boundary of M.

We can transfer this picture to translation surfaces. Since our translation surfaces do not have a boundary, the integral for the boundary vanishes. The Gaussian curvature is 0 almost everywhere except for the singularities, where it is not well-defined, we therefore cannot use the classical Gauß–Bonnet formula in this context. However, one can use a nice heuristic to visualize curvature with excess angle: The sum of the external angles of a geodesic triangle (in $\mathbb{C}$) is equal to 2π minus the total curvature within the triangle. So, after triangulating our translation surface and since the external angle is equal to π minus the interior angle, the left-hand side integral can be understood to add together the total negative of the excess angle $2\pi(k_\sigma - 1)$ for each singularity. Dividing this by -2π corresponds to our version of the Gauss-Bonnet formula.

The Gauß–Bonnet Formula is especially useful to calculate genus very easily:

Example 3.1.12 (Flat torus)
For our flat torus $\mathbb{T}_\tau$, see Example 2.0.15, the classical fundamental domain $\mathcal{F}$ of our lattice Λ is a parallelogram, where all four corners are identified. So, we only have one singularity $\sigma \in \Sigma(\mathbb{T}_\tau)$. Since the total interior angle of a quadrilateral is 2π, so is the total angle around σ and the sole singularity σ is a removable singularity. The genus of the flat torus is $g(\mathbb{T}_\tau) = 1$, since $2g(\mathbb{T}_\tau) - 2 = 1 - 1$ by Proposition 3.1.10.

Example 3.1.13 (Veech's double n–gon)
Let n be fixed and $\mathbb{V}_n$ be Veech's double n–gon from Example 2.1.6. Fix one corner v of one of the n–gons. The edge e adjacent to v in clockwise direction is identified with an edge e' of the other n–gon, so v is identified with a corner v' adjacent to e'. Gluing the other edge adjacent to v' identifies v' with v'' which is a corner of the first polygon again. Vertex v'' is thereby the corner that is two edges apart from v in clockwise direction.

Since v is identified with every second corner of the first n–gon and analogously with every second corner of the second n–gon, the number of singularities depends only on n: for even n, there are two singularities and for odd n, there is only one. See Figures 2.3 and 3.2 for an odd and even case, respectively.

Since the sum of interior angles in an n–gon is $\pi(n-2)$, for even n, both singularities have an angle of $2\pi\frac{n-2}{2}$ by symmetry, so the multiplicity of each singularity is $\frac{n-2}{2}$. The genus of Veech's double n–gon is $g(\mathbb{V}_n) = \frac{n-2}{2}$ for even n, since $2g - 2 = 2(\frac{n-2}{2} - 1)$.

For odd n, the sole singularity has an angle of $2\pi(n-2)$ and thus the multiplicity is $n - 2$.

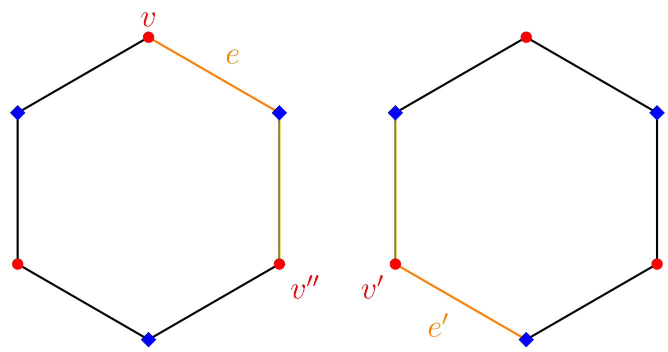

Figure 3.2: Veech's double hexagon

The genus of Veech's double n–gon is $g(\mathbb{V}_n) = \frac{n-1}{2}$ for odd n, since $2g - 2 = n - 2 - 1$. In particular, exactly the double triangles and double quadrilaterals have removable singularities and genus 1.

Example 3.1.14 (Eierlegende Wollmilchsau)
The Eierlegende Wollmilchsau is an 8–fold covering of the punctured torus with four singularities. All of these are conical with a multiplicity of 2 and an angle 4π. Due to Gauß–Bonnet, $2g - 2 = 1 + 1 + 1 + 1$, so the Eierlegende Wollmilchsau has genus 3.

For infinite translation surfaces, there are two more types of singularities.

Definition 3.1.15 (Infinite angle and wild singularity)
A singularity $\sigma \in \Sigma$ of a translation surface (X, ω) is called *infinite angle singularity* or *cone angle singularity of multiplicity* ∞, if there exists a neighborhood U of σ in $\overline{X}$, such that there is an infinite translation covering from $U \setminus \{\sigma\}$ to the punctured disk $\mathbb{D}^*$.

A singularity that is neither removable, nor a cone angle singularity, nor an infinite angle singularity is called *wild*.

These definitions are quite coarse, for a better understanding of wild singularities see [Ran18].

Example 3.1.16 (Baker's map surfaces)
The family of baker's map surfaces all have one wild singularity. In 2.4.5, we have seen that there is only one singularity. Let σ be this singularity on the baker's map surface for some $\alpha \in (0, 1)$. For every $\varepsilon > 0$, the neighborhood $B_\varepsilon(\sigma)$ contains a segment joining σ with itself. This can be seen in Figure 2.12: Infinitely many of these arbitrarily small segments accumulate towards the bottom left and top right corner. Therefore $B_\varepsilon(\sigma) \setminus \{\sigma\}$ is not simply connected and cannot be a translation covering of a once-punctured disk.

3.2 From saddle connections to cylinders

Translation surfaces can be investigated by understanding how they behave around singularities, since elsewhere we have a flat structure. Naturally, we want to understand paths coming from their singularities.

Definition 3.2.1 (Separatrices & saddle connections)
Let (X, ω) be a translation surface.

- A *separatrix* (or *critical trajectory*) is a geodesic ray $\gamma\colon \mathbb{R}_{\geq 0} \to \overline{X}$ that starts at a singularity and does not contain any other singularity.
- A *saddle connection* is a geodesic segment $\gamma\colon\ [0, t] \to \overline{X}$ in $\overline{X}$ that connects two, not necessarily distinct, singularities and does not contain any other singularity.

Convention 3.2.2 (Separatrices & saddle connections)
The image of a separatrix in $\overline{X}$ is also called a separatrix and the image of a saddle connection is called saddle connection, respectively.

Saddle connections in particular are a powerful tool to understand combinatorics on translation surfaces. For example, the set of saddle connections up until a given length encode some information about the complexity of the surface:

Definition 3.2.3 (Set of saddle connections)
Let (X, ω) be a translation surface. The *set of saddle connections* shorter than l is denoted by $V_{\text{sc}}(X, l)$.

Convention 3.2.4 (On V_{sc})
We will omit X from $V_{\text{sc}}(X, l)$ when the translation surface (X, ω) is clear from the context. Similarly, we will omit l from $V_{\text{sc}}(X, l)$ when $l = \infty$, referring to the set of all saddle connections of any length on (X, ω).

Since the interior of saddle connections and separatrices stay away from the singularities of $\overline{X}$ and thus are defined with respect to a translation structure on X, it makes sense to speak of global directions of these trajectories.

Definition 3.2.5 (Holonomy vector)
Let (X, ω) be a translation surface and $\gamma\colon I \to X$ a geodesic on X. We can choose charts (U_i, ϕ_i) with neighborhoods U_i around $x_i \in \gamma(I) \subsetneq X$, such that

- two consecutive points share a neighborhood $x_i, x_{i+1} \in U_i$,
- the geodesic γ is covered by the union of U_i and
- for each i, the intersection $\gamma \cap U_i$ is connected.

Now consider the $\phi_i(U_i)$ in $\mathbb{R}^2$. We transform these with transition maps between charts so that $\phi_{i-1}(x_i)$ and $\phi_i(x_i)$ coincide.

The transformed image of γ then becomes an open geodesic in $\mathbb{R}^2$. The difference vector between the endpoint and the starting point of the closure of this geodesic is called the *holonomy vector*

$$\operatorname{hol}(\gamma) = \int_\gamma \omega$$

of the geodesic γ.

If one specifies a direction or a holonomy vector as a direction vector, it is possible to examine whether a geodesic in this direction is closed for points on the translation surface. If this is the case, one can also look at it for a neighborhood of the point. This local behavior works until encountering singularities. We get a Cartesian product of an (open) interval with a circle, which is a cylinder topologically. If this process is applied to the entire surface, a cylinder decomposition is obtained. Note that this approach does not work for every direction.

Definition 3.2.6 (Cylinder & cylinder decomposition)
Let (X, ω) be a translation surface.

- A *cylinder* in (X, ω) is an open subset of X isometric to a Euclidean cylinder of the form $\mathbb{R}/_{c\mathbb{Z}} \times (0, h)$. Here, $c, h \in \mathbb{R}_{>0}$ and we call c the *circumference* and h the *height* of the cylinder.
- The direction of a cylinder is defined by the direction of a closed geodesic that maps to $\mathbb{R}/_{c\mathbb{Z}} \times \{h'\}$ with $h' \in (0, h)$.
- Let C be a cylinder. We call C *maximal*, if for every other cylinder D with $C \subseteq D$ this already implies that $C = D$.
- The *modulus* $\mu := \mu(C)$ of a cylinder C is the ratio of circumference to height, which is to say, $\mu(C) := \frac{c}{h}$.
- A *cylinder decomposition* of (X, ω) (with direction $d \in S^1$) is a set of maximal cylinders $\{C_i\}_{i \in I}$ in (X, ω) (with direction d) such that
  (a) the surface $\overline{X}$ is the union of these cylinders: $\overline{X} = \bigcup_{i \in I} \overline{C_i}$ and
  (b) the intersection $C_i \cap C_j = \emptyset$ for all pairs $i \neq j$.

Example 3.2.7 (Veech's double n–gon)
Let us consider Veech's double n–gon. Choose the direction d given by the saddle connection between two neighboring vertices in the n–gon. For even n, we get a cylinder decomposition given by $\frac{n-2}{2}$ cylinders and for odd n, we get a cylinder decomposition given by $\frac{n-1}{2}$ cylinders similar to Figure 3.3. Veech showed in [Vee89], that all cylinders for each decomposition have a common modulus of $\mu(C_i) = 2 \cot\left(\frac{\pi}{n}\right)$.

Those maximal cylinders are bounded by objects from which we started this endeavor.

Remark 3.2.8 (Boundaries of maximal cylinders)
The fact that a maximal cylinder cannot be further extended generally arises (when $\overline{X}$ is not a torus) because there is a singularity in the closure of the cylinder in $\overline{X}$. The boundary of the cylinder in $\overline{X}$ then consists of saddle connections.

While it is true that every maximal cylinder is bounded by saddle connections, the opposite statement that every saddle connection is the boundary of a maximal cylinder is false in general.

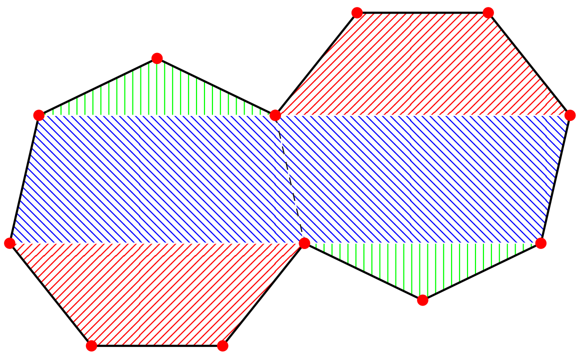

Figure 3.3: Cylinder decomposition of Veech's double heptagon

Furthermore, on a finite translation surface there cannot be infinitely maximal cylinders.

Proposition 3.2.9 (Cylinder decompositions of finite translation surfaces)
If (X, ω) is a finite translation surface, then a cylinder decomposition of (X, ω) can only consist of finitely many cylinders.

Proof. Let (X, ω) be a finite translation surface. If there are infinitely many cylinders, they could be extended with additional open sets to form an open cover of $\overline{X}$, such that no cylinder could be omitted from the cover. However, this would contradict the compactness of $\overline{X}$ in Definition 2.1.1. □

Cylinders can be skewed in the direction of the cylinder and almost stay the same, if we skew by a multiple of the circumference. This skewing procedure is closely related to Dehn twists. The question which arises is the following: Does there exist a transformation of our surface which stabilizes every cylinder of a maximal cylinder decomposition and therefore stabilizes the entire translation surface?

3.3 Translations, affinities, and Veech groups

To motivate this section, let us return to our family of tori from Example 2.0.15 and consider the parameter as an element of $\mathbb{R}^2$ instead of $\mathbb{C}$. For now, we do not want to fix one of the sides of our parallelogram to $(1, 0)$. Instead, we consider a surface $P(a, b, c, d)$ obtained by gluing together opposite edges of a parallelogram with one vertex at the origin, one edge ending at $(a, c) \in \mathbb{R}^2$ and the second edge ending at $(b, d) \in \mathbb{R}^2$, see Figure 3.4.

The surface is thus parameterized with coordinates in $\mathbb{R}^4$. Furthermore, each non-degenerate surface $P(a, b, c, d)$ can be obtained from the unit square $P(1, 0, 0, 1)$ by multiplying with the matrix $A = \begin{pmatrix} a & b \\ c & d \end{pmatrix} \in \mathrm{GL}_2^+(\mathbb{R}) := \{A \in \mathrm{GL}_2(\mathbb{R}) \mid \det A > 0\}$. For non-degenerate surfaces with positive orientation, we have $\det(A) > 0$.

The following question now arises: for which $A \in \mathrm{GL}_2^+(\mathbb{R})$ is the torus $A \cdot P(1, 0, 0, 1)$ isomorphic to $P(1, 0, 0, 1)$ again?

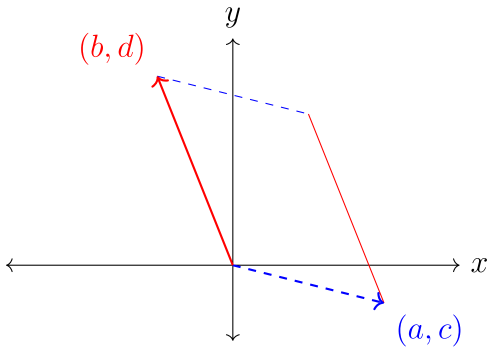

Figure 3.4: Parallelogram $P(a,b,c,d) \subsetneq \mathbb{R}^2$

The answer to this question depends on how one interprets the underlying objects. When viewed as purely topological manifolds, all surfaces constructed in this way are isomorphic to the torus according to Theorem 2.2.16, the classification of compact surfaces.

We obtain an isomorphism of Riemann surfaces between $A \cdot P(1,0,0,1)$ and $P(1,0,0,1)$, when multiplication by A is a $\mathbb{C}$–linear map, which is to say, when $A = \begin{pmatrix} a & -b \\ b & a \end{pmatrix}$ for $(a,b) \in \mathbb{R}^2 \setminus \{(0,0)\}$. Consequently, all $P(\tilde{a}, \tilde{b}, \tilde{c}, \tilde{d})$ can be transformed by some $\mathbb{C}$–linear map, such that is isomorphic as a Riemann surface to $P(1,b,0,d)$, bringing us back to the case of parameterization only with $\tau = b + \mathrm{i}d \in \mathbb{C}$, such that $\mathbb{T}_{b+\mathrm{i}d} \cong P(1,b,0,d)$. Furthermore, for $\tau = 1 + \mathrm{i}$, we can regain our unit square $\mathbb{T}_{\mathrm{i}}$ by cutting and regluing as seen in Figure 3.5.

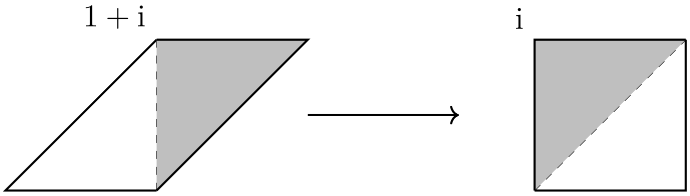

Figure 3.5: Cutting and regluing $\mathbb{T}_{\mathrm{i}+1}$ to obtain $\mathbb{T}_{\mathrm{i}}$

This works for all lattice points $\tau \in (\mathbb{Z}+\mathrm{i}\mathbb{Z}) \setminus \{(0,0)\}$. Thus, $\mathbb{T}_\tau$ and $\mathbb{T}_{\tau'}$ are isomorphic Riemann surfaces if and only if their *lattices* $\mathbb{Z} + \tau\mathbb{Z}$ and $\mathbb{Z} + \tau'\mathbb{Z}$ are equivalent.

Definition 3.3.1 (Equivalence of lattices)
A lattice $\mathbb{Z} + \tau\mathbb{Z}$ is *equivalent* to $\mathbb{Z} + \tau'\mathbb{Z}$ if and only if there exists $\alpha \in \mathbb{C}^\times := \mathbb{C} \setminus \{0\}$, such that $\alpha\,(\mathbb{Z} + \tau\mathbb{Z}) = \mathbb{Z} + \tau'\mathbb{Z}$.

Lemma 3.3.2 (Isomorphism)
Let $\tau, \tau' \in \mathbb{H}$. The corresponding Riemann surfaces $\mathbb{T}_\tau, \mathbb{T}_{\tau'}$ are complex isomorphic if

and only if there exists a *Möbius transformation* $\gamma = \begin{pmatrix} a & b \\ c & d \end{pmatrix} \in \mathrm{SL}_2(\mathbb{Z})$ such that

$$\tau' = \gamma\tau = \frac{a\tau + b}{c\tau + d}.$$

Proof. "$\Rightarrow$": First, let us consider the lattices $\mathbb{Z}+\tau\mathbb{Z}$ and $\mathbb{Z}+\tau'\mathbb{Z}$ to be equivalent, so there exists an $\alpha \in \mathbb{C}^\times$ such that $\alpha(\mathbb{Z}+\tau'\mathbb{Z}) = \mathbb{Z}+\tau\mathbb{Z}$. Write $\alpha\tau' = a\tau+b$ and $\alpha = c\tau + d$. Then, according to the assumption, $(\alpha\tau', \alpha)$ forms another basis of $\mathbb{Z} + \tau\mathbb{Z}$ and hence the matrix $\gamma = \begin{pmatrix} a & b \\ c & d \end{pmatrix}$ is invertible over the integers, meaning $\det(\gamma) = \pm 1$. Since the Möbius transformation $\tau' = \frac{a\tau+b}{c\tau+d}$ maps $\mathbb{H}$ to $\mathbb{H}$ and $\tau' \in \mathbb{H}$, it follows that $\det(\gamma) = 1$.

"$\Leftarrow$": Conversely, let $\gamma = \begin{pmatrix} a & b \\ c & d \end{pmatrix} \in \mathrm{SL}_2(\mathbb{Z})$ with $\tau' = \frac{a\tau+b}{c\tau+d}$. Because $\det(\gamma) = 1$, the set $\{a\tau + b, c\tau + d\}$ forms another basis of $\mathbb{Z}+\tau\mathbb{Z}$. With $\alpha = c\tau + d$, it follows that

$$\alpha(\mathbb{Z} + \tau'\mathbb{Z}) = (c\tau + d)\mathbb{Z} + (a\tau + b)\mathbb{Z} = \mathbb{Z} + \tau\mathbb{Z},$$

meaning the two lattices are equivalent. □

For translation surfaces, the translation structure must also be preserved. In the case of the torus as a translation surface, the considerations with the equivalent lattices work analogously here. However, scaling, which is to say, multiplication by an α in $\mathbb{C}^\times$, is incompatible with the translation structure.

Another observation we can make here is that the *moduli space*, that is to say, the geometric space of isomorphism classes of objects, consists of just one point as a real, topological, or differentiable manifold, since all these objects are isomorphic to the torus. While for Riemannian manifolds, we obtain an interesting space:

Let E be a compact Riemannian surface of genus 1. Then, the *universal cover* $\tilde{E} / E$ is isomorphic to $\mathbb{C}$ and the *deck transformation group* $\mathrm{Deck}\left(\tilde{E} / E\right)$ is isomorphic to the *fundamental group* $\pi_X(E) \cong \mathbb{Z}^2$, that is to say, $\mathrm{Deck}\left(\tilde{E} / E\right)$ forms a lattice in $\mathbb{C}$. As seen earlier, we can assume that the lattices are in the form $\mathbb{Z} + \tau\mathbb{Z}$ with $\tau \in \mathbb{H}$. Additionally, $\mathbb{C} / \tau$ and $\mathbb{C} / \tau'$ are isomorphic Riemannian surfaces if $\tau' = \gamma\tau$ for a Möbius transformation $\gamma \in \mathrm{SL}_2(\mathbb{Z})$. Thus, the moduli space M_1 for compact Riemannian surfaces of genus 1 is precisely given by

$$M_1 = \mathbb{H} \big/ \mathrm{PSL}_2(\mathbb{Z}).$$

Note the use of $\mathrm{PSL}_2(\mathbb{Z})$ instead of $\mathrm{SL}_2(\mathbb{Z})$, as $\begin{pmatrix} -1 & 0 \\ 0 & -1 \end{pmatrix}$ operates as the identity comprehended as a Möbius transformation.

Furthermore, $\mathrm{PSL}_2(\mathbb{Z})$ acts discontinuously on $\mathbb{H}$ and a popular choice for the fundamental domain can be found in Figure 3.6. The corresponding orbit space of this action is isomorphic to $\mathbb{C}$ as a Riemannian surface.

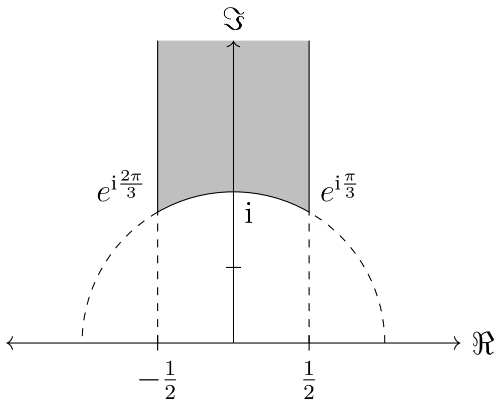

Figure 3.6: Fundamental domain $\left\{z \in \mathbb{H} \;\middle|\; -\frac{1}{2} < \Re(z) \leq \frac{1}{2}, |z| > 1\right\}$ in gray

A subtlety worth mentioning here is that by defining the lattice as a subgroup of $(\mathbb{C}, +)$, we have distinguished a point, namely our neutral element 0 and its orbits. So, $\mathbb{H} \big/ \mathrm{PSL}_2(\mathbb{Z})$ is actually the moduli space $M_{1,1}$ of Riemannian surfaces of genus 1 with one marked point.

To obtain the moduli space for translation structures or surfaces, we can proceed analogously. Now, the translation structure depends only on the lattice and not on the lattice basis. The oriented lattice bases correspond to the elements in $\mathrm{GL}_2^+(\mathbb{R})$. Therefore, the moduli space of translation surfaces of genus 1 (with a marked point) is the quotient space

$$\Omega M_1 := \mathrm{GL}_2^+(\mathbb{R}) \big/ \mathrm{PSL}_2(\mathbb{Z}).$$

The action of $\mathbb{C}^\times$ is given by the subgroup $\left\{\begin{pmatrix} a & -b \\ b & a \end{pmatrix} \;\middle|\; (a,b) \in \mathbb{R}^2 \setminus \{(0,0)\}\right\}$.

Since $\mathbb{C}^\times \big\backslash \mathrm{GL}_2^+(\mathbb{R}) \cong \mathbb{H}$, we obtain a surjective map

$$\psi\colon \mathrm{GL}_2^+(\mathbb{R}) \big/ \mathrm{PSL}_2(\mathbb{Z}) = \Omega M_1 \to M_1 = \mathbb{H} \big/ \mathrm{PSL}_2(\mathbb{Z}).$$

For each $m \in M_1$, we have $\psi^{-1}(m) = \mathbb{C}^\times$ and because the actions of $\mathbb{C}^\times$ and $\mathrm{PSL}_2(\mathbb{Z})$ on $\mathrm{GL}_2^+(\mathbb{R})$ commute, we even have

$$\Omega M_1 \cong \mathbb{C}^\times \times M_1.$$

Different translation structures on a fixed Riemann surface of genus 1 differ only by multiplication with an $\alpha \in \mathbb{C}^\times \cong \mathbb{R}_{>0} \times S^1$. Therefore, apart from scaling and rotation, there is only one translation structure on $\mathbb{T}_{\mathrm{i}}$, which is generally not the case for translation surfaces of higher genus.

The observations made here can now be considered more generally for arbitrary translation surfaces. We can now proceed to understand spaces of translation surfaces as such by first considering morphisms in the category of translation surfaces, which are *maps* on translation surfaces.

Definition 3.3.3 (Orientation)
Let $f : (X, \omega) \to (Y, \zeta)$ be a non-degenerate continuous map between two translation surfaces.

The map f is called *orientation-preserving* if for any charts $(U, \phi) \in \omega$ and $(V, \psi) \in \zeta$ with $f(U) \subseteq V$, the Jacobian matrix of $\psi \circ f \circ \phi^{-1} : \phi(U) \to \psi(V)$ has a positive determinant.

The map f is called *orientation-reversing* if the corresponding Jacobian matrix has a negative determinant.

Since translation surfaces are generally orientable, it suffices to consider *orientation-preserving linear transformations* $\mathrm{GL}_2^+(\mathbb{R})$ of the plane $\mathbb{R}^2$ to understand isomorphism classes of translation surfaces, which will be defined later.

Remark 3.3.4 (On $\mathrm{GL}_2(\mathbb{R})$)
The topology on $\mathrm{GL}_2(\mathbb{R})$ is induced by the embedding into the space $\mathbb{R}^{2\times 2} \cong \mathbb{R}^4$. The space $\mathrm{GL}_2(\mathbb{R})$ is Zariski-open in $\mathbb{R}^4$ since it is topologically the complement of the *zero set*

$$Z(ad - bc) = \left\{(a, b, c, d) \in \mathbb{R}^4 \;\middle|\; ad - bc = 0\right\}$$

for any $A = \begin{pmatrix} a & b \\ c & d \end{pmatrix} \in \mathrm{GL}_2(\mathbb{R})$ The total space $\mathrm{GL}_2(\mathbb{R})$ is split by $Z(ad - bc)$ into two components where $ad - bc$ is positive or negative. The positive connected component, which contains the identity, is $\mathrm{GL}_2^+(\mathbb{R})$. The other connected component

$$\mathrm{GL}_2^-(\mathbb{R}) = \mathrm{GL}_2(\mathbb{R}) \setminus \mathrm{GL}_2^+(\mathbb{R})$$

corresponds to orientation-reversing linear transformations.

We obtain an action of $\mathrm{GL}_2^+(\mathbb{R})$ on the moduli space of translation surfaces.

Lemma 3.3.5 (Action of $\mathrm{GL}_2^+(\mathbb{R})$)
The group $\mathrm{GL}_2^+(\mathbb{R})$ acts on translation surfaces. That is to say, for every $A \in \mathrm{GL}_2^+(\mathbb{R})$ with its associated linear transformation

$$\varphi_A : \mathbb{R}^2 \to \mathbb{R}^2, \quad x \mapsto Ax$$

and for every translation surface (X, ω) with translation atlas $\{(U_i, \phi_i)\}_{i\in I}$, the set of charts $\{(U_i, \varphi_A \circ \phi_i)\}_{i\in I}$ is also a translation atlas with associated translation structure $A \cdot \omega$ on a translation surface $A \cdot (X, \omega) \coloneqq (X, A \cdot \omega)$.

Proof. Let $i, j \in I$ and $U \subseteq U_i \cap U_j$. By Definition 2.0.3, the transition map $\phi_i \circ \phi_j^{-1}$ on $\phi_j(U)$ is given by $x \mapsto x + c$ for some $c \in \mathbb{R}$. Then on $\varphi_A(\phi_j(U))$,

$$\begin{aligned}(\varphi_A \circ \phi_i) \circ (\varphi_A \circ \phi_j)^{-1}(x) &= A(\phi_i \circ \phi_j^{-1})(A^{-1}x) \\ &= A(A^{-1}x + c) = x + Ac,\end{aligned}$$

thus the transition functions are also translations and $A \cdot \omega$ is a translation structure on X. □

Next let us understand the $\mathrm{GL}_2^+(\mathbb{R})$–action from the perspective of the three different definitions of finite translation surfaces.

Remark 3.3.6 (Action of $\mathrm{GL}_2^+(\mathbb{R})$ on finite translation surfaces)
Let (X, ω) be a finite translation surface and (X_A, ω_A) be the translation surface after the action of $A \in \mathrm{GL}_2^+(\mathbb{R})$.

(I) The surface X and the translation structure ω get multiplied by A. The Euclidean metric on AX differs from that on X as a Riemannian metric by multiplication with A as well, thus inducing the same topology. The metric completion is the same in both cases.

(II) If $P_1, \dots P_n$ are the polygons with gluing instructions T describing the atlas ω, then the polygons $\varphi_A(P_1), \dots, \varphi_A(P_n)$ with the gluing instructions $\varphi_A T \varphi_A^{-1}$ correspond to the atlas ω_A.

(III) Write the holomorphic differential ω on $\overline{X}$ as:

$$\omega = \Re(\omega) + \Im(\omega), \quad \mathrm{d}z = \mathrm{d}x + \mathrm{i}\,\mathrm{d}y.$$

Then let $\omega_A := A \begin{pmatrix} \Re(\omega) \\ \Im(\omega) \end{pmatrix}$, that is to say, $(a + \mathrm{i}c)\,\mathrm{d}x + (b + \mathrm{i}d)\,\mathrm{d}y$ for $A = \begin{pmatrix} a & b \\ c & d \end{pmatrix}$. The form ω_A is generally not holomorphic on X, but only $\mathcal{C}^\infty$. We now choose the compact structure on the surface $\overline{X}$ so that ω_A is holomorphic. This Riemann surface is called X_A. This complex structure is unique. We obtain it from the construction as in the proof of Lemma 2.1.25: For $\overline{X} \setminus \Sigma$, we obtain charts through $\int_{P_i}^{P} \omega_A$ on simply connected open subsets.

An important class of maps between translation surfaces to understand isomorphism classes are translation maps.

Definition 3.3.7 (Translation)
Let (X, ω) and (Y, ζ) be translation surfaces. A continuous map $f\colon (X, \omega) \to (Y, \zeta)$ is called a *translation map* or just *translation*, if for all charts (U, ϕ) for X and (V, ψ) for Y, there exists $c \in \mathbb{R}^2$ such that

$$(\psi \circ f \circ \phi^{-1})(x) = x + c$$

for all $x \in \phi(U \cap f^{-1}(V))$, provided $U \cap f^{-1}(V)$ is connected; otherwise, c may depend on the component.

Translations are not necessarily bijective. However, bijective translations are remarkably interesting and have their own group.

Definition 3.3.8 (Translation group)
The *translation group* $\mathrm{Trans}(X, \omega)$ of a translation surface (X, ω) is the group of bijective translations of (X, ω).

We can now finally define isomorphism classes of translation surfaces.

Definition 3.3.9 (Isomorphic translation surfaces)
Two translation surfaces are called *isomorphic* if there exists a bijective translation between them.

Example 3.3.10 (L-shape and Eierlegende Wollmilchsau)
Let $L_{2,2}$ be the L-shape origami from Example 2.3.3. Then the map $p : L_{2,2} \to \mathbb{T}_i$, which maps each square of $L_{2,2}$ onto the unit square by translations, is a translation map, which is not injective.

Let W be the Eierlegende Wollmilchsau, whose squares are labeled with elements of the quaternion group as in Example 2.3.8. Then the map $f : W \to W$ which sends squares of W to squares of W by $x \mapsto x \cdot \mathrm{i}$ is a bijective translation map.

After defining translations, the next object of interest are affinities. For translation surfaces, affine maps can be defined in the following way.

Definition 3.3.11 (Affine maps)
Let (X, ω) and (Y, ζ) be translation surfaces. A continuous map $f\colon (X, \omega) \to (Y, \zeta)$ is called *affine*, if for all charts (U, ϕ) for X and (V, ψ) for Y, there exists an $A_{\phi,\psi} \in \mathrm{GL}_2(\mathbb{R})$ and a $c \in \mathbb{R}^2$ such that

$$(\psi \circ f \circ \phi^{-1})(x) = A_{\phi,\psi} x + c$$

for all $x \in \phi(U \cap f^{-1}(V))$, provided $U \cap f^{-1}(V)$ is connected; otherwise, c may depend on the component.

Next let us see how these matrices $A_{\phi,\psi}$ are independent of the choice of charts.

Proposition 3.3.12 (Chart independence of affine maps)
Let $f : X \to Y$ be an affine map of translation surfaces. The matrix $A_f := A_{\phi,\psi}$ from Definition 3.3.11 is independent of the choice of charts.

Proof. Let $(U_1, \phi_1), (U_2, \phi_2)$ be charts for X and $(V_1, \psi_1), (V_2, \psi_2)$ be charts for Y, each pair with non-empty intersections, without loss of generality, having exactly one connected component.

By assumption, there exist $c, t, s \in \mathbb{R}^2$ such that:

$$\begin{aligned}
(\psi_1 \circ f \circ \phi_1^{-1})(x) &= A_{\phi_1,\psi_1} x + c,\\
(\phi_1 \circ \phi_2^{-1})(y) &= y + t,\\
(\psi_2 \circ \psi_1^{-1})(z) &= z + s
\end{aligned}$$

for $x \in \phi_1(U_1 \cap U_2 \cap f^{-1}(V_1 \cap V_2))$, $y \in \phi_2(U_1 \cap U_2)$, and $z \in \psi_1(V_1 \cap V_2)$.

For $y \in \phi_2(U_1 \cap U_2 \cap f^{-1}(V_1 \cap V_2))$, we have

$$\begin{aligned}
(\psi_2 \circ f \circ \phi_2^{-1})(y) &= \left((\psi_2 \circ \psi_1^{-1}) \circ (\psi_1 \circ f \circ \phi_1^{-1}) \circ (\phi_1 \circ \phi_2^{-1})\right)(y)\\
&= \left((\psi_2 \circ \psi_1^{-1}) \circ (\psi_1 \circ f \circ \phi_1^{-1})\right)(y + t)
\end{aligned}$$

$$\begin{aligned} &= \left(\psi_2 \circ \psi_1^{-1}\right)(A_{\phi_1,\psi_1}(y+t)+c) \\ &= A_{\phi_1,\psi_1}(y+t)+c+s \\ &= A_{\phi_1,\psi_1}y + (A_{\phi_1,\psi_1}t+c+s). \end{aligned}$$

Hence, $A_{\phi_2,\psi_2} = A_{\phi_1,\psi_1}$. □

It is easy to show that the set of all orientation-preserving homeomorphisms is closed under inversion and composition, we therefore obtain the affine group.

Definition 3.3.13 (Affine group)
The *affine group* $\mathrm{Aff}^+(X,\omega)$ of a translation surface (X,ω) is defined by

$$\mathrm{Aff}^+(X,\omega) \coloneqq \{f\colon X \to X \mid f \text{ is an affine orientation-preserving homeomorphism}\}.$$

Let us fix the linear part of the affine map.

Definition 3.3.14 (Derivative)
Let $f\colon X \to Y$ be an affine map of translation surfaces and let $A \coloneqq A_f \in \mathrm{GL}_2(\mathbb{R})$ be the associated matrix of the linear part. Then A is called the *derivative* of f, denoted by $A = \mathrm{der}(f)$.

The group homomorphism $\mathrm{der}\colon \mathrm{Aff}^+(X,\omega) \to \mathrm{GL}_2(\mathbb{R})$, which assigns to each affine orientation-preserving homeomorphism its derivative, is called the *derivative map*.

We can calculate an easy example for warm-up.

Example 3.3.15 (Derivative)
If $\mathbb{T}_{\mathrm{i}}$ denotes the standard torus and $f\colon \mathbb{T}_{\mathrm{i}} \to \mathbb{T}_{\mathrm{i}}$ is the map induced by

$$\tilde{f}\colon \mathbb{C} \to \mathbb{C}, \quad z \mapsto 2z,$$

then f is an unbranched covering of degree 4. f is affine and $\mathrm{der}(f) = \begin{pmatrix} 2 & 0 \\ 0 & 2 \end{pmatrix}$.

This map is not area preserving, compared to derivatives of translations.

Remark 3.3.16 (Derivative of translations)
A continuous map is a translation if and only if it is affine and its derivative is the identity. In particular, $\mathrm{Trans}(X,\omega) \subseteq \mathrm{Aff}^+(X,\omega)$ and $\mathrm{Trans}(X,\omega)$ is the kernel of the map $\mathrm{der} : \mathrm{Aff}^+(X,\omega) \to \mathrm{GL}_2(\mathbb{R})$.

We would like to understand the image of der. For that consider:

Proposition 3.3.17 (Image of der)
Let (X,ω) be a finite translation surface and $f\colon (X,\omega) \to (X,\omega)$ be affine.

- If $g(X) \geq 2$, then f is a homeomorphism.
- If f is a homeomorphism, then $\mathrm{der}(f) \subseteq \mathrm{SL}_2(\mathbb{R})$.

Proof. Let us show the two parts of the statement individually.

- Every affine map is a local homeomorphism outside the singularity set Σ_X and even a topological covering $\overline{X} \setminus \Sigma_X \to \overline{X} \setminus \Sigma_X$. Thus, f can be extended to a possibly branched covering $\overline{f}\colon \overline{X} \to \overline{X}$. For such maps, the Riemann–Hurwitz formula from Proposition 3.1.3 applies:

$$2g(\overline{X}) - 2 = \deg(\overline{f}) \cdot (2g - 2) + \sum_{x \in \overline{X}} (\mathrm{ord}_x(\overline{f}) - 1).$$

  For $g \geq 2$, this is only possible for $\sum_{x \in \overline{X}} (\mathrm{ord}_x(\overline{f}) - 1) = 0$ and $\deg(\overline{f}) = 1$, so $\mathrm{ord}_x(\overline{f}) = 1$ everywhere and f must be a homeomorphism.

- Let $\mathrm{area}(X)$ be the area of (X, ω) with respect to the Euclidean metric. Since f is injective, $\mathrm{area}\,(\mathrm{der}(f)) = 1$, so

$$\mathrm{der}(f) \in \mathrm{SL}_2(\mathbb{R}) = \{A \in \mathrm{GL}_2(\mathbb{R}) \mid \det(A) = \pm 1\}. \qquad \square$$

In particular, if $f \in \mathrm{Aff}^+(X, \omega)$ for some finite translation surface (X, ω), then the image of the derivative map is contained in $\mathrm{SL}_2(\mathbb{R})$.

Definition 3.3.18 (Veech group)
Let (X, ω) be a translation surface. We call the image of the derivative map

$$\mathrm{der}\colon \mathrm{Aff}^+(X, \omega) \to \mathrm{GL}_2(\mathbb{R})$$

the *Veech group* of (X, ω) and denote it by $\mathrm{GL}^+(X, \omega)$.

The group homomorphism from $\mathrm{Aff}^+(X, \omega)$ to $\mathrm{GL}_2(\mathbb{R})$ can be extended to the group of all affine homeomorphisms $\mathrm{Aff}(X, \omega)$. The image of this new map, denoted by $\mathrm{GL}(X, \omega)$, is called the *extended Veech group* of (X, ω).

Remark 3.3.19 (Maximal Veech groups)
Since we look at the image of orientation-preserving homeomorphisms for a translation surface (X, ω), we have

$$\mathrm{GL}^+(X, \omega) \subseteq \mathrm{GL}_2^+(\mathbb{R}).$$

If (X, ω) is finite, we even get

$$\mathrm{GL}^+(X, \omega) \subseteq \mathrm{SL}_2(\mathbb{R}),$$

as seen in Proposition 3.3.17.

This remark gives us an upper bound in some sense of which elements can be at most in a Veech group, which is an actual group since:

Remark 3.3.20 (Veech groups are groups)
The Veech group is a group, since it is defined as the image of the derivative map, which is a homomorphism.

For the first example, we calculate the Veech group of an infinite translation surface with maximal symmetry and therefore a big Veech group.

Example 3.3.21 (Euclidean plane)
Let $(\mathbb{R}^2, \omega)$ be the Euclidean plane. For every $A \in \mathrm{GL}_2^+(\mathbb{R})$ (and $t \in \mathbb{R}^2$), the map

$$f\colon (\mathbb{R}^2, \omega) \to (\mathbb{R}^2, \omega), \quad x \mapsto A \cdot x \ (+\ t)$$

is an orientation-preserving affine map. Therefore, the Veech group of $(\mathbb{R}^2, \omega)$ is entirely $\mathrm{GL}_2^+(\mathbb{R})$.

There is another way to perceive Veech groups, which we already mentioned in an earlier chapter, namely as the stabilizer of the $\mathrm{GL}_2^+(\mathbb{R})$–action:

Remark 3.3.22 (Stabilizer of $\mathrm{GL}_2^+(\mathbb{R})$)
If (X, ω) is a translation surface and $A \in \mathrm{GL}^+(X, \omega)$, then there exists an $f \in \mathrm{Aff}^+(X, \omega)$ such that $\mathrm{der}(f) = A^{-1} \in \mathrm{GL}^+(X, \omega)$. The map defined by

$$f_A\colon (X, \omega) \to (X, A \cdot \omega), \quad x \mapsto f(x),$$

is a bijective translation and $(X, A \cdot \omega)$ and (X, ω) are isomorphic. $\mathrm{GL}^+(X, \omega)$ is therefore the stabilizer of the $\mathrm{GL}_2^+(\mathbb{R})$–action.

If we know the Veech group of a translation surfaces (X, ω), we can also deduce the Veech group of $A \cdot (X, \omega)$ for $A \in \mathrm{GL}_2^+(\mathbb{R})$:

Proposition 3.3.23 (Veech groups under the $\mathrm{GL}_2^+(\mathbb{R})$–action)
Let (X, ω) be a translation surface and $A \in \mathrm{GL}_2^+(\mathbb{R})$. Then,

$$\mathrm{GL}^+(X, A \cdot \omega) = A \cdot \mathrm{GL}^+(X, \omega) \cdot A^{-1}.$$

Proof. Let $B \in \mathrm{GL}^+(X, \omega)$, so there exists a map $f\colon X \to X$ such that for any two charts $(U, \phi), (V, \psi) \in \omega$ with $f(U) \subseteq V$, we have:

$$\psi \circ f \circ \phi^{-1}(z) = B \cdot z + t$$

for some $t \in \mathbb{R}^2$. Then, $(U, A \cdot \phi), (V, A \cdot \psi) \in A \cdot \omega$ are two charts with:

$$\begin{aligned}
\left((A \cdot \psi) \circ f \circ (A \cdot \phi)^{-1}\right)(z) &= ((A \cdot \psi) \circ f)\left(\phi^{-1}\left(A^{-1} \cdot z\right)\right) \\
&= A\left(\psi \circ f \circ \phi^{-1}\right)\left(A^{-1} \cdot z\right) \\
&= A\left((BA^{-1}) \cdot z + t\right) \\
&= ABA^{-1} \cdot z + A \cdot t.
\end{aligned}$$

Since for every point $x \in X$, there exist corresponding charts $(U, A \cdot \phi)$ and $(V, A \cdot \psi)$, the map f is also an affine homeomorphism on $(X, A \cdot \omega)$ with

$$\mathrm{der}(f) = ABA^{-1} \in \mathrm{GL}^+(X, A \cdot \omega).$$

Thus,

$$A \cdot \mathrm{GL}^+(X, \omega) \cdot A^{-1} \subseteq \mathrm{GL}^+(X, A \cdot \omega).$$

Similarly,

$$A^{-1} \cdot \mathrm{GL}^+(X, A \cdot \omega) \cdot A \subseteq \mathrm{GL}^+(X, A^{-1}A \cdot \omega) = \mathrm{GL}^+(X, \omega),$$

which shows this proposition. □

For the Veech group of a finite translation surface, consider the following example.

Example 3.3.24 (Veech group of tori)
Let us reconsider the tori from the introduction of this section. We have already seen that

$$\mathrm{GL}^+(\mathbb{T}_\mathrm{i}) = \mathrm{SL}_2(\mathbb{Z}).$$

For all other tori $(\mathbb{T}, \omega)$, there exists an $A \in \mathrm{GL}_2(\mathbb{R})$, such that $(\mathbb{T}, \omega) = A \cdot \mathbb{T}_\mathrm{i}$. Because of Proposition 3.3.23, conjugating by A yields our Veech group and therefore

$$\mathrm{GL}^+(\mathbb{T}, \omega) = A \cdot \mathrm{SL}_2(\mathbb{Z}) \cdot A^{-1}.$$

The elements of $\mathrm{SL}(2, \mathbb{R})$, except for $\pm I_2$, can be classified as parabolic, elliptic, and hyperbolic elements. This classification can be based on the traces of the matrices, their fixed points, or their conjugacy classes; see Table 3.1.

As seen in the end of the previous section, there is a connection between cylinders and shears, which we now call parabolic elements.

To see the connection between cylinders and parabolic elements, let us fix the notion of commensurability.

Definition 3.3.25 (Commensurable)
Let $A \subsetneq \mathbb{R}$ be countable. We call A *commensurable* if there exists a $c \in \mathbb{R}$, such that $a = m_a c$ with $m_a \in \mathbb{Z}$ for all $a \in A$. In this case, we call c a *common divisor*.

Proposition 3.3.26 (Cylinders and parabolic elements)
Let (X, ω) be a translation surface.

(a) If $(C_i)_{i \in I}$ is a cylinder decomposition of (X, ω), such that the cylinder C_i has height h_i and circumference c_i and the inverse moduli $(m(C_i))^{-1} = \frac{h_i}{c_i}$ are commensurable with common divisor μ, then the Veech group contains a parabolic element:

$$\begin{pmatrix} 1 & \frac{1}{\mu} \\ 0 & 1 \end{pmatrix} \in \mathrm{GL}^+(X, \omega).$$

(b) If $(X, \mathcal{A})$ is a finite translation surface and the Veech group contains a parabolic element, then there exists a cylinder decomposition of $(X, \mathcal{A})$, whose direction corresponds to the eigenvectors of the parabolic element.

Proof. For finite translation surfaces, (a) was shown by [Vee89]. The same arguments work for the infinite case. (b) was shown in Lemma 4 of [HS06]. □

A is	$\lvert\mathrm{tr}(A)\rvert$	Fixed point(s) of Möbius transformation on $\mathbb{C}$	Conjugacy class(es)
elliptic	< 2	two fixed points in $\mathbb{C} \setminus \mathbb{R}$, (conjugated to each other)	rotations conjugated to $\begin{pmatrix} \cos(\theta) & -\sin(\theta) \\ \sin(\theta) & \cos(\theta) \end{pmatrix}$ for $\theta \in (0, 2\pi)$
parabolic	$= 2$	one fixed point in $\mathbb{R} \sqcup \{\infty\}$	shears conjugated to $\begin{pmatrix} 1 & t \\ 0 & 1 \end{pmatrix}$ for $t \in \mathbb{R} \setminus \{0\}$
hyperbolic	> 2	two fixed points in $\mathbb{R} \sqcup \{\infty\}$	squeeze maps conjugated to $\begin{pmatrix} \lambda & 0 \\ 0 & \frac{1}{\lambda} \end{pmatrix}$ for $\lambda \in \mathbb{R} \setminus (-1, 1)$

Table 3.1: Classification of $\mathrm{SL}(2, \mathbb{R})$ into elliptic, parabolic, and hyperbolic elements

Since every cylinder decomposition of a finite translation surface contains only finitely many cylinders, the number μ can always be chosen such that each cylinder can be subdivided, yielding a new cylinder decomposition where all cylinders share the same modulus. This will be useful for us particularly in Chapter 4.

Even though Veech groups can be hard to compute, there have been various levels of success for special types of translation surfaces. The best understood subclass of translation surfaces regarding their Veech groups are square-tiled surfaces. Unfortunately, the Veech group does not depend continuously on the translation surfaces, so we cannot extend this knowledge to all translation surfaces by arguments on square-tiled surfaces being dense in the moduli space of translation surfaces. However, it is still remarkable what can be achieved there:

Proposition 3.3.27 (Veech groups of square-tiled surfaces)
Let (X, ω) be a square-tiled surface. Then the Veech group $\mathrm{GL}^+(X, \omega)$ and $\mathrm{SL}_2(\mathbb{Z})$ share a common subgroup of finite index with each other.

Proof. This is shown in Theorem 5.5 of [GJ00]. For a general algorithm for calculating the Veech group of a square-tiled surfaces, see Corollary 2.9. of [Sch04]. $\square$

Example 3.3.28 (Eierlegende Wollmilchsau)
Let W be the Eierlegende Wollmilchsau from Example 2.3.8. It is easy to check that the parabolic elements

$$S \coloneqq \begin{pmatrix} 1 & 1 \\ 0 & 1 \end{pmatrix} \text{ and } T \coloneqq \begin{pmatrix} 1 & 0 \\ 1 & 1 \end{pmatrix}$$

are elements of $\mathrm{GL}^+(W)$ since their action stabilizes W. The same is true for $-I_2$. Since $\mathrm{GL}^+(W)$ is a group, we know that

$$\mathrm{SL}_2(\mathbb{Z}) = \langle S, T, -I_2 \rangle \subseteq \mathrm{GL}^+(W).$$

The Eierlegende Wollmilchsau W has four essential singularities. Saddle connections between those essential singularities are, without loss of generality, elements of $\mathbb{Z} + \mathrm{i}\mathbb{Z}$, since W is a square-tiled surface. Since stabilizing elements of $\mathrm{GL}_2^+(\mathbb{R})$ map saddle connections to saddle connections, we know that $\mathrm{GL}^+(W) \subseteq \mathrm{SL}_2(\mathbb{Z})$, analogously to $\mathrm{GL}^+(\mathbb{T}_i) \subseteq \mathrm{SL}_2(\mathbb{Z})$, so $\mathrm{GL}^+(W) = \mathrm{SL}_2(\mathbb{Z})$.

The next best understood class consists of finite translation surfaces, for which holonomy vectors are a powerful tool to use.

Proposition 3.3.29 (Holonomy vectors of finite translation surfaces are discrete)
Let (X, ω) be a finite translation surface. Then the *set of holonomy vectors* $H_{\mathrm{sc}} :- \mathrm{hol}\,(V_{\mathrm{sc}})$ of saddle connections in (X, ω) is discrete in $\mathbb{R}^2$.

Proof. Let $v \in \mathbb{R}^2$. Consider the set of all geodesic paths in $\overline{X}$ that begin in a singularity and have holonomy vector v. Since (X, ω) has only finitely many singularities, which are all conical, this set is finite.

For every point $x \in \overline{X}$, there exists $\varepsilon(x) > 0$ such that $B_{\varepsilon(x)}(x) \setminus \{x\}$ does not contain a singularity. Let $\tilde{\varepsilon}$ be the smallest $\varepsilon(x)$, minimizing over all $x \in E$, where E is the set of endpoints of geodesic paths, beginning in a singularity and having holonomy vector v.

By construction, there are no saddle connections ending in $B_{\tilde{\varepsilon}}(x) \setminus \{x\}$ for any such endpoint x. This is also true for any non-constant sequence of saddle connections whose holonomy vectors converge to v. Thus, v cannot be an accumulation point and the set of holonomy vectors of saddle connections H_{sc} is discrete in $\mathbb{R}^2$. □

For finite translation surfaces, the Veech group therefore must also be discrete:

Proposition 3.3.30 (Discreteness of Veech groups of finite translation surfaces)
Let (X, ω) be a finite translation surface. Then the Veech group of (X, ω) is a discrete subgroup of $\mathrm{SL}_2(\mathbb{R})$.

Proof. Proposition 3.3.17 shows that $\mathrm{GL}^+(X, \omega)$ is a subgroup of $\mathrm{SL}_2(\mathbb{R})$ for a finite translation surface (X, ω).

For finite translation surfaces of genus one, we showed discreteness in Example 3.3.24. For surfaces of higher genus, the Gauß–Bonnet formula of Proposition 3.1.10 implies the existence of at least one essential singularity. Since X is not simply connected, we find two nontrivial geodesics in $\overline{X}$ connecting our singularity to itself. These geodesics in $\overline{X}$ consist of finitely many saddle connections and therefore there are saddle connections in at least two directions.

Choose a sequence $(A_n)_{n\in\mathbb{N}} \subseteq \mathrm{GL}^+(X,\omega)$ with $A_n \to A \in \mathrm{GL}^+(X,\omega)$ and linearly independent holonomy vectors $v, w \in H_{\mathrm{sc}}$ of saddle connections in (X,ω). Since affine homeomorphisms preserve singularities and geodesic paths, A_n maps each saddle connection back to a saddle connection for each $n \in \mathbb{N}$. However, the set of holonomy vectors of saddle connections is discrete by Proposition 3.3.29.

Therefore, from $A_n v \to Av$ and $A_n w \to Aw$, it follows that for large enough $m > N$ with $N \in \mathbb{N}$, we have $A_m v = Av$ and $A_m w = Aw$. Due to the linear independence of v and w, we conclude that $A_m = A$ for $m > N$ and $\mathrm{GL}^+(X,\omega)$ is discrete. □

A large Veech group corresponds to many symmetries in the surface. A random translation surface will have no symmetry on average, so we expect the Veech group to be minimal generically.

3.4 Dynamics

In this section, we lay the groundwork for the most important concept of dynamics on translation surfaces, which will be immensely helpful for Chapters 5 and 6. One of the main goals is to express translation surfaces as suspensions of interval exchange maps which highlight the dynamical origin of a lot of work related to translation surfaces.

Given a set X, we can define a flow on X:

Definition 3.4.1 (Flow)
Let X be a set. A *flow* on X is an action of $\mathbb{R}$ on X by a map $\varphi : X \times \mathbb{R} \to X$, if

(a) for all $x \in X : \varphi(x, 0) = x$ and

(b) for all $x \in X,\ s, t \in \mathbb{R} : \varphi(\varphi(x, s), t) = \varphi(x, s + t)$.

Usually, this flow should be chosen in a way, that it preserves some structure of the underlying space.

Remark 3.4.2 (On flows)
If the set X has an additional structure, this structure is typically asked to be preserved by the action.

- Flows on topological spaces should be continuous.
- Flows on differentiable manifolds should be differentiable.

Flows on translation surfaces can be defined in several ways, we use the geodesic flow.

Definition 3.4.3 (Geodesic flow)
The *geodesic flow* $\varphi_\theta(x,t)$ on a translation surface (X,ω) in the direction $\theta \in S^1$ is defined as follows: Let v_θ be the unit vector in direction θ in $\mathbb{R}^2$. If there exists a geodesic starting in $x \in X$ and whose holonomy vector is $r \cdot v_\theta$ for $r \in \mathbb{R}$, then $\varphi_\theta(x,r)$ is defined as the endpoint of this geodesic. If there is no such geodesic, we leave $\varphi_\theta(x,t)$ undefined.

We can parametrize geodesic flows with angles:

Convention 3.4.4 (Angle versus direction)
For every $\theta \in S^1$, we can associate an angle $\alpha \in {}^{\mathbb{R}}/_{2\pi\mathbb{Z}}$ by fixing an underlying coordinate system. We therefore use the following convention: the horizontal direction to the right corresponds to the angle 0. Going around counterclockwise the direction going vertically upwards corresponds to the angle $\frac{\pi}{2}$ and so on.
In particular, we will abuse notation and sometimes talk about direction in S^1 and angles interchangeably.

Singularities can break our geodesic flow.

Remark 3.4.5 (On geodesic flows)
Geodesic flows are generally not flows on X and even less on $\overline{X}$ for a translation surface (X,ω) since $\varphi_\theta(x,t)$ is undefined when the ray in direction θ starting at x exits the surface X, that is to say, it runs into a singularity. Nevertheless, we will continue to use the notions from flows.

On finite translation surfaces, singularities are rare, so for almost all points and directions, let us define trajectories:

Definition 3.4.6 (Trajectory)
Let (X,ω) be a translation surface and φ_θ be the geodesic flow on (X,ω) in direction $\theta \in S^1$. A *trajectory* $\mathrm{tr}_{x,\theta}$ of a point $x \in X$ under φ_θ is the path

$$\mathrm{tr}_{x,\theta}\colon \mathbb{R} \to X, \quad t \mapsto \varphi_\theta(x,t),$$

as long as it is well-defined.

So now for almost any point, we can determine a trajectory on a finite translation surface. Some useful notions for the behavior of flows are given in the following way:

Definition 3.4.7 (Periodic, recurrent, ergodic, and uniquely ergodic flows)
Let (X,ω) be a translation surface and φ_θ be the geodesic flow on (X,ω) in direction $\theta \in S^1$. Let the flow be well-defined for every time for almost every point.

- The flow φ_θ is called *periodic* if all trajectories are closed or finite.
- A point $x \in X$ is called *recurrent* for φ_θ if for every neighborhood U of x and every $R \in \mathbb{R}$, there exists an $r > R$ such that $\varphi_\theta(x,r) \in U$.

- The geodesic flow φ_θ is called *recurrent* if almost every point on X is recurrent for φ_θ.
- The flow φ_θ is called *ergodic* with respect to a probability measure μ on X if
  (a) it is measure-preserving and
  (b) for all $t \in \mathbb{R}$, every measurable set $Y \subseteq X$ with $\varphi_\theta^{-1}(Y, t) = Y$ has measure 0 or 1.
- The flow φ_θ is called *uniquely ergodic* if there is exactly one invariant probability measure μ' on X under φ_θ. In this case, φ_θ is already ergodic with respect to μ' and Lebesgue.

There are several strong results concerning flows on translation surfaces that we would like to mention, although we will not provide the proofs ourselves.

Theorem 3.4.8 (Poincaré recurrence — Carathéodory)
Let X be a finite measure space and $\varphi\colon X \to X$ a measure-preserving transformation. Then φ is recurrent.

Proof. This is shown on pages 296–301 of [Car56]. □

This immediately implies the following corollary.

Corollary 3.4.9 (Poincaré recurrence on translation surfaces of finite area)
Let (X, ω) be a translation surface of finite area and φ_θ be the geodesic flow on (X, ω) in direction $\theta \in S^1$. Let the flow be well-defined for every time for almost every point. Then φ_θ is recurrent.

Proof. Theorem 3.4.8 is applicable for translation surfaces of finite area. □

An even stronger statement can be made for Veech surfaces, for whose definition we need to define lattices for subgroups of $\mathrm{SL}(2, \mathbb{R})$.

Definition 3.4.10 (Lattice)
A discrete subgroup Γ of $\mathrm{SL}(2, \mathbb{R})$ is called a *lattice* in $\mathrm{SL}(2, \mathbb{R})$ if the hyperbolic area of ${}^{\mathbb{H}}/_{\Gamma}$ is finite.

Definition 3.4.11 (Veech surface)
A translation surface (X, ω) is called a *Veech surface* if its Veech group is a lattice.

For Veech surfaces, a strong statement is known:

Theorem 3.4.12 (Veech's dichotomy — Veech)
Let (X, ω) be a finite Veech surface. Then (X, ω) satisfies Veech's dichotomy: For every direction $\theta \in S^1$, the geodesic flow φ_θ is either periodic or uniquely ergodic.

This means that for any angle θ, one of following two possibilities arises:

- All trajectories in direction θ are either periodic, or they intersect a singularity in the forward direction, as well in the backward direction and give therefore rise to saddle connections.
- No trajectory in direction θ intersects a singularity in both forward and backward directions and all infinite trajectories are uniformly distributed on X.

Proof. This is shown in [Vee89]. $\square$

Returning to flows more generally, it is not necessary to fix a direction all the time:

Remark 3.4.13 (Vertical flows)
We have seen in Lemma 3.3.5, that $\mathrm{GL}_2(\mathbb{R})$ and in particular the elliptic elements

$$R_\theta := \begin{pmatrix} \cos(\theta) & -\sin(\theta) \\ \sin(\theta) & \cos(\theta) \end{pmatrix} \text{ for } \theta \in [0, 2\pi)$$

act on the space of all translation surfaces by Möbius transformations.

Since $\det(R_\theta) = 1$, the action of R_θ is area preserving on (X, ω) and corresponds to rotating (X, ω).

$$\begin{tikzcd}
(X,\omega) \arrow[r, "R_{\frac{\pi}{2}-\theta}"] \arrow[d, "\varphi_\theta"] & R_{\frac{\pi}{2}-\theta}(X,\omega) \arrow[d, "\varphi_{\frac{\pi}{2}}"] \\
(X,\omega) \arrow[r, "R_{\frac{\pi}{2}-\theta}"] & R_{\frac{\pi}{2}-\theta}(X,\omega)
\end{tikzcd}$$

Let φ_θ be a flow in direction θ, then $R_{\frac{\pi}{2}-\theta} \circ \varphi_\theta$ corresponds to a flow on $R_{\frac{\pi}{2}-\theta}(X, \omega)$ in vertical direction upwards. On the other hand, every vertical flow can be rotated in any other direction. Since the space of translation surfaces is closed under the R_θ–action we can just study *vertical* flows, that is to say vertically upwards corresponding to the angle $\frac{\pi}{2}$, to understand flows in all directions.

Convention 3.4.14 (Vertical flows)
If we do not define the direction of a flow on a translation surface, we use the vertical flow. The same convention is used for trajectories.

Finally, we have laid the groundwork to understand translation surfaces as suspensions of interval exchange transformation. Let us first describe the origin of interval exchange transformations.

In dynamical systems, an irrational rotation is a map

$$T_\theta \colon \mathbb{R}/\mathbb{Z} \to \mathbb{R}/\mathbb{Z}, \quad x \mapsto x + \theta \mod 1,$$

where $\theta \in \mathbb{R} \setminus \mathbb{Q}$ is an irrational number. With re-scaling by a factor of 2π, this map can be understood as a circle rotation with Convention 3.4.4. Since θ is irrational, the rotation has infinite order and the map T_θ has no periodic orbits. This map is a useful toy example for dynamical systems. A generalization is given by so-called interval exchange transformations, which we want to formalize.

Definition 3.4.15 (Interval exchange transformation)
Let $n \in \mathbb{N}^+$, $\pi \in \mathrm{Sym}_n$ be a permutation of $[n] := \{1, \dots, n\}$ and $\lambda = (\lambda_1, \dots, \lambda_n)$ be a vector of positive real numbers, such that

$$\sum_{i=1}^{n} \lambda_i = 1.$$

For $i \in [n]$, let

$$a_i := \sum_{j \in [i-1]} \lambda_j \quad \text{and} \quad b_i := \sum_{j \in [\pi(i)-1]} \lambda_{\pi^{-1}(j)}.$$

Define the map

$$T_{\pi,\lambda} : [0,1) \to [0,1), \quad x \mapsto x - a_i + b_i \text{ if } x \in [a_i, a_i + \lambda_i),$$

which we call the *interval exchange transformation* of the pair (π, λ).

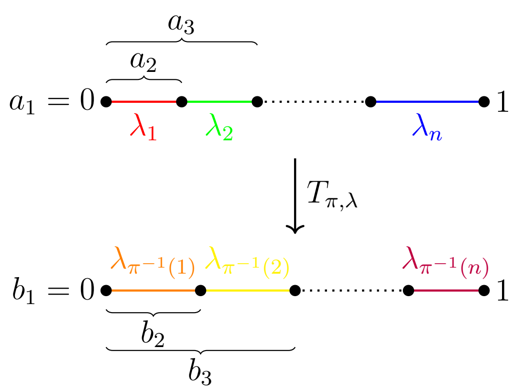

Figure 3.7: Interval exchange transformation $T_{\pi,\lambda}$

Remark 3.4.16 (On interval exchange transformations)
While the λ_i correspond to the widths of the intervals $[a_i, a_i + \lambda_i)$ into which we decompose the unit interval, $T_{\pi,\lambda}$ permutes the intervals of the form $[a_i, a_i + \lambda_i)$ according to π: the interval at position i is moved to position $\pi(i)$.

On one hand, interval exchange transformations give rise to translation surfaces:

Definition 3.4.17 (Suspension datum)
A *suspension datum* for the interval exchange transformation $T_{\pi,\lambda}$ with $\pi \in \mathrm{Sym}_n$ is a vector $\tau \in \mathbb{R}^n$ such that $\sum_{j \in [n]} \tau_j = 0$ and for every $i \in [n-1]$:

$$\sum_{j \in [i]} \tau_j > 0 \quad \text{and} \quad \sum_{j \in [i]} \tau_{\pi^{-1}(j)} < 0.$$

This suspension datum describes all lengths necessary to obtain the corresponding suspension surface.

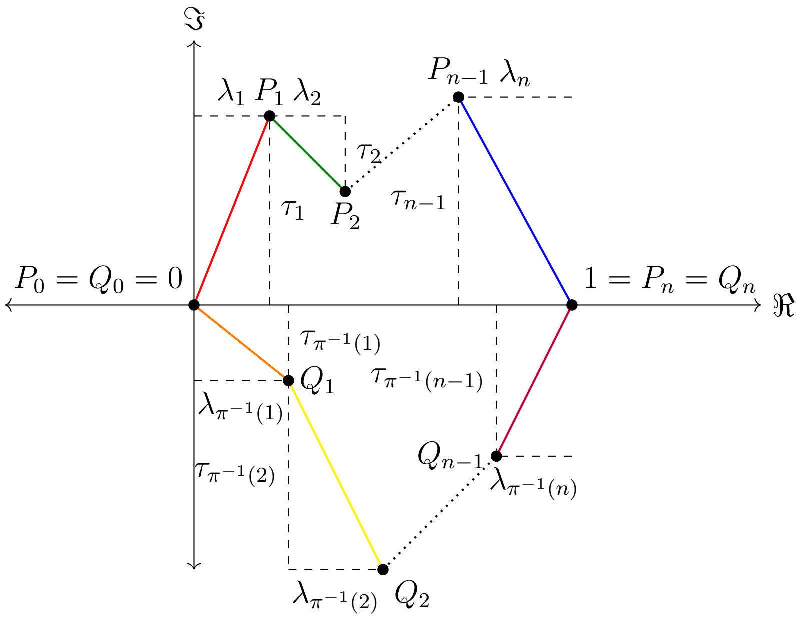

Figure 3.8: Suspension surface $S_{\pi,\lambda,\tau}$ obtained from the suspension datum $\tau \in \mathbb{R}^n$ for the interval exchange transformation $T_{\pi,\lambda}$

Definition 3.4.18 (Suspension surface)
Let $T_{\pi,\lambda}$ be an interval exchange transformation and $\tau \in \mathbb{R}^n$ a suspension datum for $T_{\pi,\lambda}$.

We construct the translation surface $S_{\pi,\lambda,\tau}$ as shown in Figure 3.8 in the following manner. Take a $2n$–gon in $\mathbb{C}$, whose vertices are cyclically ordered like

$$P_0, P_1, \dots, P_n = Q_n, Q_{n-1}, \dots Q_1.$$

Define the vertices with $P_0 = Q_0 = 0$ and for $j \in [n]$ recursively

$$P_j = P_{j-1} + \lambda_j + \tau_j \mathrm{i}, \quad Q_j = Q_{j-1} + \lambda_{\pi(j)} + \tau_{\pi(j)} \mathrm{i}.$$

By construction and the choice of the suspension datum, the first $n-1$ vertices have positive imaginary part, while the last $n-1$ edges have negative imaginary part. The resulting $2n$–gon is well-defined, non-degenerated and closed since $P_n = Q_n = 1 + 0i$. For each edge exists an opposite edge of the same length, so we constructed a finite translation surface $S_{\pi,\lambda,\tau}$.

How does $S_{\pi,\lambda,\tau}$ correlate to $T_{\pi,\lambda}$? By construction, $T_{\pi,\lambda}$ is the first return map of $S_{\pi,\lambda,\tau}$ to $[0,1]$:

Definition 3.4.19 (First return map)
Let (X,ω) be a translation surface, φ be a flow on (X,ω), and Y be a subset of X. We define the *first return time* of φ to Y as

$$r_{Y,\varphi} \colon Y \to \mathbb{R}_{>0}, \quad x \mapsto \inf \{t > 0 \mid \varphi(x,t) \in Y\}.$$

If this is well-defined for Y, we can define the *first return map* by

$$T_{Y,\varphi}\colon Y \to Y, \quad x \mapsto \varphi(x, r_{Y,\varphi}(x)).$$

Proposition 3.4.20 (Zippered rectangle)
The first return map of φ to a segment Y is an interval exchange map on the n subintervals of Y. The return times of φ are constant on each of these subintervals, which decomposes the surface $S_{\pi,\lambda,\tau}$ into n rectangles $(R_1, \dots, R_n)$, referred to as a *zippered rectangle*. The widths of these rectangles are the lengths $(\lambda_1, \lambda_2, \dots, \lambda_n)$ and the heights $(h_1, h_2, \dots, h_n)$ are the return times of φ to Y on each of the n subintervals of Y, see Figure 3.9.

Proof. This is shown in [Via06] and follows immediately from the construction of the suspension surface $S_{\pi,\lambda,\tau}$. □

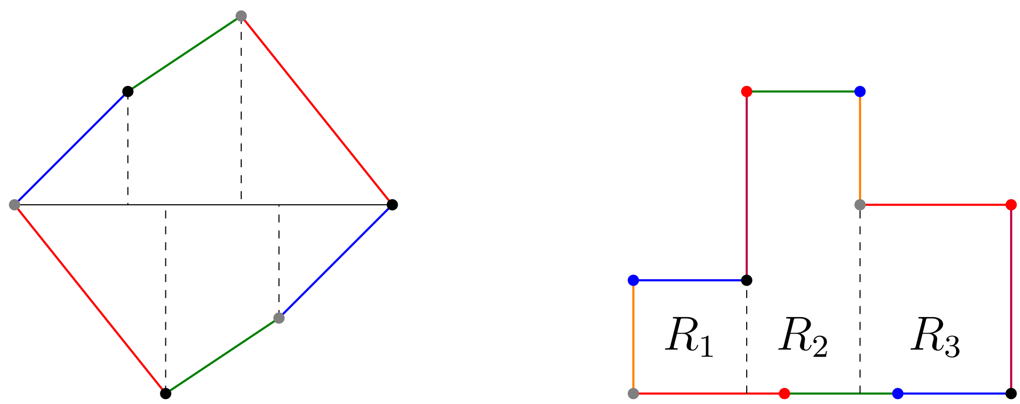

(a) Suspension surface $S_{\pi,\lambda,\tau}$ (b) Corresponding zippered rectangle

Figure 3.9: A zippered rectangle (R_1, R_2, R_3) obtained from cutting and regluing a suspension surface $S_{\pi,\lambda,\tau}$ from the interval exchange transformation of the pair (π, λ) and the suspension datum $\tau = (0.3, 0.2, -0.5)$ with permutation $\pi = (1\ 3)$, lengths $\lambda = (0.3, 0.3, 0.4)$, and heights $h = (0.3, 0.8, 0.5)$

One can obtain the zippered rectangle from $S_{\pi,\lambda,\tau}$ by cutting and regluing the shapes of $S_{\pi,\lambda,\tau}$ with negative imaginary values to those with positive imaginary values, see Figure 3.9.

On the other hand, interval exchange transformations arise naturally from translation surfaces:

Proposition 3.4.21 (Interval exchange transformation from translation surfaces)
Suppose (X, ω) is a translation surface with no vertical saddle connections. Then there exists a horizontal interval I in X such that (X, ω) can be obtained as a suspension surface from I.

Proof. This follows from [Via06]. □

3.5 Stratification

To gain a better understanding of the space of all translation surfaces, we first focus on the space of finite translation surfaces, hoping to regard infinite translation surfaces ideally as limits. To better understand the space of finite translation surfaces and classify them, it is useful to divide them according to useful properties. Due to the classification of compact surfaces, we know that the genus classifies the underlying Riemann surface. However, the singularities also have a considerable influence on the translation surface, as they can vary greatly. For example, Veech's double pentagon has genus 2 and one singularity that locally resembles a triple cover of the punctured disk, while Veech's double hexagon, also with genus 2, has two singularities, each locally resembling a double cover of the punctured disk.

At the same time, Proposition 3.1.10 provides a connection between genus and singularities, where the essential singularities can only be conical. Overall, this naturally leads to the following stratification of the space of finite translation surfaces.

Definition 3.5.1 (Partition)
Let $n \in \mathbb{N}^+$. We call a tuple $\kappa = (k_1, \ldots, k_l)$ with $1 \leq l \leq n$ elements a *partition* of n, if $n = \sum_{i=1}^{l} k_i$ and $k_i \geq 1$ for all $i \in [l]$.

Convention 3.5.2 (Ordered partition)
Let κ be a partition of n. We always order the elements of $\kappa = (k_1, \ldots, k_l)$, such that $k_i \geq k_{i+1}$ for all $i \in [l]$.

We fix a subspace of the moduli space of translation surfaces by the singularities that occur.

Definition 3.5.3 (Stratum)
Let $\kappa = (k_1, \ldots, k_l)$ be a partition of $2g - 2$. The *stratum* $\mathcal{H}(\kappa)$ of translation surfaces is defined as the set of all isomorphism classes of finite translation surfaces (X, ω) of genus g with l singularities of orders $k_1, \ldots, k_l$. The subset of translation surfaces of *unit area* is denoted by $\mathcal{H}_1(\kappa)$.

Remark 3.5.4 (Unnamed singularities)
Having a translation surface in $\mathcal{H}(\kappa)$ does not retain information about the labeling or names of the singularities.

Remark 3.5.5 (Unit area)
Every finite translation surface of area A can be scaled by a factor of $\frac{1}{\sqrt{A}}$. This scaled translation surface has area 1 and the same topological data, the same singularity-related data, the same flow behavior (after re-scaling the speed of the flow) and the same Veech group as the non-scaled finite translation surface. It is therefore quite common to only study unit-area translation surfaces.

There are only finitely many partitions of $2g - 2$. The extreme cases, where one singularity has all the excess angle of $(4g - 4)\pi$ and where there are $2g - 2$ essential singularities in total, each with the smallest excess angle of 2π, were given their own names. In the space of translation surfaces, if there are at least two singularities, one can degenerate a translation surface by letting two singularities get arbitrarily close and then joining them together. This insight will be in particular important for Chapter 7. By doing so, we obtain a translation surface with less singularities as a point in the boundary of the stratum. The boundary is a lower-dimensional object and rare in the sense of some measure, which we also will define in Chapter 7. This behavior explains the name of the two most extreme cases:

Definition 3.5.6 (Minimal stratum)
The stratum $\mathcal{H}\,(2g-2)$ is called the *minimal stratum* of genus g. Its translation surfaces contain one singularity of order $2g-2$.

Definition 3.5.7 (Principal stratum)
The stratum $\mathcal{H}\,(1^{2g-2}) = \mathcal{H}(\underbrace{1,\ldots,1}_{2g-2})$ is called the *principal stratum* of genus g. Its translation surfaces contain $2g-2$ singularities of order 1.

Sometimes we have non-essential singularities like in the case of tori.

Convention 3.5.8 (Tori)
In the case of the torus, so for example $\mathbb{T}_{\mathrm{i}}$, where we only have a marked point, we still attribute a stratum to these surfaces and write $\mathbb{T}_{\mathrm{i}} \in \mathcal{H}\,(0) = \Omega M_1 = {\mathrm{GL}_2^+(\mathbb{R})} \big/ {\mathrm{PSL}_2(\mathbb{Z})}$.

We now assign the corresponding strata to selected examples of translation surfaces.

Example 3.5.9 (Strata)

- Veech's double n–gons of Example 2.1.6 are elements of the corresponding minimal stratum for odd n, so $\mathbb{V}_n \in \mathcal{H}\,(n-3)$. For even n, Veech's double n–gons are elements of $\mathcal{H}\left(\frac{n-4}{2}, \frac{n-4}{2}\right)$.
- The L-shape origami $L_{2,2}$ of Example 2.3.3 is an element of the same stratum as Veech's double pentagon $\mathbb{V}_5$: $L_{2,2} \in \mathcal{H}\,(2)$.
- The Eierlegende Wollmilchsau W of Example 2.3.8 has four singularities of multiplicity 2, so $W \in \mathcal{H}\,(1,1,1,1)$.

Strata can be globally complicated spaces, which are hard to understand generally as their dimension, connectivity and even more highly depend on the underlying partition. However, they can be understood well locally:

Remark 3.5.10 (Local picture)
Fix a translation surface $(X_0, \omega_0) \in \mathcal{H}(\kappa)$ with singularities $\Sigma_0 = \{\sigma_1, \ldots, \sigma_l\}$. Choose a basis of cycles for the relative homology $H_1(\overline{X_0}, \Sigma_0; \mathbb{Z})$, in such a way, that they are each represented by a saddle connection in (X_0, ω_0). This is possible, since each path between singularities on (X_0, ω_0) is homotopic to a chain of saddle connections.

In the polygonal picture of (X_0, ω_0) for example, we can choose some sides of our polygons. We can then locally transform these edges by changing the length and orientation of these edges or in other words the homology vectors of the corresponding saddle connections. Since we want to obtain a translation surface of the same stratum again, we are restricted in our deformations. In particular, we cannot degenerate our chosen set of saddle connections nor add new elements. Furthermore, the surface needs to stay a translation surface. So glued partner edges need to adjust their length accordingly.

In the case of the tori $\mathbb{T}_\tau$, the homology vector of $\tau \in \mathbb{H}$ is the only free parameter if we fix the base edge from 0 to 1, since the other two opposite sides are fixed by τ as well.

For any translation surface (X, ω) obtained locally by changing (X_0, ω_0), we get local coordinates for (X, ω) near (X_0, ω_0) by keeping track of the homology vectors $\operatorname{hol}\left(\overline{\sigma_i \sigma_j}\right)$ of our chosen basis of saddle connections, see Figure 7.1. These vectors are called the *relative periods* of ω by construction, since $\operatorname{hol}\left(\overline{\sigma_i \sigma_j}\right) = \int_{\sigma_i}^{\sigma_j} \omega$.

So, locally our strata looks like Euclidean space, making it a manifold again.

Lemma 3.5.11 (Locally Euclidean)
Let $\mathcal{H}(\kappa)$ be a stratum of translation surfaces of genus g with singularities of order $\kappa = (k_1, \ldots, k_l)$. Then the neighborhood around each point in the interior of $\mathcal{H}(\kappa)$ is homeomorphic to $\mathbb{R}^{4g+2l-2}$.

Proof. We have seen in Remark 3.5.10, that we get relative periods for each base point (X_0, ω_0) in the interior of $\mathcal{H}(\kappa)$. So, we get a domain in the space of relative cohomology $H^1(X_0, \Sigma_0; \mathbb{C})$ as a local coordinate chart, where $\mathbb{R}^{4g+2l-2} \cong H^1(X_0, \Sigma_0; \mathbb{C})$ by [KZ03]. □

The dimension of $\mathcal{H}(\kappa)$ equates to the dimension of these neighborhoods which can be calculated by:

Corollary 3.5.12 (Dimension)
Let $\mathcal{H}(\kappa)$ be a stratum of translation surfaces of genus g and l singularities. Locally the real dimension as a vector space over $\mathbb{R}$ and therefore the real dimension of the manifold is

$$\dim_{\mathbb{R}} \mathcal{H}\left(\kappa\right) = 4g + 2l - 2.$$

Proof. This follows immediately with Lemma 3.5.11. □

In this way, we can talk about distance of translation surfaces in their respective strata by looking at minimal rectifiable paths on local coordinates. We can also talk more generally about the topology of each stratum.

In general, the strata $\mathcal{H}_1\left(\kappa\right)$ are not connected. To better understand $\mathcal{H}_1\left(\kappa\right)$, before finishing this chapter, we want to classify the connected components. For this, we need the so-called parity of spin structure.

Before we can define the invariant parity of spin structure, we first need to introduce the term index.

Definition 3.5.13 (Index)
Let (X, ω) be a translation surface and γ be a smooth simple curve on X. We define the *index* $\operatorname{ind}(\gamma) \in \mathbb{N}$ the following way: Choose some foliation (for example the horizontal foliation) on X. The total change of the angle between the vector tangent to the curve and the vector tangent to the chosen foliation then equals $2\pi \cdot \operatorname{ind}(\gamma)$.

Since X is flat everywhere, the change in total angle does not depend on the chosen foliation. Our index measures the integral of the absolute value of the change of angle, while following its path and therefore is equal to the degree of the corresponding Gauß map.

Definition 3.5.14 (Canonical basis)
Let (X, ω) be a translation surface of genus g with singularities Σ, all of which have an even order. A symplectic homology basis $\{a_i, b_i \mid i \in [g]\}$ of $H_1(\overline{X}, \Sigma; \mathbb{Z})$ is called a *canonical basis*, if for all $i, j \in [g]$, it holds:

$$\iota(a_i, a_j) = \iota(b_i, b_j) = 0, \quad \iota(a_i, b_j) = \chi_{\{i=j\}},$$

where $\iota(\cdot, \cdot)$ denotes the intersection form on $H_1(\overline{X}, \Sigma; \mathbb{Z})$.

Since all singularities have an even order, we can actually choose a symplectic basis. The canonical basis for a finite translation surface (X, ω) is not unique, but can be generated by the Gram–Schmidt process from any symplectic homology basis. The Gram–Schmidt process keeps the symplectic structure and therefore yields a symplectic canonical basis.

Convention 3.5.15 (Curves and homology elements)
Let (X, ω) be a translation surface with singularities Σ. Choose a canonical basis $\{a_i, b_i \mid i \in [g]\}$ of $H_1(\overline{X}, \Sigma; \mathbb{Z})$. Consider a collection of smooth closed curves representing the chosen basis and denote them by the same symbols $\{a_i, b_i \mid i \in [g]\}$. With this correspondence, we abuse notation and write $a \in H_1(\overline{X}, \Sigma; \mathbb{Z})$ and a is a curve on X at the same time.

Definition 3.5.16 (Parity of the spin structure)
Let (X, ω) be a finite translation surface of genus g with singularities Σ, all of which have an even order and let $\{a_i, b_i \mid i \in [g]\}$ be a canonical basis of $H_1(\overline{X}, \Sigma; \mathbb{Z})$. We define the *parity of the spin structure* $\psi(X, \omega)$ by

$$\psi(X, \omega) \coloneqq \sum_{i=1}^{g} (\operatorname{ind}(a_i) + 1)(\operatorname{ind}(b_i) + 1) \mod 2.$$

The parity of the spin structure does not depend on the basis.

Lemma 3.5.17 (Independence for the parity of the spin structure)
The parity of the spin structure is independent of the choice of representatives and the choice of the canonical basis.

Proof. This is shown in [Joh80], where further background information on spin structures is available. □

Additionally, the parity of spin structure does not change under the action of $\mathrm{GL}_2^+(\mathbb{R})$:

Lemma 3.5.18 (Invariance of the $\mathrm{GL}_2^+(\mathbb{R})$–action)
The parity of spin structure $\psi(X,\omega)$ is invariant under transformation by the $\mathrm{GL}_2^+(\mathbb{R})$–action.

Proof. This is shown in [KZ03]. □

Using the independence of the spin structure's parity and the invariance under the $\mathrm{GL}_2^+(\mathbb{R})$–action, Kontsevich and Zorich demonstrated the classification of the connected components in strata with only even singularities, depending on the underlying parity of the spin structure. For a complete classification, we furthermore need the notion of hyperelliptic.

Definition 3.5.19 (Hyperelliptic)
We call a translation surface $(X,\omega) \in \mathcal{H}(2g-2)$ *hyperelliptic*, if the hyperelliptic involution τ acts on (X,ω) by $\tau(\omega) = -\omega$.

We call a translation surface $(X,\omega) \in \mathcal{H}(g-1, g-1)$ with singularities $\{\sigma_1, \sigma_2\}$ hyperelliptic, if the hyperelliptic involution τ acts on (X,ω) by $\tau(\omega) = -\omega$ and

$$\tau\colon \sigma_1 \mapsto \sigma_2, \quad \sigma_2 \mapsto \sigma_1.$$

The different types of connected components for strata will be of the following types:

Definition 3.5.20 (Hyperelliptic, even and odd strata)
Let $\mathcal{H}(\kappa)$ be a stratum of finite translation surfaces.

- Define $\mathcal{H}^{\mathrm{hyp}}(\kappa)$ as the subset of $\mathcal{H}(\kappa)$, whose elements are hyperelliptic.
- Define $\mathcal{H}^{\mathrm{nonhyp}}(\kappa)$ as the subset of $\mathcal{H}(\kappa)$, whose elements are not hyperelliptic.

Furthermore, let all elements of κ be even, in this case:

- Define $\mathcal{H}^{\mathrm{even}}(\kappa)$ as the subset of $\mathcal{H}(\kappa)$, whose elements have an even spin structure parity.
- Define $\mathcal{H}^{\mathrm{odd}}(\kappa)$ as the subset of $\mathcal{H}(\kappa)$, whose elements have an odd spin structure parity.

Remark 3.5.21 (Unit area)
The subsets of translation surfaces with unit area are denoted by $\mathcal{H}_1^{\cdot\cdot}(\kappa)$ analogously.

However, which component really exists is a bit more complicated, but can be summarized by:

Theorem 3.5.22 (Classification of connected components in the stratification — Kontsevich and Zorich)
Let $\mathcal{H}(\kappa)$ be the stratum of finite translation surfaces of genus g and κ be a partition of $2g-2$ with singularities $\Sigma = \{\sigma_1, \ldots \sigma_l\}$ of order $\mathrm{ord}(\sigma_i) = k_i$.

1. If $g = 1$, the stratum $\mathcal{H}(0)$ is connected.
2. If $g = 2$, all translation surfaces are hyperelliptic and $\mathcal{H}(2)$ and $\mathcal{H}(1,1)$ are connected.
3. If $g = 3$, only hyperelliptic translation surfaces can have even parity of the spin structure and we get the following decomposition in connected components:
   - For $\kappa = (4) : \mathcal{H}(4) = \mathcal{H}^{\mathrm{hyp}}(4) \sqcup \mathcal{H}^{\mathrm{odd}}(4)$.
   - For $\kappa = (2,2) : \mathcal{H}(2,2) = \mathcal{H}^{\mathrm{hyp}}(2,2) \sqcup \mathcal{H}^{\mathrm{odd}}(2,2)$.

   The other strata $\mathcal{H}(3,1), \mathcal{H}(2,1,1), \mathcal{H}(1,1,1,1)$ are connected.
4. If $g \geq 4$:
   (a) If $\kappa = (2g-2)$, there are three connected components:
   $$\begin{aligned}\mathcal{H}(2g-2) &= \mathcal{H}^{\mathrm{hyp}}(2g-2) \sqcup \mathcal{H}^{\mathrm{nonhyp}}(2g-2) \\ &= \mathcal{H}^{\mathrm{hyp}}(2g-2) \sqcup \mathcal{H}^{\mathrm{even}}(2g-2) \sqcup \mathcal{H}^{\mathrm{odd}}(2g-2).\end{aligned}$$
   (b) If $\kappa = (g-1, g-1)$:
   - If g is even, there are two connected components:
   $$\mathcal{H}(g-1,g-1) = \mathcal{H}^{\mathrm{hyp}}(g-1,g-1) \sqcup \mathcal{H}^{\mathrm{nonhyp}}(g-1,g-1).$$
   - If g is odd, there are three connected components:
   $$\begin{aligned}\mathcal{H}(g-1,g-1) &= \mathcal{H}^{\mathrm{hyp}}(g-1,g-1) \sqcup \mathcal{H}^{\mathrm{nonhyp}}(g-1,g-1) \\ &= \mathcal{H}^{\mathrm{hyp}}(g-1,g-1) \sqcup \mathcal{H}^{\mathrm{even}}(g-1,g-1) \sqcup \mathcal{H}^{\mathrm{odd}}(g-1,g-1).\end{aligned}$$
   (c) If $(g-1,g-1) \neq \kappa \neq (2g-2)$:
   - If κ only contains even elements, there are two connected components:
   $$\mathcal{H}(\kappa) = \mathcal{H}^{\mathrm{even}}(\kappa) \sqcup \mathcal{H}^{\mathrm{odd}}(\kappa).$$
   - If κ contains an odd element, $\mathcal{H}(\kappa)$ is connected.

Analogously for strata of translation surfaces with unit area.

Proof. This is shown in [KZ03]. □

Before ending this chapter, let us quickly denote some extended strata, which can be put together with additional data.

Similar to Convention 3.5.8, we often encounter additional marked points on translation surfaces, especially in the construction of Chapter 7, where we also encounter spaces of disconnected translation surfaces.

Definition 3.5.23 (Strata of translation surfaces with marked points)
Let $\kappa = (k_1, \ldots, k_l)$ be a partition of $2g-2$ and $0^z = (0, \ldots, 0)$ be a z–tuple. Define $\tilde{\kappa} := \kappa \oplus 0^z$ as the concatenation of κ with 0^z. The *stratum* $\mathcal{H}(\tilde{\kappa})$ of translation surfaces with marked points is defined as the set of all equivalence classes of finite translation surfaces (X, ω) of genus g with l singularities of orders $k_1, \ldots, k_l$ and z marked points.

Convention 3.5.24 (Restricted subsets)
Subsets of unit area, even/odd spin parity and more on strata with marked points are denoted analogously to the normal strata.

Remark 3.5.25 (Named marked points)
The marked points on each translation surface are assumed to be named.

Our dimension formula can be easily extended.

Lemma 3.5.26 (Dimension)
Let $\mathcal{H}(\kappa)$ be a stratum of translation surfaces (with marked points) of genus g, l singularities and z marked points. Locally, the dimension as a vector space over $\mathbb{R}$ and therefore the real dimension of the manifold is

$$\dim_{\mathbb{R}} \mathcal{H}\left(\kappa \oplus 0^z\right) = 4g + 2l + 2z - 2.$$

Proof. Since the marked points on each translation surface are named, a stratum with at least one marked point is a fiber bundle over the corresponding stratum with one less marked point and the underlying translation surface as a fiber, so

$$\dim_{\mathbb{R}} \mathcal{H}\left(\kappa \oplus 0^z\right) = \dim_{\mathbb{R}} \mathcal{H}\left(\kappa \oplus 0^{z-1}\right) + 2.$$

Thus after z iterations:

$$\dim_{\mathbb{R}} \mathcal{H}\left(\kappa \oplus 0^z\right) = \dim_{\mathbb{R}} \mathcal{H}\left(\kappa\right) + z \cdot 2 = 4g + 2l - 2 + 2z. \qquad \square$$

For disconnected surfaces we define:

Definition 3.5.27 (Strata of disconnected translation surfaces)
For $i \in [m]$, where $m \in \mathbb{N}^+$, let $\kappa_i = (k_{i,1}, \ldots, k_{i,l_i})$ be partitions of $2g_i - 2$. Define

$$\kappa' := \bigsqcup_{i=1}^{m} \kappa_i$$

as the union of $\{\kappa_i\}_{i\in[m]}$. The *stratum* $\mathcal{H}(\kappa')$ of m disconnected translation surfaces is defined as the set of all equivalence classes of m disconnected finite translation surfaces $\{(X_i,\omega)\}_{i\in[m]}$ of genus g_i respectively with l_i singularities of orders $k_{i,1},\ldots,k_{i,l_i}$:

$$\mathcal{H}(\kappa') = \prod_{i=1}^{m} \mathcal{H}(\kappa_i).$$

In this way, the dimension needs to be the sum of the dimension of the separated spaces, so

$$\dim_{\mathbb{R}} \mathcal{H}\left(\kappa'\right) = \sum_{i=1}^{m} \dim_{\mathbb{R}} \mathcal{H}\left(\kappa_i\right).$$

Remark 3.5.28 (Marked points)
We combine Definitions 3.5.23 and 3.5.27 and allow strata of disconnected translations surfaces with marked points.

Remark 3.5.29 (Named surfaces)
The different translation surfaces in each stratum of disconnected translation surfaces are assumed to be named.

Convention 3.5.30 (Restricted subsets)
Restricted subsets of unit area, even/odd spin parity and more on strata of disconnected translation surfaces are denoted analogously.

Example 3.5.31 (Cutting a translation surface into two)
In the space $\mathcal{H}\left(2,0\sqcup 2,0\right)$, each point represents two translation surfaces of genus 2, each with one marked point and a singularity of order 2.

Part II

An asymptotic construction

4 Hooper–Thurston–Veech cut

There exists a special kind of infinite translation surfaces, namely Hooper–Thurston–Veech surfaces, which can be constructed from an infinite graph. In this chapter, we cut this graph to generate a sequence of finite graphs, which then can be used to construct finite Hooper–Thurston–Veech surfaces with the classical Thurston–Veech construction from the induced subgraphs. This approach yields a sequence of Veech groups of Bouillabaisse surfaces, whose parabolic elements approach the parabolic elements in the Veech group of the initial Hooper–Thurston–Veech surface. For more details on infinite Hooper–Thurston–Veech surfaces, refer to [DHV24].

4.1 Hooper–Thurston–Veech surfaces

We start this chapter by providing a brief introduction to why Hooper–Thurston–Veech surfaces have garnered significant attention and utility in the study of translation surfaces. A key feature that makes these surfaces particularly powerful is the size and structure of their Veech groups, which are known to contain a freely generated subgroup.

Definition 4.1.1 (Hooper–Thurston–Veech surface)
A translation surface is called a *Hooper–Thurston–Veech surface* if it admits two cylinder decompositions in noncollinear directions, such that all cylinders have the same modulus. The common modulus μ of the cylinders is called the *modulus* of the Hooper–Thurston–Veech surface.

Remark 4.1.2 (On Hooper–Thurston–Veech surfaces)
It is not necessary for the cylinder decomposition in Definition 4.1.1 to be maximal. The choice to not define Hooper–Thurston–Veech surfaces by maximal cylinders allows us to use this definition for surfaces which combinatorially are close to having the same modulus in each maximal cylinder.

For surfaces to be combinatorially close to having the same modulus in each maximal cylinder, we mean that they have a commensurable modulus, see Definition 3.3.25. The concept of commensurability is useful to construct Hooper–Thurston–Veech surfaces, as shown by the following lemma.

Lemma 4.1.3 (Commensurability implies Hooper–Thurston–Veech)
Let (X, ω) be a translation surface with two maximal cylinder decompositions in noncollinear directions. If all maximal cylinder moduli are commensurable, then (X, ω) is a Hooper–Thurston–Veech surface.

Proof. Without loss of generality, let the two maximal cylinder decompositions in non-collinear directions be in horizontal and vertical direction. We can achieve this by first rotating (X, ω) until the first direction is horizontal. We can then multiply by some parabolic element, such that the second direction becomes vertical.

Let $\{H_i\}_{i \in I}$ and $\{V_j\}_{j \in J}$ be the horizontal and vertical cylinder decomposition of (X, ω). Let $\tilde{\mu}$ be a common divisor of the inverse moduli. Then for each horizontal cylinder H_i, there exists an $m_i \in \mathbb{N}$, such that $\frac{1}{m(H_i)} = m_i \cdot \tilde{\mu}$ and for each vertical cylinder V_j, there exists a $\tilde{m}_j \in \mathbb{N}$, such that $\frac{1}{m(V_j)} = \tilde{m}_j \cdot \tilde{\mu}$.

A division of each horizontal cylinder H_i into m_i different cylinders of equal modulus $\frac{1}{\tilde{\mu}}$ (likewise the vertical cylinders) yields new cylinder decompositions $\{\tilde{H}\}_{i \in \tilde{I}}$ and $\{\tilde{V}\}_{j \in \tilde{J}}$ with common modulus $\frac{1}{\tilde{\mu}}$. Therefore (X, ω) is a Hooper–Thurston–Veech surface. □

The reason we are interested in Hooper–Thurston–Veech surfaces is that they allow for a relatively large group as a subgroup of their Veech group.

Definition 4.1.4 (The group G_λ)
For every $\lambda \in \mathbb{R}$, we define G_λ as the subgroup of $\mathrm{SL}_2(\mathbb{R})$ generated by

$$h_\lambda := \begin{pmatrix} 1 & \lambda \\ 0 & 1 \end{pmatrix} \text{ and } v_\lambda := \begin{pmatrix} 1 & 0 \\ \lambda & 1 \end{pmatrix}.$$

Proposition 4.1.5 (The group G_λ is a subgroup)
If (X, ω) is a Hooper–Thurston–Veech surface of modulus $\frac{1}{\lambda}$ with $\lambda \geq 2$, then G_λ is a conjugated free subgroup of the Veech group of (X, ω).

Proof. Let (X, ω) be a Hooper–Thurston–Veech surface of modulus $\frac{1}{\lambda}$, with a horizontal and vertical cylinder decomposition $\{H_i\}_{i \in I}$ and $\{V_j\}_{j \in J}$ in (X, ω), such that each cylinder has modulus $m(H_i) = \frac{1}{\lambda} = m(V_j)$. From Proposition 3.3.26, we know of the existence of an affine automorphism acting on the horizontal direction that fixes the boundaries of the cylinders with derivative $\begin{pmatrix} 1 & \lambda \\ 0 & 1 \end{pmatrix}$. Rotating (X, ω) by $\frac{\pi}{2}$ in either direction (without loss of generality counterclockwise), swaps horizontal and vertical direction, such that Proposition 3.3.26 for $\begin{pmatrix} 0 & -1 \\ 1 & 0 \end{pmatrix} (X, \omega)$ yields the existence of an affine automorphism acting as a Dehn twist on the horizontal direction that fixes the boundaries of the cylinders with derivative $\begin{pmatrix} 1 & \lambda \\ 0 & 1 \end{pmatrix}$. Therefore (X, ω) has an affine automorphism in vertical direction by Proposition 3.3.23 with derivative

$$\begin{pmatrix} 0 & -1 \\ 1 & 0 \end{pmatrix} \begin{pmatrix} 1 & \lambda \\ 0 & 1 \end{pmatrix} \begin{pmatrix} 0 & 1 \\ -1 & 0 \end{pmatrix} = \begin{pmatrix} 1 & 0 \\ -\lambda & 1 \end{pmatrix}.$$

This also implies the existence of the inverse element as an affine automorphism in vertical direction with derivative $\begin{pmatrix} 1 & 0 \\ -\lambda & 1 \end{pmatrix}^{-1} = \begin{pmatrix} 1 & 0 \\ \lambda & 1 \end{pmatrix}$.

Hence G_λ is contained in the Veech group. We now will show that G_λ is free, consider

$$U = \left\{ \begin{pmatrix} x \\ y \end{pmatrix} \in \mathbb{Z}^2 \;\middle|\; |x| > |y| \right\} \text{ and}$$
$$L = \left\{ \begin{pmatrix} x \\ y \end{pmatrix} \in \mathbb{Z}^2 \;\middle|\; |x| < |y| \right\}.$$

The groups $\langle h_\lambda \rangle = \left\{ \begin{pmatrix} 1 & \lambda n \\ 0 & 1 \end{pmatrix} \;\middle|\; n \in \mathbb{Z} \right\}$ and $\langle v_\lambda \rangle = \left\{ \begin{pmatrix} 1 & 0 \\ \lambda n & 1 \end{pmatrix} \;\middle|\; n \in \mathbb{Z} \right\}$ are nontrivial subgroups of $\mathrm{SL}_2(\mathbb{R})$ with order greater than 2 that act on U and L with $MU \subseteq L$ for $M \in \langle v_\lambda \rangle \setminus I_2$ and $NL \subseteq U$ for $N \in \langle h_\lambda \rangle \setminus I_2$. Using the ping-pong lemma, we conclude $\langle v_\lambda, h_\lambda \rangle \cong \mathbb{F}_2$. For more general Hooper–Thurston–Veech surfaces with two cylinder decompositions in noncollinear directions, we can transform them, such that these cylinder decompositions become horizontal and vertical, respectively. Using Proposition 3.3.23, we see that the Veech group contains a free subgroup which is conjugated to G_λ. □

4.2 Graph construction

In this section, we establish a connection between graphs and Hooper–Thurston–Veech surfaces, providing us with a way to generate Hooper–Thurston–Veech surfaces. With this, we will later be able to define an explicit construction that yields an in various respects interesting approximation of infinite Hooper–Thurston–Veech surfaces using finite translation surfaces.

Definition 4.2.1 (λ–harmonic function)
Let $G = (V, E)$ be a graph of finite maximal valence. Let $A : V \times V \to \mathbb{N}$ be the associated adjacency operator. An eigenvector $h : V \to \mathbb{N}$ of A with eigenvalue λ (that is, $Ah = \lambda h$) is called a *λ–harmonic function*.

Definition 4.2.2 (Locally finite and multicurves)
Let X be a topological surface.

- A disjoint union $\alpha = \bigcup_{i \in I} \alpha_i$ of simple closed curves $\{a_i\}_{i \in I}$ with index set I is *locally finite* if for all connected compact sets K in X, the number of connected components of $K \cap \alpha$ is finite.
- A *multicurve* in X is a locally finite union $\alpha = \bigcup_{i \in I} \alpha_i$ of essential simple closed curves $\{a_i\}_{i \in I}$. Those curves do not necessarily need to be pairwise isotopic.

Definition 4.2.3 (Minimal position and filling)
Let $\alpha = \bigcup_{i \in I} \alpha_i$ and $\beta = \bigcup_{j \in J} \beta_j$ be two multicurves in the topological surface X. We say that α and β

- are in *minimal position*, if for every $\alpha_i \in \alpha$ and $\beta_j \in \beta$, $|\alpha_i \cap \beta_j|$ realizes the minimal number of intersection points between representatives in the free isotopy classes of α_i and β_j.
- *fill* X if every connected component of $X \setminus (\alpha \cup \beta)$ is an at most once-punctured disk.

Definition 4.2.4 (Configuration graph)
Let $\alpha = \bigcup_{i \in I} \alpha_i$ and $\beta = \bigcup_{j \in J} \beta_j$ be two multicurves in the topological surface X in minimal position. The *configuration graph* $\mathcal{G}(\alpha \cup \beta)$ is the bipartite graph with vertices $I \cup J$ and edges from $i \in I$ to $j \in J$ for every intersection between the curves α_i and β_j.

Theorem 4.2.5 (Hooper–Thurston–Veech construction — Hooper)
Let X be a topological surface, $\alpha = \bigcup_{i \in I} \alpha_i$ and $\beta = \bigcup_{j \in J} \beta_i$ two multicurves in minimal position that fill X. Let $h : \mathcal{G}(\alpha \cup \beta) \to \mathbb{R}_{>0}$ be a positive λ–harmonic function with $\lambda > 1$. Furthermore, the following conditions hold:

(a) The configuration graph $\mathcal{G}(\alpha \cup \beta)$ has finite degree, that is to say, there is an upper bound on the degree of the vertices in $\mathcal{G}(\alpha \cup \beta)$.

(b) For every component D of the complement of $\alpha \cup \beta$ in X, its boundary ∂D in X is connected.

(c) For every component D of the complement of $\alpha \cup \beta$ for which ∂D intersects infinitely many curves in $\alpha \cup \beta$, D is a disk without punctures.

Then, there exists a translation structure ω on X such that $M(\alpha, \beta, h) \coloneqq (X^*, \omega)$ is a Hooper–Thurston–Veech surface of modulus $\frac{1}{\lambda}$ whose horizontal cylinders have core curves $\{\alpha_i\}_{i \in I}$ and vertical cylinders have core curves $\{\beta_j\}_{j \in J}$.

Proof. This is shown in [Hoo15] and [DHV24]. □

Remark 4.2.6 (Finite-type)
If X is compact then the conditions (a), (b) and (c) in Theorem 4.2.5 are satisfied and the result follows from the regular Thurston–Veech construction, described in [Hoo13a].

Definition 4.2.7 (Bouillabaisse surface)
A translation surface obtained by Theorem 4.2.5 for compact X is called a *Bouillabaisse surface*.

Remark 4.2.8 (Etymology of Bouillabaisse surface)
The original Thurston–Veech construction for finite-type translation surfaces by [Thu88] and [Vee89] received relatively little attention for a long time. However, this changed after a traditional Bouillabaisse dinner at the Centre International de Rencontres Mathématiques (France, Marseille), when John Hamal Hubbard resuscitated the construction by explaining it to a large audience.

For the construction of a sequence of finite translation surfaces approaching an infinite one, we want to forget the underlying topological space. It is therefore useful to give an alternative construction of Hooper–Thurston–Veech surfaces only based on the associated graph structure.

Definition 4.2.9 (Ribbon structure)
Let $\mathcal{G}$ be a bipartite graph with vertices $I \sqcup J$. A *ribbon structure* on $\mathcal{G}$ is a choice for each vertex v of a cyclic ordering of the edges adjacent to v.

Theorem 4.2.10 (Graph construction — Hooper)
Let $\mathcal{G}$ be a connected bipartite graph of finite degree endowed with a ribbon structure. Then for every positive λ–harmonic function h of $\mathcal{G}$, there is a surface $M = M(\mathcal{G}, h)$ which is a Hooper–Thurston–Veech surface of modulus $\frac{1}{\lambda}$. Let α and β be the multicurves given by the core curves of the corresponding horizontal and vertical cylinder decompositions. Then $\mathcal{G}$ is the configuration graph $\mathcal{G}(\alpha \cup \beta)$.

Proof. This is shown in [Hoo15]. □

Remark 4.2.11 (Surfaces $M(\mathcal{G}, h)$ & $M(\alpha, \beta, h)$ coincide)
If we consider α and β to be the multicurves formed by the core curves of the horizontal and vertical cylinder decompositions of $M(\mathcal{G}, h)$, then $M(\mathcal{G}, h)$ is equal to the Hooper–Thurston–Veech surface $M(\alpha, \beta, h)$ given by Theorem 4.2.5.

Corollary 4.2.12 (Finite graph construction)
For every finite connected bipartite graph of finite degree endowed with a ribbon structure $\mathcal{G}$, there exists a Hooper–Thurston–Veech surface, whose cylinders' heights and circumferences can be explicitly calculated.

Proof. Let $\mathcal{G}$ be a finite connected bipartite graph of finite degree endowed with a ribbon structure. Let r and s denote the number of vertices in each partition set. Let $E \in \mathbb{N}_0^{r \times s}$, where $E_{i,j}$ is the number of edges between the i–th vertex of the first and s–th vertex of the second part. Then the adjacency matrix A of $\mathcal{G}$ is a symmetric matrix in the form $A = \begin{pmatrix} 0 & E \\ E^{\intercal} & 0 \end{pmatrix} \in \mathbb{N}_0^{(r+s)\times(r+s)}$. The biggest eigenvalue λ of A has a corresponding eigenvector $v = \begin{pmatrix} v_H \\ v_V \end{pmatrix} \in \mathbb{R}^{r+s}$. By Theorem 4.2.10, we get a Hooper–Thurston–Veech surface $M(\mathcal{G}, v)$ of modulus $\frac{1}{\lambda}$.

The length of the core curves of the horizontal and vertical cylinders are encoded in v_H and v_V correspondingly by construction. Specifically, the n–th element of v_H is the circumference of the n–th horizontal cylinder, and similarly, the n-th element of v_V is the circumference of the n–th vertical cylinder. The heights can be calculated since the sum of two cylinder heights corresponds to the circumference of the corresponding cylinder in vertical direction, except for the initial cylinder, where the heights are directly equal. □

A special case, we want to study further, are staircases. These surfaces allow a particularly nice construction for the finite Thurston–Veech construction, since we can show that our underlying matrix can be described in an alternative and numerically more efficient way.

Definition 4.2.13 (Staircase)
A *staircase* is a translation surface, which admits a maximal horizontal and vertical cylinder decomposition, such that the configuration graph of the core curves is a tree with a maximal valence of at most 2. The corresponding surface consists of rectangles, which can be drawn in such a way that it resembles a staircase like in Figure 4.1.

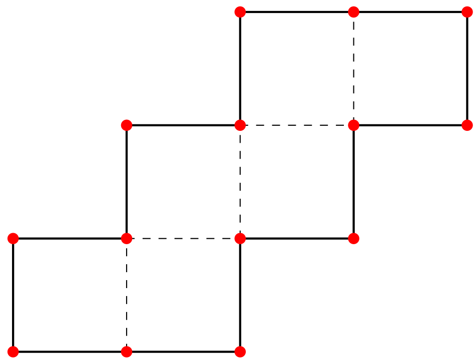

Figure 4.1: Staircase illustration with configuration graph of seven nodes

Definition 4.2.14 (Hooper–Thurston–Veech Staircase)
A *Hooper–Thurston–Veech staircase* is a Hooper–Thurston–Veech surface, which is also a staircase.

For these Hooper–Thurston–Veech staircases, we get a configuration graph of the following form.

Definition 4.2.15 (The graph $\mathcal{G}(m, \tilde{m})$)
Let $m = (m_i)_{i\in[k]} \in \mathbb{N}^k$ for $k \in \mathbb{N}$ and $\tilde{m} = (\tilde{m}_j)_{j\in[k-1]} \in \mathbb{N}^{k-1}$ or $\tilde{m} = (\tilde{m}_j)_{j\in[k]} \in \mathbb{N}^k$.
We define $\mathcal{G}(m, \tilde{m})$ as the bipartite graph with $\sum_{i=1}^{k} m_i$ vertices in one set and $\sum_{j=1}^{k-1} \tilde{m}_j$ or $\sum_{j=1}^{k} \tilde{m}_j$ vertices in the other set and edges between these sets in the form of complete bipartite subgraphs $K_{m_i,\tilde{m}_j}$ for all $(i, j) = (n + 1, n)$ for $n \in [k - 1]$ and all $(i, j) = (n, n)$ for $n \in [k - 1]$ or $n \in [k]$ respectively.

Remark 4.2.16 (Staircase configuration)
On the one hand, given a bipartite graph $\mathcal{G}(m, \tilde{m})$, we can construct a finite staircase surface with commensurable moduli in the cylinder decompositions, which is therefore a Hooper–Thurston–Veech surface. On the other hand, we can get m and $\tilde{m}$ from a finite staircase surface by sorting these multiples of the common modulus in such a way, that the corresponding cylinder of m_i and $\tilde{m}_j$ intersect.

For infinite staircases, we also need to fix some ribbon structure. The natural choice for the ribbon structure is to order the edges adjacent to each vertex in the same cyclic order as they are numbered for one partition set and in reverse order for the other partition set.

Lemma 4.2.17 (Staircase construction)
For a finite staircase obtained from $\mathcal{G}(m, \tilde{m})$, the eigenvalue equation of Corollary 4.2.12 is equivalent to the eigenvalue equation

$$Ah := \begin{pmatrix} 0 & \tilde{m}_1 & & & & & \\ m_1 & 0 & m_2 & & & & \\ & \tilde{m}_1 & 0 & \ddots & & & \\ & & m_2 & \ddots & \tilde{m}_{k-1} & & \\ & & & \ddots & 0 & m_k & \\ & & & & \tilde{m}_{k-1} & 0 & (\tilde{m}_k) \\ & & & & & (m_k) & (0) \end{pmatrix} h = \lambda h.$$

Proof. Let (X, ω) be a finite staircase obtained from $\mathcal{G}(m, \tilde{m})$. With Corollary 4.2.12, we obtain a harmonic function $Bv = \lambda v$, where B is the configuration matrix of the cylinder decomposition of (X, ω).

Notice that $A \neq B$, while B encodes the configuration graph as an adjacency matrix and is symmetric, A encodes it without doubling information, is generally not symmetric and they are generally not of the same dimension.

Linear algebra shows that the underlying eigenvalue equations for $Bv = \lambda v$ are equivalent to $Ah = \lambda h$ for finite staircase surfaces. In particular, the biggest eigenvalue coincides. □

Remark 4.2.18 (Hooper–Thurston–Veech operator)
We can generalize the adjacency matrix from the proof of Corollary 4.2.12 or the matrix from Lemma 4.2.17 on an infinite-dimensional space via an operator $\mathcal{A}$. Let A be the original matrix and $k = \operatorname{rank}(A)$. The operator $\mathcal{A}$ acts on a k–dimensional real vector space V_k linear by matrix multiplication with A.
We therefore can calculate the spectral norm $\|\mathcal{A}\|_2 = \left\|\mathcal{A}|_{V_k}\right\|_2 = \|A\|_2$ and the maximal eigenvalue $\lambda_{max}(\mathcal{A}) = \|\mathcal{A}\|_2^2$. In this way, it is easier to talk about the convergence of infinite matrices of different dimensions. After transforming a sequence of matrices to their corresponding operator, they live in the same infinite dimensional space $\mathbb{R}^{\mathbb{N}}$ and we can use classical operator theory to describe them.

4.3 Finite approximations of infinite translation surfaces

In this section, we define an explicit construction that provides a way to approximate infinite Hooper–Thurston–Veech surface in various respects using finite translation surfaces. In particular, due to [DHV24], a subgroup of the Veech group will behave well and converge in some sense, described in Theorem 4.3.3.

Definition 4.3.1 (Hooper–Thurston–Veech cut)
Let $(X, \omega) = M(\alpha, \beta, h)$ be a Hooper–Thurston–Veech surface of modulus $\frac{1}{\lambda}$ as in Theorem 4.2.5. This can be constructed from its configuration graph $\mathcal{G}(\alpha \cup \beta)$ as

in Theorem 4.2.10. Consider a connected induced subgraph $\mathcal{G}'$ of the configuration graph $\mathcal{G}(\alpha \cup \beta)$.

If there exists a λ–harmonic function h' corresponding to the maximal eigenvalue of $\mathcal{G}'$. Then the translation surface $C(\mathcal{G}') := M(\mathcal{G}', h')$ is called the *Hooper–Thurston–Veech cut* of (X, ω) induced by $\mathcal{G}'$.

Definition 4.3.2 (Growing Hooper–Thurston–Veech sequence)
A sequence of Hooper–Thurston–Veech cuts $(C(\mathcal{G}_n))_{n\in\mathbb{N}}$ is called a *growing Hooper–Thurston–Veech sequence*, if the associated partial configuration graphs fulfill $\mathcal{G}_n \subsetneq \mathcal{G}_{n+1}$ for all $n \in \mathbb{N}$.

Theorem 4.3.3 (Hooper–Thurston–Veech sequence convergence)
Let (X, ω) be an infinite Hooper–Thurston–Veech surface with configuration operator $\mathcal{A}$ and $(C(\mathcal{G}_i))_{i\in\mathbb{N}}$ be a growing Hooper–Thurston–Veech sequence of (X, ω). If $\|\mathcal{A}\| < \infty$ and $\bigcup_{i\in\mathbb{N}} \mathcal{G}_i = \mathcal{G}$, then the sequence of moduli $(\lambda_i)_{i\in\mathbb{N}}$ of the Hooper–Thurston–Veech surfaces coming from $(C(\mathcal{G}_i))_{i\in\mathbb{N}}$ converges to the modulus λ of the original Hooper–Thurston–Veech surface $M(\mathcal{G}, h)$. This yields a sequence of finite translation surfaces (X_i, ω_i) whose Veech groups contain a conjugate of G_{λ_i} with $\lambda_i \to \lambda$.

Proof. Consider the corresponding operator in each step as in Remark 4.2.18. This yields a sequence of embedded spaces $V_1 \subseteq V_2 \subseteq \ldots$ such that $\mathcal{A}_k = \mathcal{A}|_{V_k}$ converges to the Hooper–Thurston–Veech operator of our original Hooper–Thurston–Veech surface in the spectral norm, since $\bigcup_{i\in\mathbb{N}} \mathcal{G}_i = \mathcal{G}$ and $\|\mathcal{A}\| < \infty$. We therefore also know that the corresponding maximal eigenvalues also converge to the maximal eigenvalue of the original surface and we get a sequence of Hooper–Thurston–Veech cuts. Thus, the Thurston–Veech construction yields a sequence of finite translation surfaces given by the Hooper–Thurston–Veech cuts.

The biggest eigenvalue for each Hooper–Thurston–Veech cut will be at least 2, this follows more generally for Hooper–Thurston–Veech surfaces from Appendix B in [DHV24]. The Veech group of $C(\mathcal{G}_i)$ will therefore contain a conjugate of G_{λ_i} for each $i \in \mathbb{N}$ by Proposition 4.1.5. $\square$

We can use this theorem in some cases of α for baker's map surfaces from Definition 2.4.3. These surfaces were the inspiration behind this theorem.

Proposition 4.3.4 (The baker's map surface $B_{1/q}$ is a Hooper–Thurston–Veech surface)
For $\alpha = \frac{1}{q}$ with $q \in \mathbb{N}_{\geq 2}$, baker's map surfaces are Hooper–Thurston–Veech surfaces.

Proof. We use Lemma 4.1.3 and only have to show the existence of two cylinder decompositions of B_α in noncollinear directions, whose moduli are commensurable. For this, consider the two maximal cylinder decompositions obtained in the direction of ac and ac_1 as seen in Figure 4.2.

By multiplying with $M_1 := \begin{pmatrix} 1 & 0 \\ \alpha & 1 \end{pmatrix}$, we can force the cylinder decomposition in direction of ac_1 to be horizontal. The multiplication by $M_2 := \begin{pmatrix} 1 & \frac{1}{1-\alpha} \\ 0 & 1 \end{pmatrix}$ allows us to

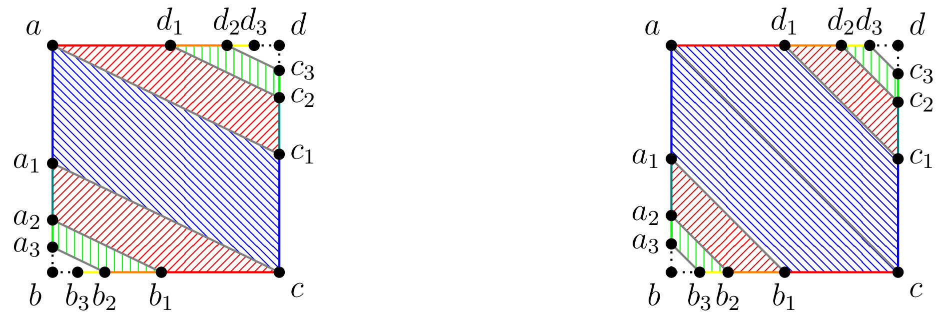

(a) Cylinder in direction ac_1 (horizontal after transformation)

(b) Cylinder in direction ac (vertical after transformation)

Figure 4.2: Two maximal cylinder decompositions in B_α

make the cylinder decomposition in direction ac to be vertically. The corresponding surfaces can be seen in Figure 4.3.

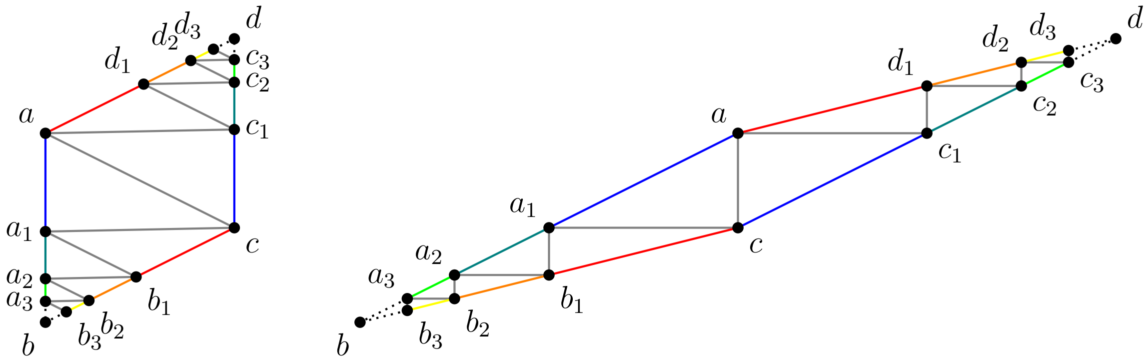

(a) $M_1 B_\alpha$

(b) $M_2 M_1 B_\alpha$

Figure 4.3: Transformation to a vertical and horizontal decomposition

By cutting and regluing, we can transform this surface into an infinite staircase, which can be seen in Figure 4.4.

The calculation of the modulus of these cylinder decompositions shows that the vertical cylinders have the same modulus of

$$\begin{aligned}\mu\left(V_j\right) &= \frac{\operatorname{height}(V_j)}{\operatorname{circumference}(V_j)} = \frac{\frac{\alpha^{j+1}}{1-\alpha}}{\alpha^{j+1}+\alpha^{j+2}} \\ &= \frac{\alpha^{j+1}}{(1-\alpha)(\alpha^{j+1}+\alpha^{j+2})} = \frac{1}{(1+\alpha)(1-\alpha)}\end{aligned}$$

for all $j \in \mathbb{N}_0$. For the horizontal cylinder, however, almost all cylinders have the same modulus of

$$\mu\left(H_k\right) = \frac{\operatorname{height}(H_k)}{\operatorname{circumference}(H_k)} = \frac{\alpha^{k+1}}{\frac{\alpha^k}{1-\alpha}+\frac{\alpha^{k+1}}{1-\alpha}}$$

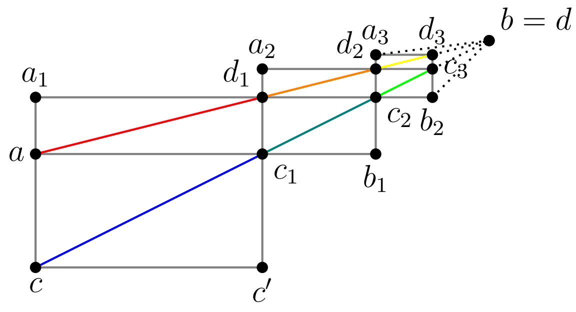

Figure 4.4: Infinite staircase presentation of $M_2 M_1 B_\alpha$

$$= \frac{\alpha^{k+1}(1-\alpha)}{\alpha^k + \alpha^{k+1}} = \frac{\alpha(1-\alpha)}{1+\alpha}$$

for all $k \in \mathbb{N}^+$ except for $\mu(H_0) = \frac{\alpha}{\frac{\alpha}{1-\alpha}} = 1 - \alpha$.

A multiplication by $M_3 = \operatorname{diag}\left(\kappa, \frac{1}{\kappa}\right)$ with $\kappa = \sqrt[4]{\alpha(1-\alpha)^2}$ yields a common modulus for almost all horizontal and all vertical cylinders, which can be seen in Figure 4.5.

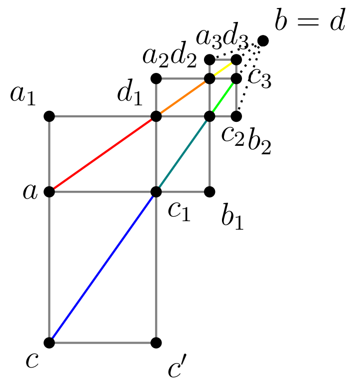

Figure 4.5: Infinite staircase presentation of $M_3 M_2 M_1 B_{\frac{1}{2}}$

Since $\alpha = \frac{1}{q}$, the modulus of H_0 is a rational multiple of the common modulus κ^2. And therefore $B_{\frac{1}{q}}$ is a Hooper–Thurston–Veech surface. $\square$

Proposition 4.3.5 (Veech group of $B_{1/q}$)
The Veech group of the baker's map surface B_α with $\alpha = \frac{1}{q}$ and $q \in \mathbb{N}_{\geq 2}$ contains a free subgroup that is conjugated in $\mathrm{SL}_2(\mathbb{R})$ to the group G_λ with $\lambda = \frac{q+1}{\sqrt{q}}$.

Proof. From the proof of Proposition 4.3.4 we know that applying

$$M := M_3 M_2 M_1 = \begin{pmatrix} \sqrt{\frac{\alpha}{1-\alpha}} & \sqrt{\frac{\alpha}{1-\alpha}} \\ \sqrt{\frac{\alpha}{1-\alpha}} & \sqrt{\frac{1}{\alpha(1-\alpha)}} \end{pmatrix} = \sqrt{\frac{1}{q-1}} \begin{pmatrix} 1 & 1 \\ 1 & q \end{pmatrix}$$

to B_α yields a Hooper–Thurston–Veech surface by construction. Its Veech group contains the free subgroup G_λ with $\lambda = \frac{q+1}{\sqrt{q}}$ by Proposition 4.1.5. Therefore, the Veech group of the baker's map surface contains the free subgroup $M^{-1} G_\lambda M$ by Proposition 3.3.23. $\square$

Remark 4.3.6 (Equality)
Chamanara showed that the Veech group of the baker's map surface B_α with $\alpha \in (0,1)$ is conjugated to a free subgroup G_λ up to $-I_2$ in [Cha04].

Example 4.3.7 (Hooper–Thurston–Veech sequence of $B_{1/2}$)
To apply Theorem 4.3.3 to the baker's map surface $B_{\frac{1}{2}}$, we first have to choose a growing Hooper–Thurston–Veech sequence. The configuration graph of $B_{\frac{1}{2}}$ is the infinite bipartite graph $\mathcal{G}(m, \tilde{m})$ by Remark 4.2.16 with $I = J = \mathbb{N}^+$, $\tilde{m}_j = 1\ \forall j \in J$, $m_i = 1\ \forall i \in I \setminus \{1\}$ and $m_1 = \frac{\alpha}{1+\alpha} = 3$, see Figure 4.6 for the first few steps.

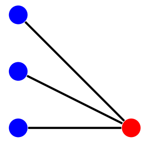

(a) $\mathcal{G}_1 = \mathcal{G}((3),(1))$

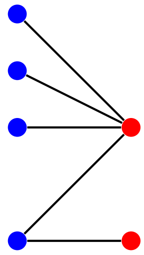

(b) $\mathcal{G}_2 = \mathcal{G}((3,1),(1,1))$

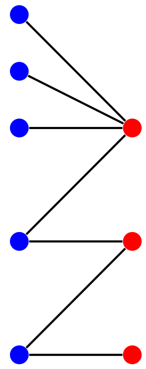

(c) $\mathcal{G}_3 = \mathcal{G}((3,1,1),(1,1,1))$

Figure 4.6: Configuration graphs for the first few steps of the Hooper–Thurston–Veech sequence of the baker's map surface

For each $n \in \mathbb{N}^+$, we define our Hooper–Thurston–Veech cut $\mathcal{G}_n$ by restricting $\mathcal{G}$ on the vertices $I = J = \{1, \ldots, n\}$. The sequence of maximal eigenvalues λ_n on the restricted $\mathcal{G}_n = \mathcal{G}\left((3, 1^{n-1}), (1^n)\right)$ is a sequence by Theorem 4.3.3 that converges to a value of $\lambda = \frac{q+1}{\sqrt{q}} = \frac{3\sqrt{2}}{2} \approx 2.121\,320\,3$, see Table 4.1 for the first few values, which are calculated with SageMath, see the code in [Rei24a].

The Veech groups of the Hooper–Thurston–Veech surfaces corresponding to a growing Hooper–Thurston–Veech sequence are not necessarily equal to G_λ up to $-I_2$ for some λ as the following example (that can occur naturally) shows.

Example 4.3.8 (Sometimes there is more)
On a genus 2 surface, consider the multicurve, chosen as in Figure 4.7.

The corresponding configuration graph is the bipartite graph $\mathcal{G}\left((1,1,1),(2,1)\right)$. This corresponds to a staircase surface such that we get the following eigenvalue equation for a λ–harmonic h:

$$\begin{pmatrix} 0 & 2 & & & \\ 1 & 0 & 1 & & \\ & 2 & 0 & 1 & \\ & & 1 & 0 & 1 \\ & & & 1 & 0 \end{pmatrix} h = \lambda h.$$

n	λ_n	$\lambda - \lambda_n$
1	$\approx 2.074\,313\,3$	$\approx 4.700\,705 \times 10^{-2}$
2	$\approx 2.111\,990\,7$	$\approx 9.329\,607 \times 10^{-3}$
3	$\approx 2.119\,165\,8$	$\approx 2.154\,561 \times 10^{-3}$
4	$\approx 2.120\,795\,9$	$\approx 5.244\,133 \times 10^{-4}$
5	$\approx 2.121\,190\,4$	$\approx 1.299\,720 \times 10^{-4}$
6	$\approx 2.121\,287\,9$	$\approx 3.240\,564 \times 10^{-5}$
7	$\approx 2.121\,312\,2$	$\approx 8.094\,866 \times 10^{-6}$
8	$\approx 2.121\,318\,3$	$\approx 2.023\,239 \times 10^{-6}$
9	$\approx 2.121\,319\,8$	$\approx 5.057\,755 \times 10^{-7}$
10	$\approx 2.121\,320\,2$	$\approx 1.264\,415 \times 10^{-7}$

Table 4.1: Numerical convergence of the Hooper–Thurston–Veech sequence for $B_{\frac{1}{2}}$

The maximal eigenvalue is given by $\lambda_{\max} = \sqrt{3+\sqrt{3}}$. Choosing $h_1 = 1$ and scaling in vertical direction by $\lambda_{\max}^{-1}$ yields a Hooper–Thurston–Veech surface $\tilde{M}$ consisting of three squares of side lengths $1, \alpha+1$ and α glued on opposite sides as illustrated in Figure 4.8 with $\alpha = 1+\sqrt{3}$.

The direction between the *Weierstrass points* W_1 and W_2 in the center of the squares with side length 1 and α, see Figure 4.8, yield a parabolic element λ_W in $\mathrm{SL}_2(\mathbb{R})$ corresponding to the cylinder decomposition with slope $\frac{1}{2}$. We get two commensurable cylinders whose boundary curve contains the Weierstrass points W_1 and W_2. In his work on Teichmüller geodesics of infinite complexity [McM03], McMullen showed the existence of a family of genus 2 surfaces whose Veech groups are infinitely generated. In particular, he showed that λ_W coming from two Weierstrass points cannot be generated by the other two parabolic elements obtained from the Thurston–Veech construction in the horizontal and vertical direction.

4.4 New infinite-type constructions

In Question 3.5.8 of [DHV24], Delecroix–Hubert–Valdez ask whether there exists an infinite translation surface with finite area whose Veech group is a lattice in $\mathrm{SL}_2(\mathbb{R})$. For Hooper–Thurston–Veech surfaces, we know that G_λ is a subgroup of the Veech group and we have seen in the previous sections that surfaces constructed this way sometimes can be infinite translation surfaces of finite area. A fundamental domain of G_λ is of the

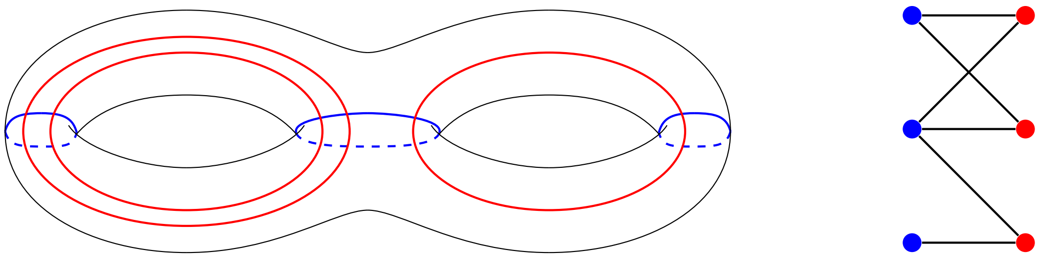

(a) Multicurves in minimal position and filling S_2

(b) Corresponding configuration graph

Figure 4.7: Hooper–Thurston–Veech surface on a double torus

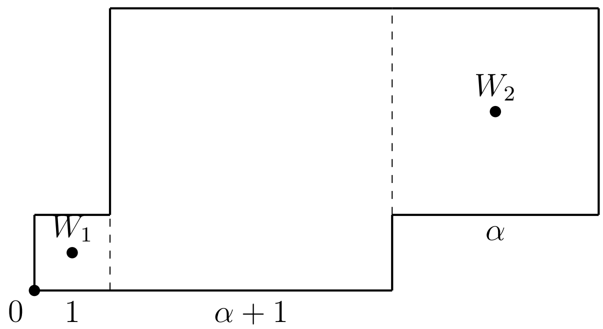

Figure 4.8: Surface $\tilde{M}$ with Weierstrass points W_1 and W_2

shape as in Figure 4.9. So, to get a lattice group which corresponds to finite hyperbolic area of the fundamental domain of the Veech group, all we would need is to close the hole between $-\frac{1}{\lambda}$ and $\frac{1}{\lambda}$.

The hole in the fundamental domain is the inspiration for Anja Randecker, Erick Gordillo, and me to investigate Hooper–Thurston–Veech surfaces with additional rotational symmetry to answer Question 3.5.8 of [DHV24]. We hope the fundamental domain of the additional elliptic element r_θ coming from the rotational symmetry will be in a form which allows the use of Poincaré's theorem, see for example Section 9.8 of [Bea95]. To obtain the total fundamental domain of $\langle h_\lambda, v_\lambda, r_\theta \rangle$, we then could just intersect the domains of G_λ and $\langle r_\theta \rangle$.

The immediate thought was to consider a 4–symmetry, given by $r_{\frac{\pi}{2}} = \begin{pmatrix} 0 & -1 \\ 1 & 0 \end{pmatrix}$. Although this approach does not yield a lattice, it serves as a useful starting point for our motivation. We realized that symmetries in the underlying configuration graph can correspond to symmetries of the Hooper–Thurston–Veech surface. So, we want an infinite configuration graph since we want an infinite translation surface with 4–fold rotational

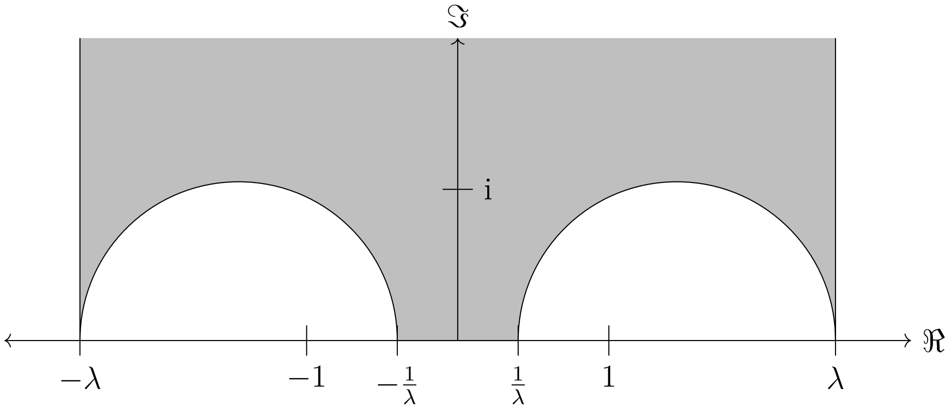

Figure 4.9: Fundamental domain of G_λ in gray for $\lambda = \frac{5}{2}$

symmetry on a bipartite graph. This 4–symmetry also needs to respect the bipartiteness of the graph, sending vertices in one part to vertices of the other part, since our parts correspond to vertical or horizontal cylinders and a rotation by $r_{\frac{\pi}{2}}$ would exchange these vertices. The graph we constructed in the end is the clover graph.

Definition 4.4.1 (Clover graph)
We call the graph given by a square or 4–cycle in the center with infinite path graphs attached to each center vertex, see Figure 4.10, the *clover graph*.

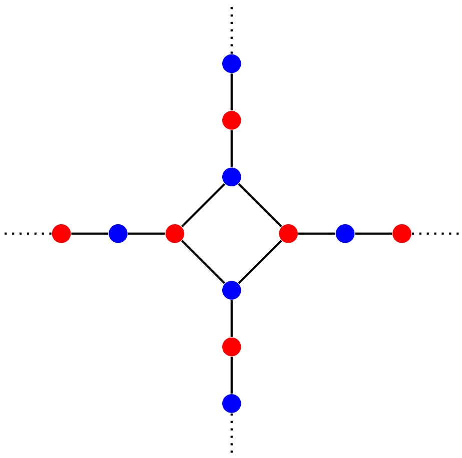

Figure 4.10: Clover graph

We can calculate the recurrence relations of the Hooper–Thurston–Veech operator and obtain $\lambda = \frac{5}{2}$. We can also create Hooper–Thurston–Veech sequences on this graph to create a sequence of finite translation surfaces. By choosing to cut off all path graphs at the same length, the argument for the symmetry on the finite graph holds as well. In total, we obtain a sequence of finite translation surfaces with 4–symmetry, whose Veech group contains r_θ and G_{λ_i}. It approaches an infinite translation surface with 4–symmetry, whose

Veech groups contains r_θ and G_λ. For those interested in the fast convergence of $\lambda_i \to \lambda$, see the code in [Rei24b]. The surface these surfaces converges to is the (un-)lucky clover surface.

Definition 4.4.2 ((Un-)lucky clover surface)
We call the surface obtained from the clover graph by the Hooper–Thurston–Veech construction the *(un-)lucky clover surface*. See Figure 4.11 for an illustration.

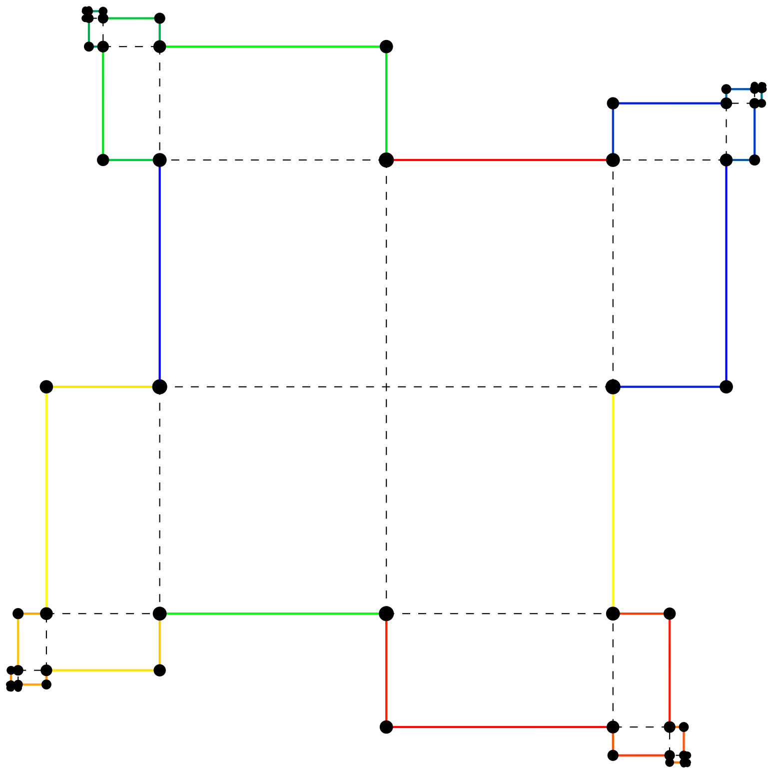

Figure 4.11: (Un-)lucky clover surface

Remark 4.4.3 (Etymology of (un-)lucky & clover)
Because of its 4–symmetry, the (un-)lucky clover surface has a clover-like look, which explains the latter part of its naming. The actual construction of the surface, however, did not start with the graph, but rather by the idea of overlapping four rotated baker's map surfaces. The problem in this construction is that it is not possible to directly align them in a suitable way. We can adjust the scaling for each cylinder and as an example decide to pick $\lambda = 3$. This value, however, was too big for the recurrence construction to converge. So, next we try $\frac{5}{2}$ and get our clover surface. As it turns out, its area converges to some finite value which we will show in Proposition 4.4.8. This is extremely lucky, every other real number does not work. The recurrence relations for the Hooper–Thurston–Veech construction produce negative values for the cylinder lengths when the value of λ is below $\frac{5}{2}$, while the lengths diverge for values of λ above $\frac{5}{2}$. Now to the unlucky part of this story: it sadly is not an answer to the original question. By construction this is not

a suitable candidate for a lattice Veech group since G_λ is a finite index subgroup of this Veech group.

Before we show that the clover surface is a new example of an infinite translation surface with finite area, let us understand staircase arms.

Definition 4.4.4 (Staircase arm)
The subsurface obtained from the Hooper–Thurston–Veech constructions of a one-sided infinite path is an infinite staircase and shall be denoted as a *staircase arm*.

The clover surface has four intersecting staircase arms.

Remark 4.4.5 (Staircase arm data)
Since a staircase arm is constructed as the subsurface of a Hooper–Thurston–Veech construction of a one-sided infinite path, the infinite staircase can be described as the one-sided infinite sequence of rectangles $(R_n)_{n\in\mathbb{N}_0}$. Without loss of generality, let the first two rectangles be glued together vertically. So R_0 will have height h_0 with width v_0 and R_1 will have height h_1 with width v_0. Continuing the gluing patterns, we see that rectangle R_{2n} will have height h_n with width v_n and R_{2n+1} will have height h_n with width v_{n+1}. The sequences $h, v \in \mathbb{R}_{>0}^{\mathbb{N}_0}$ encode the data of a staircase arm.

The staircase arm data is already given for some initial value v_0, h_0 since the rest can be calculated recursively.

Lemma 4.4.6 (Staircase arm recurrence)
Consider a staircase arm of a Hooper–Thurston–Veech surface of modulus $\frac{1}{\lambda}$ and encode the horizontal and vertical length data by $h, v \in \mathbb{R}_{>0}^{\mathbb{N}_0}$ as in Remark 4.4.5. Then for $i \in \mathbb{N}_0$

$$v_{i+1} = \lambda \cdot h_i - v_i, \quad h_{i+1} = \lambda \cdot v_{i+1} - h_i.$$

Proof. Since each horizontal cylinder has a modulus of $\frac{1}{\lambda}$, we know that for every $i \in \mathbb{N}_0$:

$$\frac{1}{\lambda} = \frac{v_{i+1} + v_i}{h_i}.$$

Analogously for the vertical cylinders, except that because of the asymmetry in the definition, where we assumed to start in horizontal direction, we get

$$\frac{1}{\lambda} = \frac{h_{i+1} + h_i}{v_{i+1}}.$$ □

So, a staircase arm is already encoded by $(\lambda, v_0, h_0) \in \mathbb{R}_{>0}^3$. We can also read the area of a staircase arm from this data.

Lemma 4.4.7 (Staircase arm area)
Let X be a staircase arm of a Hooper–Thurston–Veech surface encoded by (λ, v_0, h_0). Then

$$\operatorname{area}(X) = \lambda \sum_{n=0}^{\infty} h_n^2,$$

where h_n can be constructed with Remark 4.4.5.

Proof. Using Remark 4.4.5 and Lemma 4.4.6, this problem becomes a quick calculation:

$$\begin{aligned}\operatorname{area}(X) &= \sum_{n=0}^{\infty} \operatorname{area}(R_n) = \sum_{n=0}^{\infty} \operatorname{area}(R_{2n}) + \operatorname{area}(R_{2n+1}) \\ &= \sum_{n=0}^{\infty} h_n v_n + h_n v_{n+1} \\ &= \sum_{n=0}^{\infty} h_n v_n + h_n(\lambda \cdot h_n - v_n) \\ &= \lambda \sum_{n=0}^{\infty} h_n^2. \end{aligned}$$ □

Since we can scale our surface, we can fix $h_0 = 1$ and the problem of finding staircase arms such that the staircase data is well-defined with finite area becomes two-dimensional over a pair of parametrizations $(\lambda, v_0) \in \mathbb{R}_{>2} \times \mathbb{R}_{>0}$. We want $\lambda > 2$ for the Hooper–Thurston–Veech construction. One such solution is given by the staircase arms of the clover surface. We can use Lemma 4.4.7 to explicitly calculate the area of the (un-)lucky clover surface.

Proposition 4.4.8 (Clover surface has finite area)
The clover surface has an area of $\frac{20}{3}$.

Proof. Let C be the clover surface and X be a staircase arm beginning with two neighboring center squares of C as the first rectangle. In the case of the clover surface, this pair is $(\lambda, v_0) = (\frac{5}{2}, 2)$. Here our recurrence relations deliver $h_n = \frac{1}{4^n}$ and $v_n = \frac{2}{4^n}$. Since $v_0 = 2 \cdot h_0$, we can interlace four of these arms with each other, see Figure 4.11. We double count the interior four squares, so in total with Lemma 4.4.7, we get an area of

$$\begin{aligned}\operatorname{area}(C) &= 4 \cdot \operatorname{area}(X) - 4 \\ &= 4 \cdot \frac{5}{2} \sum_{n=0}^{\infty} \frac{1}{16^n} - 4 \\ &= 10 \cdot \frac{16}{15} - \frac{60}{15} = \frac{20}{3}. \end{aligned}$$ □

The (un-)lucky clover surface C is an example of an infinite translation surface with finite area and a large Veech group

$$\mathrm{GL}^+(C) \supseteq \left\langle \begin{pmatrix} 1 & \frac{5}{2} \\ 0 & 1 \end{pmatrix}, \begin{pmatrix} 1 & 0 \\ \frac{5}{2} & 1 \end{pmatrix}, \begin{pmatrix} 0 & -1 \\ 1 & 0 \end{pmatrix} \right\rangle.$$

Analyzing the behavior of the recurrence relation from Lemma 4.4.6 for initial conditions (λ, v_0) fixing $h_0 = 1$, we see the following behavior in Figure 4.12. For a fixed v_0, a too high λ causes h_n to diverge to ∞, so the area diverges as well. For a fixed v_0, a too low λ causes the equations for our recurrence to imply negative lengths and the data is not well-defined. Computing simulations seem to imply that the value for which this recurrence converges to some finite value is given by a curve, which disconnects the phase space in such a way that one side corresponds to area divergence and the other to non-constructability, see Figure 4.12.

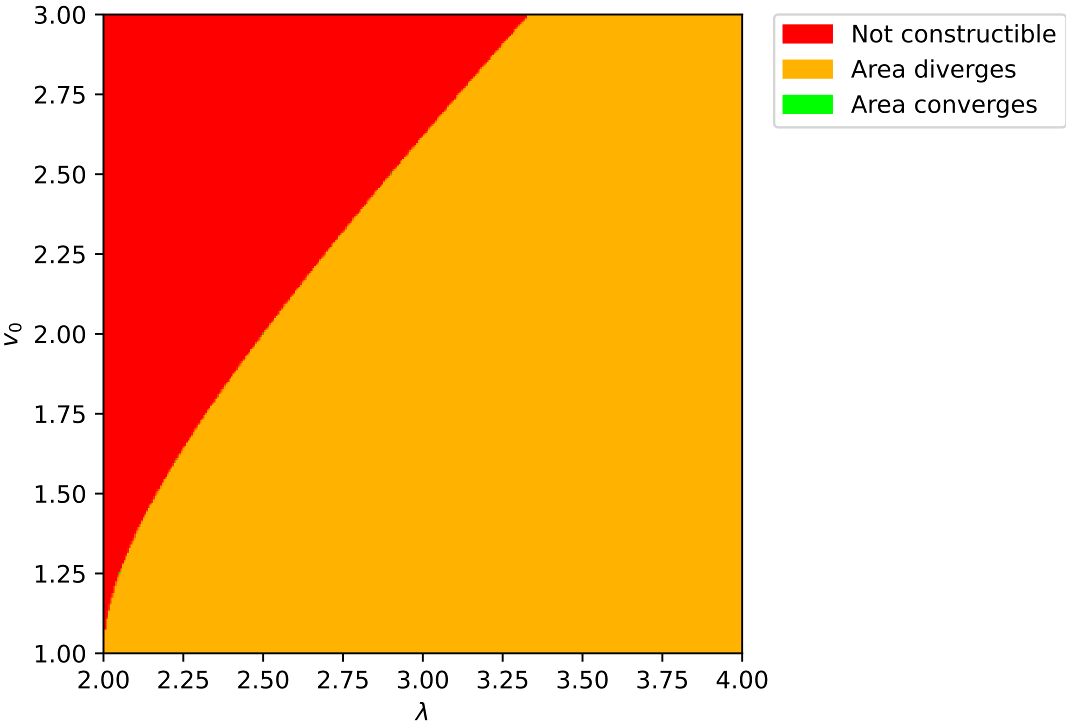

Figure 4.12: Recurrence behavior for the area for initial (λ, v_0) fixing $h_0 = 1$, figure is generated with the code in [Rei24d]

However, explicitly calculating points on this line is not straight forward. Some examples of these values were constructed by fixing the recurrence relation, requiring the ratio $\frac{h_{n+1}}{h_n}$ to be constant to simultaneously enforce area convergence, since we can then use the geometric series for finite area.

For $\lambda = 3$, we get the iteration $h_{n+1} = 3 \cdot h_n + 1$, in which case $\lim_{n\to\infty} \frac{h_{n+1}}{h_n} = \varphi_+^2$, where $\varphi_+ = \frac{1+\sqrt{5}}{2}$ is the golden ratio. So $(3, \varphi_+^2) \approx (3, 2.62)$ is another allowed configuration pair. All other rational λ, which we evaluated, were explicitly calculable and yielded metallic ratios as well. To create a translation surface by overlapping staircase arms, these arms must fit together seamlessly. Therefore, we require v_0 and h_0 to be commensurable, which is a problem since theses metallic ratios are not rational.

However, if it is true that the boundary is a continuous line, we should get infinitely many more examples of clover-like surfaces having finite area and being of infinite type corresponding to the rational values.

Part III

Cutting sequences

5 Word dynamics

The goal of this chapter is to set up the framework needed to understand symbolic dynamics on translation surfaces. For a comprehensive book on word dynamics and substitutions, one can refer to [Fog02]. We will need the notions introduced in this chapter, particularly to understand new results on the complexity of word dynamics on the regular octagon in Chapter 6.

5.1 Complexity

Let us start by introducing some terminology in combinatorics on words. These concepts have corresponding counterparts in symbolic dynamics.

Definition 5.1.1 (Alphabets & letters)
Let $\mathcal{A}$ be a finite set referred to as the *alphabet*. The elements of the alphabet $\mathcal{A}$ are referred to as *letters*.

Remark 5.1.2 (On letters)
In our case, the letters of our alphabet $\mathcal{A}$ will be usually represented either as numbers ($\mathcal{A} = \{(0,)1, \ldots, d\}$) or as classical letters ($\mathcal{A} = \{A, B, \ldots\}$).

Definition 5.1.3 ((Finite) words)
A *(finite) word* is a (finite) sequence of elements in $\mathcal{A}$.

Definition 5.1.4 (Length)
Let $w = w_1 w_2 \ldots w_n$ be a finite word in $\mathcal{A}$. We define the *length* of w as the number of letters in w and denote this by $|w| = n$.

Convention 5.1.5 (Extreme length cases)
There exists only one word of length 0, the *empty word*, denoted by ε. Infinite words w have infinite length, denoted by $|w| = \infty$.

Definition 5.1.6 (Some word sets)
Let $\mathcal{A}$ be an alphabet.

- The *set of words of length* n over $\mathcal{A}$ is denoted by $\mathcal{A}^n$.
- The *set of all finite words* over $\mathcal{A}$ is denoted by $\mathcal{A}^\star = \{w \mid \exists n \in \mathbb{N}_0 \colon w \in \mathcal{A}^n\}$.

Definition 5.1.7 (Concatenation)
Let $v = v_1 \dots v_n$ be a finite word and $w = w_1 \dots$ be a word in $\mathcal{A}$. We define the *concatenation* of these words as the word

$$vw = v_1 \dots v_n w_1 \dots .$$

Proposition 5.1.8 (A free monoid)
The set $\mathcal{A}^\star$ together with concatenation is endowed with the structure of a monoid: the free monoid generated by $\mathcal{A}$.

Proof. Concatenation is associative and has a unit element: the empty word ε. □

For infinite words, we differentiate between two different types of words.

Definition 5.1.9 ((Bi-)infinite words)
Let $\mathcal{A}$ be an alphabet.

- A *(right) infinite word* on $\mathcal{A}$ is a one-sided sequence of elements of $\mathcal{A}$, denoted by $(w_n)_{n\in\mathbb{N}^+}$.
- A *biinfinite word* on $\mathcal{A}$ is analogously a two-sided sequence of elements of $\mathcal{A}$, denoted by $(w_n)_{n\in\mathbb{Z}}$.

Definition 5.1.10 (More word sets)
Let $\mathcal{A}$ be an alphabet.

- The *set of infinite words* over $\mathcal{A}$ is denoted by $\mathcal{A}^\mathbb{N}$.
- The *set of biinfinite words* over $\mathcal{A}$ is denoted by $\mathcal{A}^\mathbb{Z}$.

It will be useful to have a *metric* on $\mathcal{A}^\mathbb{N}$ and $\mathcal{A}^\mathbb{Z}$ to talk about distance.

Definition 5.1.11 (Metric & topology)
We define for $v, w \in \mathcal{A}^\mathbb{Z}$

$$d(v,w) = d_{\mathcal{A}^\mathbb{Z}}(v,w) := 2^{-|\min\{n\in\mathbb{Z},\ v_n \neq w_n\}|}.$$

This yields a *topology* on the set $\mathcal{A}^\mathbb{Z}$, which is equivalent to the product topology of the discrete topology on each copy of $\mathcal{A}$.

Proposition 5.1.12 (Metric $d_{\mathcal{A}^\mathbb{Z}}$ is well-defined)
The map $d_{\mathcal{A}^\mathbb{Z}} \colon \mathcal{A}^\mathbb{Z} \times \mathcal{A}^\mathbb{Z} \to \mathbb{R} \cup \{\infty\}$ is a metric.

Proof. Let $u, v, w \in \mathcal{A}^\mathbb{Z}$.

- *Definiteness*: Let $u \neq v$, so there exists some index $m \in \mathbb{Z}$ where $u_m \neq v_m$, then $d_{\mathcal{A}^\mathbb{Z}}(u,v) \geq 2^{-m} > 0$.
- *Positivity* & *Symmetry*: This immediately follows from the symmetric definition of $d_{\mathcal{A}^\mathbb{Z}}$.

- *Triangle inequality*: Let $|m_{u,v}|$ be the smallest index such that $u_{m_{u,v}} \neq v_{m_{u,v}}$, so $d_{\mathcal{A}^{\mathbb{Z}}}(u,v) = 2^{-|m_{u,v}|}$ and $|m_{v,w}|$ be the smallest index such that $v_{m_{v,w}} \neq w_{m_{v,w}}$, so $d_{\mathcal{A}^{\mathbb{Z}}}(v,w) = 2^{-|m_{v,w}|}$, then

$$\begin{aligned} d_{\mathcal{A}^{\mathbb{Z}}}(u,w) &= 2^{-|\min\{n\in\mathbb{Z},\ u_n\neq w_n\}|} \\ &\leq 2^{-|\min\{m_{u,v},m_{v,w}\}|} \\ &= \max\left\{2^{-|m_{u,v}|}, 2^{-|m_{v,w}|}\right\} \\ &= \max\{d_{\mathcal{A}^{\mathbb{Z}}}(u,v), d_{\mathcal{A}^{\mathbb{Z}}}(v,w)\} \\ &\leq d_{\mathcal{A}^{\mathbb{Z}}}(u,v) + d_{\mathcal{A}^{\mathbb{Z}}}(v,w). \end{aligned}$$ □

For word dynamics, we are interested in subsets of $\mathcal{A}^{\mathbb{Z}}$ with interesting properties, these can often be described by subwords occurring in infinite words.

Definition 5.1.13 (Occurrence)
Let $\mathcal{A}$ be an alphabet. We say a word v *occurs (at position m)* in a word w, if v is a subsequence of w (starting in index m). We then also call v a *factor* of w.

Let us consider an easy example to better understand these definitions.

Example 5.1.14 (Occurrence)
Let $w = (\chi_{\{n\in 2\mathbb{Z}\}})_{n\in\mathbb{Z}} = \dots 010101 \dots \in \{0,1\}^{\mathbb{Z}}$. This is an example of a biinfinite word. The word 101 is a factor of w. It occurs at position -1, 1, 3, and so on. The infinite word $w' = 10101\dots \in \{0,1\}^{\mathbb{N}}$ is also a factor occurring also at all odd positions.

Definition 5.1.15 (Language)
Let $w \in \mathcal{A}^{\mathbb{Z}}$. The *language* $\mathcal{L}(w)$ (or the language $\mathcal{L}_n(w)$ of length n) of the infinite word w is the set of all words (or all words of length n) which occur in w.

Example 5.1.16 (Language)
Our example $w = \dots 010101 \dots \in \{0,1\}^{\mathbb{Z}}$ is a biinfinite word, in which all words from $\{0,1\}^\star$ with no double letters can occur. We get all one-letter words $\mathcal{L}_1(w) = \{0,1\}$ as the language of length 1, but only $\mathcal{L}_2(w) = \{01,10\}$ as the language of length 2. The other two-letter words $\{00,11\}$ are not in $\mathcal{L}_2(w)$.

Definition 5.1.17 (Properties of infinite words)
Let $w \in \mathcal{A}^{\mathbb{N}}$ be an infinite word.

- We call w *recurrent* if every finite factor occurs infinitely often.
- We call w *periodic* if there exists a positive integer $T \in \mathbb{N}^+$, called *periodicity*, such that $w_m = w_{m+T}$ for all $m \in \mathbb{N}^+$.
- We call w *ultimately periodic* if there exists a positive integer $T \in \mathbb{N}^+$, also called *periodicity* and an $M \in \mathbb{N}_0$, such that $w_m = w_{m+T}$ for all $m \geq M$.

- We call w *uniformly recurrent* if every word v occurring in w occurs in an infinite number of positions with bounded gaps. That is, if there exists an $m \in \mathbb{N}^+$ such that for every $n \in \mathbb{N}^+$, the word v is a factor of $w_n \dots w_{n+m-1}$.

Remark 5.1.18 (On periodicity)
We do not speak about the unique periodicity T of an (ultimately) periodic infinite word w, since w is for example also a (ultimately) periodic infinite word of periodicity $2T$.

Example 5.1.19 (Periodic)
Our example $w = \dots 010101 \dots \in \{0,1\}^{\mathbb{Z}}$ is periodic for every even periodicity. Every periodic word is (uniformly) recurrent: we can use the periodicity T to find every factor v in $w_n \dots w_{n+T+|v|-1}$ for all $n \in \mathbb{N}^+$.

A question which arises naturally when investigating languages is how fast is the rate of growth in the count of words occurring in a language depending on word length. We formalize this in the following way.

Definition 5.1.20 (Complexity function)
Let $w \in \mathcal{A}^{\mathbb{N}}$ be an infinite word. We define the *complexity function* p_w of w by

$$p_w \colon \mathbb{N}_0 \to \mathbb{N}^+, \quad n \mapsto |\mathcal{L}_n(w)| \,.$$

Example 5.1.21 (Complexity function)
For our example $w = \dots 010101 \dots \in \{0,1\}^{\mathbb{Z}}$, there are exactly two factors of length n occurring in w for $n > 0$ corresponding to starting with the letter 0 or 1. We therefore get the complexity function

$$p_w \colon \mathbb{N}_0 \to \mathbb{N}^+, \quad 0 \mapsto 1, \quad n \mapsto 2 \ \forall n \in \mathbb{N}^+.$$

The complexity function can be viewed as a measure of disorder in an infinite word since we measure how many unique word exists. It is easy to see that the complexity function must be non-decreasing.

Lemma 5.1.22 (Non-decreasing property)
Let $w \in \mathcal{A}^{\mathbb{N}}$ be an infinite word. The complexity function of w is non-decreasing, so

$$p_w(n+1) \geq p_w(n) \text{ for all } n \in \mathbb{N}_0.$$

Proof. Let w be an infinite word, $n \in N^+$ and $u, v \in \mathcal{L}_n(w)$ and $u \neq v$. Let m_u be the position in which u occurs in w. Then $\tilde{u} = w_{m_u} \dots w_{m_u+n+1} = u w_{m_u+n+1}$ occurs in w. Analogously for $\tilde{v} = v w_{m_v+n+1}$. Since $u \neq v$, so is $\tilde{u} \neq \tilde{v}$ and therefore $|\mathcal{L}_{n+1}(w)| \geq |\mathcal{L}_n(w)|$. $\square$

Furthermore, we can give already some explicit bound in n.

Proposition 5.1.23 (Bounded complexity)
Let $w \in \mathcal{A}^{\mathbb{N}}$ be an infinite word. The complexity function of w fulfills

$$1 \leq p_w(n) \leq d^n,$$

where $d \coloneqq |\mathcal{A}|$.

Proof. Since $\mathcal{L}_0(w) = \{\varepsilon\}$, $p_w(0) = 1$ and the lower bound holds by Lemma 5.1.22.

Since $\mathcal{A}$ is finite, so is $\mathcal{A}^n$ as well with $|\mathcal{A}^n| = |\mathcal{A}|^n = d^n$. Furthermore is $\mathcal{L}_n(w) \subseteq \mathcal{A}^n$, so $|\mathcal{L}_n(w)| \leq d^n$ for any $w \in \mathcal{A}^{\mathbb{N}}$. □

An ultimately periodic word is very ordered and therefore has a small value for the complexity function:

Proposition 5.1.24 (Complexity of periodic infinite words)
If w is an ultimately periodic infinite word, $p_w(n)$ is a bounded function. If there exists an integer n such that $p_w(n) \leq n$, w is an ultimately periodic infinite word.

Proof. Let w be an ultimately periodic infinite word, so there exists a positive integer $T \in \mathbb{N}^+$ and an $M \in \mathbb{N}_0$, such that $w_m = w_{m+T}$ for all $m \geq M$. In the worst case, every word of length n is unique for each word starting with one of the first $M + T$ letters of the infinite word. But afterwards, every word of length n starting with a letter from position $M + T + m$ of the infinite word is already obtained by the word of length n starting with a letter from position $M + m$ for every $m \in \mathbb{N}^+$. So $|\mathcal{L}_n(w)| \leq M + T$ and therefore p_w is a bounded function.

Now we show the second part of this proposition. If $p_w(1) = 1$, this implies that only one single letter has been used, so w is periodic with periodicity 1. So consider the case, where $p_w(1) \geq 2$. Since $p_w(n) \leq n$ for some n, Lemma 5.1.22 and the fact that $p_w(n) \in \mathbb{N}^+$ imply that there exists some $k \in 1, \dots n-1$ with $p_w(k+1) = p_w(k)$. We have seen in the proof of Lemma 5.1.22, that the elements of $\mathcal{L}_{k+1}(w)$ can be constructed from $\mathcal{L}_k(w)$ by extending with the next letter in the infinite word and since $p_w(k+1) = p_w(k)$, this extension is unique and $\mathcal{L}_k(w)$ and $\mathcal{L}_{k+1}(w)$ are in one-to-one correspondence by extension respectively by forgetting the last letter. That is to say, if $w_i \dots w_{i+k-1} = w_j \dots w_{j+k-1}$, then $w_{i+k} = w_{j+k}$. So, we know how to continue w from k letters already. As the set $\mathcal{L}_k(w)$ is finite, at some point in the infinite word w, there exist indices $j > i$ such that $w_i \dots w_{i+k-1} = w_j \dots w_{j+k-1}$ and hence $w_{i+p} = w_{j+p}$ for every $p \geq 0$, with one periodicity being $j - i$. □

To calculate the complexity function of an infinite word, we can understand the growth recursively by investigating, how our words can grow through extensions.

Definition 5.1.25 (Right & left extension)
Let v be a factor of the infinite word $w \in \mathcal{A}^{\mathbb{N}}$. A *right extension* (respectively *left extension*) of the factor v is a word vx (respectively xv), where $x \in \mathcal{A}$, such that vx (respectively xv) is also a factor of the infinite word w.

Definition 5.1.26 (Right, left and bispecial factor)
A factor is a *right special factor* (respectively *left special factor*) if it has more than one right (respectively left) extension. A factor is called a *bispecial factor* if it is a right and left special factor.

Proposition 5.1.27 (Complexity growth)
Let $w \in \mathcal{A}^{\mathbb{N}}$ be an infinite word and let $W^+(v)$ (respectively $W^-(v)$) denote the number of right (respectively left) extensions of a factor $v \in \mathcal{A}^\star$. Then for all $n \in \mathbb{N}_0$

$$p_w(n+1) - p_w(n) = \sum_{v \in \mathcal{L}_n(w)} (W^+(v) - 1) = \sum_{v \in \mathcal{L}_n(w)} (W^-(v) - 1).$$

Proof. We get this formula by considering elements in $\mathcal{L}_{n+1}(w)$ as right or left extensions of elements in $\mathcal{L}_n(w)$ and counting all the possible ways of extending, so

$$p_w(n+1) = \sum_{v \in \mathcal{L}_n(w)} W^+(v) = \sum_{v \in \mathcal{L}_n(w)} W^-(v).$$

Finally, we remove $p_w(n) = \sum_{v \in \mathcal{L}_n(w)} 1$. □

Equipped with this knowledge, we can now start doing symbolic dynamical systems. For the dynamical part, we use the classical one-sided shift operation.

Definition 5.1.28 (One-sided shift operator)
Define the *one-sided shift operator* S by

$$S \colon \mathcal{A}^{\mathbb{Z}} \to \mathcal{A}^{\mathbb{Z}}, \quad (w_n)_{n \in \mathbb{Z}} \mapsto (w_{n+1})_{n \in \mathbb{Z}}.$$

Remark 5.1.29 (On the one-sided shift operator)
The map S is uniformly continuous and bijective on $\mathcal{A}^{\mathbb{Z}}$. Its restriction to $\mathcal{A}^{\mathbb{N}}$, where we set the first element of the shifted infinite word to some fixed element of $\mathcal{A}$, usually $0, 1$, or A, is still uniformly continuous, but only injective. The shift S is a continuous map, since $d(Sx, Sy) \leq \frac{1}{2} d(x, y)$. This continuity implies that if $x = \lim_{n \to \infty} S^{k_n} w$, then $Sx = \lim_{n \to \infty} S^{k_n + 1} w$.

Definition 5.1.30 (Symbolic dynamical system)
A *symbolic dynamical system* is a pair (X, S), where $X \subseteq \mathcal{A}^{\mathbb{Z}}$ is an S–invariant subset in the space of infinite words, that is to say $SX \subseteq X$.

Example 5.1.31 (Symbolic dynamical system of the shift)
Let $\overline{O(w)} \subseteq \mathcal{A}^{\mathbb{Z}}$ (respectively $\mathcal{A}^{\mathbb{N}}$) be the closure of the orbit of the infinite word w under the action of the shift S, so $O(w) = \{S^n w, n \in \mathbb{Z}\}$ (respectively $O(w) = \{S^n w, n \in \mathbb{N}\}$). The *symbolic dynamical system* associated with a biinfinte (respectively infinite) word w with values in $\mathcal{A}$ is then the tuple $(\overline{O(w)}, S)$.

Remark 5.1.32 (On symbolic dynamical systems)
The set $\overline{O(w)}$ is finite if and only if w is periodic. Furthermore, $\overline{O(w)}$ is a compact space, since it is a closed subset of the compact set $\mathcal{A}^{\mathbb{Z}}$.

5.2 Substitutions

A lot of words in a language can be described by some initial seed and substitution rules. The kind of words we aim to obtain in Chapter 6 fall into this category and some information, such as complexity, can be derived with the help of substitutions.

Definition 5.2.1 (Substitution)
A *substitution* σ is a map of the form

$$\sigma\colon \mathcal{A} \to \mathcal{A}^\star$$

from the alphabet $\mathcal{A}$ into the set of finite words $\mathcal{A}^\star$. It is called to be *of constant length k* if $\sigma(a)$ is of length k for all $a \in \mathcal{A}$.

Remark 5.2.2 (On substitutions)
A substitution σ extends to a morphism of $\mathcal{A}^\mathbb{Z}$ (or $\mathcal{A}^\star$, $\mathcal{A}^\mathbb{N}$) by concatenation

$$\sigma(vw) = \sigma(v)\sigma(w)$$

for all infinite words v and w.

We can define words as fixed points of substitutions.

Definition 5.2.3 (Fixed point, periodic point and n–word)
Let $\sigma\colon \mathcal{A} \to \mathcal{A}^\star$ be a substitution.

- A *fixed point* of σ is an infinite word $w \in \mathcal{A}^\mathbb{Z}$ (or $w \in \mathcal{A}^\mathbb{N}$) such that $\sigma(w) = w$.
- A *periodic point* of σ is an infinite word w such that there exists some $k \in \mathbb{N}^+$, such that $\sigma^k(w) = w$.
- An *n–word* for σ is a word of the form $\sigma^n(a)$ for $a \in A$.

In [Mor21], Harold Calvin Marston Morse studied non-closed infinite geodesics on connected surfaces with constant negative curvature.

He affirmed the existence of recurrent flows by encoding the flow with infinite words of zeroes and ones, indicating which edge of a polygon constituting the surface they meet. Closed geodesics in this setting corresponded to periodic infinite words while uniformly recurrent infinite words give rise to recurrent geodesics.

The uniformly recurrent infinite word he found is called the Morse sequence, even though it had already been discovered by Prouhet in [Pro51].

Example 5.2.4 (Morse sequence)
Consider the substitution

$$\sigma\colon \{0,1\} \to \{0,1\}^\star, \quad 0 \mapsto 01, \quad 1 \mapsto 10$$

of constant length 2. The infinite word $u \in \{0,1\}^\mathbb{N}$ obtained by infinitely iterating σ on 0 is called the *Morse sequence*.

Remark 5.2.5 (On Morse sequence)
Since $\sigma^n(0) = \sigma^{n-1}(\sigma(0)) = \sigma^{n-1}(01) = \sigma^{n-1}(0)\sigma^{n-1}(1)$, the nested n–words $\sigma^n(0)$ converge in $\{0,1\}^{\mathbb{N}}$ to the only infinite word that begins with $\sigma^n(0)$ for every n. Therefore, the Morse sequence starts with $u = (0,1,1,0,1,0,0,1,1,0,0,1,0,1,1,0,\ldots)$ and is a fixed point of σ.

Another interesting example is the Fibonacci sequence:

Example 5.2.6 (Fibonacci sequence)
Consider the substitution

$$\sigma\colon \{0,1\} \to \{0,1\}^\star, \quad 0 \mapsto 01,\ 1 \mapsto 0.$$

The infinite word $v \in \{0,1\}^{\mathbb{N}}$ obtained by infinitely iterating σ on 0 is called the *Fibonacci sequence*.

Remark 5.2.7 (On the Fibonacci sequence)
As before, the Fibonacci sequence is a fixed point of σ and therefore starts with

$$v = (0,1,0,0,1,0,1,0,0,1,0,0,1,0,1,0,\ldots).$$

The Fibonacci sequence is an example of an infinite word whose complexity growth is as small as possible without being constant, called Sturmian words:

Definition 5.2.8 (Sturmian words)
A *Sturmian word* is defined as an infinite word w such that the complexity function p_w satisfies for all $n \in \mathbb{N}$:

$$p_w(n) = n + 1.$$

Another way to represent a substitution, which can be useful to encode some data on the account of occurring letters in an n–word, is given by the incidence matrix.

Definition 5.2.9 (Incidence matrix)
Let $\sigma\colon \mathcal{A} \to \mathcal{A}^\star$ be a substitution and $\mathcal{A} = \{a_1, \ldots, a_d\}$. The *incidence matrix* of the substitution σ is the $d \times d$ matrix M_σ with

$$(M_\sigma)_{i,j} := |\sigma(a_j)|_{a_i}$$

for $i, j \in [d]$, where $|w|_v$ is the count of occurrences of v in w.

Remark 5.2.10 (On incidence matrices)
The incidence matrix M_σ encodes the number of occurrences of the letters $(a_i)_{i\in[d]}$ in $(\sigma(a_j))_{i\in[d]}$ and therefore M_σ^n does encode the number of occurrences of the letters $(a_i)_{i\in[d]}$ in $(\sigma^n(a_j))_{i\in[d]}$. However, the incidence matrix cannot be used to construct a word directly from the entries of the matrix alone.

Example 5.2.11 (Fibonacci & Morse sequence)
Let σ be the Morse substitution and τ be the Fibonacci substitution. The corresponding incidence matrices are given by

$$M_\sigma = \begin{pmatrix} 1 & 1 \\ 1 & 1 \end{pmatrix}, \quad M_\tau = \begin{pmatrix} 1 & 1 \\ 1 & 0 \end{pmatrix}.$$

5.3 Words from cutting sequences

In this section, we want to define the notion of encoding data obtained by trajectories on translation surfaces with words of languages similar to Morse's work in [Mor21].

We are in the setting of Section 3.4. Let θ be some globally defined direction on a finite translation surface (X, ω). Let φ_θ be the geodesic flow on (X, ω) and define $\tau \coloneqq \mathrm{tr}_{x,\theta}$ as the trajectory of $x \in X$ under φ_θ for as long as it is well-defined, meaning not hitting any singularity including marked points.

Remark 5.3.1 (Straight line trajectory)
In the view of translation surfaces as glued polygons as in Definition 2.1.4, the trajectory τ has a constant velocity vector making a globally defined angle θ with the horizontal, until it hits the edge at which time it re-enters another polygon of (X, ω) at the corresponding point on the glued side and continues with the same direction and velocity. We refer to these trajectories also as *straight line trajectories*.

We now describe a symbolic coding for these trajectories.

Definition 5.3.2 (Cutting sequence)
Let (X, ω) be a finite translation surface given by Definition 2.1.4 and τ be a straight line trajectory. Label each pair of glued edges of (X, ω) with a letter of an alphabet $\mathcal{A}$. We define the *cutting sequence* $c(\tau)$ of τ as the word with letters from $\mathcal{A}$, obtained by reading the labels of the pairs of identified sides crossed by the trajectory τ as time increases.

Remark 5.3.3 (On cutting sequences)
We usually use $\mathcal{A} = \{A, B, \ldots\}$ to encode these words. If we talk about infinite words, we start the encoding with the first intersection of our trajectory τ including the start point $\tau(0)$. If we talk about biinfinite words, we also flow in reverse with $\overleftarrow{\tau}$ and denote the word as the concatenate of $c(\overleftarrow{\tau})$ in reversed order with $c(\tau)$ without doubling the encoding of the start point, if $\tau(0)$ is on an edge of (X, ω) according to Definition 2.1.4.

The encoding of the cutting sequence depends on the gluing chosen in Definition 2.1.4, which is non-unique for translation surfaces.

As usual, we start to consider the torus $\mathbb{T}_\mathrm{i}$ from Example 2.0.15. The methods and principle we develop for the torus can be extended to the upcoming octagon in several ways. We encode the horizontal and vertical edge by A and B respectively.

Example 5.3.4 (Torus)
Let us consider the trajectories τ_1 starting in the center of the horizontal boundary edge flowing diagonally in direction $\frac{\pi}{4}$ and τ_2 starting in the center of the square in direction $\frac{\pi}{2} + 1$, see Figure 5.1. The infinite words obtained from their cutting sequences are

$$c(\tau_1) = ABABABA\ldots, \quad c(\tau_2) = BABABBA\ldots.$$

Since τ_1 is periodic, its cutting sequence must also be periodic. While the periodicity for τ_1 is $\sqrt{2}$ in the underlying square torus, $c(\tau_1)$ has periodicity 2 in word length. The

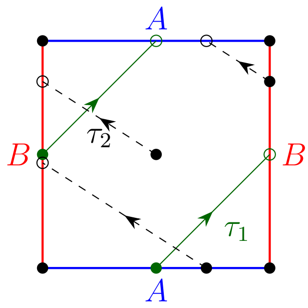

Figure 5.1: Square torus with labeled sides illustrating cutting sequences

infinite word $c(\tau_2)$ is not periodic and the corresponding trajectory τ_2 is not periodic either. Since Theorem 3.4.12 holds, τ_2 uniformly distributes and would fill the whole torus in Figure 5.1 for any positive linewidth, while the picture colored by τ_1 would approach some measure 0 set for decreasing linewidth.

This naturally gives rise to differentiate between two kinds of angles, directions, and slopes.

Definition 5.3.5 ((Ir-)rational angle)
We call an angle *rational* if it is a rational multiple of π and *irrational* otherwise. Analogously, we denote (ir-)rational direction and slope if the according angle is also (ir-)rational.

Remark 5.3.6 (On periodicity on the torus)
On one hand, trajectories on the torus, whose directions are rational, are periodic and therefore their cutting sequences as well. On the other hand, trajectories, whose directions are irrational, are uniquely ergodic and their cutting sequences are aperiodic.

Remark 5.3.7 (On calculating cutting sequences)
Let (X, ω) be a finite translation surface and τ a rational trajectory on X in direction θ. We can calculate the cutting sequence by describing an almost global flow on X in direction θ and then calculating the interval exchange transformation.

On the square, the flow $\varphi_{\frac{\pi}{4}}$ in the direction τ_1 from Example 5.3.4 on the orthogonal diagonal then corresponds to the interval exchange transformation

$$(\pi, \lambda) = \left((1, 2), \left(\frac{1}{2}, \frac{1}{2}\right)\right).$$

We normalized the length of the diagonal to length 1. λ_1 and λ_2 correspond to A and B as an encoding for the cutting sequence. The permutation $\tau = (1, 2)$ describes that the successor in the cutting sequence of A is B and vice versa. Each interval corresponds to a set of trajectories encoding $\ldots ABAB \ldots$, starting with either A or B depending on the starting point.

We are interested in the set of all cutting sequences and not only the ones corresponding to rational directions. For this, we can use transition diagrams as a useful tool.

Definition 5.3.8 (Transition diagrams)
For a subset of trajectories on a translation surface (X, ω) with a fixed gluing structure on (X, ω), we define the *transition diagram* as the directed graph $\mathcal{D} := (V, E)$. The vertex set $V \subseteq \mathcal{A}$ is the set of all possible letters appearing in the cutting sequences of our subset of trajectories. The directed edges E contain an edge (v, w) if vw is factor of any cutting sequence of our subset of trajectories.

These diagrams can sometimes be used to exclude some words as cutting sequences, though not every word obtained from a diagram is necessarily a cutting sequence.

For actual calculations, such as those implemented in software to compute a word from specific initial conditions, the appropriate tool is given by interval exchange transformations.

Example 5.3.9 (Transition diagram of $\mathbb{T}_{\mathrm{i}}$ for all trajectories)
The transition diagram in Figure 5.2 on the square torus for all trajectories contains every edge. It is easy to check that all combinations can appear.

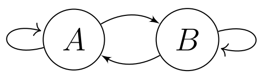

Figure 5.2: Transition diagram of $\mathbb{T}_{\mathrm{i}}$ for all trajectories

Not every cutting sequence is actually realizable. On the torus, a cutting sequence containing the factor AA needs a direction for its trajectory of $\theta \in \overline{D_u}$, where

$$D_u := \left\{ \theta \in S^1 \;\middle|\; \frac{\pi}{4} < \theta < \frac{3\pi}{4} \text{ or } \frac{5\pi}{4} < \theta < \frac{7\pi}{4} \right\}.$$

In the direction of elements in D_u, no cutting sequence has BB as a factor. The cutting sequences with the factor BB on the other hand come from $\overline{D_r}$, where $D_r := S^1 \setminus \overline{D_u}$, see Figure 5.3.

(a) D_u

(b) D_r

Figure 5.3: Transition diagram of $\mathbb{T}_{\mathrm{i}}$ for trajectories with direction in D_u and D_r

In particular, words containing the factor AA and BB are not cutting sequences of $\mathbb{T}_{\mathrm{i}}$. Because of the previous argument, they would need to be in a direction

$$\theta \in \overline{D_u} \cap \overline{D_r} = \left\{ \frac{(2k-1)\pi}{4} \;\middle|\; k \in [4] \right\}$$

corresponding to the diagonals, where it is easy to check that all cutting sequences start with either $ABA\ldots$ or $BAB\ldots$.

Definition 5.3.10 (Admissibility on $\mathbb{T}_{\mathrm{i}}$)
We say a word w is *admissible* on $\mathbb{T}_{\mathrm{i}}$ if it corresponds to an infinite path on one of the transition diagrams given by Figure 5.3.

Every cutting sequence is admissible by construction. However, not every (bi)infinite word which is admissible is also a cutting sequence. So, the question on how to detect or describe all cutting sequences is not answered with admissibility alone. In the case of the torus, we need to introduce and construct derived words to answer this question.

Definition 5.3.11 (Derived word)
Let w be an admissible word. Denote by w' the *derived word* obtained by erasing one B from each block of consecutive B's, if w has no factor AA (respectively erase A from consecutive A's, if w has no factor BB).

Example 5.3.12 (First derivation example)
Consider the following word w and its derived word w' and w'' and so on:

$$\begin{aligned} w &= \ldots ABBABBBABBABBBABBABBB\ldots, \\ w' &= \ldots ABABBABABBABABB\ldots, \\ w'' &= \ldots AABAABAAB\ldots, \\ w''' &= \ldots ABABAB\ldots. \end{aligned}$$

Definition 5.3.13 (Infinitely derivable)
A word w is *infinitely derivable*, if it is admissible and every derived word $w', w'', \ldots$ is admissible.

The construction of derived words is chosen such that:

Proposition 5.3.14 (Cutting sequences are infinitely derivable)
Cutting sequences on $\mathbb{T}_{\mathrm{i}}$ are infinitely derivable.

Proof. This was first shown in [Ser85].
Let $w = c(\tau)$ be a cutting sequence of a trajectory τ. Without loss of generality, let $0 \leq \theta \leq \pi/4$. The other directions can be transformed into this direction with an element of the symmetry group of the square or the substitution

$$\sigma\colon \{A, B\} = \mathcal{A} \to \mathcal{A}, \quad A \mapsto B, \quad B \mapsto A.$$

Let us add the diagonal to $\mathbb{T}_{\mathrm{i}}$ in Figure 5.4 labeled by the letter C.
We obtain a cutting sequence $\tilde{c}(\tau)$ on an alphabet $\tilde{\mathcal{A}} = \{A, B, C\}$ by recording the crossings of the sides of the square and the diagonal. The diagonal C is only crossed during a segment of the trajectory corresponding to the cutting sequence BB, not during the segments of the trajectory corresponding to the cutting sequences of BA or AB, as shown in Figure 5.4. Thus, the cutting sequence with the additional edge C can be determined from the cutting sequence without the edge C by substituting BB by BCB.

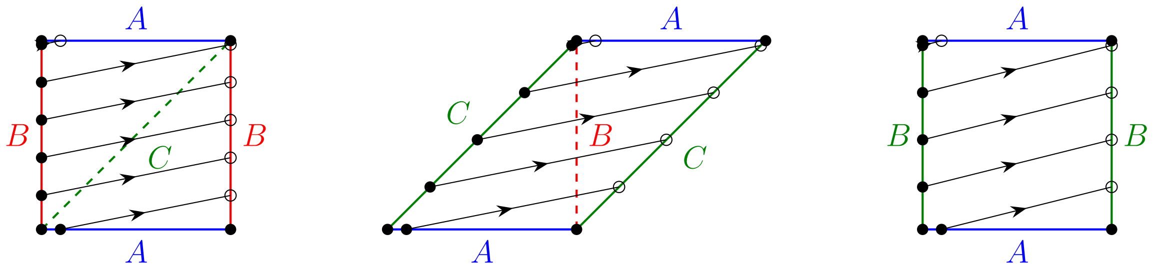

(a) Initial $\mathbb{T}_i$ (b) After regluing (c) After transformation

Figure 5.4: Renormalization of a cutting sequence

By cutting the square corresponding to the underlying surface of $\mathbb{T}_i$ along the edge C and regluing along the edge B, we obtain the parallelogram $P(1,1,0,1)$ corresponding to the underlying surface of $\mathbb{T}_{i+1}$ in Figure 5.4 whose sides are labeled by A and C. The word obtained by erasing B in the word $\tilde{c}(\tau)$ is the cutting sequence of $\mathbb{T}_{i+1}$. We renormalize $\mathbb{T}_{i+1}$ by applying the Veech group element that sends it back to a square, so the linear transformation is given by the matrix $\begin{pmatrix} 1 & -1 \\ 0 & 1 \end{pmatrix}$.

Since the map is affine, linear trajectories in $\mathbb{T}_{i+1}$ are sent to linear trajectories on $\mathbb{T}_i$. Thus, if we replace the C's with B's, the word we obtain is a cutting sequence of a trajectory τ' in a new direction θ'.

The effect of the combined operation on w is the same as that of deriving the word. Thus, the new cutting sequence $c(\tau')$ coincides with the derived word w'. $\square$

Remark 5.3.15 (Almost equivalence)
The converse statement, that every infinitely derivable word is also a cutting sequence, is not true. For example, the word $w = \dots AAABAAA\dots$ is infinitely derivable but not a cutting sequence.

However, every factor of w can be realized as a cutting sequence of a finite trajectory. This is equivalent to saying that w is in the closure of the space of cutting sequences. It turns out, that the closure of the space of cutting sequences is the set of infinitely derivable words, see [Ser85].

The key insight in the proof of Proposition 5.3.14 is the fact that the operation of deriving cutting sequences corresponds to some renormalization of trajectories. Consider the map which associates to the direction $0 \le \theta \le \pi/2$ of a trajectory τ the direction θ' of the renormalized trajectory τ' as used in the proof of Proposition 5.3.14, then the corresponding cutting sequences have the same encoding $c(\tau') = c(\tau)'$. We call this map F and it is defined on the first quadrant. Instead of using the angle coordinate θ, one can choose the coordinate transformation $t = t(\theta) = \frac{\sin\theta}{\cos\theta + \sin\theta}$, obtained by projecting radially to the line $\{(t, 1-t), 0 \le t \le 1\}$. Then F is the classical *Farey map*, defined by

$$F(t) = \begin{cases} \frac{t}{1-t}, & \text{if } 0 \le t < \frac{1}{2} \\ \frac{1-t}{t}, & \text{if } \frac{1}{2} \le t \le 1. \end{cases}$$

In this way, one can see that the number of B's between two A's is related to the count of times the iterates of $0 < t(\theta) < 1/2$ under the Farey map are in the sector $[0, 1/2]$. If we form an infinite word $(s_k)_{k\in\mathbb{N}}$ where s_k is 0 when the k–th iterate of $t(\theta)$ is an element of $[0, 1/2]$ and 1 otherwise, then we call it the *Farey expansion* of θ. We refer to this as the additive continued fraction expansion of the slope of θ. The usual continued fraction expansion is obtained by counting the number of symbols in each block of zeroes or ones. Thus, one can recover the continued fraction expansion of the slope of θ from the cutting sequence. We will extend this insight from [Ser85] to the regular octagon.

6 Octagon

The goal of this chapter is to understand more about the complexity function of the octagon as a translation surface. We prove how to explicitly count the connected components in the phase space of cutting sequences on the octagon, which will be introduced in Definition 6.3.1, such that the count depends solely on the word encoding the component. This is a key step towards computing the complexity function with Theorem 6.1.7 for cutting sequences arising from geodesic trajectories on the regular octagon, a task we have not yet accomplished.

The proof of our theorem will be presented in Section 6.3. One of the key steps in the proof is understanding the relationship between angles and word encodings via a renormalization scheme from [SU11], as detailed in Section 6.2. Before that, we set up the framework in Section 6.1.

6.1 Billiard & cutting sequence complexity

In this section, we discuss some ideas and the progress made for the complexity function of words obtained on the octagon. While the general growth type of its complexity function is already known, this is not the case for the exact growth.

These kinds of questions are motivated by billiards, in which a point "mass" moves with unit speed inside a polygon $P \subsetneq \mathbb{R}^2$ and reflects instantaneously at the boundary ∂P with the rule "the angle of incidence is equal to the angle of reflection". The question which arises naturally is on the complexity of this billiard game, or how many possible, truly distinct paths there are.

By adding a mirrored copy of a polygon along each edge instead of instantaneous reflection at the boundary, we can understand a billiard path by continuing in some straight line flow on copies of different polygons. This unfolding [ZK75] gives rise to a translation surface and even a finite translation surface if all angles of P are rational. To measure complexity, we want to understand generalized diagonals:

Definition 6.1.1 (Generalized diagonals)
A *generalized diagonal* is an (oriented) orbit segment which begins and ends at a vertex of the polygon and contains no vertex of the polygon in its interior. The segments of this generalized diagonal are the connected components within the interior, connecting points on the boundary of the polygon.

The number of segments of a generalized diagonal is called its *combinatorial length*, while its *geometric length* is simply the sum of the lengths of the segments. Define $N_g(t)$

(respectively $N_c(n)$) as the number of generalized diagonals of geometric (respectively combinatorial) length at most $t \in \mathbb{R}_{\geq 0}$ (respectively $n \in \mathbb{N}_0$).

Convention 6.1.2 (What counts as a generalized diagonal)
We define $N_c(0)$ in such a way that it corresponds to the number of vertices of the polygon. The sides of P themselves, however, do not count as generalized diagonals.

The combinatorial count $N_c(n)$ is closely related to the geometric count $N_g(t)$:

Proposition 6.1.3 (Combinatorial and geometric counts are similar)
For every polygon P, there exists some constant $D \in \mathbb{R}_{>0}$, such that

$$N_g(D^{-1} \cdot n) \leq N_c(n) \leq N_g(D \cdot n).$$

Proof. Let $D' := \operatorname{diam}(P)$ be the diameter of P, then every geodesic path on P has at most length D'. Therefore, every path with combinatorial length n has a geometric length of at most $D' \cdot n$. Analogously, we define D'' as the minimum of all corner distances of the polygon for the other direction. Thus, we define $D := \max\left\{D', \frac{1}{D''}\right\}$ to obtain this statement. □

A strong statement about the asymptotic growth of the count of saddle connections for translation surfaces is known. Alex Eskin and Howard Masur showed that it behaves in a quadratic way with respect to length. This insight will be important in Part IV again, where this asymptotic behavior is used for different kind of counting problems of saddle connections, which will give rise to Siegel–Veech constants.

Theorem 6.1.4 (Quadratic saddle connection length count — Eskin and Masur)
Let (X, ω) be a finite translation surface, then

$$\lim_{t \to \infty} \frac{|V_{\mathrm{sc}}(X, t)|}{t^2} \in \mathbb{R}_{>0},$$

where $V_{\mathrm{sc}}(X, t)$ is the set of saddle connections on (X, ω) with length smaller than t.

Proof. This is shown in [EM01]. □

This implies that for polygonal billiards with rational angles, the combinatorial count as well as the geometric count of generalized diagonals have quadratic growth.

We motivate this section with the square, for which the exact growth is known. We consider billiards in a square and code each orbit by the sequence of sides it hits.

Definition 6.1.5 (Square torus language and complexity)
Let $\mathcal{L}_S(n)$ denote the set of all words of length n obtained from billiards in the square S, using the alphabet $\mathcal{A} = \{A, B, C, D\}$, where each letter corresponds to one of the sides of S.

Its cardinality $p_S(n) = |\mathcal{L}_S(n)|$ is called the *complexity function of the square.*

The most general results, which are known about the complexity function for billiards in arbitrary polygons is an upper bound of exponential [Kat87] and a lower bound of at least quadratic [Tro98] growth. For the square and regular octagon we obtain quadratic growth with Theorem 6.1.4.

Instead of encoding the words obtained by playing billiards, we could also consider the cutting sequences of the square torus. This corresponds to the substitution:

$$\sigma\colon \{A, B, C, D\} \to \{A, B\}, \quad A \mapsto A, \quad B \mapsto B, \quad C \mapsto A, \quad D \mapsto B.$$

The complexity function $p_{\mathbb{T}_\mathrm{i}}$ according to this edge labeling can be transformed by:

Proposition 6.1.6 (Complexity interchange)
Let $p_{\mathbb{T}_\mathrm{i}}$ denote the complexity function obtained as the cardinality of cutting sequences on the square torus, then

$$p_S(n) = 4p_{\mathbb{T}_\mathrm{i}}(n) - 4.$$

Proof. If $n = 1$, every one-letter word from $\{A, B, C, D\}$ can be realized on the square, so $p_S(1) = 4$. Every one-letter word from $\{A, B\}$ can be realized on $\mathbb{T}_\mathrm{i}$, so $p_{\mathbb{T}_\mathrm{i}}(1) = 2$. Every word of $\mathcal{L}_S(n+1)$ can be obtained from $\mathcal{L}_S(n)$ by adding a letter in the front or in the back. Since σ maps A and C to A and maps B and D to B, we get at most

$$p_{\mathbb{T}_\mathrm{i}}(n+1) - p_{\mathbb{T}_\mathrm{i}}(n) \leq \frac{1}{4}\left(p_S(n+1) - p_S(n)\right)$$

additional cutting sequences. Every cutting sequence can be lifted to the universal cover, which is a 4–fold covering map to the square. There can be at most

$$p_S(n+1) - p_S(n) \leq 4\left(p_{\mathbb{T}_\mathrm{i}}(n+1) - p_{\mathbb{T}_\mathrm{i}}(n)\right)$$

according continuations in the original billiards in the square. The statement holds by induction since $p_S(1) = 4p_{\mathbb{T}_\mathrm{i}}(1)$ and $p_S(n+1) - p_S(n) = 4\left(p_{\mathbb{T}_\mathrm{i}}(n+1) - p_{\mathbb{T}_\mathrm{i}}(n)\right)$. ☐

So we can answer the question of exact growth for p_S if and only if we can answer it for $p_{\mathbb{T}_\mathrm{i}}$. Moreover, Cassaigne, Hubert, and Troubetzkoy showed that the complexity function is closely related to the combinatorial count of generalized diagonals.

Theorem 6.1.7 (Complexity combinatorics — Cassaigne, Hubert, and Troubetzkoy)
Let P be a polygon, p_P be the complexity function coming from billiards in P and N_c the combinational count of generalized diagonals for P. Then the following equality holds:

$$p_P(n) = \sum_{k=0}^{n-1} N_c(k).$$

Proof. This is shown in [CHT02] for convex polygons. Bédaride extended the statement to more cases, see Remark 7 in [Béd03], his proof can be used for all polygons. ☐

One of the main ingredients for the proof of Theorem 6.1.7 is a modified version of Proposition 5.1.27, which combines left and right extensions and sums over bispecial factors instead.

Example 6.1.8 (Square)
The square S has four corners, so $N_c(0) = 4$. It also has four generalized diagonals of combinatorial length 1, so $N_c(1) = N_c(0) + 4 = 8$. Using Theorem 6.1.7 we obtain $p_S(2) = N_c(0) + N_c(1) = 12$. These twelve admissible billiard paths on the octagon correspond to the encodings

$$\{AB, AC, AD, BA, BC, BD, CA, CB, CD, DA, DB, DC\}.$$

If we investigate billiards in the square S after unfolding it to a translation surface T_{i}, then Definition 6.1.1 coincides with the definition of a saddle connection from Definition 3.2.1 up to the sides of S and $N_g(t) \sim |V_{\mathrm{sc}}(T_{\mathrm{i}}, t)|$. Extending this heuristics we obtain cubic growth for the complexity p_S of the square. By Theorem 6.1.4, we know there exists some $c \in \mathbb{R}_{>0}$, such that

$$\lim_{t\to\infty} \frac{|V_{\mathrm{sc}}(X,t)|}{t^2} = c.$$

Since $N_g(t) \sim |V_{\mathrm{sc}}(X,t)|$ by our heuristics and $N_g(D^{-1} \cdot n) \leq N_c(n) \leq N_g(D \cdot n)$ for some $D \in \mathbb{R}_{>0}$, we know there exist $C, C' \in \mathbb{R}_{>0}$, such that

$$C \leq \frac{N_c(n)}{n^2} \leq C'$$

for all $n \in \mathbb{N}^+$. We therefore get a cubical growth of $p_S(n)$ from Theorem 6.1.7.

More generally, this is true for every convex polygon:

Corollary 6.1.9 (Cubical complexity)
Let P be a convex polygon and p_P the complexity function of P. Then p_P has cubical growth in word length, so there exist $C, C' \in \mathbb{R}_{>0}$, such that

$$C \leq \frac{p_P(n)}{n^3} \leq C'$$

for all $n \in \mathbb{N}^+$.

Proof. This is Corollary 1.2 in [CHT02]. □

With Proposition 6.1.6 and Corollary 6.1.9 we obtain a cubic growth for the complexity of the square torus, so there exist $C, C' \in \mathbb{R}_{>0}$, such that

$$C \leq \frac{p_{\mathbb{T}_{\mathrm{i}}}(n)}{n^3} \leq C'$$

for all $n \in \mathbb{N}^+$.

The heuristic is the following: On a finite translation surface, the cutting sequences for finite trajectories almost stay the same when changing direction locally unless one crosses a saddle connection. The count of words therefore corresponds to the count of saddle connections, which grows quadratically. Each word corresponds to a factor of a

Sturmian word whose complexity grows linearly. In total, the complexity of the whole language grows cubical.

Even though we know the growth class for the complexity for the billiard paths for all convex polygons, it is hard to explicitly calculate the limit for a given polygon. In the case of billiards in a square, we know that $\frac{p_S(n)}{n^3} \to \frac{2}{3\pi^2}$ for $n \to \infty$ by [CHT02] and the square torus has therefore a complexity $\frac{p_{\mathbb{T}_1}(n)}{n^3} \to \frac{1}{6\pi^2}$ for $n \to \infty$. Analogous results are known for the complexity function on an isosceles right triangle and the equilateral triangle [CHT02].

Cutting sequences on the regular octagon have been extensively studied and are quite well understood, particularly due to the work of Smillie–Ulcigrai [SU11]. In collaboration with Athreya, Bédaride, and Cassaigne, we aim to expand the list of polygons whose complexity is explicitly known by the regular octagon.

Definition 6.1.10 (Octagon letters & language)
Let $\Sigma := \{A, B, C, D\}$ be the *letters* encoding the four edges of the regular *octagon* O with side lengths chosen to be 1. After opposite edges are identified as in Figure 6.1, we obtain a translation surface (O, ω_O).

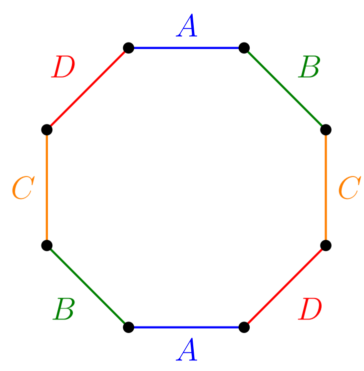

Figure 6.1: Octagon with labeled sides

Let $\mathcal{L}_n \subseteq \Sigma^n$ denote the set of all *cutting sequences* of length n obtainable via straight line trajectories on (O, ω_O) and $\mathcal{L} = \bigcup_{n=0}^{\infty} \mathcal{L}_n$.

Remark 6.1.11 (Octagon coming from billiards)
The billiards in the rational triangles with angles $\left(\frac{\pi}{2}, \frac{3\pi}{8}, \frac{\pi}{8}\right)$ or $\left(\frac{3\pi}{8}, \frac{3\pi}{8}, \frac{\pi}{4}\right)$ both unfold to the octagon (O, ω_O).

To explicitly calculate the steps in the proof of Theorem 6.1.7, there are different methods to determine the first finite iterates of $p_O(n)$. Cassaigne utilized an algorithm based on substitution rules from [SU11] to construct all relevant words. One can also apply the heuristics previously discussed after Corollary 6.1.9, aiming to compute N_c explicitly. Upon comparing these approaches, we can observe discrepancies: for $n = 2$, the results are off by a factor of 4, and for larger values of n, the results are off by a factor greater than 2. The root of this problem lies in the heuristics; the same words can occur in different directions, leading to variations in the calculated results.

In the case of the square torus, this becomes clear by realizing that the reverse flow in the opposite direction can always encode the same word: If a word $w = c(\tau)$ is encoded by a trajectory τ, rotate τ around the center point of the square to obtain τ', then $c(\tau') = w$. This happens for all words and cannot occur in other directions because of the bijection between directions and words occurring via the Farey map. So, the two methods mentioned to calculate the complexity before are always off by a factor of 2. This is however not the case in the octagon, we noticed some words appearing only in two and some appearing in four different directions. We hope that solving the exact relationship will allow us to use results on saddle connections to calculate the complexity.

6.2 Renormalization scheme

In this section, we reintroduce concepts like infinitely derivable or the continued fraction expansion we obtained from some renormalization scheme on the square torus but for the octagon. Some of these statements are easily transferable while other ones require completely different notions.

Refer to the definition of the language on the regular octagon from Definition 6.1.10. We now subdivide these sets based on the direction in which they appear.

Definition 6.2.1 (Sectors and more languages)
Let $\Sigma_i := [i\frac{\pi}{8}, (i+1)\frac{\pi}{8}) \mod 2\pi\mathbb{Z}$ for $i \in \{0, \dots, 15\}$ be the *sector* decomposition of all possible directions in the plane as seen in Figure 6.2.

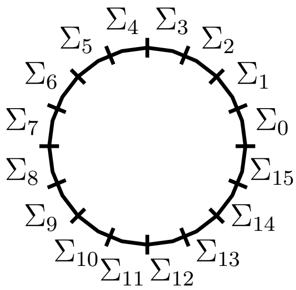

Figure 6.2: Definitions of direction sectors in S^1

Let $\mathcal{L}_n(\Sigma_i)$ be the *sublanguage* of $\mathcal{L}_n$ and $\mathcal{L}(\Sigma_i)$ be the *sublanguage* of $\mathcal{L}$, whose words can be found in direction Σ_i. A word w can be found in direction Σ_i, if there exists a trajectory τ on (O, ω_O), such that w is a factor of $c(\tau)$ and the direction of τ is in Σ_i.

Let $\mathcal{L}_n^\star$ be the *sublanguage* of $\mathcal{L}_n$ and $\mathcal{L}^\star$ be the *sublanguage* of $\mathcal{L}$, whose words have a factor AA, BB, CC or DD.

Given our direction sectors, let us define admissibility for (O, ω_O) like we did for the square torus.

Definition 6.2.2 (Admissible)
A word $w \in \Sigma^* \cup \Sigma^{\mathbb{Z}}$ is *admissible (admissible in diagram i)* if it describes a path on one of the *diagrams* (on $\mathcal{D}_i$) given by Figure 6.3.

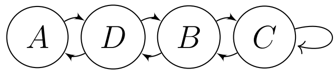

(a) $\mathcal{D}_0, \mathcal{D}_8$

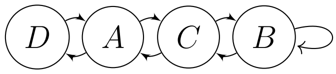

(b) $\mathcal{D}_1, \mathcal{D}_9$

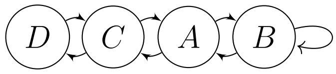

(c) $\mathcal{D}_2, \mathcal{D}_{10}$

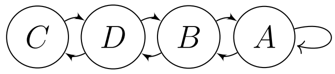

(d) $\mathcal{D}_3, \mathcal{D}_{11}$

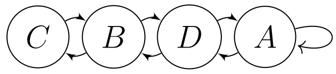

(e) $\mathcal{D}_4, \mathcal{D}_{12}$

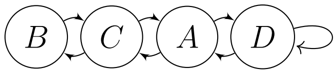

(f) $\mathcal{D}_5, \mathcal{D}_{13}$

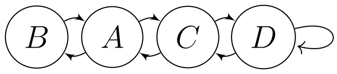

(g) $\mathcal{D}_6, \mathcal{D}_{14}$

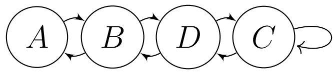

(h) $\mathcal{D}_7, \mathcal{D}_{15}$

Figure 6.3: Transition diagrams

Lemma 6.2.3 (Admissible is necessary)
The words of $\mathcal{L}_n(\Sigma_i)$ are admissible in diagram $\mathcal{D}_i$.

Proof. This is shown in Lemma 2.1.7. of [SU11]. □

We want to define an adjusted version of derived words which respects some renormalization scheme. For this, we can do the following:

Definition 6.2.4 (Sandwiched letters property)
A letter m of an biinfinite word $w \in \Sigma^{\mathbb{Z}}$ is *(l–)sandwiched*, if it is preceded and followed by the same letter l.

Example 6.2.5 (Sandwiched letters)
In the biinfinite word
$$w = \dots AABAABAABAAB \dots,$$
every letter B is A–sandwiched, but not the other way around.

Definition 6.2.6 (Derivation)
Given a word $w \in \Sigma^{\mathbb{Z}}$, the *derived word*, which we denote by w', is the word obtained by keeping only the letters of w which are sandwiched.

Definition 6.2.7 (Normalization)
Given a trajectory τ with direction in Σ_k, we call $n(\tau) \coloneqq \nu_k \tau$ the *normal form* of the trajectory τ, obtained by applying the isometry ν_k which maps Σ_k to Σ_0. The

corresponding eight permutations of $\{A, B, C, D\}$ will be denoted by π_i for $i \in \{0, \dots, 7\}$ and the corresponding *normal form* of the word $n(w) := \pi_k w$. These maps in their natural basis representation and permutations in cycle notation are explicitly given by:

$$\begin{array}{llll}
\nu_0 = \begin{pmatrix} 1 & 0 \\ 0 & 1 \end{pmatrix} & \nu_1 = \begin{pmatrix} \frac{1}{\sqrt{2}} & \frac{1}{\sqrt{2}} \\ \frac{1}{\sqrt{2}} & -\frac{1}{\sqrt{2}} \end{pmatrix} & \nu_2 = \begin{pmatrix} \frac{1}{\sqrt{2}} & \frac{1}{\sqrt{2}} \\ -\frac{1}{\sqrt{2}} & \frac{1}{\sqrt{2}} \end{pmatrix} & \nu_3 = \begin{pmatrix} 0 & 1 \\ 1 & 0 \end{pmatrix} \\
\nu_4 = \begin{pmatrix} 0 & 1 \\ -1 & 0 \end{pmatrix} & \nu_5 = \begin{pmatrix} -\frac{1}{\sqrt{2}} & \frac{1}{\sqrt{2}} \\ \frac{1}{\sqrt{2}} & \frac{1}{\sqrt{2}} \end{pmatrix} & \nu_6 = \begin{pmatrix} -\frac{1}{\sqrt{2}} & \frac{1}{\sqrt{2}} \\ -\frac{1}{\sqrt{2}} & -\frac{1}{\sqrt{2}} \end{pmatrix} & \nu_7 = \begin{pmatrix} -1 & 0 \\ 0 & 1 \end{pmatrix} \\
\pi_0 = id & \pi_1 = (A\ D)(B\ C) & \pi_2 = (A\ B\ C\ D) & \pi_3 = (A\ C) \\
\pi_4 = (A\ C)(B\ D) & \pi_5 = (A\ B)(C\ D) & \pi_6 = (D\ C\ B\ A) & \pi_7 = (B\ D)
\end{array}$$

Lemma 6.2.8 (Renormalization scheme)
If w is a non-periodic cutting sequence, then the renormalization scheme

$$w_{k+1} := n(w_k)', \quad w_0 = w$$

is well-defined for all $k \in \mathbb{N}$. In this case, w determines an infinite sequence

$$(d_k)_{k \in \mathbb{N}_0} \in \{0, \dots, 7\}^{\mathbb{N}_0}$$

such that w_k is admissible in diagram $\mathcal{D}_{d_k}$.

Proof. This is shown in Proposition 2.2.1. of [SU11]. □

Definition 6.2.9 (Sequence of admissible diagrams)
We refer to the sequence $(d_k)_{k \in \mathbb{N}}$ as the *sequence of admissible diagrams.*

We can also create a version of the continued fraction expansion on the octagon by developing its direction on the sequence of admissible diagrams. The main idea is that d_{k+1} encodes information to further reduce the range of direction in the range obtained after the steps $d_1, \dots, d_k$. So we can develop the angle by reducing the range in each step. After iterating for k steps, we obtain a direction range given by:

Definition 6.2.10 (Direction segment)
Given $(s_k)_{k \in \mathbb{N}}$ with $s_k \in \{0, \dots, 7\}$, let

$$\overline{\Sigma}[s_0; s_1, \dots, s_k] := \bigcap_{k \in \mathbb{N}} F_{s_0}^{-1} F_{s_1}^{-1} \dots F_{s_k}^{-1} [0, \pi]$$

be the *direction segment*, constructed with the *octagon Farey map*:

$$F(\alpha) = F_i(\alpha) := \cot^{-1} \left(\frac{a \cot \alpha + b}{c \cot \alpha + d} \right), \text{ where } \begin{pmatrix} a & b \\ c & d \end{pmatrix} = \begin{pmatrix} -1 & 2\left(1 + \sqrt{2}\right) \\ 0 & 1 \end{pmatrix} \nu_i$$

if $\alpha \in \Sigma_i$.

Remark 6.2.11 (Initial segment coincides)
Notice that $\overline{\Sigma}[s_0] = F_{s_0}^{-1}[0,\pi] = \Sigma_{s_0}$, so the first element in the sequence corresponds to the main direction segment Σ_0 to Σ_7. We also only consider angles $\theta \in [0,\pi)$ in this definition. For $\theta \in [\pi, 2\pi)$, we get the same sequence of admissible diagrams by construction.

Definition 6.2.12 (Octagon additive continued fraction expansion)
If

$$\{\theta\} = \bigcap_{k\in\mathbb{N}} \overline{\Sigma}[s_0; s_1, \dots, s_k],$$

we write $\theta \coloneqq [s_0; s_1, \dots]$ and say that $[s_0; s_1, \dots]$ is an *octagon continued fraction expansion* of θ.

We can also extend the renormalization scheme to its trajectories.

Proposition 6.2.13 (Direction recognition)
If w is a non-periodic cutting sequence, the direction of trajectories τ such that w is the encoding of the trajectory τ is uniquely determined and given by

$$\theta = [d_0(w); d_1(w), \dots, d_k(w), \dots],$$

where $(d_k(w))_{k\in\mathbb{N}}$ is the sequence of admissible diagrams.

Proof. This follows from Proposition 2.2.1. of [SU11], the uniqueness of $d_k(w) = s_k$, and Lemma 2.2.17. of [SU11]. □

Definition 6.2.14 (Derived trajectory)
Let τ be a trajectory. Define the *derived trajectory* τ' via

$$c(\tau') = c(\tau)'.$$

This is unique as shown in the proof of Proposition 2.2.1. of [SU11].

Definition 6.2.15 (Renormalization on trajectories)
Given a trajectory τ, define the *renormalized trajectory sequence* $(\tau_k)_{k\in\mathbb{N}}$ by

$$\tau_k \coloneqq n(\tau)', \tau_0 \coloneqq \tau.$$

Definition 6.2.16 (Sequence of sectors)
Given a trajectory τ, define the *sequence of sectors* $(s_k)_{k\in\mathbb{N}}$ by

$$s_k(\tau) \coloneqq s(\tau_k),$$

where $s(\tau_k)$ is the corresponding sector of τ_k.

Compared to the square torus, on the octagon “infinitely derivable” is not enough to understand the closure of cutting sequences. For this we need a stronger definition.

Definition 6.2.17 (Coherence)
A derivable word $w \in \Sigma^{\mathbb{Z}}$ is *coherent with respect to* (i, j), if the following conditions hold:

(C0) The word w is admissible (in diagram i).

If we normalize w by setting $n(w) \coloneqq \pi_i w$, then:

(C1) Sandwiched letters occurring in $n(w)$ fall into one of these groups G_k:

$$G_0 \coloneqq \{D\text{–sandwiched } A, C\text{–sandwiched } B, B\text{–sandwiched } C, A\text{–sandwiched } D\},$$
$$G_1 \coloneqq \{D\text{–sandwiched } A, C\text{–sandwiched } B, B\text{–sandwiched } C, B\text{–sandwiched } D\},$$
$$G_2 \coloneqq \{D\text{–sandwiched } A, C\text{–sandwiched } B, C\text{–sandwiched } C, B\text{–sandwiched } D\},$$
$$G_3 \coloneqq \{D\text{–sandwiched } A, D\text{–sandwiched } B, C\text{–sandwiched } C, B\text{–sandwiched } D\}.$$

(C2) The derived word of $n(w)$ is admissible (in diagram j).

(C3) The condition $k = [j/2]$ holds, where $[x]$ denotes the integer part of x. We obtain j and k corresponding to conditions (C2) and (C1), respectively.

A derivable word $w \in \Sigma^{\mathbb{Z}}$ is *coherent*, if there exists a pair $(i, j) \in \{1, \dots, 7\}^2$, such that w is coherent with respect to (i, j).

Analogously, the renormalization scheme can also be extended to its words:

Definition 6.2.18 (Renormalization on a word sequence)
Given a word $w \in \Sigma^{\mathbb{Z}}$ and a sequence $s \in \{0, \dots, 7\}^{\mathbb{N}}$, define the *renormalized word sequence* $(w_k)_{k \in \mathbb{N}}$ by

$$w_k \coloneqq (\pi_{s_{k-1}} \cdot w_{k-1})', \quad w_0 \coloneqq w.$$

Definition 6.2.19 (Infinite coherence)
A word $w \in \Sigma^{\mathbb{Z}}$ is *infinitely coherent* (with respect to a sequence $s \in \{0, \dots, 7\}^{\mathbb{N}}$), if it is infinitely derivable and for each $k \in \mathbb{N}$, the renormalized word w_k in Definition 6.2.18 is coherent (with respect to (s_k, s_{k+1})).

With the following lemma, we can associate infinitely coherent words with a specific direction, given the first direction segment. Notice that this cannot be true globally without the first direction, because cutting sequences can be obtained from trajectories coming from different direction segments. In fact, it is this count that we aim to understand in this chapter.

Lemma 6.2.20 (Unique continuation)
Let w be infinitely coherent and admissible in diagram s_0. Then there exists a sequence $s \in \{0, \dots, 7\}^{\mathbb{N}}$, starting with s_0 with respect to which w is infinitely coherent.

Proof. This is shown in Lemma 2.4.4. of [SU11]. □

Now infinite coherence is the right way to understand biinfinite cutting sequences and the right analog for infinitely derivable in the square torus case.

Lemma 6.2.21 (Infinite coherence of cutting sequences)
A cutting sequence $c(\tau)$ is infinitely coherent.

Proof. This is shown in Proposition 2.4.5. of [SU11]. □

Theorem 6.2.22 (Closure of the space of cutting sequences — Smillie and Ulcigrai)
The closure of the space of cutting sequences coincides with the set of infinitely coherent words.

Proof. This is shown in Theorem 2.4.8 of [SU11]. □

In particular, we get all finite subwords:

Lemma 6.2.23 (Finite factors are cutting sequences)
If w is an infinitely coherent word with respect to $(s_0, s_1, s_2, \ldots)$, each finite factor of w is a cutting sequence of some segment of a periodic trajectory τ in direction $\theta \in \Sigma_{s_0}$.

Proof. This is shown in Proposition 2.4.21. of [SU11]. The direction is a consequence of Proposition 2.4.5. of [SU11]. □

Since we now understand how to encode finite cutting sequences as factors of infinitely coherent words and how to associate directions with a continued fraction expansion, we begin our work on how to calculate how often finite cutting sequences appear in different direction sections.

6.3 Connected components

In this section, we solve the counting problem arising from understanding complexity by investigating cutting sequences given by straight line trajectories for different starting points and directions. We show that all words which are bounded cyclically by saddle connections appear either exactly two or four times in the case of the octagon and we can predict the exact number by the word alone.

To get the big picture, we parameterize the straight line trajectories with initial conditions by using the following phase space.

Definition 6.3.1 (Phase space)
Let $\mathcal{P}_n$ denote the *phase space* of linear flow trajectories with cutting sequences of truncated length n on our octagon via parametrization $[0, 8) \times (-\infty, \infty)$. The first component parameterizes a cutting point of a trajectory with the boundary ∂O of the octagon, where each side has length 1. The upper-left corner between the edges labeled D and A corresponds to 0. We continue the parameterization clockwise, so the upper-right corner between A and B corresponds to 1, and so on. The second component measures the slope of the trajectory with respect to the inward orthogonal to each side, see Figure 6.4. We truncated non-closed trajectories to encode the first n letters.

Let $\mathcal{P}(w)$ denote the part of the phase space $\mathcal{P}_n$ corresponding to the word $w \in \mathcal{L}_n$.

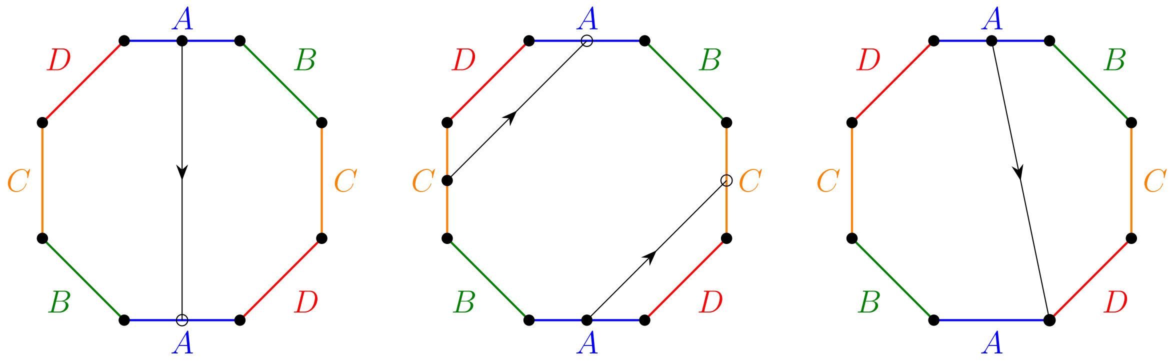

(a) $\left(\frac{1}{2}, 0\right)$ (b) $\left(\frac{5}{2}, 1\right)$ or $\left(\frac{13}{2}, 1\right)$ (c) $\left(\frac{1}{2}, \frac{1}{2}\left(\sqrt{2}-1\right)\right)$

Figure 6.4: Octagon with trajectories parametrized by position and slope

Remark 6.3.2 (Exceptions)
Let $(x, s) \in \mathcal{P}_n$ be some starting condition of our trajectory. If $x \in \{0, \dots, 7\}$, we do not get a well-defined trajectory for every $n \in \mathbb{N}_0$, similar for $\left(\frac{1}{2}, \frac{1}{2}\left(\sqrt{2}-1\right)\right)$ for large enough n and in general a lot of other points in $[0, 8) \times (-\infty, \infty)$ corresponding to separatrices and saddle connections. However, for each $n \in \mathbb{N}^+$, these points in $\mathcal{P}_n$ correspond to sets of measure 0, so almost all pairs of starting position and directions will be well-defined. These sets will correspond to the boundaries of the connected components, as we will see later.

Convention 6.3.3 (Generality)
Since almost all initial conditions in $(x, s) \in \mathcal{P}_n$ yield well-defined cutting sequences coming from biinfinite words, we will omit to write "almost all" and talk about the whole set $[0, 8) \times (-\infty, \infty)$ when discussing the initial conditions corresponding to biinfinite words.

A nice fact we can use when working with the phase space, is that projecting on one of its components preserves connectivity.

Remark 6.3.4 (Projection preserves connectivity)
Consider the projection

$$\phi\colon \mathcal{P}_n \to S^1, \quad (x, s) \mapsto \arctan(s).$$

If a domain D is connected in $\mathcal{P}_n$, so must be $\phi(D) \subseteq S^1$. This insight will be helpful later, to show disconnectivity in $\mathcal{P}_n$.

Proposition 6.3.5 (Convex polygons)
For all words $w \in \mathcal{L}_n$, the connected components of $\mathcal{P}(w)$ are convex polygons in $\mathcal{P}_n$.

Proof. We show this by induction over word length. For $|w| = 1$, the slope for each trajectory does not matter and the word is solely encoded by the starting point on ∂O. The closure of the phase space $\mathcal{P}_1$ therefore consists of eight infinitely long stripes $[n-1, n] \times [-\infty, \infty]$ for $n \in [8]$, which are convex polygons, see Figure 6.6a.

Let $w \in \mathcal{L}_n$. Let the connected components of $\mathcal{P}(w)$ be convex polygons. Consider the universal cover of (O, ω_O). Fix some connected component C of $\mathcal{P}_n(w)$. The union of trajectories with cutting sequence w constitute a set T in the universal cover. The last letter of w is obtained by intersecting with an edge $\tilde{e}$ in the universal cover. Consider the octagon $\tilde{O}$ in the universal cover, which shares the edge $\tilde{e}$ and in which the trajectories encoding w extend. Continue the word w by a letter $s \in \Sigma$. We obtain the possible word continuations as encodings of the edges in $\left(T \cap \partial\tilde{O}\right) \setminus \tilde{e}$, see Figure 6.5.

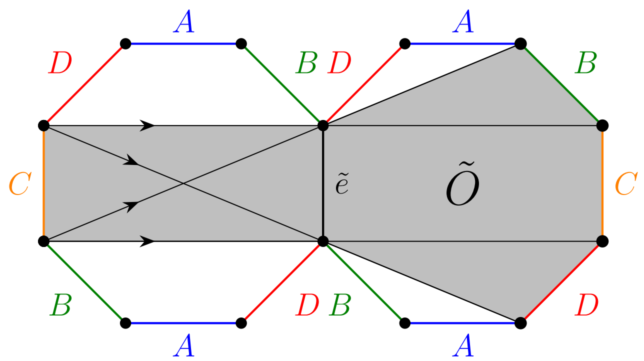

Figure 6.5: Word extensions of $w = CC$ in the connected component containing $\left(\frac{13}{2}, 0\right)$, set T in gray, possible word continuations from $\left(T \cap \partial\tilde{O}\right) \setminus \tilde{e}$ are in $\{B, C, D\}$

Now fix some word continuation $s \in \Sigma$. The boundary of a connected component in $\mathcal{P}(ws)$ will correspond to trajectories, where some local deformation can result in a transition to a new encoding. This transition corresponds to trajectories starting on the edge which encode w_1 and ending in the corners of $\left(T \cap \partial\tilde{O}\right) \setminus \tilde{e}$.

To solve for the set of these trajectories for each corner individually, we need to calculate the trajectories parametrized by $(x, m) \in \mathcal{P}(w)$, which go through a specific corner P from $\left(T \cap \partial\tilde{O}\right) \setminus \tilde{e}$ in the universal cover. These conditions are all linear, so every connected component of $\mathcal{P}(ws)$ is obtained as the intersection of C with at most two half spaces.

Since C is convex, by the induction hypothesis the connected components of $\mathcal{P}(ws)$ in C will be convex polygons. Every connected component in $\mathcal{P}_{n+1}$ can be obtained this way. $\square$

We want to count the number of connected components for different words, for which we introduce the following notation.

Definition 6.3.6 (Set of connected components)
Let $CC(A) := \{\mathcal{C}_i\}_{i \in I}$ be the *set of connected components* for some set A. In particular $|CC(A)|$ is the number of connected components in A.

A crucial step to understand the number of connected components is to understand its growth locally for each step in word length.

Lemma 6.3.7 (Unique continuation)
Let $w \in \mathcal{L}_n$ with $n \geq 2$, let $l \in \Sigma$, such that $wl \in \mathcal{L}_{n+1}$. Let $\mathcal{C}$ be a connected component of $\mathcal{P}(w)$. Then

$$|CC\left(\mathcal{P}(wl) \cap \mathcal{C}\right)| \leq 1.$$

Proof. If $\mathcal{P}(wl) \cap \mathcal{C} = \emptyset$, the statement is trivially true. So assume that $\mathcal{P}(wl) \cap \mathcal{C}$ is the non-empty region in the convex polygon $\mathcal{P}(w)$ obtained via the intersection with some half space(s) used in the induction of the proof of Proposition 6.3.5.

Two or more letters restrict the possible direction already to a range of directions in S^1 with cone angle smaller than or equal to $\frac{\pi}{4}$. There are at most the same number of words of the form wl in $\mathcal{C}$ as there are connected components in $\mathcal{C}$, since in a cone angle smaller than or equal to $\frac{\pi}{3}$, each letter range for continuation can appear only once.

Since each word extension in $\mathcal{P}(wl) \cap \mathcal{C}$ is non-empty, there is also at least one connected component. So, by the pigeonhole principle $|CC\left(\mathcal{P}(wl) \cap \mathcal{C}\right)| = 1$ for those words. □

Lemma 6.3.8 (Non-increasing property)
Word continuations cannot increase the number of connected components for words of length at least 2.

$$\forall w \in \mathcal{L}_n, n \geq 2, \forall l \in \Sigma\colon\ |CC(\mathcal{P}(wl))| \leq |CC(\mathcal{P}(w))|\,.$$

Proof. Let $w \in \mathcal{L}_n$ with length at least 2 and $l \in \Sigma$ be fixed.
If $wl \in \mathcal{L}_{n+1}$, then by Lemma 6.3.7 $|CC\left(\mathcal{P}(wl) \cap \mathcal{C}\right)| \leq 1$ for all $\mathcal{C} \in CC(\mathcal{P}(w))$.
If $wl \notin \mathcal{L}_{n+1}$, then $|CC\left(\mathcal{P}(wl) \cap \mathcal{C}\right)| = |CC\left(\emptyset\right)| = 0$. Therefore:

$$\begin{aligned} |CC(\mathcal{P}(w))| &= \sum_{\mathcal{C} \in CC(\mathcal{P}(w))} 1 \\ &\geq \sum_{\mathcal{C} \in CC(\mathcal{P}(w))} \chi_{\{\mathcal{P}(wl) \cap \mathcal{C} \neq \emptyset\}} \\ &\geq \sum_{\mathcal{C} \in CC(\mathcal{P}(wl))} 1 = |CC(\mathcal{P}(wl))|\,. \end{aligned}$$ □

We can use these lemmas for an induction with the following base case.

Lemma 6.3.9 (Base case)
For all $p, q \in \Sigma$:

$$\begin{aligned} |CC(\mathcal{P}(p))| &= 2, \\ |CC(\mathcal{P}(pq))| &= 4 - 2\delta_{p,q}. \end{aligned}$$

Proof. The first few connected components can be computed directly. We already described the phase space for $\mathcal{P}_1$ as eight stripes. Similar but longer calculation can explicitly give the connected components for $\mathcal{P}_2$, see Figure 6.6 from which we can read of this statement. □

These statements are enough for a global upper bound, which is even optimal in word length as we will see later.

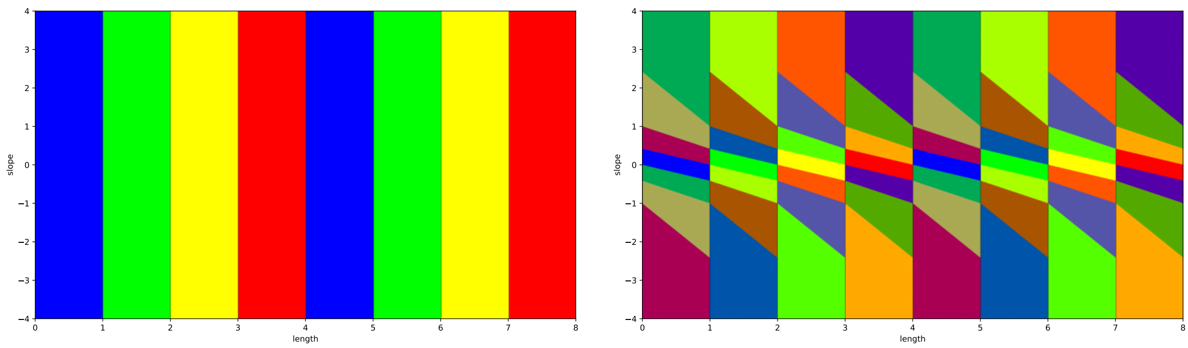

(a) $\mathcal{P}_1$ contains four different words and colors (b) $\mathcal{P}_2$ contains 16 different words and colors

Figure 6.6: Phase space picture for $\mathcal{P}_1$ and $\mathcal{P}_2$, each color represents another word, figure is generated with the code in [Rei24c]

Lemma 6.3.10 (Upper limit)
For every word $w \in \mathcal{L}_n$, $\mathcal{P}(w)$ has at most four connected components in $\mathcal{P}_n$:

$$|CC(\mathcal{P}(w))| \leq 4.$$

Proof. This follows immediately from Lemma 6.3.8 and Lemma 6.3.9. □

For a lower bound, we need to understand symmetries that will force the existence of the same cutting sequences in other directions. The easiest one corresponds to reversing the flow, which is also the case on the square torus.

Lemma 6.3.11 (Reverse direction)
If $w \in \mathcal{L}_n(\Sigma_i)$, then $w \in \mathcal{L}_n(\Sigma_{i+8 \mod 16})$.

Proof. Let $w \in \mathcal{L}_n(\Sigma_i)$ and $\tau \colon \mathbb{R} \to O$ be the corresponding trajectory. Let C be the center of O. Rotating (each segment) of τ around C with angle π yields a new trajectory $\tilde{\tau}$ with the same cutting sequence as τ, but in reverse direction, so

$$w \in \mathcal{L}_n(\Sigma_{i+8 \mod 16}).$$ □

We can also exclude some directions, if we know a cutting sequence appears in one direction segment.

Lemma 6.3.12 (Barrier)
If $w \in \mathcal{L}_n(\Sigma_i)$ with $n \geq 2$, then $w \notin \mathcal{L}_n(\Sigma_{i+2 \mod 16})$.

Proof. For every word $w \in \mathcal{L}_n(\Sigma_i)$ that contains at least two letters, we can list all factors of length 2. For example for $i = 1$, we obtain a subset of

$$\{AD, DA, DB, BD, BC, CB, CC\}.$$

None of these factors can be obtained from the transition diagram $\mathcal{D}_{i+2 \mod 16}$ in Definition 6.2.2, which implies that $w \notin \mathcal{L}_n(\Sigma_{i+2 \mod 16})$. □

These lemmas are enough to get a global lower bound on the connected components.

Lemma 6.3.13 (Lower bound)
For every word $w \in \mathcal{L}_n$, $\mathcal{P}(w)$ has at least two connected components in $\mathcal{P}_n$.

Proof. Let $w \in \mathcal{L}_n(\Sigma_i) \subseteq \mathcal{L}_n$. Using Lemma 6.3.11, we know that $w \in \mathcal{L}_n(\Sigma_{i+8 \mod 16})$. This implies there are trajectories parametrized by (x_1, m_1) and (x_2, m_2) in the phase space.

Next we show, that these trajectories lie in different connected components of the phase space. Because of Remark 6.3.4, it is enough to check if their image under the projection onto S_1 are not connected.

Because of Lemma 6.3.12, we know that w can not occur as en encoding in the direction segment $\Sigma_{i+2 \mod 16}$ and $\Sigma_{i+10 \mod 16}$. Therefore, the image of the projection must contain at least two connected components, as illustrated in Figure 6.7. □

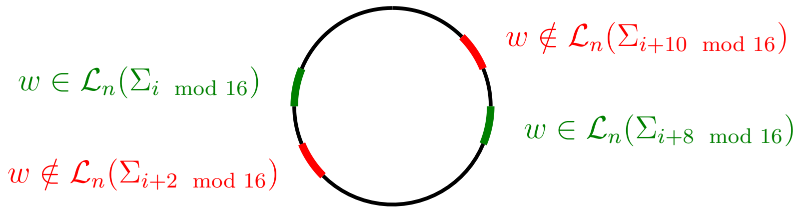

Figure 6.7: Directions in S^1, word cannot occur in red domains and needs to occur in green domains

There is an invariant for the count of connected components by reversing words, which does not correspond to finding the same word in another direction, but rather equating the count of connected components for different words.

Definition 6.3.14 (Reverse word)
Let $w \in \mathcal{L}_n$. Define the word $\overleftarrow{w} \in \mathcal{L}_n$ as the *reversion* of w by writing the letters in reversed order.

Remark 6.3.15 (On reversion)
Be reversing the flow of a trajectory, every word in $\mathcal{L}$ can be reversed and if $w \in \mathcal{L}_n(\Sigma_i)$, then $\overleftarrow{w} \in \mathcal{L}_n(\Sigma_{i+8 \mod 16})$.

Lemma 6.3.16 (Reversion invariant)
The number of connected components is invariant under reversion:

$$|CC(\mathcal{P}(w))| = |CC(\mathcal{P}(\overleftarrow{w}))| .$$

Proof. This follows directly from the phase space construction. A trajectory of $\overleftarrow{w}$ is the same as a trajectory of w with reversed flow. So, there is a bijective map $\psi\colon \mathcal{P}_n \to \mathcal{P}_n$ mapping $w \mapsto \overleftarrow{w}$. This involution sends connected components to connected components, such that

$$|CC(\mathcal{P}(w))| = |CC(\mathcal{P}(\overleftarrow{w}))| .$$
□

Let $w \in \mathcal{L}$ finite. We already know that $|CC(\mathcal{P}(w))| \in \{2,3,4\}$, which enables us to establish both upper and lower bounds that relate the two distinct counting problems from Section 6.1. However, this is insufficient to determine the exact asymptotic constant. Looking at short word examples, one can realize that words having double letters only appear as cutting sequences of trajectories in two direction segments.

Recall that we denote by $\mathcal{L}^{\star}_{(n)}$ the sublanguage of words in $\mathcal{L}_{(n)}$ that contain double letters $\{AA, BB, CC, DD\}$ as a factor.

Proposition 6.3.17 (Double letter factor)
If $w \in \mathcal{L}^{\star}_{n}$, then $|CC(\mathcal{P}(w))| = 2$.

Proof. Let $w \in \mathcal{L}^{\star}_{n} \subseteq \mathcal{L}_{n}$. Without loss of generality, let $w = w_1 AA w_2$ with $|w_1| < \infty$. From Lemma 6.3.9, we know that $|CC(\mathcal{P}(AA))| = 2$. Using Lemma 6.3.8, we know that $|CC(\mathcal{P}(AA\overleftarrow{w_1}))| \leq 2$. Since

$$\overleftarrow{AA\overleftarrow{w_1}} = w_1 AA,$$

we see $|CC(\mathcal{P}(w_1 AA))| \leq 2$ by Lemma 6.3.16. Lastly using Lemma 6.3.8 again, we can see that $|CC(\mathcal{P}(w))| = |CC(\mathcal{P}(w_1 AA w_2))| \leq 2$ and Lemma 6.3.13 yields equality. □

Words not containing these double letters can be found in an almost perpendicular direction.

Lemma 6.3.18 (Almost orthogonal)
If $w \in \mathcal{L}_n(\Sigma_i) \setminus \mathcal{L}^{\star}_{n}$, then $w \in \mathcal{L}_n(\Sigma_{i+4 \mod 16})$.

Proof. Without loss of generality, let $w \in \mathcal{L}_n(\Sigma_0) \setminus \mathcal{L}^{\star}_{n}$. Since $w \in \mathcal{L}_n(\Sigma_0)$, there exists a trajectory τ, such that $w \in c(\tau)$. Because $c(\tau)$ is a cutting sequence, it is infinitely coherent by Lemma 6.2.21.

Because of Lemma 6.2.23, each factor of $c(\tau)$ is contained in a cutting sequence for some periodic $\tilde{\tau}$ in some direction $\theta \in \Sigma_0$. Let $\tilde{w} \coloneqq c(\tilde{\tau}) \in \mathcal{L}(\Sigma_0) \setminus \mathcal{L}^{\star}$.

We can choose $\tilde{\tau}$ in Lemma 6.2.23, such that $c(\tilde{\tau}) \notin \mathcal{L}^{\star}$. We are able to achieve this, since $w \notin \mathcal{L}^{\star}_{n}$, so we can extend w to $\tilde{w}$ with no additional double letters in the set of infinitely coherent words. The extended word $\tilde{w}$ is infinitely coherent with respect to $s = (0, s_1, s_2, \ldots)$ as a cutting sequence.

We can see that the diagrams $\mathcal{D}_0$ and $\mathcal{D}_4$ in Definition 6.2.2 are the same, if one does not allow loops on nodes, which we do not need, since $\tilde{w} \notin \mathcal{L}^{\star}$.

Furthermore, we can see that the Diagrams $\mathcal{D}_0$ and $\pi_4(\mathcal{D}_4)$ in Figure 6.3 are the same.

So $\tilde{w}$ is infinitely coherent with respect to $\tilde{s} = (4, s_1, s_2, \ldots)$ by Definition 6.2.19. In particular, w is a factor of $\tilde{w}$ by construction, so $w \in \mathcal{L}_n(\Sigma_4)$ with Lemma 6.2.23. □

Proposition 6.3.19 (No double letter factor)
Let $n \geq 2$. If $w \in \mathcal{L}_n(\Sigma_i) \setminus \mathcal{L}^{\star}_{n}$, then $|CC(\mathcal{P}(w))| = 4$.

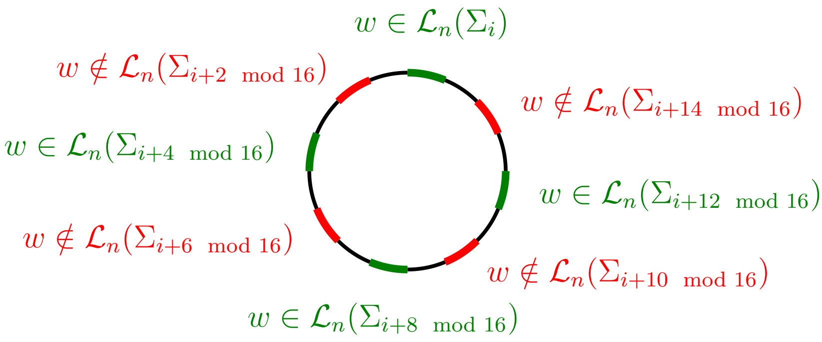

Figure 6.8: Directions in S^1, word cannot occur in red domains and needs to occur in green domains

Proof. Let $w \in \mathcal{L}_n(\Sigma_i) \subseteq \mathcal{L}_n, n \geq 2$. Applying Lemmas 6.3.12 and 6.3.18 implies in which section w must occur at least once or can never occur, this is visualized in Figure 6.8.

Since w can be found in four different directions which cannot be path-connected in $\mathcal{P}(w)$ by Remark 6.3.4, we get $|CC(\mathcal{P}(w))| \geq 4$. Finally, Lemma 6.3.10 yields equality. □

Theorem 6.3.20 (Double letter encodes case — Athreya, Bédaride, Cassaigne, and R.) For every word $w \in \mathcal{L}$:

$$|CC(\mathcal{P}(w))| = \begin{cases} 2, & \text{if } w \in \mathcal{L}^\star \cup \mathcal{L}_1 \\ 4, & \text{otherwise.} \end{cases}$$

Proof. Using Lemma 6.3.9 for the base case and Propositions 6.3.17 and 6.3.19 yields this theorem. □

Part IV

Geometric invariants

7 Volume calculation of strata

The goal of this chapter is to formalize the volume form in spaces of translations surfaces in order to make quantitative statements in the remaining chapters. In particular, we are interested in statements on asymptotics in growing genus. So, calculating some volume estimates on specific strata of translation surfaces will be of highest importance. The proofs and concepts in this chapter are based on [EMZ03].

7.1 Volume form and asymptotics

To construct a volume form in the space of translation surfaces, consider the set of holonomy vectors H_{sc} introduced in Proposition 3.3.29 on a translation surface $(X, \omega) \in \mathcal{H}(\kappa)$ with singularities Σ. For every saddle connection, we get a *holonomy vector* in $\mathbb{C}$ via the translation structure ω on X. Associate each saddle connection to an element of the first relative cohomology group $H^1(X, \Sigma; \mathbb{C})$ as we did in Remark 3.5.10. In particular, we saw that these so-called *period coordinates* describe locally

$$H^1(X, \Sigma; \mathbb{C}) \cong \mathbb{R}^{4g+2l-2},$$

around (X, ω), where l is the count of singularities on (X, ω). Furthermore, the gluings between different linear coordinate charts on $\mathcal{H}(\kappa)$ correspond to automorphisms of $H^1(X, \Sigma; \mathbb{C})$, induced by the diffeomorphisms of X.

The cohomology group with complex coefficients contains a lattice $H^1(X, \Sigma; \mathbb{Z} \oplus \mathrm{i}\mathbb{Z})$ within $H^1(X, \Sigma; \mathbb{C})$ that is invariant under these automorphisms. An abelian differential ω for $(X, \omega) \in \mathcal{H}(\kappa)$ corresponds to an integer point in the moduli space if its image under the period map is in this lattice. Such surfaces are square-tiled surfaces.

We can now define a volume element in $H^1(X, \Sigma; \mathbb{C})$ and normalize it with the natural choice, such that the volume of a unit cube of the lattice is one. It is now very intuitive to define the volume form by a pullback. Since the coordinate changes in $\mathcal{H}(\kappa)$ are linear transformations preserving the lattice, the volume element in $H^1(X, \Sigma; \mathbb{C})$ induces a volume element $\mathrm{d}\nu$ on $\mathcal{H}(\kappa)$ independent of the choice of basis.

Definition 7.1.1 (Masur–Veech volume)
The *Masur–Veech volume* ν on a stratum $\mathcal{H}(\kappa)$ can be defined locally on each neighborhood U as the pullback of the Lebesgue measure from $\mathbb{R}^{4g+2l-2}$ to U. This gives rise to a global form of the same name on $\mathcal{H}(\kappa)$.

Let (X,ω) be a translation surface, let A_i and B_i be its periods. The area of X, denoted by area(X), is given in the flat structure ω by

$$\operatorname{area}(X) = \frac{i}{2}\int_X \omega \wedge \overline{\omega} = \frac{i}{2}\sum_{i=1}^{g}(A_i\overline{B_i} - \overline{A_i}B_i).$$

With this, it is easy to see that for all $t \in \mathbb{C}$:

$$\operatorname{area}(tX) = |t|^2 \operatorname{area}(X).$$

The volume element $\mathrm{d}\nu$ induces a volume element $\mathrm{d}\tilde{\nu} = \frac{\mathrm{d}\nu}{\mathrm{d}S}$ on the hyperboloid $\mathcal{H}_1(\kappa)$. We can view this as a cone constructed in $\mathcal{H}(\kappa)$, where $\mathcal{H}_1(\kappa)$ forms the base plane.

Definition 7.1.2 (Cone)
Let S be a subset of $\mathcal{H}_1(\kappa)$. We define the *cone* $C(S) \in \mathcal{H}(\kappa)$ of S by

$$C(S) \coloneqq \{(X,\omega) \in \mathcal{H}(\kappa) \mid (X,\omega) = t(X',\omega'), (X',\omega') \in S, t \in (0,1]\}.$$

Lemma 7.1.3 (Masur–Veech volume for translation surfaces of area 1)
Let κ be a partition of $2g-2$, then

$$\tilde{\nu}\left(\mathcal{H}_1(\kappa)\right) = d \cdot \nu\left(C\left(\mathcal{H}_1(\kappa)\right)\right),$$

where $d \coloneqq \dim_{\mathbb{R}}\left(\mathcal{H}(\kappa)\right) = 4g + 2l - 2$.

Proof. Let $d = \dim_{\mathbb{R}}\left(\mathcal{H}(\kappa)\right)$. For $(X,\omega) = t(X',\omega')$, we know that

$$\mathrm{d}\nu(X,\omega) = t^{d-1}\,\mathrm{d}t\,\mathrm{d}\tilde{\nu}(X',\omega').$$

In particular, we can calculate

$$\begin{aligned}
\nu\left(C\left(\mathcal{H}_1(\kappa)\right)\right) &= \int_{(X,\omega)\in C(\mathcal{H}_1(\kappa))} \mathrm{d}\nu(X,\omega) \\
&= \int_{(X',\omega')\in \mathcal{H}_1(\kappa)} \int_0^1 t^{d-1}\,\mathrm{d}t\,\mathrm{d}\tilde{\nu}(X',\omega') \\
&= \int_{(X',\omega')\in \mathcal{H}_1(\kappa)} \frac{1}{d}\,\mathrm{d}\tilde{\nu}(X',\omega') = \frac{1}{d}\tilde{\nu}\left(\mathcal{H}_1(\kappa)\right).
\end{aligned}$$

Multiplying by d yields the statement. ☐

Convention 7.1.4 (Masur–Veech volumes)
We denote the Masur–Veech volume for $\mathcal{H}(\kappa)$, as well as the Masur–Veech volume for $\mathcal{H}_1(\kappa)$ with ν. It will be clear from the context, which one we want to use.

In Chapters 8 and 9, we will construct translation surfaces by separating them along separating curves related to the Cheeger constant. This process results in disconnected surfaces. When a surface is separated into disconnected surfaces, we get a point in a stratum of disconnected surfaces $\mathcal{H}(\kappa') = \prod_{i=1}^{p}\mathcal{H}(\kappa_i')$.

The volume $\tilde{\nu}\left(\mathcal{H}_1\left(\kappa'\right)\right)$ of $\mathcal{H}_1\left(\kappa'\right)$ can be expressed with our regular volume ν in the following way:

Lemma 7.1.5 (Masur–Veech volume for disconnected surfaces)
Let $\mathcal{H}_1(\kappa')$ be a stratum of disconnected surfaces of total area 1, where $\kappa' = \sqcup_{i=1}^{p}\kappa_i'$. Then,

$$\tilde{\nu}(\mathcal{H}_1(\kappa')) = \frac{1}{2^{p-1}} \cdot \frac{\prod_{i=1}^{p}\left(\frac{d_i}{2}-1\right)!}{\left(\frac{d}{2}-1\right)!} \cdot \prod_{i=1}^{p} \nu(\mathcal{H}_1(\kappa_i')),$$

where $d_i = \dim_{\mathbb{R}} \mathcal{H}(\kappa_i')$ and $d = \dim_{\mathbb{R}} \mathcal{H}(\kappa')$.

Proof. This is shown after Convention 5 in [EMZ03]. Since this proof is helpful for understanding the relationship with the volume form, we still choose to present it here for clarity. Let $(X,\omega) \in \mathcal{H}_1(\kappa')$ for $\kappa' = \sqcup_{i=1}^{p}\kappa_i'$. So $X = \bigsqcup_{i=1}^{p} X_i$ with $X_i \in \mathcal{H}(\kappa_i')$ for all $i \in [p]$. Since each connected component of X has at most area 1, we can normalize each disconnected surface (X_i,ω_i) to unit area with $(X_i,\omega_i) = t_i(X_i',\omega_i')$ such that $\operatorname{area}(X_i') = 1$ and therefore $\operatorname{area}(X_i) = t_i^2$. Let $d_i = \dim_{\mathbb{R}} \mathcal{H}(\kappa_i')$ be the dimension of each stratum $\mathcal{H}(\kappa_i')$ and $d = \dim_{\mathbb{R}} \mathcal{H}(\kappa') = \sum_{i=1}^{p} d_i$ be the dimension of the total stratum. Let $\mathrm{d}\nu_i'$ be the volume element on the stratum $\mathcal{H}(\kappa_i')$ and $\mathrm{d}\tilde{\nu}_i'$ be the volume element of the corresponding hyperboloid $\mathcal{H}_1(\kappa_i')$. Then the volume element on $\mathcal{H}(\kappa')$ can be written as

$$\begin{aligned}
\mathrm{d}\nu(X,\omega) &= \prod_{i=1}^{p} d\nu_i'(X_i,\omega_i) \\
&= \prod_{i=1}^{p} \left(t_i^{d_i-1}\,\mathrm{d}t_i\,\mathrm{d}\tilde{\nu}_i'(X_i',\omega_i')\right),
\end{aligned}$$

similar to the proof of Lemma 7.1.3.

For $(X,\omega) \in \mathcal{H}_1(\kappa')$, these t_i must be in $\partial B_1(0) = \left\{(t_1,\ldots,t_p) \;\middle|\; t_1^2 + \ldots + t_p^2 = 1\right\}$. Then,

$$\begin{aligned}
\nu(C(\mathcal{H}_1(\kappa'))) &= \int_{(X,\omega)\in C(\mathcal{H}_1(\kappa'))} \mathrm{d}\nu(X,\omega) \\
&= \prod_{i=1}^{p} \nu(\mathcal{H}_1(\kappa_i')) \cdot \int_{\overline{B}_1(0)} \prod_{i=1}^{p} t_i^{d_i-1}\,\mathrm{d}t_i,
\end{aligned}$$

which we can solve with the substitutions $x_i = t_i^2$. Then $t_i^{d_i-1}\,\mathrm{d}t_i = \frac{1}{2}x_i^{\frac{d_i}{2}-1}\,\mathrm{d}x_i$ for each $i \in [p]$ and

$$\nu(C(\mathcal{H}_1(\kappa'))) = \frac{1}{2^p} \cdot \prod_{i=1}^{p} \nu(\mathcal{H}_1(\kappa_i')) \cdot \int_{\sum_{i=1}^{p} x_i \le 1} \prod_{i=1}^{p} x_i^{\frac{d_i}{2}-1}\,\mathrm{d}x_i.$$

We can use the identity

$$\int_0^y x^a (y-x)^b\,\mathrm{d}x = \frac{a!\,b!}{(a+b+1)!} y^{a+b+1}$$

on our integral p times and obtain

$$\nu(C(\mathcal{H}_1(\kappa'))) = \frac{1}{2^p} \cdot \prod_{i=1}^{p} \nu(\mathcal{H}_1(\kappa_i')) \cdot \frac{\prod_{i=1}^{p}\left(\frac{d_i}{2}-1\right)!}{\left(\sum_{i=1}^{p}\left(\frac{d_i}{2}-1\right)+p\right)!}.$$

Since $\sum_{i=1}^{p}\left(\frac{d_i}{2}-1\right)+p=\sum_{i=1}^{p}\frac{d_i}{2}=\frac{d}{2}$, we get

$$\nu\left(C\left(\mathcal{H}_1\left(\kappa'\right)\right)\right)=\frac{1}{2^p}\cdot\prod_{i=1}^{p}\nu\left(\mathcal{H}_1\left(\kappa_i'\right)\right)\cdot\frac{\prod_{i=1}^{p}\left(\frac{d_i}{2}-1\right)!}{\left(\frac{d}{2}\right)!}.$$

Using Lemma 7.1.3, we finally see

$$\begin{aligned}\tilde{\nu}\left(\mathcal{H}_1\left(\kappa'\right)\right)&=d\cdot\nu\left(C\left(\mathcal{H}_1\left(\kappa'\right)\right)\right)\\&=\frac{d}{2^p}\cdot\prod_{i=1}^{p}\nu\left(\mathcal{H}_1\left(\kappa_i'\right)\right)\cdot\frac{\prod_{i=1}^{p}\left(\frac{d_i}{2}-1\right)!}{\left(\frac{d}{2}\right)!}\\&=\frac{2}{2^p}\cdot\frac{\frac{d}{2}\cdot\prod_{i=1}^{p}\left(\frac{d_i}{2}-1\right)!}{\left(\frac{d}{2}\right)!}\cdot\prod_{i=1}^{p}\nu\left(\mathcal{H}_1\left(\kappa_i'\right)\right)\\&=\frac{1}{2^{p-1}}\cdot\frac{\prod_{i=1}^{p}\left(\frac{d_i}{2}-1\right)!}{\left(\frac{d}{2}-1\right)!}\cdot\prod_{i=1}^{p}\nu\left(\mathcal{H}_1\left(\kappa_i'\right)\right).\end{aligned}$$ □

Remark 7.1.6 (Masur–Veech volume element for disconnected surfaces)
For the sake of completeness, the volume form can analogously be given by

$$\mathrm{d}\tilde{\nu}\left(X,\omega\right)=\frac{1}{2^{p-1}}\cdot\frac{\prod_{i=1}^{p}\left(\frac{d_i}{2}-1\right)!}{\left(\frac{d}{2}-1\right)!}\cdot\prod_{i=1}^{p}\mathrm{d}\tilde{\nu}_i'\left(X_i',\omega_i'\right).$$

Lastly, to extend our volume form to more general strata, we want to consider strata with marked points. Since marked points can be added or removed arbitrarily from each translation surface of a stratum, we see that

$$\nu\left(\mathcal{H}_1(\kappa\sqcup 0^n)\right)=\nu\left(\mathcal{H}_1(\kappa)\right)$$

for every $n\in\mathbb{N}_0$. With Lemmas 7.1.3 and 7.1.5, we see that it is enough to understand ν for strata of translation surfaces of area 1.

While these constructions are useful to understand the ideas behind the volume form, it can be quite challenging to actually calculate the volume of subsets or even the full strata. It is for example not immediately clear, given a partition κ, whether $\nu\left(\mathcal{H}_1(\kappa)\right)$ is finite or not. To see that it is finite for every κ, we want to shortly introduce a way on how to actually compute the volume of unit area strata with the help of square-tiled surfaces and some combinatorics, as it was done by [Zor02]. The underlying idea has been independently suggested by [EM01] and a preprint of [KZ03] earlier.

One way to estimate the volume of a set $V\in\mathbb{R}^n$ is to count how many points

$$\operatorname{grid}(V):=|V\cap\Lambda|$$

of a lattice Λ are inside of V. An estimate for the volume of V is then just this count multiplied by the volume of the fundamental domain of the lattice, also called the covolume $\mathrm{d}(\Lambda)$. To approximate the volume, one can take finer and finer grids. Equivalently we can scale V by some factor $r > 1$ to get $V(r)$ and divide by r^n to normalize, so

$$\lim_{r\to\infty} \frac{\mathrm{grid}\,(V(r)) \cdot \mathrm{d}(\Lambda)}{r^n} = \mathrm{vol}\,(V(1))\,.$$

In particular, we also know the hyper surface area of ∂V, since $\mathrm{vol}(V(r)) = \mathrm{vol}(V(1)) \cdot r^n$ and

$$\mathrm{vol}(\partial V) = \frac{\mathrm{vol}(V(r))}{dr}(1) = n \cdot \mathrm{vol}(V(1)).$$

To calculate the volume of ∂V, it suffices to know the leading term coefficient in the asymptotic formula for the number of lattice points inside the scaled body. This strategy can be extended to our problem.

Proposition 7.1.7 (First volume calculation formula)
Let $\mathcal{H}_1(\kappa)$ be some stratum and let $f\colon \mathbb{N}_0 \to \mathbb{N}_0$ be the count of square-tiled surfaces of $\mathcal{H}_1(\kappa)$ tiled by at most $N \in \mathbb{N}_0$ squares. Then the Masur–Veech volume of $\mathcal{H}_1(\kappa)$ can be calculated with

$$\nu\left(\mathcal{H}_1(\kappa)\right) = 2\frac{df}{dN}\,(1)\,.$$

Proof. This is shown in [Zor02]. To understand the “integer points” $\left(\tilde{X}, \tilde{\omega}\right) \in \mathcal{H}(\kappa)$, let $\tilde{\omega} \in H^1(X, \Sigma; \mathbb{Z} \oplus \mathrm{i}\mathbb{Z})$. Let $\Sigma = \{P_1, \ldots P_l\}$ be the l singularities of $\left(\tilde{X}, \tilde{\omega}\right)$. The map

$$f_{\tilde{X}} : \tilde{X} \to \mathbb{T}^2, \quad P \mapsto \left(\int_{P_1}^{P} \tilde{\omega}\right) \quad \bmod \mathbb{Z} \oplus \mathrm{i}\mathbb{Z},$$

is a ramified covering containing Σ in its ramification points.

The covering map $f_{\tilde{X}}$ endows the Riemann surface $\tilde{X}$ with a tiling by unit squares, therefore the “integer points” in $\mathcal{H}(\kappa)$ correspond to square-tiled surfaces.

The problem of calculating the volume of $\mathcal{H}_1(\kappa)$ can be deduced from the problem of how many different square-tiled surfaces of the given topological type encoded by κ can be constructed using at most $N \in \mathbb{N}^+$ squares.

In the strategy mentioned before, we want to count the translation surfaces corresponding to “integer points” $\left(\tilde{X}, \tilde{\omega}\right) \in \mathcal{H}(\kappa)$, while scaling our surfaces by some large factor r. Here, however, we scale area $\left(\tilde{X}\right)$ by some large number $N \in \mathbb{N}^+$. Since area is a homogeneous function of degree 2, we get an additional factor of 2 when determining the hypersurface volume.

Similar to before, the leading term of f can be extracted by differentiating and evaluating at 1. The additional factor of n is eliminated by $\frac{1}{n}$ coming from the definition of the unit Masur–Veech volume. Multiplying by 2 yields the final formula. $\square$

Since some strata are not connected, see Theorem 3.5.22, we sometimes want to know the volume of each connected component separately.

With the method from Proposition 7.1.7, it is possible to calculate the stratum of translation surfaces containing all unit area tori $\mathcal{H}_1(0)$.

Proposition 7.1.8 (Volume of $\mathcal{H}_1(0)$)
The Masur–Veech volume of $\mathcal{H}_1(0)$ is finite and

$$\nu\left(\mathcal{H}_1(0)\right) = \frac{\pi^2}{3}.$$

Proof. This proof originates from [Zor02]. Let $(X, \omega) \in \mathcal{H}(0)$ be a square-tiled surface. The translation surface (X, ω) is topologically a torus and tiled by unit squares whose edges are horizontally and vertically aligned. By cutting the flat torus along a horizontal curve γ, we obtain a cylinder of length $c = \text{length}(\gamma)$ and a height h. The number of squares in the cylinder is given by $c \cdot h$.

We have some choice of regluing the cylinder to a torus. Since we get a topological cylinder, the interval exchange transformation going upwards from γ must be a permutation of the form $(1 \dots c)^k$ in cycle notation for some $k \in \mathbb{Z}$. There are in total c unique gluings obtainable this way. In other words, fixing the integer perimeter c and height h of a cylinder, we obtain c non-diffeomorphic square-tiled tori. Therefore, the number of square-tiled tori constructed using at most $N \in \mathbb{N}^+$ squares is approximately

$$\begin{aligned} \sum_{c=1}^{N} \sum_{h=1}^{\frac{N}{c}} h &\approx \sum_{c=1}^{\infty} \frac{1}{2} \left(\frac{N}{c}\right)^2 \\ &= \frac{N^2}{2} \sum_{c=1}^{\infty} \frac{1}{c^2} = \frac{N^2}{2} \frac{\pi^2}{6}. \end{aligned}$$

This approximation does not consider that some of the tori are equivalent by diffeomorphism, leading to multiple counts. This multi counting as well as the extension to the infinite sum does not affect the leading term for $N \to \infty$. Using Proposition 7.1.7, we get

$$\nu\left(\mathcal{H}_1(0)\right) = \frac{\pi^2}{3}.$$ □

Masur and Veech already showed more generally, that:

Theorem 7.1.9 (Finite volume of $\mathcal{H}_1(\kappa)$ — Masur; Veech)
The Masur–Veech volume of $\mathcal{H}_1(\kappa)$ is finite for all κ.

Proof. This is shown in [Mas82; Vee82]. □

The method of calculating the volume of strata of translation surfaces introduced in Section 7.1 can be quite complicated for arbitrarily large strata.

If we interpret $\nu\left(\mathcal{H}_1(\kappa)\right)$ as the asymptotics in the enumeration of square-tiled surfaces as their degree goes to ∞ while the ramification type is fixed, we transfer the problem to a counting problem. For this counting problem, Eskin–Okounkov [EO01] proposed a general algorithm that determines the volume of the stratum $\nu\left(\mathcal{H}_1(\kappa)\right)$ for every partition κ. Although this algorithm did not yield closed-form identities, Eskin–Okounkov successfully employed it to establish interesting properties of these volumes. For example, they demonstrated that $\nu\left(\mathcal{H}_1(\kappa)\right)$ is a rational multiple of π^{2g} for any partition κ of $2g - 2$.

A natural question is how these volumes behave as the genus g tends to infinity. In the analogous context of Weil–Petersson volumes, such questions were extensively and successfully explored by Mirzakhani and Zograf in [Mir13; MZ15].

Eskin was able to implement the Eskin–Okounkov algorithm as a computer program to evaluate the volumes $\nu\left(\mathcal{H}_1(\kappa)\right)$ for the partitions κ of $2g-2$ for $g \leq 10$. Based on the numerical data from this program, Eskin and Zorich predicted in 2003 and published their conjecture in 2015 [EZ15], that

$$\nu\left(\mathcal{H}_1(\kappa)\right) = \frac{4}{\prod_{i=1}^{l}(k_i+1)}\left(1+\mathcal{O}\left(\frac{1}{g^{1/2}}\right)\right)$$

uniformly in g for all partitions $\kappa = (k_1, \dots k_l)$ of $2g-2$.

They also noticed that the error is the largest for the minimal and the smallest for the principal stratum. These extreme cases were the first ones for which the conjecture of Eskin and Zorich has been proven to be true in [CMZ18] for the principal and in [Sau18] for the minimal strata, respectively.

Finally, Amol Aggarwal proved the conjecture for all strata:

Theorem 7.1.10 (Large-genus volume asymptotics — Aggarwal)
Let $g \geq 2$ and $\kappa = (k_1, \dots, k_l)$ be a partition of $2g-2$. Then,

$$\frac{4}{\prod_{i=1}^{l}(k_i+1)}\left(1-\frac{2^{2^{200}}}{g}\right) \leq \nu\left(\mathcal{H}_1(\kappa)\right) \leq \frac{4}{\prod_{i=1}^{l}(k_i+1)}\left(1+\frac{2^{2^{200}}}{g}\right).$$

Proof. This is included in Theorem 1.4 of [Agg20]. ☐

The proof of Theorem 7.1.10 is based on a combinatorial analysis of the original algorithm proposed by Eskin and Okounkov for evaluating $\nu\left(\mathcal{H}_1(\kappa)\right)$. After breaking it down, the algorithm expresses the Masur–Veech volume through the composition of three identities. Each of these identities involves a sum whose number of terms increases exponentially with the genus g. Aggarwal showed that each of these sums is dominated by a single term, while the remaining terms decay rapidly and are negligible for the asymptotic behavior.

7.2 Calculating volumes recursively

Another method for calculating the volume of different strata was developed by Eskin, Masur, and Zorich in [EMZ03]. Their approach focused on establishing relations via Siegel–Veech formulas. By leveraging these formulas, they constructed a recursive method for calculating the volumes of more complicated strata. This method involves expressing the volume of a given stratum in terms of simpler strata, multiplied by combinatorial constants derived from the Siegel–Veech formulas.

To understand these Siegel-type formulas, we need to encode some data on the configurations of saddle connections. As we explore different translation surfaces, it is practical to focus solely on generic translation surfaces. This approach helps exclude special edge cases, which have measure 0 with respect to the Masur–Veech volume. But what does it mean for a translation surface to be non-generic?

By examining the set of saddle connections $V_{\mathrm{sc}}(X)$, as defined in Definition 3.2.3, one can determine if a translation surface (X, ω) is generic.

Definition 7.2.1 (Homologous)
Let β and γ be two paths on a translation surface (X, ω), connecting $z_1 \in \overline{X}$ with $z_2 \in \overline{X}$ each. We call β and γ *homologous*, if $\beta\gamma^{-1}$ separates the surface $\overline{X}$ into different components. We call a collection of paths $\{\gamma_i\}_{i \in I}$ homologous if they are pairwise homologous.

Remark 7.2.2 (Homologous saddle connections' holonomy)
Saddle connections $\beta, \gamma \in H_1(X, \Sigma; \mathbb{Z})$ connecting the same singularities in Σ, which are homologous have the same holonomy, so $\mathrm{hol}(\beta) = \mathrm{hol}(\gamma)$, since

$$\mathrm{hol}(\beta) - \mathrm{hol}(\gamma) = \int_{\beta\gamma^{-1}} \omega = 0.$$

The reverse implication that $\mathrm{hol}(\beta) = \mathrm{hol}(\gamma)$ implies homologous saddle connections is false in general. It is however true generically, which we will see in the next example.

Example 7.2.3 (Homologous saddle connection stability)
Consider the L-shape $L_{2,2}$ from Example 2.3.3 glued together from three unit squares. The L-shape $L_{2,2} = (X, \omega)$ is a closed surface of genus 2. It has one conical singularity σ with a total angle of 6π.

Every saddle connection on $L_{2,2}$ is therefore closed with start and end point σ. Let us consider the set of all saddle connections of length at most 1. There are six different saddle connections $\alpha_1, \alpha_2, \beta, \gamma_1, \gamma_2, \delta$ of length at most 1, see Figure 7.1.

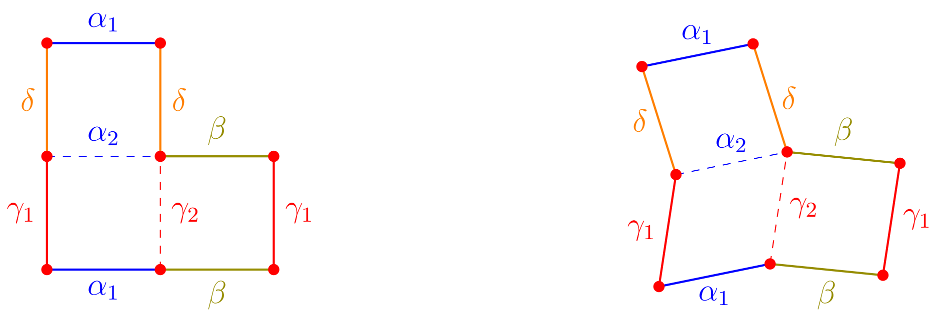

(a) L-shape with saddle connections

(b) Deformed L-shape

Figure 7.1: Generic deformation changes that holonomies are equal for non-homologous, but not for homologous saddle connections

We see that,

$$\mathrm{hol}(\alpha_1) = \mathrm{hol}(\alpha_2) = \mathrm{hol}(\beta) = (1, 0),$$

$$\mathrm{hol}(\gamma_1) = \mathrm{hol}(\gamma_2) = \mathrm{hol}(\delta) = (0, 1).$$

On one hand, α_1 and β are not homologous. The relation above does not persist under a generic deformation of this translation surface, as can be seen in the right-hand side of Figure 7.1. On the other hand, the pair of saddle connections α_1 and α_2 are homologous and maintain the same holonomy, under any small deformation of the surface.

This observation suggests that non-homologous saddle connections with the same holonomy are rare, since small deformations generically destroy them.

Proposition 7.2.4 (Non-homologous saddle connections have different holonomy vectors)
Almost any translation surface (X, ω) in any connected component of any stratum does not have a single pair of non-homologous saddle connections sharing the same holonomy vector.

Proof. This is shown in Proposition 3.1 of [EMZ03]. □

Similarly to the torus case, the set $H_{\mathrm{sc}}(X)$ introduced in Proposition 3.3.29 is a discrete subset of $\mathbb{R}^2$. However, when $\overline{X}$ is not a torus, the map hol from the set of saddle connections $V_{\mathrm{sc}}(X)$ to $H_{\mathrm{sc}}(X)$ is not necessarily injective and different saddle connections can have the same holonomy.

Definition 7.2.5 (Multiplicity)
We define the *multiplicity* of an element $v \in H_{\mathrm{sc}}(X)$ to be the number p of distinct saddle connections $\gamma_1, \dots, \gamma_p$ such that $\mathrm{hol}(\gamma_i) = v$.

Proposition 7.2.4 implies that generically two saddle connections β, γ have the same holonomy, if and only if they are homologous. In this case, the corresponding saddle connections join the same singularities.

Convention 7.2.6 (Thinking generically)
Since we do want to understand strata generically, we will write statements like “two saddle connections β, γ have the same holonomy, if and only if they are homologous” without mentioning that this is false in general.

Higher multiplicity, however, is quite common even on generic surfaces. For example, [EMZ03] showed on page 10 that for a surface with genus at least 3, the number of saddle connections in $V_{\mathrm{sc}}(X, l)$ of multiplicity 1, as well as the number of saddle connections of multiplicity 2, both display quadratic growth with respect to l.

Multiplicity is not the only property distinguishing elements in $V_{\mathrm{sc}}(X)$. Some of them correspond to closed saddle connections, while others correspond to saddle connections joining distinct singularities. Sometimes we also want to fix elements in $V_{\mathrm{sc}}(X)$, which correspond to saddle connections joining a particular pair of singularities. We therefore need to fix some data.

Definition 7.2.7 (Configuration data)
Let $p \in \mathbb{N}^+$, $m_1, m_2 \in \mathbb{N}_0$, and $a', a'' \in \mathbb{N}_0^p$, such that the equations $\sum_{i=1}^p a'_i = m_1 + 1 - p$ and $\sum_{i=1}^p a''_i = m_2 + 1 - p$ hold. The *configuration* $\mathcal{C}$ is a finite sequence (m_1, m_2, a', a''), encoding the following information.

Suppose that we have precisely p homologous saddle connections $\gamma_1, \dots, \gamma_p$ joining a singularity σ_1 of order m_1 to a singularity σ_2 of order m_2, see Figure 7.5. Furthermore, let all the γ_i have the same holonomy for $1 \le i \le p$ oriented from σ_1 to σ_2. The cyclic order of the γ_i at z_1 is chosen to be clockwise in the orientation defined by the flat structure. Let the angle between γ_i and γ_{i+1} at σ_1 be $2\pi(a'_i + 1)$. Let the angle between γ_i and γ_{i+1} at σ_2 be $2\pi(a''_i + 1)$. Since the saddle connections are homologous, the cyclic order of $\{\gamma_i\}_{i \in [p]}$ at σ_2 will be the reverse of the order of $\{\gamma_i\}_{i \in [p]}$ at σ_1.

With the configuration data at hand, we can specify our counting problem in H_{sc}.

Definition 7.2.8 (Configured set of saddle connections and holonomy vectors)
Given a translation surface (X, ω) and a configuration $\mathcal{C}$, let $H_{\mathcal{C}}(X) \subset H_{\text{sc}}(X)$ denote the vectors $v \in \mathbb{R}^2$, such that there are precisely p homologous saddle connections $\gamma_1, \dots, \gamma_p$ with configuration $\mathcal{C}$ and having holonomy $\operatorname{hol}(\gamma_i) = v$. Denote the corresponding set of collections of saddle connections $\{\gamma_1, \dots, \gamma_p\}$ by $V_{\mathcal{C}}(X)$.

Eskin–Masur–Zorich aimed to compute the number of collections $\{\gamma_1, \dots, \gamma_p\}$ in configuration $\mathcal{C}$ and holonomy vector length at most l. In other words, they want to compute the asymptotics of

$$\lim_{l \to \infty} |V_{\mathcal{C}}(X, l)| .$$

Eskin and Masur showed beforehand, that:

Theorem 7.2.9 (Asymptotics of saddle connection count — Eskin and Masur)
Given a configuration $\mathcal{C}$ and a connected component $\mathcal{H}$ of $\mathcal{H}_1(\kappa)$, there exists a constant $c = c(\kappa, \mathcal{C}, \mathcal{H})$ such that for almost all $(X, \omega) \in \mathcal{H}$, it holds

$$\lim_{l \to \infty} \frac{|V_{\mathcal{C}}(X, l)|}{\pi l^2} = c(\kappa, \mathcal{C}, \mathcal{H}) .$$

The constant c depends only on the connected component of the stratum and on the configuration $\mathcal{C}$. For connected strata, we write $c(\kappa, \mathcal{C})$.

Proof. This is shown in [EM01]. □

So, in [EMZ03], they actually wanted to calculate the numerical values for $c(\kappa, \mathcal{C}, \mathcal{H})$. But how do these values relate to the volume of strata, in which we are interested?

Define an operator $f \mapsto \hat{f}$ from the space $\mathcal{C}_0^\infty(\mathbb{R}^2)$ of integrable functions with compact support in $\mathbb{R}^2$ to functions on $\mathcal{H}$ by

$$\hat{f}(X) := \sum_{v \in H_{\mathcal{C}}(X)} f(v).$$

Averaging $\hat{f}$ over $\mathcal{H}$, we obtain an interesting functional, which was shown to be $\mathrm{SL}_2(\mathbb{R})$–invariant in [Vee98]. This implies the following Siegel-type formula for each configuration $\mathcal{C}$ and for each connected component of $\mathcal{H}_1(\kappa)$:

Proposition 7.2.10 (Siegel–Veech formula)
Let $\mathcal{C}$ be a configuration and $\mathcal{H}$ be a connected component of $\mathcal{H}_1(\kappa)$. Then there exists a constant $\tilde{c}\,(\kappa, \mathcal{C}, \mathcal{H})$ such that for any $f \in \mathcal{C}_0^\infty(\mathbb{R}^2)$, the *Siegel–Veech formula*

$$\frac{1}{\nu\,(\mathcal{H})} \int_{\mathcal{H}} \hat{f}(X)\,\mathrm{d}\nu(X,\omega) = \tilde{c}\,(\kappa, \mathcal{C}, \mathcal{H}) \int_{\mathbb{R}^2} f(x,y)\,\mathrm{d}x\,\mathrm{d}y$$

holds. The constant $\tilde{c}\,(\kappa, \mathcal{C}, \mathcal{H})$ is called the *Siegel–Veech constant* of $\mathcal{H}$ and configuration $\mathcal{C}$.

Proof. This follows immediately from Theorem 2.2 of [EM01]. □

It was shown in [EM01] that the Siegel–Veech constant $\tilde{c}\,(\kappa, \mathcal{C}, \mathcal{H})$ and the constant $c\,(\kappa, \mathcal{C}, \mathcal{H})$ from before are coinciding.

Corollary 7.2.11 (Disk Siegel–Veech formula)
For all $\varepsilon > 0$, for each configuration $\mathcal{C}$ and each connected component $\mathcal{H}$ of each stratum $\mathcal{H}_1(\kappa)$

$$\frac{1}{\nu\,(\mathcal{H})} \int_{\mathcal{H}} |V_{\mathcal{C}}(X,\varepsilon)|\,\mathrm{d}\nu(X,\omega) = c(\kappa, \mathcal{C}, \mathcal{H}) \cdot \pi\varepsilon^2,$$

where $V_{\mathcal{C}}(X,\varepsilon)$ is the set of collections of saddle connections on (X,ω) in configuration $\mathcal{C}$ smaller than ε.

Proof. Since Proposition 7.2.10 works for any integrable function with compact support in $\mathbb{R}^2$, let us insert the function

$$f_\varepsilon \colon \mathbb{R}^2 \to \mathbb{R}, \quad (x,y) \mapsto \chi_{\overline{B}_\varepsilon(0)}.$$

The integral on the right in Proposition 7.2.10 is equal to $\pi\varepsilon^2$. The integral on the left gives the average number of saddle connections on translation surfaces in configuration $\mathcal{C}$ having holonomy vector shorter than ε. □

We can use this to estimate the volume of surfaces of a special configuration type:

Corollary 7.2.12 (Siegel–Veech upper bound)
For all $\varepsilon > 0$, for each configuration $\mathcal{C}$ and each connected component $\mathcal{H}$ of each stratum $\mathcal{H}_1(\kappa)$, let $\mathcal{H}\,(\mathcal{C},\varepsilon)$ be the subset of translation surfaces that contains saddle connections of the configuration $\mathcal{C}$ with length at most ε. Then,

$$\nu\,(\mathcal{H}\,(\mathcal{C},\varepsilon)) \le c(\kappa, \mathcal{C}, \mathcal{H}) \cdot \pi\varepsilon^2 \cdot \nu\,(\mathcal{H})\,.$$

Proof. Using Corollary 7.2.11 and the fact that $|V_{\mathcal{C}}(X,\varepsilon)| \ge 1$ for any surfaces in $\mathcal{H}\,(\mathcal{C},\varepsilon)$, we get

$$\begin{aligned} \frac{\nu\,(\mathcal{H}\,(\mathcal{C},\varepsilon))}{\nu\,(\mathcal{H})} &= \frac{1}{\nu\,(\mathcal{H})} \int_{\mathcal{H}(\mathcal{C},\varepsilon)} 1\,\mathrm{d}\nu(X,\omega) \\ &\le \frac{1}{\nu\,(\mathcal{H})} \int_{\mathcal{H}} |V_{\mathcal{C}}(X,\varepsilon)|\,\mathrm{d}\nu(X,\omega) \\ &= c(\kappa, \mathcal{C}, \mathcal{H}) \cdot \pi\varepsilon^2. \end{aligned}$$

Multiplying by $\nu\,(\mathcal{H})$ yields the statement. □

Eskin–Masur–Zorich were not interested in explicitly calculating these ratios $\frac{\nu(\mathcal{H}(\mathcal{C},\varepsilon))}{\nu(\mathcal{H})}$ for a given ε, this however will be especially important for us later. For them, it was enough to know how to compute the leading term in front of ε^2 in the asymptotics as $\varepsilon \to 0$ to calculate the Siegel–Veech constant. The insights they obtained in doing so, are useful for our case as well.

Let us fix some notation which slightly deviates from the definitions of Eskin–Masur–Zorich:

Definition 7.2.13 (Thin-thick decomposition)
For $g \geq 2$ and $\varepsilon > 0$, define the following subsets of $\mathcal{H}_1(\kappa)$:

- Let $\mathcal{H}_1^{\varepsilon,\text{thick}}(\kappa)$ be the subset of translation surfaces whose saddle connections are all larger than ε.
- Let $\mathcal{H}_1^{\varepsilon,\text{thin}}(\kappa)$ be the subset of translation surfaces that contain at least one saddle connection shorter than ε.
  - Let $\mathcal{H}_1^{\varepsilon,\text{thin-thick}}(\kappa)$ be the subset of $\mathcal{H}_1^{\varepsilon,\text{thin}}(\kappa)$ with exactly one collection of homologous saddle connections shorter than ε and all other saddle connections being longer than 3ε.
  - Let $\mathcal{H}_1^{\varepsilon,\text{thin-thin}}(\kappa)$ be the subset of $\mathcal{H}_1^{\varepsilon,\text{thin}}(\kappa)$ having at least one additional (collection of homologous) saddle connection(s) shorter than 3ε in addition to the collection smaller to ε given by $\mathcal{H}_1^{\varepsilon,\text{thin}}(\kappa)$.

Remark 7.2.14 (On the thin-thick decomposition)
We chose 3ε in the definition of $\mathcal{H}_1^{\varepsilon,\text{thin-thick}}(\kappa)$, because it is then compatible with constructions described later. The following decompositions hold:

- For all $\varepsilon > 0$: $\mathcal{H}_1(\kappa) = \mathcal{H}_1^{\varepsilon,\text{thick}}(\kappa) \sqcup \mathcal{H}_1^{\varepsilon,\text{thin}}(\kappa)$.
- For all $\varepsilon > 0$: $\mathcal{H}_1^{\varepsilon,\text{thin}}(\kappa) = \mathcal{H}_1^{\varepsilon,\text{thin-thick}}(\kappa) \sqcup \mathcal{H}_1^{\varepsilon,\text{thin-thin}}(\kappa)$.

To find a recursive formula for the volume of strata, we first want to represent the Siegel–Veech constant as the limit of some volume ratio and afterwards as the ratio of the volume of different strata and some combinatorial data. Combining these two perspectives will then yield our recursion formula.

For the first step, where we want to express the Siegel–Veech constant as the limit of some volume ratio, we need the following lemma:

Lemma 7.2.15 (Masur–Smillie)
Let $\mathcal{H}_1(\kappa)$ be some fixed stratum. There is a constant $M = M(\kappa)$ such that for all $\varepsilon, \delta > 0$, the Masur–Veech volume of the subset of $\mathcal{H}_1(\kappa)$ consisting of translation surfaces with at least one short saddle connection of length ε, is at most $M\varepsilon^2$. The volume of the subset of $\mathcal{H}_1(\kappa)$ consisting of translation surfaces with at least two non-homologous short saddle connections of length ε and δ respectively, is at most $M\varepsilon^2\delta^2$.

Proof. This is contained in the proof of Theorem 10.3 of [MS91]. □

This lemma can be used to show that:

Corollary 7.2.16 (Thin-thick dominates)
For any connected component of any stratum $\mathcal{H}_1(\kappa)$ and any configuration $\mathcal{C}$, we have

$$\nu\left(\mathcal{H}_1^{\varepsilon,\text{thin}}(\kappa,\mathcal{C})\right) = \nu\left(\mathcal{H}_1^{\varepsilon,\text{thin-thick}}(\kappa,\mathcal{C})\right) + o\left(\varepsilon^2\right).$$

Proof. By definition

$$\nu\left(\mathcal{H}_1^{\varepsilon,\text{thin}}(\kappa,\mathcal{C})\right) = \nu\left(\mathcal{H}_1^{\varepsilon,\text{thin-thick}}(\kappa,\mathcal{C})\right) + \nu\left(\mathcal{H}_1^{\varepsilon,\text{thin-thin}}(\kappa,\mathcal{C})\right).$$

Using Lemma 7.2.15, we get

$$\nu\left(\mathcal{H}_1^{\varepsilon,\text{thin}}(\kappa,\mathcal{C})\right) = \nu\left(\mathcal{H}_1^{\varepsilon,\text{thin-thick}}(\kappa,\mathcal{C})\right) + o\left(\varepsilon^2\right). \qquad \square$$

The second lemma we need for the volume limit formula is a consequence of the following theorem.

Theorem 7.2.17 (Upper bound for the functional — Eskin and Masur)
Let

$$f_\varepsilon \colon \mathbb{R}^2 \to \mathbb{R}, \quad (x,y) \mapsto \chi_{\overline{B_\varepsilon(0)}}.$$

Let length(X) denote the length of the shortest saddle connection on $(X,\omega) \in \mathcal{H}_1(\kappa)$. For any connected component of any stratum $\mathcal{H}_1(\kappa)$, there exist constants $0 < \delta(\kappa) < 1$ and $c'(\kappa)$, such that for any $(X,\omega) \in \mathcal{H}_1(\kappa)$ for which length(X) is sufficiently small, the following holds:

$$\hat{f}_\varepsilon(X) \leq c'(\kappa)\,(\text{length}(X))^{-(1+\delta(\kappa))}.$$

Proof. This is shown in [EM01]. $\square$

Lemma 7.2.18 (Functional on thin-thin negligible)
For any connected component of any stratum $\mathcal{H}_1(\kappa)$ and any configuration $\mathcal{C}$, the integral of the function $\hat{f}_{\varepsilon,\mathcal{C}}$ over the thin-thin part is negligible for $\varepsilon \to 0$:

$$\int_{\mathcal{H}_1^{\varepsilon,\text{thin-thin}}(\kappa,\mathcal{C})} \hat{f}_{\varepsilon,\mathcal{C}}(X)\,\mathrm{d}\nu(X) = o\left(\varepsilon^2\right).$$

Proof. The function $\hat{f}_{\varepsilon,\mathcal{C}}(X)$ only counts those saddle connections arranged in the configuration $\mathcal{C}$:

$$\hat{f}_{\varepsilon,\mathcal{C}}(X) \coloneqq |V_{\mathcal{C}}(X,\varepsilon)|.$$

For $\hat{f}_\varepsilon(X)$, we get

$$\hat{f}_\varepsilon(X) \coloneqq |V_{\text{sc}}(X,\varepsilon)|,$$

which counts all short saddle connections regardless of configuration type.

Since $V_{\mathcal{C}}(X) \subseteq V_{\text{sc}}(X)$, we see that $\hat{f}_\varepsilon \geq \hat{f}_{\varepsilon,\mathcal{C}}$ and it is enough to show the lemma for the function $\hat{f}_\varepsilon$. Separate $\mathcal{H}_1^{\varepsilon,\text{thin-thin}}(\kappa,\mathcal{C}) = \bigsqcup_{n\in\mathbb{N}_0} U_n$ into the sets

$$U_n = \left\{ X \in \mathcal{H}_1^{\varepsilon,\text{thin-thin}}(\kappa,\mathcal{C}) \;\middle|\; \text{for the smallest saddle connection } \gamma \text{ it holds:}\right.$$

$$2^{-n-1}\varepsilon < \text{length}(\gamma) \leq 2^{-n}\varepsilon \Big\}.$$

On each surface in U_n, there is by definition a saddle connection with length between $\frac{\varepsilon}{2^{n+1}}$ and $\frac{\varepsilon}{2^n}$ and a non-homologous saddle connection with length at most 3ε. By Lemma 7.2.15, there is a constant $M = M(\kappa)$ such that

$$\nu\left(U_n\right) \leq 9M \cdot 2^{-2n}\varepsilon^4.$$

Together with Theorem 7.2.17, this implies that for some new constant $\tilde{M}$, the integral of $\hat{f}_\varepsilon$ over U_n is bounded by

$$\tilde{M} \cdot 2^{(\delta-1)n}\varepsilon^{3-\delta}.$$

Summing over n, yields this lemma. □

Finally, we get:

Proposition 7.2.19 (Volume limit formula)
For any connected component $\mathcal{H}$ of any stratum $\mathcal{H}_1(\kappa)$ and for any configuration $\mathcal{C}$, the following limit exists and is equal to the corresponding Siegel–Veech constant:

$$c(\kappa, \mathcal{C}, \mathcal{H}) = \lim_{\varepsilon\to 0} \frac{1}{\pi\varepsilon^2} \frac{\nu\left(\mathcal{H}_1^{\varepsilon,\text{thin}}\left(\kappa, \mathcal{C}\right) \cap \mathcal{H}\right)}{\nu\left(\mathcal{H}\right)}.$$

Proof. This follows from Proposition 7.2.10 and Lemma 7.2.18. □

As mentioned before, Eskin–Masur–Zorich were interested in the case where $\varepsilon \to 0$ for which the translation surfaces in the thin-thick part degenerate to "simpler" translation surfaces. In the case of a single saddle connection joining a pair of distinct singularities, these singularities collapse to a higher order singularity. So, the translation surface will have the same genus, though being from another stratum. For this to work, the real dimension has to decrease by two. The surface can be disconnected if the configuration has multiplicity 2 or more. We say that the resulting surface belongs to the *principal boundary* of the original stratum.

Eskin–Masur–Zorich proved that the thin-thick part $\mathcal{H}_1^{\varepsilon,\text{thin-thick}}\left(\kappa, \mathcal{C}\right)$ has the structure of a ramified covering over a direct product $\mathcal{H}_1\left(\kappa'\right) \times \overline{B}_\varepsilon(0)$ of the corresponding stratum of disconnected translation surfaces obtained after degeneration to the principal boundary with $\mathcal{C}$ and a two-dimensional disk $\overline{B}_\varepsilon(0)$. The degree of the covering, let us call it M, encodes combinatorial data, the number of ways to perform some constructions, we will define in the next Section 7.3. We therefore can express the volume of the thin part by

$$\nu\left(\mathcal{H}_1^{\varepsilon,\text{thin}}\left(\kappa, \mathcal{C}\right)\right) = M \cdot \pi\varepsilon^2 \cdot \nu\left(\mathcal{H}_1\left(\kappa'\right)\right) + o\left(\varepsilon^2\right).$$

Using Proposition 7.2.19, the factor $\pi\varepsilon^2$ cancels and we obtain our *volume recursion formula*

$$c(\kappa, \mathcal{C}) = M \cdot \frac{\nu\left(\mathcal{H}_1\left(\kappa'\right)\right)}{\nu\left(\mathcal{H}_1(\kappa)\right)}.$$

If one perceives strata as complex polyhedra, the set of faces of the polyhedron corresponds to the collection of all types $\mathcal{C}$ of configurations of homologous saddle connections describing all generic degenerations of our stratum.

7.3 The work of Eskin–Masur–Zorich

We have seen the idea on how to calculate the volume recursively. For this, we need to know the combinatorial data M. For its calculation, we first need to introduce and describe some surgeries we actually perform to switch between $\mathcal{H}_1(\kappa')$ and $\mathcal{H}_1(\kappa)$.

First, we look at the simpler case where we have only one short saddle connection joining two singularities and this saddle connection has multiplicity 1, meaning there are no other saddle connections with the same holonomy joining the same pair of singularities. We also assume this whole section, that our stratum of translation surfaces $\mathcal{H}_1(\kappa)$ is connected, which is the case for the minimal and principal stratum.

Since we want to be able to reverse the surgeries up to some non-uniqueness, we explain both directions, first breaking up a singularity into two and then collapsing two singularities into one back again. All these constructions originate from [EMZ03].

Construction 7.3.1 (Breaking up a singularity)
Let (X', ω') be a translation surface and σ a singularity in (X', ω') of order $m \geq 2$. Furthermore let $m_1, m_2 \in \mathbb{N}_0$, such that $m = m_1 + m_2$ and let $\gamma \in \mathbb{R}^2$ be a vector of length $2\delta \leq \varepsilon$. Suppose that (X', ω') does not have any saddle connection or closed geodesic of length smaller than 2ε. Let $\Sigma \ni \sigma$ be the set of all singularities of (X', ω').

Next, we want to build the relative homology group $H_1(X', \Sigma; \mathbb{Z})$ in a suitable way for the construction. If σ is the only singularity, choose a basis in $H_1(X', \Sigma; \mathbb{Z})$, which all miss σ. If there are other singularities, choose a basis in $H_1(X', \Sigma; \mathbb{Z})$, such that exactly one curve β_1 contains σ as an endpoint.

Now, we can focus on the actual construction. Without loss of generality, let γ be horizontal. Take a disk of radius ε around σ that misses all other singularities. Break up the singularity σ of order m in (X', ω') into two singularities σ_1 and σ_2 of orders m_1 and m_2 respectively, such that the vector γ is joining them, yielding a new translation surface (X, ω) in the following way, see Figure 7.2 for illustration purposes:

- Create $2m + 2$ half-disks of radius ε.
- For two of these half-disks, along the real axis, mark the two points $(0, \delta)$ and $(0, -\delta)$.
- For m of these half-disks, mark a point at $(0, \delta)$.
- For the remaining m half-disks, mark a point at $(0, -\delta)$.
- Glue together the first two half-disks along the side with length 2δ, leaving a pair of free segments of length $\varepsilon - \delta$ on each.
- Glue the remaining segments of all other half-disks isometrically to each other in a circular fashion. Multiple choices may be available in this step.

And now replace the original disk by this new construction.

In how many ways can we do this construction?

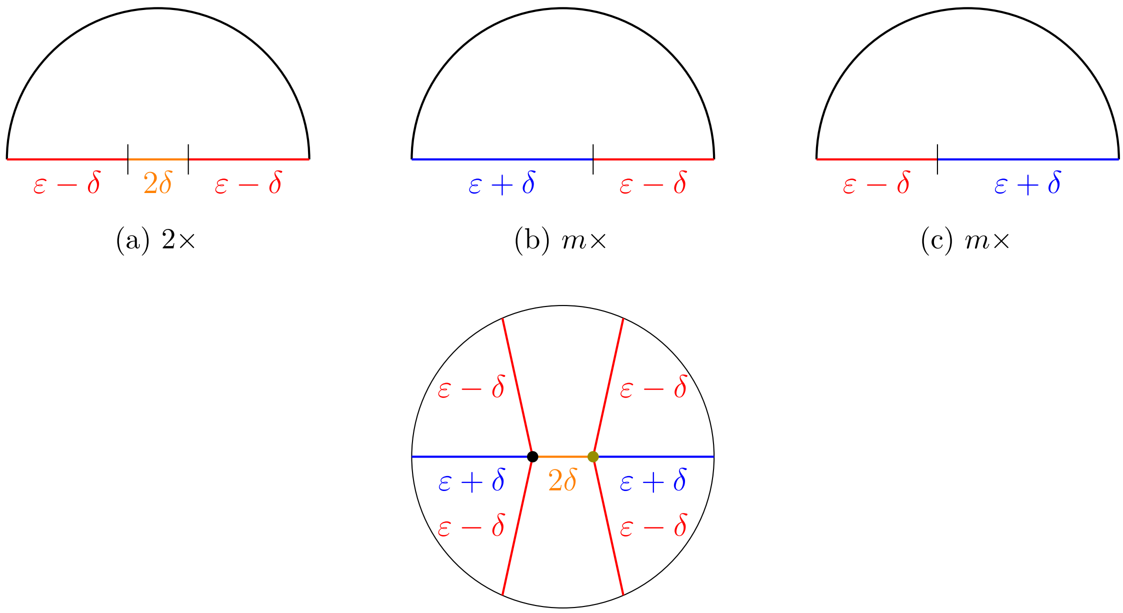

(a) $2\times$ (b) $m\times$ (c) $m\times$

(d) Circular gluing pattern for $m=2$

Figure 7.2: Breaking up a singularity into two singularities

Lemma 7.3.2 (Number of ways to break up a singularity)
Let (X',ω') be a translation surface and σ a singularity in (X',ω') of order $m\geq 2$, such that we can perform Construction 7.3.1 on (X',ω') for a vector $\gamma\in\mathbb{R}^2$ of length $2\delta\leq\varepsilon$. We can then perform Construction 7.3.1 in $m+1$ many ways.

Proof. This is shown in Lemma 8.1 of [EMZ03]. If $m_1\neq m_2$, the number of ways of effecting the breakup is $2m+2$. Half of which have $\overrightarrow{\sigma_1\sigma_2}=\gamma$, while the other half will have $\overrightarrow{\sigma_1\sigma_2}=-\gamma$. So, we actually only get $m+1$ ways of construction where $\overrightarrow{\sigma_1\sigma_2}=\gamma$ is fixed.

If $m_1=m_2=\frac{m}{2}$, the number of the resulting surfaces is $m+1$. For every such surface, there are two ways to name σ_1 and σ_2 to the newborn singularities of order $\frac{m}{2}$. This doubles the number of resulting surfaces with named singularities. However, we again only have $m+1$ surfaces with $\overrightarrow{\sigma_1\sigma_2}=\gamma$ and $\overrightarrow{\sigma_2\sigma_1}=\gamma$ each. So, we again only get $m+1$ surfaces. □

For future reference, we want to fix such an assignment by:

Definition 7.3.3 (Assignment)
We denote the *assignment* by

$$(X',\gamma,m)\to(X,m_1,m_2).$$

Let the curve β_1 which had the endpoint at w keep the corresponding endpoint at σ_1 during the deformation. The fact that this construction was local means that except for the curve β_1, the holonomy is preserved along the homology basis of (X',ω'). The holonomy of β_1 is changed exactly by $-\frac{\gamma}{2}$. Furthermore, every saddle connection other than $\overrightarrow{\sigma_1\sigma_2}$ has length at least ε.

For the constructed surface $(X,\omega) \in \mathcal{H}_1(\kappa)$, the partition κ is obtained from the partition κ' by replacing the entry m by two entries m_1 and m_2. Since all the singularities on the translation surface (X',ω') are named, we keep this naming structure for all other singularities.

For the reversion of Construction 7.3.1:

Construction 7.3.4 (Collapsing a pair of singularities)
Let $(X,\omega) \in \mathcal{H}_1(\kappa)$ and a saddle connection of length $2\delta \leq \varepsilon$ joining distinct singularities σ_1 and σ_2 of orders m_1 and m_2 with holonomy γ and no other saddle connection of length smaller than 3ε. We can now exactly reverse the breaking-up procedure to collapse the saddle connection of length 2δ to a singularity σ of order $m = m_1 + m_2$ to construct a flat surface (X',ω'). For more details, see Section 8.2 of [EMZ03].

We say that $\mathcal{H}_1(\kappa')$ is the principal boundary of $\mathcal{H}_1(\kappa)$ corresponding to this configuration.

Lemma 7.3.5 (Correspondence of 1 to $m+1$)
For γ a vector in $\mathbb{R}^2$ of length at most ε, except for a set of volume 0, there are exactly $m+1$ surfaces in $\mathcal{H}_1^{\varepsilon,\text{thin}}(\kappa)$, that are the result of the assignment

$$(X',\gamma,m) \to (X,m_1,m_2).$$

Moreover, every surface in $\mathcal{H}_1^{\varepsilon,\text{thin-thick}}(\kappa)$ is the result of such an assignment.

Proof. This is shown in Lemma 8.1 of [EMZ03]. The idea is to choose a simply connected subset of $\mathcal{H}_1(\kappa')$ of full volume and remove the set of translation surfaces with a saddle connection or closed geodesic of length at most 2ε. Call this set $\mathcal{F}' \subset \mathcal{H}_1(\kappa')$. With Lemma 7.2.15, we see:

$$\nu\left(\mathcal{H}_1(\kappa') \setminus \mathcal{F}'\right) = o\left(\varepsilon^2\right).$$

Let the configuration $\mathcal{C}$ correspond to a single saddle connection. Suppose that for fixed $(X',\omega') \in \mathcal{F}'$, two of the $m+1$ surfaces (X,ω) built from (X',ω') are isomorphic. Since by construction each of these surfaces has a single short saddle connection, the isomorphism sends the newborn saddle connection on one surface to the newborn saddle connection on the other surface. Therefore, it sends the corresponding "disk" on one surface to the corresponding "disk" on the other surface. Hence, it is an isomorphism of the complements of the "disks", which implies that it induces an automorphism of the surface (X',ω') and the set of translation surfaces that have automorphisms has measure 0. □

Remark 7.3.6 (On the 1 to $m+1$ correspondence)
The previous lemma shows that the map

$$\mathcal{H}_1^{\varepsilon,\text{thin-thick}}(\kappa,\mathcal{C}) \to \mathcal{F}' \times \overline{B}_\varepsilon(0)$$

is a ramified covering of order $m+1$ almost everywhere and

$$\mathrm{d}\nu(X,\omega) = \mathrm{d}\nu(X',\omega')\,\mathrm{d}\gamma,$$

where $\gamma = \overrightarrow{\sigma_1\sigma_2}$.

In Constructions 7.3.1 and 7.3.4, we showed how we can split or merge two singularities in some ε–neighborhood. For this thesis, however, we also need to understand how we can split and merge three singularities in some local neighborhood. Extending the previous construction directly is quite difficult. In Construction 7.3.1, we decided for a symmetric construction around $\overrightarrow{\sigma_1\sigma_2} = \gamma$ with singularities σ_1 and σ_2 of degree m_1 and m_2 correspondingly. If we change this construction to be one-sided, meaning we extend γ in all possible ways from σ_2 extending the holonomy of $\overrightarrow{\sigma_1\sigma_2}$ by $\delta' = 2\delta$, we get a similar construction, see Figure 7.3 for illustration. Here we have to pick m_2 marked points for our construction.

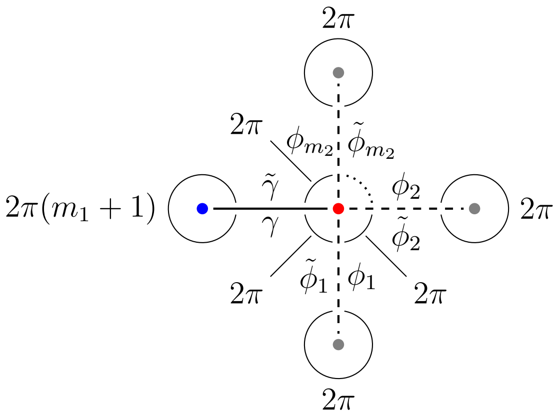

(a) Breaking up of a singularity into two

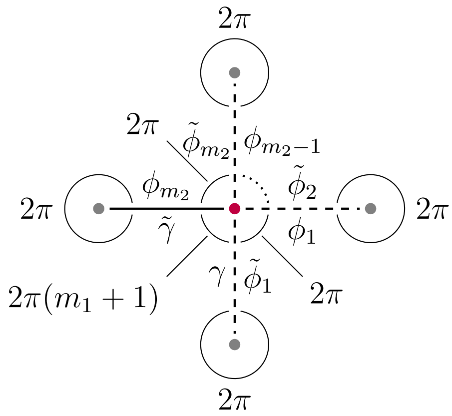

(b) Collapsing two singularities

Figure 7.3: Local picture for one-sided Constructions 7.3.1 and 7.3.4

We now cut along $\gamma = \overrightarrow{\sigma_1\sigma_2}$ and the extensions $\phi_i = \overrightarrow{\sigma_1\sigma_{i+2}}$ for all $i \in [m_2]$, where σ_{i+2} is a marked point chosen such that $\mathrm{hol}(\phi_i) = \mathrm{hol}(\gamma)$ for all $i \in [m_2]$. We label the sides of γ and ϕ_i accordingly $\tilde{\gamma}, \gamma$ and $\tilde{\phi}_i, \phi_i$ for $i \in [m_2]$ so we can better illustrate the gluing.

This construction will still have the same 1 to $m+1$ correspondence. However, we can extend this construction more easily to collapse three singularities at once.

Construction 7.3.7 (Collapsing or creating three close singularities)
Let $(X,\omega) \in \mathcal{H}_1(\kappa)$. Consider a saddle connection of length $\delta_1' \leq \varepsilon$ joining distinct singularities σ_1 and σ_2 of orders m_1 and m_2 with holonomy $\gamma_1 = \overrightarrow{\sigma_1\sigma_2}$. Consider a second saddle connection of length $\delta_2' \leq \varepsilon$ joining distinct singularities σ_1 and σ_3 of orders m_1 and m_3 with holonomy $\gamma_2 = \overrightarrow{\sigma_1\sigma_3}$, such that σ_2 and σ_3 are distinct as well. Choose $\phi_{1,i}$ for $i \in [m_1]$ and $\phi_{2,j}$ for $j \in [m_2]$, such that $\mathrm{hol}(\phi_{1,i}) = \mathrm{hol}(\gamma_1)$ and $\mathrm{hol}(\phi_{2,j}) = \mathrm{hol}(\gamma_2)$.

Furthermore, we need that all $\gamma_{1,i}, \gamma_{2,j}, \phi_1, \phi_2$ for $i \in [m_2]$ and $j \in [m_3]$ are pairwise not intersecting and that there is no other saddle connection or segment in the ε–neighborhood of all of these singularities. Let the angle between γ_1 and γ_2 be denoted by θ.

Then we can use the one-side construction of collapsing two singularities for γ_1 and γ_2 independently by our choice. The resulting surface will contain the combined singularity σ of order $m_1 + m_2 + m_3$ with no other singularity in an ε–neighborhood around it, see Figure 7.4 for an illustration in the principal stratum for the sake of clarity with $m_2 = m_3 = 1$ and $\phi_1 := \phi_{1,1}$ and $\phi_2 := \phi_{2,1}$.

We can reverse this collapsing given two holonomy vectors $\mathrm{hol}(\gamma_1), \mathrm{hol}(\gamma_2)$ for a singularity of order $m = m_1 + m_2 + m_3$, where we have

$$m_1 \cdot (m + 1) = m_1 \cdot (m_1 + m_2 + m_3 + 1)$$

many possibilities of choosing our construction.

To see this, remember how we calculated the correspondence in the proof of Lemma 7.3.5. The same arguments holds here for both single collapsing procedures. The first collapse can pick a disk, such that the holonomy of the boundary of the disk is γ_1 for both, from the total $(m + 1) \cdot 2\pi$ angle around σ. The second collapsing procedure needs to pick a covering of a disk with total angle $(m_2) \cdot 2\pi$ out of the remaining $(m_2) \cdot 2\pi$ with an holonomy vector for the boundary of γ_2. This disk has an offset of θ as a local angle from the previous disk, so we get a total offset in the covering of $2k\pi + \theta$ for some $k \in \mathbb{N}_0$.

We can restrict $k < (m + 1) - m_2 - (m_3 + 1) = m_1$, since $(m_2) \cdot 2\pi$ of the angle is used for the previous construction and we need to keep a distance of $(m_3 + 1) \cdot 2\pi$, such that the remaining angle of $(m_3) \cdot 2\pi$ fits in. So we get in total $m_1 \cdot (m + 1)$ many ways to do this construction.

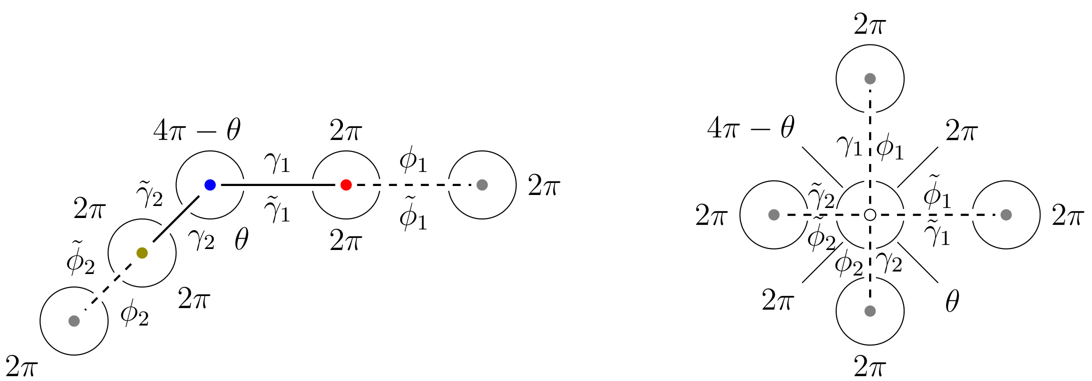

(a) Breaking up of a singularity into three

(b) Collapsing three singularities

Figure 7.4: Local picture for Construction 7.3.7 in the principal stratum

The Constructions 7.3.1 and 7.3.4 allow us to calculate M of our recursion formula.

Proposition 7.3.8 (First recursion formula)
Let $\mathcal{H}(\kappa)$ be a connected stratum and $\mathcal{H}(\kappa')$ be a stratum of the principal boundary of $\mathcal{H}(\kappa)$ obtained through Construction 7.3.1 from the configuration

$$\mathcal{C} = (m_1, m_2, (m_1), (m_2))$$

corresponding to one short saddle connection joining two fixed singularities σ_1 and σ_2, where this saddle connection has multiplicity 1. Furthermore if $m_1 = m_2$, we require the singularities themselves to be different; that is, $\sigma_1 \neq \sigma_2$. Then

$$c\left(\kappa, \mathcal{C}\right) = (m_1 + m_2 + 1)\frac{\nu\left(\mathcal{H}_1\left(\kappa'\right)\right)}{\nu\left(\mathcal{H}_1(\kappa)\right)}.$$

Proof. Let $d = \dim_{\mathbb{R}}\left(\mathcal{H}(\kappa)\right)$ and $d' = \dim_{\mathbb{R}}\left(\mathcal{H}(\kappa')\right) = d-2$. For (X', ω') being an element of the cone $C(\mathcal{F}')$ of $\mathcal{F}'$ defined in the proof of Lemma 7.3.5, we normalize $X' = tX''$ where $\operatorname{area}\left(X''\right) = 1$. Because of Lemma 7.1.3 and Remark 7.3.6, we obtain the volume element

$$\mathrm{d}\nu(X, \omega) = t^{d'-1}\,\mathrm{d}t\,\mathrm{d}\nu(X'', \omega'')\,\mathrm{d}\gamma.$$

Since

$$\nu\left(\mathcal{H}_1^{\varepsilon,\text{thin}}\left(\kappa, \mathcal{C}\right) \setminus \mathcal{H}_1^{\varepsilon,\text{thin-thick}}\left(\kappa, \mathcal{C}\right)\right) = \mathcal{O}\left(\varepsilon^4\right)$$

by Lemma 7.2.15, we obtain with Lemma 7.3.5 and Remark 7.3.6:

$$\begin{aligned}
\nu\left(\mathcal{H}_1^{\varepsilon,\text{thin}}\left(\kappa, \mathcal{C}\right)\right) &= d \cdot \nu\left(C\left(\mathcal{H}_1^{\varepsilon,\text{thin}}\left(\kappa, \mathcal{C}\right)\right)\right) \\
&= d(m_1 + m_2 + 1)\nu\left(\mathcal{F}'\right)\int_0^1 t^{d'-1}\int_{\overline{B}_{t\varepsilon}(0)} 1\,\mathrm{d}\gamma\,\mathrm{d}t + \mathcal{O}\left(\varepsilon^4\right) \\
&= d\pi\varepsilon^2(m_1 + m_2 + 1)\nu\left(\mathcal{F}'\right)\int_0^1 t^{d'-1}t^2\,\mathrm{d}t + \mathcal{O}\left(\varepsilon^4\right) \\
&= d\pi\varepsilon^2(m_1 + m_2 + 1)\nu\left(\mathcal{F}'\right)\int_0^1 t^{d'+1}\,\mathrm{d}t + \mathcal{O}\left(\varepsilon^4\right) \\
&= \frac{d}{d'+2}\pi\varepsilon^2(m_1 + m_2 + 1)\nu\left(\mathcal{F}'\right) + \mathcal{O}\left(\varepsilon^4\right) \\
&= \pi\varepsilon^2(m_1 + m_2 + 1)\nu\left(\mathcal{F}'\right) + \mathcal{O}\left(\varepsilon^4\right).
\end{aligned}$$

So, inserting this into the formula for the Siegel–Veech constant in Proposition 7.2.19:

$$\begin{aligned}
c(\kappa, \mathcal{C}) &= \lim_{\varepsilon\to 0}\frac{1}{\pi\varepsilon^2}\frac{\nu\left(\mathcal{H}_1^{\varepsilon,\text{thin}}\left(\kappa, \mathcal{C}\right)\right)}{\nu\left(\mathcal{H}_1(\kappa)\right)} \\
&= (m_1 + m_2 + 1)\lim_{\varepsilon\to 0}\frac{\nu\left(\mathcal{F}'\right)}{\nu\left(\mathcal{H}_1(\kappa)\right)} \\
&= (m_1 + m_2 + 1)\frac{\nu\left(\mathcal{H}_1\left(\kappa'\right)\right)}{\nu\left(\mathcal{H}_1(\kappa)\right)}.
\end{aligned}$$

□

Furthermore, this can easily be expanded to the case where we do not fix σ_1 and σ_2 and allow any singularities of order m_1 and m_2 respectively.

Definition 7.3.9 (Singularity of order)
Define $\operatorname{soo}(m_i)$ as the number of *singularities of order* m_i in the partition κ of the stratum $\mathcal{H}(\kappa)$.

Proposition 7.3.10 (Second recursion formula)
Let $\mathcal{H}(\kappa)$ be a connected stratum and $\mathcal{H}(\kappa')$ be a stratum of the principal boundary of $\mathcal{H}(\kappa)$ obtained through Construction 7.3.1 from the configuration

$$\mathcal{C} = (m_1, m_2, (m_1), (m_2)),$$

corresponding to one short saddle connection joining two singularities, where this saddle connection has multiplicity 1. If $m_1 \neq m_2$, then

$$c(\kappa, \mathcal{C}) = \mathrm{soo}(m_1)\,\mathrm{soo}(m_2)(m_1 + m_2 + 1)\frac{\nu(\mathcal{H}_1(\kappa'))}{\nu(\mathcal{H}_1(\kappa))}.$$

If $m_1 = m_2$, then

$$c(\kappa, \mathcal{C}) = \frac{\mathrm{soo}(m_1)(\mathrm{soo}(m_1) - 1)}{2}(2m_1 + 1)\frac{\nu(\mathcal{H}_1(\kappa'))}{\nu(\mathcal{H}_1(\kappa))}.$$

Proof. If $m_1 \neq m_2$, there are $\mathrm{soo}(m_1)\,\mathrm{soo}(m_2)$ ways of choosing the singularities σ_1 and σ_2 of orders m_1 and $o(m_2)$. Thus, we get an additional factor $\mathrm{soo}(m_1)\,\mathrm{soo}(m_2)$ for Proposition 7.3.8. For $m_1 = m_2$, the question of how many unordered pairs (σ_1, σ_2) exist with the same order m_1 is the same as the number of ways to choose 2 out of m_1 singularities, so we get the additional factor of $\frac{\mathrm{soo}(m_1)(\mathrm{soo}(m_1)-1)}{2}$ for Proposition 7.3.8. $\square$

Now that we understood the case of a saddle connection having multiplicity 1, we want to generalize to multiplicity p. Here we consider new constructions generalizing Constructions 7.3.1 and 7.3.4. Keep in mind Figure 7.5 for all these following constructions.

Let us start with extending Construction 7.3.4.

Construction 7.3.11 (Separating the surface)
Let $(X, \omega) \in \mathcal{H}_1^{\varepsilon,\text{thin-thick}}(\kappa)$ be a translation surface with a fixed pair of singularities σ_1 and σ_2 of orders m_1 and m_2 correspondingly in configuration $\mathcal{C}$ of p homologous saddle connections $\gamma_1, \ldots, \gamma_p$ joining σ_1 and σ_2 of length at most ε and no other saddle connections shorter than 3ε. Call the surface, which is bounded by the pair γ_i and γ_{i+1}, X_i. The surfaces X_i and X_{i+1} share the saddle connection γ_{i+1}. By Definition 7.2.7, the cyclic order of the γ_i at σ_1 is clockwise in the orientation defined by the flat structure. The angle between γ_i and γ_{i+1} at σ_1 is $2\pi(a_i' + 1)$ and at σ_2 is $2\pi(a_i'' + 1)$. Cut $\overline{X}$ along all $\{\gamma_i\}_{i\in[p]}$. For each connected component X_i, glue together the boundaries γ_i with $\gamma_{i+1 \bmod p}$.

By construction, we get p translation surfaces (X_i^*, ω_i) for $i \in [p]$, each with two singularities $\sigma_{1,i}$ and $\sigma_{2,i}$ of orders a_i' and a_i'', such that $\overrightarrow{\sigma_{1,i}\sigma_{2,i}} = \gamma$. Note that neither $\sigma_{1,i}$ nor $\sigma_{2,i}$ needs to be essential. Furthermore (X_i^*, ω_i) has a single saddle connection of length shorter than ε and every other saddle connection has length at least 3ε.

Now use Construction 7.3.4 to collapse $\sigma_{1,i}$ and $\sigma_{2,i}$ into σ_i of order $a_i = a_i' + a_i''$. We obtain a translation surface $(X_i', \omega_i') \in \mathcal{H}(\kappa_i')$ for each $i \in [p]$. The surface

$$\bigsqcup_{i=1}^{p} (X_i', \omega_i') = (X', \omega') \in \mathcal{H}(\kappa') = \mathcal{H}\left(\bigsqcup_{i=1}^{p} \kappa_i'\right)$$

is in the principal boundary of the configuration $\mathcal{C}$ and the result of this construction.

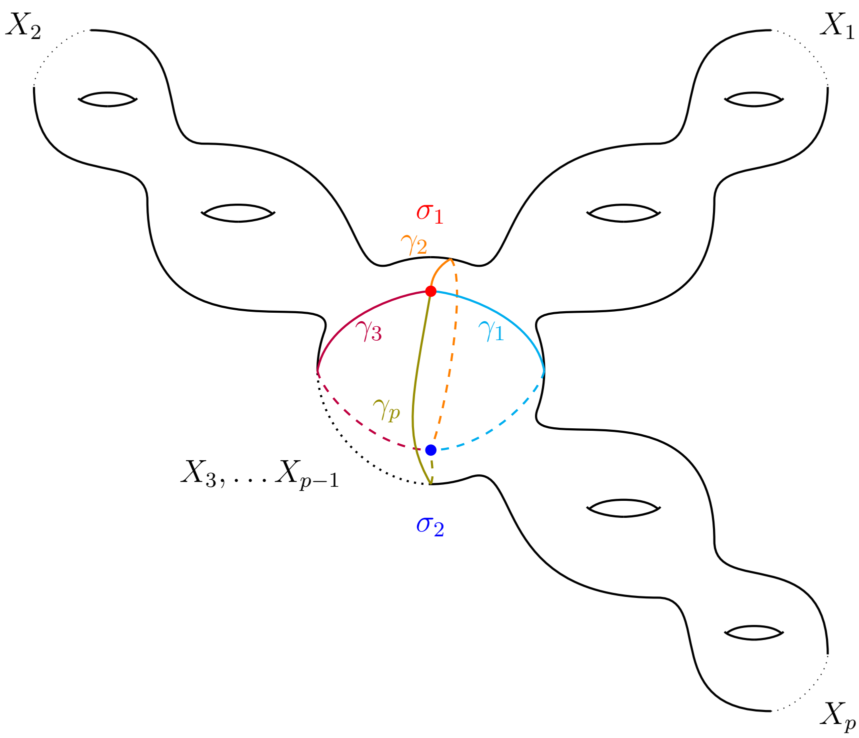

Figure 7.5: p homologous saddle connections

We can also reverse this and generalize Construction 7.3.1 with the help of a slit construction before building surfaces with multiple homologous saddle connections.

Construction 7.3.12 (Slit construction)
Let (X', ω') be a translation surface with a singularity of order $a \in \mathbb{N}_0$, containing no saddle connections of length shorter than 2ε. Let $a', a'' \in \mathbb{N}_0$, such that $a = a' + a''$. Let $\gamma \in \mathbb{R}^2$, such that $\|\gamma\| \leq \varepsilon$.

Use Construction 7.3.1 on this setup to break up the singularity. If $a' = 0$ or $a'' = 0$, we need to artificially create a singularity as a marked point. In this case, define the points $\sigma_1 = \sigma - \frac{\gamma}{2}$ and $\sigma_2 = \sigma + \frac{\gamma}{2}$ in local coordinates on (X', ω').

Then cut the resulting surface along the saddle connection joining the two singularities σ_1 and σ_2. This cut, which corresponds to a slit, gives the name of this construction. We obtain a surface with one boundary component consisting of two arcs γ' and γ'' and glue the endpoints of these arcs together. The angles between γ' and γ'' at the points σ_1 and σ_2 are $2\pi(a' + 1)$ and $2\pi(a'' + 1)$ inherited by the construction.

The translation structure ω' fixes the choice of the orientation. For consistency, we give the names γ' and γ'' to the arcs in such a way that turning around σ_1 in a clockwise direction from γ'' to γ', we do not leave the surface.

We can now do this slit construction for all surface components separately:

Construction 7.3.13 (Building surfaces with multiple homologous saddle connections)
Let $(X', \omega') = \bigsqcup_{i=1}^{p} (X'_i, \omega'_i)$ be a disconnected translation surface. On every $\overline{X}'_i$, there is

a singularity (which could be just a marked point) σ_i of order a_i. Let no surface contain a saddle connection shorter than 2ε.

Let $a_i', a_i'' \in \mathbb{N}_0$ with $a_i = a_i' + a_i''$ and $\gamma \in \mathbb{R}^2$ be a vector with $\|\gamma\| \leq \varepsilon$. Perform Construction 7.3.12 on each surface. We obtain surfaces with one boundary component each of which consists of two arcs γ_i' and γ_i''. Glue together γ_i' to $\gamma_{i+1 \bmod p}''$ for $i \in [p]$ and call it $\gamma_{i+1 \bmod p}$. This gives a closed surface (X, ω), a pair of singularities σ_1 and σ_2 of orders m_1 and m_2, where

$$\sum_{i=1}^{p} a_i' = m_1 + 1 - p,$$
$$\sum_{i=1}^{p} a_i'' = m_2 + 1 - p,$$

and a set of homologous curves γ_i, joining σ_1 to σ_2, which ends this construction.

This construction assigns a translation surface (X, ω) to (X', ω'). Let us fix this assignment:

Definition 7.3.14 (Extended assignment)
We denote the *extended assignment* obtained from Construction 7.3.13 by

$$(X', \gamma, a', a'') \to (X, m_1, m_2, a', a'').$$

The extended assignment is also referred to simply as the assignment.

In the end of Construction 7.3.13, we have seen that our assignment fulfills a few identities.

Lemma 7.3.15 (Assignments are enough)
An assignment $(X', \gamma, a', a'') \to (X, m_1, m_2, a', a'')$, where we consider the translation surfaces $(X', \omega') \in \mathcal{H}_1(\kappa')$ and $(X, \omega) \in \mathcal{H}_1(\kappa)$, satisfies the following necessary conditions:

$$\sum_{i=1}^{p} a_i' = m_1 + 1 - p,$$
$$\sum_{i=1}^{p} a_i'' = m_2 + 1 - p,$$
$$\kappa = \bigsqcup_{i=1}^{p} \kappa_i' \sqcup \{m_1\} \sqcup \{m_2\},$$
$$|\kappa_i'| = a_i' + a_i'' = 1 \mod 2 \quad \text{for } i \in [p],$$

where $|(k_1, \ldots, k_l)| \coloneqq \sum_{i=1}^{l} k_i$.

Moreover, when the stratum $\mathcal{H}_1(\kappa)$ is connected, these conditions are sufficient: every surface $(X, \omega) \in \mathcal{H}_1(\kappa)$ with a configuration of p homologous saddle connections joining the pair of singularities of length at most ε and no other saddle connection with length smaller than 3ε can be obtained by an assignment $(X', \gamma, a', a'') \to (X, m_1, m_2, a', a'')$ with appropriate (X', γ, a', a'').

Proof. This is Lemma 9.1 in [EMZ03]. □

To finish the preliminaries needed for the last few chapters, we want to extend the volume recursion formulas to configurations with multiple saddle connections or in other words, calculate the Siegel–Veech constant in these cases.

For this, we need to understand again in how many ways Construction 7.3.13 can be performed. Again, let us assume $\mathcal{H}_1(\kappa)$ is connected like in the minimal and principal stratum, also consider the case where we fix the singularities and worry about the additional factor for the volume formula later.

So, the singularities $\Sigma = (\sigma_1, \dots, \sigma_l)$ of the surface (X, ω) shall be ordered. Our configuration $\mathcal{C}$ encodes the orders m_1 and m_2 of σ_1 and σ_2 respectively with some chosen a' and a''. The singularities $\sigma_3, \dots, \sigma_{l_1}$ are contained in $\overline{X}_1$, the singularities $\sigma_{\Sigma_{i=1}^{j-1} l_i + 1}, \dots, \sigma_{\Sigma_{i=1}^{j} l_i}$ are contained in $\overline{X}_j$ for $j \in [p] \setminus \{1\}$. So l_i encodes the count of singularities in $\overline{X}_i$ for $i \in [p] \setminus \{1\}$.

Definition 7.3.16 (Stratum interchange)
The cyclic group of order p acts on the collection of ordered pairs (a_i', a_i''), which themselves are in a cyclic order. This action can have a nontrivial stabilizer Γ_+, which shall be denoted as the *stratum interchange*.

In the case where the singularities are not fixed, some singularity of (X, ω) of order m_1 is joined to a singularity of order m_2 by p homologous saddle connections $\gamma_1, \dots, \gamma_p$ as encoded in $\mathcal{C}$.

We fix $(X_i', \omega_i') \in \mathcal{H}(\kappa_i')$, but we make no assumptions on the distribution of the singularities. As before, we fix the cyclic order of appearances of the surfaces (X_i, ω_i).

If $m_1 = m_2$, we can encounter an additional symmetry: let P and Q be two singularities of order m_1 in configuration $\mathcal{C}$. Assign the names $\sigma_1 \coloneqq P$ and $\sigma_2 \coloneqq Q$. Consider now the very same surface with the same configuration of homologous saddle connections joining the same two singularities P and Q, but this time choose $\sigma_1 \coloneqq Q$ and $\sigma_2 \coloneqq P$. Since the saddle connections are oriented from σ_1 to σ_2, the homology vector of the same saddle connection is now the vector $-\gamma$. Since the cyclic order on each $\overline{X}_i$ is determined by the cyclic order at the point σ_1, the new identification reverses the cyclic order of $(\alpha_1', \dots \alpha_p')$, as well as the order in the pairs (a_i', a_i'').

Definition 7.3.17 (Additional $\gamma \to -\gamma$ symmetry)
We say that we have a $\gamma \to -\gamma$ *symmetry* if and only if the assignment $\sigma_1 \coloneqq Q$ and $\sigma_2 \coloneqq P$ gives a decomposition with the same cyclic order of $(\alpha_1', \dots \alpha_p')$ as the order in the pairs (a_i', a_i'') as before. We denote the group of $\gamma \to -\gamma$ symmetries by Γ_-, where $|\Gamma_-| = 2$, if there exists such a symmetry in addition to the identity element in Γ_-. We get $|\Gamma_-| = 1$ when there is no additional $\gamma \to -\gamma$ symmetry.

Eskin–Masur–Zorich showed that the total symmetry group $\Gamma_\pm$ is generated by the subgroup Γ_+ of stratum interchange symmetries and the subgroup Γ_- of $\gamma \to -\gamma$ symmetries. The order $|\Gamma_\pm|$ is equal to the product of $|\Gamma_+|$ and $|\Gamma_-|$.

Since the symmetry group $\Gamma_\pm$ preserves the Masur–Veech volume on $\mathcal{H}(\kappa')$, it also preserves the hyperboloid $\mathcal{H}_1(\kappa')$. And therefore we get a volume element on the quotient $\mathcal{H}_1(\kappa') \big/ \Gamma_\pm$.

Our degeneration construction from Construction 7.3.11 can be understood by the map

$$\mathcal{H}_1^{\varepsilon,\text{thin}}(\kappa, \mathcal{C}) \to \mathcal{H}_1(\kappa') \big/ \Gamma_\pm \times \overline{B}_\varepsilon(0).$$

This map, restricted to some subset U, was shown in Lemma 9.8 of [EMZ03] to be a (ramified) covering, which is also volume preserving. This subset U is constructed in such a way that $\mathcal{H}_1^{\varepsilon,\text{thin-thick}}(\kappa) \subsetneq U$. This fact can then be used to equate the volumes on the left and the right side with some factor coming from the covering. This strategy will be used in a lot of these kinds of calculations and volume estimates. In particular, we will use it a lot for the volume calculation of the thin-thin part in Chapter 9 with similar arguments.

Lemma 7.3.18 (First bounded calculation)
Suppose that the stratum $\mathcal{H}(\kappa)$ is connected; let $\mathcal{C} = (m_1, m_2, a_i', a_i'')$ be a configuration of saddle connections joining a pair of fixed singularities σ_1, σ_2 connected by p homologous saddle connections. Let $(X', \gamma, a', a'') \to (X, m_1, m_2, a', a'')$ be the corresponding assignment. Then for $\varepsilon > 0$

$$\nu\left(\mathcal{H}_1^{\varepsilon,\text{thin}}(\kappa, \mathcal{C})\right) = M \cdot \nu\left(\mathcal{H}_1\left(\kappa'\right)\right) \cdot \pi\varepsilon^2 + o\left(\varepsilon^2\right),$$

where the constant M is defined as

$$M = \frac{\prod_{i=1}^p (a_i + 1)}{|\Gamma_-| \cdot |\Gamma_+|},$$

using $a_i = a_i' + a_i''$.

Proof. This is Corollary 9.9 of [EMZ03]. The error term in $o\left(\varepsilon^2\right)$ from Corollary 9.9 is coming from the thin-thin part. □

This equality can be then used to also calculate the Siegel–Veech constant, since we understand the degree of the covering.

Proposition 7.3.19 (Third recursion formula)
Let $\mathcal{H}(\kappa)$ be a connected stratum and $\mathcal{H}(\kappa')$ be a stratum of the principal boundary of $\mathcal{H}(\kappa)$ obtained through Construction 7.3.13 from the configuration $\mathcal{C}$, where the saddle connection connecting σ_1 to σ_2 has multiplicity p and $a_i = a_i' + a_i''$ encodes the angles around σ_1 and σ_2. Then

$$c\left(\kappa, \mathcal{C}\right) = \frac{\prod_{i=1}^p (a_i + 1)}{|\Gamma_\pm|} \frac{\nu\left(\mathcal{H}_1\left(\kappa'\right)\right)}{\nu\left(\mathcal{H}_1(\kappa)\right)}.$$

Proof. This is shown after the proof of Corollary 9.9 of [EMZ03]. It uses a covering map of degree $\prod_{i=1}^p (a_i + 1)$. □

Lastly, we can introduce a free choice on the permutation of our singularities of the same order, compared to Lemma 7.3.18, where we fixed σ_1 and σ_2. This extra free choice parameter $M_c(k)$, which counts all choices of naming the singularities for each order k can be calculated by

$$M_c(k) = \frac{\operatorname{soo}(k)!}{\prod_{i=1}^{p} \operatorname{soo}_i(k)!} \cdot \prod_{i \in \{j | a_j = k\}} \operatorname{soo}_i(k),$$

where $\operatorname{soo}(k)$ is the number of singularities of order k in $\mathcal{H}(\kappa')$ and $\operatorname{soo}_i(k)$ is the number of singularities of order k in $\mathcal{H}(\kappa'_i)$. A good derivation for $M_c(k)$ is at the end of page 37 in [EMZ03]:

Consider $k \neq m_1, k \neq m_2$, and $k \neq a_i$ for $i \in [p]$. Then the singularities are all "inherited" by the surfaces X_i. Since all the singularities $\sigma_1, \sigma_2, \ldots, \sigma_l$ are named, the number of ways to distribute $\operatorname{soo}(k)$ singularities of order k into groups of $\operatorname{soo}_1(k), \ldots, \operatorname{soo}_p(k)$ singularities equals

$$\frac{\operatorname{soo}(k)!}{\prod_{i=1}^{p} \operatorname{soo}_i(k)!}$$

If $k \neq m_1$ and $k \neq m_2$ but $k = a_j$ for some j, then one of the $\operatorname{soo}_j(k)$ singularities of order k on S_j is arising from the degeneration, while the other $\operatorname{soo}_j(k) - 1$ singularities of order k come from the corresponding singularities of order k on S. Thus the corresponding factor in the denominator becomes $(\operatorname{soo}_j(k) - 1)!$. Multiplying numerator and denominator by $\operatorname{soo}_j(k)$, we get $M_c(k)$.

We therefore get the following final lemma to calculate the volume of the thin part of $\mathcal{H}_1(\kappa)$ with configuration $\mathcal{C}$.

Lemma 7.3.20 (Combined formula)
Suppose that the stratum $\mathcal{H}(\kappa)$ is connected; let $\mathcal{C} = (m_1, m_2, a'_i, a''_i)$ be a configuration of saddle connections joining a pair of any two singularities of orders m_1 and m_2 connected by p homologous saddle connections. Let $(X', \gamma, a', a'') \to (X, m_1, m_2, a', a'')$ be the corresponding assignment. Then for $\varepsilon > 0$:

$$\nu\left(\mathcal{H}_1^{\varepsilon,\text{thin}}(\kappa, \mathcal{C})\right) = \frac{\prod_{i=1}^{p}(a_i + 1)}{|\Gamma_-| \cdot |\Gamma_+|} \cdot \prod_{k \in \kappa} \left(\frac{\operatorname{soo}(k)!}{\prod_{i=1}^{p} \operatorname{soo}_i(k)!}\right) \cdot \prod_{\substack{i=1 \\ a_i \neq 0}}^{p} \operatorname{soo}_i(a_i)$$
$$\cdot \frac{1}{2^{p-1}} \cdot \frac{\prod_{i=1}^{p}\left(\frac{d_i}{2} - 1\right)!}{\left(\frac{d}{2} - 1\right)!} \cdot \prod_{i=1}^{p} \nu\left(\mathcal{H}_1(\kappa_i)\right) \cdot \pi\varepsilon^2 + o\left(\varepsilon^2\right).$$

Proof. Taking the product over all singularities in κ for $M_c(k)$ since we ignore the order and using Lemmas 7.1.5 and 7.3.18 we get this combined formula. Since

$$\prod_{k \in \kappa} \prod_{i \in \{j | a_j = k\}} \operatorname{soo}_i(k) = \prod_{\substack{i=1 \\ a_i \neq 0}}^{p} \operatorname{soo}_i(a_i),$$

we get this as an additional factor. □

It is worth noting that Eskin, Masur, and Zorich extended their results also to different connected components and to the case where the saddle connection is closed. However, these cases, while interesting on their own, are not necessary for our upcoming analysis. The reader is encouraged to read up on them in [EMZ03] from page 40 onwards.

8 Geometric Cheeger constant

The standard topology on spaces of translation surfaces is often too coarse and fails to capture the subtleties of the geometric properties of these surfaces. By understanding geometric invariants, we hope to provide a more nuanced comprehension of the topology of the space of translation surfaces. The Cheeger constant is an invariant that captures how well a surface can be cut into two parts of roughly equal size with a minimal cut and therefore measure connectivity in some sense.

The Cheeger constant plays a crucial role in various areas of computer science, with applications in computer networks, distributed computing, and machine learning. In these areas, however, it is often the Cheeger constant of graphs, rather than surfaces, that is considered. In computer networks, it serves as a tool for analyzing the network's resilience against failures or attacks. In machine learning, it helps in measuring the complexity of data sets and designing algorithms for clustering and classification.

Furthermore, the Cheeger constant of graphs is connected to other crucial mathematical concepts. For instance, it is related to the eigenvalues of graphs, for which upper and lower bound inequalities have been established [Bus82]. It is also linked to expander graphs, where the Cheeger constant measures the edge expansion and to the spectral gap of Laplacian matrices, for which corresponding inequalities exist [Chu97].

It has been the subject of extensive study, particularly hyperbolic surfaces where Maryam Mirzakhani [Mir13] established a solution demonstrating convergence of the Cheeger constant for growing genus. However, no comparable results have yet been established for translation surfaces.

The Cheeger constant is related to the covering radius, for which expected value results have been obtained independently of the stratum by Masur–Rafi–Randecker [MRR22].

Definition 8.0.1 (Cheeger isoperimetric constant)
Let (X, ω) be a translation surface and let $\mathcal{A}$ be the set of all closed separating curves on $\overline{X}$, such that for $A \in \mathcal{A}$: $\overline{X} \setminus A = X_1 \sqcup X_2$. The *Cheeger isoperimetric constant* h of X is defined by

$$h(X) \coloneqq \inf_{A \in \mathcal{A}} \frac{\text{length}(A)}{\min \{\text{area}(X_1), \text{area}(X_2)\}}.$$

We will also refer to the Cheeger isoperimetric constant as the *geometric Cheeger constant*. As we disassemble translation surfaces through a separating curve in the definition of the Cheeger constant, we obtain surfaces in the stratum of disconnected surfaces.

The Cheeger constant measures the inverse of bottleneckedness. A small Cheeger constant suggests the existence of a short separating curve, which divides the underlying space into parts of similar size, suggesting a bottleneck in the surface.

8.1 Growth of the Cheeger constant

We are mainly interested in approximating the expected value $\mathbb{E}_{\mathcal{H}_1(\kappa)}(h)$ of our Cheeger constant for different strata. The goal of this section is to get a better understanding on the expected growth of the Cheeger constant for any stratum.

We have seen in Proposition 7.1.7, how to calculate volume with square-tiled surfaces. We want to extend this to the Cheeger constant.

Definition 8.1.1 (Origami graphification)
Let (X, ω) be a square-tiled surface. We define the *origami graphification* $\mathrm{OG}(X)$ as a graph in the following way:

- Fix the squares that tile (X, ω) as the vertices: $V(\mathrm{OG}(X)) = \{P_1, P_2 \dots P_n\}$.
- Add an edge $\{P_i, P_j\} \in E(\mathrm{OG}(X))$ if there exists an edge identification in ω between the polygons P_i and P_j.

As mentioned in the introduction of this chapter, the isoperimetric Cheeger constant has a well-researched analogue for graphs.

Definition 8.1.2 (Cheeger constant for graphs)
Let $G = (V, E)$ be a graph and

$$\partial A := |\{\{P_i, P_j\} \in E \mid P_i \in A, P_j \in V \setminus A\}|$$

for $A \subseteq V$. We define the *Cheeger constant for graphs* $\tilde{h}$ by

$$\tilde{h}(G) := \min_{A \subseteq V \text{conn.}} \frac{|\partial A|}{\min\{|A|, |V \setminus A|\}}.$$

This definition is closely related to the classical geometric one. It measures the inverse of bottleneckedness as well. The cardinality of the set ∂A corresponds to how connected the separated sets A and $V \setminus A$ are.

We do want to show that h and $\tilde{h}$ are closely related, for that let us introduce the following recursive construction.

Definition 8.1.3 (Origami graphification of order m)
Let (X, ω) be a square-tiled surface. We define the *origami graphification of order m* recursively:

- Define the first surface with $X_1 := X$.
- We produce a sequence of identical translation surfaces $(X_i)_{i \in \mathbb{N}}$ by dividing each square of X_i into four equal sized squares and regluing them, such that the surface X_{i+1} obtained from this procedure is equal to X_i as a translation surface.

- The origami graphification of order m is then the standard origami graphification of X_m: $\mathrm{OG}_m(X) = \mathrm{OG}(X_m)$.

We can also explicitly calculate the edge length and the area of the underlying square for $(X, \omega) \in \mathcal{H}_1(\kappa)$.

Remark 8.1.4 (Length & area)
Let $(X, \omega) \in \mathcal{H}_1(\kappa)$ be a square-tiled surface of area 1, containing n squares, and let $\mathrm{OG}_m(X)$ be the the graphification of order m.

1. The area of a square of X_m in 8.1.3 is given by $A_{m,n} = \frac{4}{4^m n}$.
2. The length of a side of a square of X_m in 8.1.3 is given by $L_{m,n} = \sqrt{A_{m,n}}$.

Lemma 8.1.5 (Graphification quasi-preserves Cheeger constant)
For every square-tiled surface (X, ω), there exists some $m \in \mathbb{N}^+$, such that the Cheeger constant of a origami graphification of X is bounded by

$$h(X) \leq \tilde{h}(\mathrm{OG}_m(X)) L_{m,n}^{-1} \leq 3\, h(X).$$

Therefore h and $\left(\tilde{h} \circ \mathrm{OG}_m\right) L_{m,n}^{-1}$ are the same up to some factor.

Proof. Let (X, ω) be a square-tiled surface consisting of n squares with origami graphification $G = (V, E)$. Let A be a curve on $\overline{X}$ with $\min\{area(X_1), area(X_2)\} = area(X_1)$ optimizing the term in 8.0.1.

Embed G on X in such a way that the vertex corresponding to P_i is placed in the center of P_i and an edge $\{P_i, P_j\}$ corresponds to a straight line intersecting the corresponding gluing exactly once without crossing other edges.

Consider the dual graph $\tilde{G}$ embedded on $\overline{X}$. Now the vertices of $\tilde{G}$ are each homotopic to one of the corners of the original polygon construction, which are also in correspondence to the (possible) singularities of $\overline{X}$. The edges of $\tilde{G}$ are homotopic to the original sides in $\overline{X}$, which are saddle connections. Without loss of generality, choose the embedding of $\tilde{G}$ in $\overline{X}$ in such a way that the vertices correspond to corners and edges to sides exactly.

We subdivide X as in Definition 8.1.3 until the curve A encloses at least one square of size $A_{m,n}$ for each of the original polygons $P_1, P_2, \ldots P_n$ if $X_1 \cap \partial P_i \neq \emptyset$.

Now we choose a path $\tilde{A}$ on $\mathrm{OG}_m(X)$ approximating A, such that $X \setminus \tilde{A} = \tilde{X}_1 \sqcup \tilde{X}_2$ and $X_1 \subseteq \tilde{X}_1$. Let us consider the squares of area A_m, n contained in $\tilde{X}_1$ and add them to a set P. In the worst case for the path length, we choose a path of length at most $3L_{m,n}$ instead of $L_{m,n}$ and therefore $|\partial P|\, L_{m,n} \leq 3\, \mathrm{length}(A)$. For the area, we enclose at least the size of each polygon in P by construction and therefore $|P|\, A_{m,n} = \mathrm{area}(\tilde{X}_1) \geq \mathrm{area}(X_1)$.

$$\begin{aligned} \frac{\tilde{h}(\mathrm{OG}_m(X))}{L_{m,n}} &\leq \frac{|\partial P|\, L_{m,n}}{\min\{|P|, |V \setminus P|\}\, A_{m,n}} \\ &= \frac{|\partial P|\, L_{m,n}}{|P|\, A_{m,n}} \end{aligned}$$

$$\begin{aligned}
&\leq \frac{3\,\mathrm{length}(A)}{\mathrm{area}(X_1)} \\
&= 3\frac{\mathrm{length}(A)}{\min\{\mathrm{area}(X_1), \mathrm{area}(X_2)\}} \\
&= 3\ h(X).
\end{aligned}$$

For the other inequality consider A to be a subset of V_m, where $\mathrm{OG}_m(X) = (V_m, E_m)$ corresponding to a minimal case of $\tilde{h}$ in 8.1.2 for (V_m, E_m). As mentioned above the dual edges of ∂A now correspond to saddle connections in $\overline{X}_m$. The union of these saddle connections is a curve C in $\overline{X}_m$, since A is connected. The length of C is by construction just $\mathrm{length}(C) \leq |\partial A|\, L_{m,n}$. The areas of X_1 and X_2 separated by C are just the number of squares in each partition of $P_1, P_2, \ldots P_n$ in A and $(V \setminus A)$ multiplied by $A_{m,n}$, so

$$h(X) \leq \frac{\mathrm{length}(C)}{\min\{\mathrm{area}(X_1), \mathrm{area}(X_2)\}} \leq \frac{|\partial A|\, L_{m,n}}{\min\{|A|, |V \setminus A|\}\, A_{m,n}} = \frac{\tilde{h}(\mathrm{OG}_m(X))}{L_{m,n}}. \qquad \square$$

Lemma 8.1.6 (Upper bound on $\tilde{h}$ for Origami-graphs)
The Cheeger constant $\tilde{h}$ for the origami graphification of every order m of a square-tiled surface (X, ω) is bounded by

$$\tilde{h}\,(\mathrm{OG}_m(X)) \leq 4.$$

Proof. Let A be a subset of V, the vertices of an origami graphification of order m. Since $\deg(P_i) = 4$ we know that $|\partial A| \leq 4\,|A|$. Furthermore, by the symmetry of the definition of ∂A, it is clear that $|\partial A| = |\partial\,(V \setminus A)|$. A small calculation shows:

$$\begin{aligned}
\frac{|\partial A|}{\min\{|A|, |V \setminus A|\}} &= \max\left\{\frac{|\partial A|}{|A|}, \frac{|\partial A|}{|V \setminus A|}\right\} \\
&= \max\left\{\frac{|\partial A|}{|A|}, \frac{|\partial\,(V \setminus A)|}{|V \setminus A|}\right\} \\
&\leq \max\left\{\frac{4\,|A|}{|A|}, \frac{4\,|V \setminus A|}{|V \setminus A|}\right\} = \max\{4, 4\} = 4.
\end{aligned}$$

And therefore $\tilde{h}\,(\mathrm{OG}_m(X)) \leq 4$. $\square$

With Lemmas 8.1.5 and 8.1.6, we see that for a square-tiled surface (X, ω) consisting of n squares, there exists some $m \in \mathbb{N}^+$, such that

$$h(X) \leq 2^{m+1}\sqrt{n}.$$

Heuristically, this m coming from the proof of Lemma 8.1.5 should be relatively small, however we can choose examples for which this m needs to be chosen arbitrarily large.

Proposition 8.1.7 (Cheeger constant can be large)
On every Stratum $\mathcal{H}_1(\kappa)$, for every $N \in \mathbb{N}^+$, there exists some $(X, \omega) \in \mathcal{H}_1(\kappa)$, such that

$$h(X) > N.$$

Proof. We proof this statement first for tori, so $(X, \omega) \in \mathcal{H}_1(0)$. Let $N \in \mathbb{N}^+$ and choose $(X, \omega) = \frac{1}{N^3}\mathbb{T}_{N^6 \mathrm{i}}$, the translation surface (X, ω) contains a maximal cylinder in vertical direction of circumference N^3 and height $\frac{1}{N^3}$. Let A be a separating curve on $\overline{X}$ with $\overline{X} \setminus A = X_1 \sqcup X_2$, optimizing Definition 8.0.1. It bounds a topological disk on both sides, since there are no essential singularities on (X, ω). The isoperimetric inequality holds for topological disks in the flat metric, this implies

$$\operatorname{area}(X_i) \leq \frac{(\operatorname{length}(A))^2}{4\pi}.$$

Substituting length for area, we obtain

$$\begin{aligned} h(X) &= \frac{\operatorname{length}(A)}{\min(\operatorname{area}(X_1), \operatorname{area}(X_2))} \\ &\geq \frac{\sqrt{4\pi \operatorname{area}(X_1)}}{\operatorname{area}(X_1)} = \sqrt{\frac{4\pi}{\operatorname{area}(X_1)}} \end{aligned}$$

if $\operatorname{area}(X_1) \leq \operatorname{area}(X_2)$. For $\operatorname{area}(X_1) < \frac{4\pi}{N^2}$ our statement is true immediately, so let $\operatorname{area}(X_1) \geq \frac{4\pi}{N^2}$. Analogously, we see $\operatorname{area}(X_2) \geq \frac{4\pi}{N^2}$.

Since our cylinder has a height of only $\frac{1}{N^3}$, the diameter of X_i needs to be at least $2\pi N$, and $\operatorname{length}(A) \geq 2\pi N$. This can be seen by realizing that the product of the projection of X_i on the horizontal and vertical component is at most the double of the area of X_i, because otherwise A would not optimize Definition 8.0.1: we could construct a better curve as the boundary of a rhombus with diagonal lengths $\frac{1}{N^3}$ and $4\pi N$.

Since $\min(\operatorname{area}(X_1), \operatorname{area}(X_2)) \leq \frac{1}{2}$, we conclude

$$\begin{aligned} h(X) &= \frac{\operatorname{length}(A)}{\min(\operatorname{area}(X_1), \operatorname{area}(X_2))} \\ &\geq \frac{2\pi N}{\frac{1}{2}} = 4\pi N > N. \end{aligned}$$

We therefore have shown that $h(X) > N$ for every $N \in \mathbb{N}^+$ and h can be arbitrarily large on $\mathcal{H}_1(0)$. We can now generalize this to other strata.

Choose a square U of length ε on the torus (X, ω) and add genus on U by decorating it locally with slits and reglue them, such that the modified surface (X', ω') is from $\mathcal{H}_1(\kappa)$. Let A be the new curve optimizing the Cheeger constant on this modified surface.

Define $A^U = A \cap U$ and $A^{X \setminus U} = A \setminus A'$. Analogously for X_i^U and $X_i^{X \setminus U}$. If $A^U = \emptyset$, we can ignore U and are done. If $A^{X \setminus U} = \emptyset$, our curve A will be in U. We can scale down ε until the optimal curve is not anymore solely in U: scaled length of A on U will be ε times the original length of A, while $\operatorname{area}(X_i) = \operatorname{area}\left(X_i^U\right) \leq \varepsilon^2$ for one of the surfaces, so

$$\lim_{\varepsilon \to 0} \frac{\operatorname{length}(A)}{\min(\operatorname{area}(X_1), \operatorname{area}(X_2))} \sim \lim_{\varepsilon \to 0} \frac{\varepsilon}{\varepsilon^2} = \infty.$$

The set $X \setminus U$ is topologically an open disk, so like before we can conclude that for $i \in \{1, 2\}$

$$\begin{aligned}
h(X) &= \frac{\operatorname{length}(A)}{\min\left(\operatorname{area}(X_1), \operatorname{area}(X_2)\right)} \\
&= \frac{\operatorname{length}\left(A^U\right) + \operatorname{length}\left(A^{X\setminus U}\right)}{\operatorname{area}\left(X_i^U\right) + \operatorname{area}\left(X_i^{X\setminus U}\right)} \\
&\geq \frac{\operatorname{length}\left(A^{X\setminus U}\right)}{\varepsilon^2 + \operatorname{area}\left(X_i^{X\setminus U}\right)} \\
&\geq \frac{\sqrt{4\pi \operatorname{area}\left(X_1^{X\setminus U}\right)}}{\varepsilon^2 + \operatorname{area}\left(X_1^{X\setminus U}\right)}.
\end{aligned}$$

We can assume $\operatorname{area}\left(X_i^{X\setminus U}\right) \geq \frac{1}{N^2}$, otherwise for $\varepsilon \to 0$, the statement becomes immediately true.

We can estimate $\operatorname{length}\left(A^{X\setminus U}\right)$ with the same projection reasoning as before:

$$\operatorname{length}\left(A^{X\setminus U}\right) \geq \operatorname{diameter}\left(X_i^{X\setminus U}\right) \geq N^3 \cdot \frac{1}{2} \operatorname{area}\left(X_i^{X\setminus U}\right) \geq \frac{N}{2},$$

which yields

$$\begin{aligned}
h(X) &= \frac{\operatorname{length}(A)}{\min\left(\operatorname{area}(X_1), \operatorname{area}(X_2)\right)} \\
&\geq \frac{\operatorname{length}\left(A^U\right) + \operatorname{length}\left(A^{X\setminus U}\right)}{\frac{1}{2}} \\
&\geq \frac{\operatorname{length}\left(A^{X\setminus U}\right)}{\frac{1}{2}} \geq N.
\end{aligned}$$

□

It is very hard to calculate the Cheeger constant given a random translation surface. However, using the method of trying to embed a large disk is already a good starting point for understanding the behavior of the geometric Cheeger constant in the minimal stratum.

8.2 Minimal stratum

We will show that the expected value of the Cheeger constant of all translation surfaces in the stratum $\mathcal{H}_1(2g-2)$ is bounded above by a term that grows like $g^{\frac{3}{2}}$ as $g \to \infty$.

We show the main theorem by dividing the stratum $\mathcal{H}_1(2g-2)$ with the thin-thick decomposition and showing the bounded growth on each part separately. For an explicit split, we need to fix some ε.

Remark 8.2.1 (The right choice for ε)
Let us consider a ball B around a singularity of $(X, \omega) \in \mathcal{H}_1^{\varepsilon,\text{thick}}(2g-2)$. Its radius can be at least $\frac{\varepsilon}{2}$ without intersecting itself. This ball can be thought of as a covering space on a disk of degree $2g-2$ and its boundary is a closed separating curve in X. It is therefore a candidate for Definition 8.0.1. An easy calculation shows that:

$$\begin{aligned} h(X) &\leq \frac{\text{length}(\partial B_{\frac{\varepsilon}{2}})}{\min\left\{\text{area}(B_{\frac{\varepsilon}{2}}), \text{area}(X \setminus B_{\frac{\varepsilon}{2}})\right\}} \\ &= \frac{\pi\varepsilon(2g-2)}{\min\left\{\pi\frac{\varepsilon^2}{4}(2g-2), 1 - \pi\frac{\varepsilon^2}{4}(2g-2)\right\}} \\ &= \max\left\{\frac{4}{\varepsilon}, \frac{4\pi\varepsilon(2g-2)}{4 - \pi\varepsilon^2(2g-2)}\right\}. \end{aligned}$$

For further calculations, we want to differentiate between the two cases depending on the dominating term. We can achieve this by restricting our ε:

$$\begin{aligned} &\frac{4}{\varepsilon} > \frac{4\pi\varepsilon(2g-2)}{4 - \pi\varepsilon^2(2g-2)} \\ \Leftarrow\ & 4\left(4 - \pi\varepsilon^2(2g-2)\right) > 4\pi\varepsilon^2(2g-2) \\ \Leftarrow\ & 4 - \pi\varepsilon^2(2g-2) > \pi\varepsilon^2(2g-2) \\ \Leftarrow\ & 4 > 2\pi\varepsilon^2(2g-2) \\ \Leftarrow\ & \varepsilon < \frac{1}{\sqrt{\pi(g-1)}}. \end{aligned}$$

Note that for $\varepsilon > \frac{2}{\sqrt{\pi(2g-2)}}$ the area of $X \setminus B$ would be negative, we therefore look at the following two cases: a small ε case with $0 < \varepsilon < \frac{1}{\sqrt{\pi(g-1)}}$ and a large ε case with $\frac{1}{\sqrt{\pi(g-1)}} < \varepsilon < \frac{2}{\sqrt{\pi(2g-2)}} = \frac{\sqrt{2}}{\sqrt{\pi(g-1)}}$. Note that the choice of ε depends on X.

In the small ε case, we are not able to show that the Cheeger constant is bounded and we have to use a further decomposition and show that the measure of surfaces with a large Cheeger constant vanishes fast enough. The Cheeger constant for our ball example is given by $h < \frac{4}{\varepsilon}$.

In the large ε case, the Cheeger constant is bounded, however using our old upper bound for large ε is not good enough. By inserting the upper bound for ε into the formula above, our estimation for the Cheeger constant divergences:

$$\lim_{\varepsilon \to \frac{2}{\sqrt{\pi(2g-2)}}} \frac{4\pi\varepsilon(2g-2)}{4 - \pi\varepsilon^2(2g-2)} = \infty.$$

To see an upper bound for the Cheeger constant in the large ε case, we will later use a Delaunay triangulation in Lemma 8.2.7, there we also will see that the thick part is empty for $\varepsilon > \frac{2}{\sqrt{\pi(2g-2)}}$. The Cheeger constant for our ball example is given by $h < \frac{4\pi\varepsilon(2g-2)}{4-\pi\varepsilon^2(2g-2)}$ in the large ε case.

Let us start by considering the small ε case. We will show our upper bound on the thick part $\mathcal{H}_1^{\frac{1}{\sqrt{\pi(g-1)}},\mathrm{thin}}(2g-2)$ with the following decomposition.

Definition 8.2.2 (Divide-and-conquer decomposition)
For $g \geq 2$, define the following subsets of $\mathcal{H}_1(2g-2)$ for $n \in \mathbb{N}_0$:

$$U_n := \left\{ (X,\omega) \in \mathcal{H}_1(2g-2) \;\middle|\; \frac{2^{-n-1}}{\sqrt{\pi(g-1)}} < \inf_{\gamma \in V_{\mathrm{sc}}(X)} \operatorname{length}(\gamma) \leq \frac{2^{-n}}{\sqrt{\pi(g-1)}} \right\}.$$

We have chosen these sets to cover the thin part.

Remark 8.2.3 (Thin stratification)
The thin part of a stratum is stratified by

$$\mathcal{H}_1^{\frac{1}{\sqrt{\pi(g-1)}},\mathrm{thin}}(2g-2) = \bigcup_{n=0}^{\infty} U_n.$$

Using a divide-and-conquer approach, we want to give an upper bound for h on each U_n separately.

Lemma 8.2.4 (Local bound)
On U_n, the Cheeger constant h is bounded by $h \leq 2^{n+3}\sqrt{\pi(g-1)}$.

Proof. Let $(X,\omega) \in U_n$. By Remark 8.2.1, we can calculate an upper bound for the geometric Cheeger constant as the Cheeger constant given by the separating boundary of a $(2g-2)$–fold cover of a disk.

$$h(X) \leq \frac{4}{\varepsilon} \leq \frac{4}{2^{-n-1}}\sqrt{\pi(g-1)} = 2^{n+3}\sqrt{\pi(g-1)}. \qquad \square$$

To control the Cheeger constant, after giving a bound on each U_n, we just need to control the volume of U_n.

Proposition 8.2.5 (Small size)
There exists a constant $M > 0$ for large enough genus g, such that for all $n \in \mathbb{N}_0$

$$\nu(U_n) \leq 2^{-2n} \cdot M \cdot (g-1) \cdot \nu(\mathcal{H}_1(2g-2)).$$

Proof. We can calculate $\nu\left(\mathcal{H}_1^{\frac{2^{-n}}{\sqrt{\pi(g-1)}},\mathrm{thin}}(2g-2)\right)$ as an upper bound for $\nu(U_n)$, since $U_n \subseteq \mathcal{H}_1^{\frac{2^{-n}}{\sqrt{\pi(g-1)}},\mathrm{thin}}(2g-2)$. There is only one singularity σ, so every saddle connection is a loop.

We now want to calculate the Siegel–Veech constant c_{loop} for all saddle connections on $\mathcal{H}_1(2g-2)$. We want to sum over all possible counts of p homologous saddle connections in the form of loops. Consequently, we will need some results from Part 2 of [EMZ03]. The surfaces from $\prod_{i=1}^{p} \mathcal{H}_1(\kappa_i')$ either arise from the figure eight construction described in Section 12.1 in [EMZ03], where two saddle connections form a figure-eight on the boundary, or their boundary consists of two separate and closed saddle connections. In the second case, we distinguish between surfaces of genus 0, which are cylinders, and surfaces of genus greater than 0, which we refer to as being of the two holes type.

These surfaces cannot all be of the figure eight type and there can be at most one cylinder or one surface of two holes type, because, otherwise, in each case, at least two singularities would be required.

We want to compute $\tilde{c}_{p,\text{cylinder}}$ for $p \in [g-1]$, which corresponds to surfaces with p surfaces of figure eight type and one cylinder. Similarly, we want to compute $\tilde{c}_{p,\text{two-hole}}$ for $p \in \{2, \dots, g-1\}$, corresponding to surfaces with $p-1$ surfaces of figure eight type and one surface of two holes type. To calculate an upper bound for c_{loop}, we can use

$$\begin{aligned} c_{\text{loop}} &= \sum_{p=1}^{g-1} \tilde{c}_{p,\text{cylinder}} + \sum_{p=2}^{g-1} \tilde{c}_{p,\text{two-hole}} \\ &\leq \sum_{p=1}^{g-1} N_{p,\text{cylinder}} \cdot c_{p,\text{cylinder}} + \sum_{p=2}^{g-1} N_{p,\text{two-hole}} \cdot c_{p,\text{two-hole}}, \end{aligned}$$

where $N_{p,\text{cylinder}}$ count the number of ways to obtain surfaces corresponding to $\tilde{c}_{p,\text{cylinder}}$ and $c_{p,\text{cylinder}}$ is the Siegel–Veech constant for surfaces of the biggest case obtainable. The number $N_{p,\text{two-hole}}$ and the Siegel–Veech constant $c_{p,\text{two-hole}}$ are defined analogously.

To calculate $c_{p,\text{cylinder}}$ and $c_{p,\text{two-hole}}$, we can therefore fix the naming in the corresponding constructions. Similar to Part 1 of [EMZ03], we look at $p+1$ homologous saddle connections in the case corresponding to $c_{p,\text{cylinder}}$ and p homologous saddle connections in the case corresponding to $c_{p,\text{two-hole}}$. We obtain the symmetry groups Γ_- and Γ_+ from the stratum interchange and $\gamma \to -\gamma$ symmetry. However, we encode new vectors b' and b'', in addition to a. For surfaces of figure eight type, we denote the order a_i of the new singularity in $\mathcal{H}(\kappa_i')$. For surfaces of two holes type, we analogously denote the order of the corresponding singularities by b_k' and b_k''.

With Theorem 3.5.22, we see that $\mathcal{H}_1(2g-2)$ is disconnected with

$$\mathcal{H}(2g-2) = \mathcal{H}^{\text{hyp}}(2g-2) \sqcup \mathcal{H}^{\text{even}}(2g-2) \sqcup \mathcal{H}^{\text{odd}}(2g-2).$$

Because of [Che+20], we know that the even and odd component have comparable volume. The volume of the hyperelliptic part is negligible [AEZ16].

In Formula 14.5 of [EMZ03], we are in the right setting of our problem. There, we can see that it is enough to use the calculations of Formula 14.4, since we only need an upper bound for the total Siegel–Veech constant.

As in Corollaries 3–5 of [Agg20], our current goal is to evaluate for

$$c \in \{c_{p,\text{cylinder}}, c_{p,\text{two-hole}}\},$$

the equation

$$c = \frac{1}{|\Gamma_-| \cdot |\Gamma_+|} \cdot \prod_{i=1}^{p} \chi_{a,i}\,(a_i+1) \cdot \prod_{k=1}^{p} \chi_{b,k}\,(b_k'+1)\,(b_k''+1)$$

$$\cdot \frac{1}{2^{p-1}} \cdot \frac{\prod_{i=1}^{p}\left(\frac{d_i}{2}-1\right)!}{\left(\frac{d}{2}-2\right)!} \cdot \frac{\prod_{i=1}^{p}\nu\left(\mathcal{H}_1\left(\kappa_i'\right)\right)}{\nu\left(\mathcal{H}_1\left(\kappa\right)\right)}.$$

Here, d denotes the real dimension of $\mathcal{H}_1(\kappa)$, and the terms d_i refer to a quantity related to the real dimension of $\mathcal{H}(\kappa_i')$, with $d_i \geq 4$. The term $\chi_{a,i} \in \{0,1\}$ is the indicator function, encoding the information whether the surface X_i is of figure eight type and the term $\chi_{b,k} \in \{0,1\}$ is the indicator function, encoding the information whether the surface X_k is of two holes type.

This formula is derived by combining the results from Section 13 and by checking all cases in Formula 14.4 of [EMZ03]. We are not in the first case, as our assignment does not consist solely of figure eight constructions; as previously mentioned, this would require at least two singularities.

In the other cases, the terms for the "singularities of order" vanishes since we are in the labeled situation of our problem. Since

$$\mathcal{H}_1(2g-2) = \mathcal{H}_1^{\text{hyp}}(2g-2) \sqcup \mathcal{H}_1^{\text{even}}(2g-2) \sqcup \mathcal{H}_1^{\text{odd}}(2g-2),$$

the terms of the volume form in the numerator can be estimated with our formula. Also, because of [Che+20], we know that the even and odd component have comparable volume and the denominator can be estimated with our formula.

Since $|\Gamma_-| \cdot |\Gamma_+| \geq 1$, we can ignore this term for an upper bound as well. The real dimension of $\mathcal{H}_1(2g-2)$ is $4g-2$.

Let $q \in \{0,1\}$ encode the number of cylinders, then

$$4g+2-2 = d = \sum_{i=1}^{p} d_i + 2q + 2.$$

Since $d_i \geq 4$, we get $d_i \leq 4g-4(p-1)-2q-2 = 4g-4p-2q+2$ as an upper bound for d_i.

We obtain the largest value for $\frac{\prod_{i=1}^{p}\left(\frac{d_i}{2}-1\right)!}{\left(\frac{d}{2}-2\right)!}$, in the numerator, when all but one term are as small as possible, so using Stirling's approximation

$$\begin{aligned}
\frac{\prod_{i=1}^{p}\left(\frac{d_i}{2}-1\right)!}{\left(\frac{d}{2}-2\right)!} &\leq \frac{\left(\left(\frac{4}{2}-1\right)!\right)^{p-1} \cdot \left(\frac{4g-4p-2q+2}{2}-1\right)!}{\left(\frac{4g}{2}-2\right)!} \\
&= \frac{(2g-2p-q)!}{(2g-2)!} \\
&\leq \frac{\sqrt{2\pi(2g-2p-q)}\left(\frac{2g-2p-q}{e}\right)^{2g-2p-q} e^{\frac{1}{12(2g-2p-q)}}}{\sqrt{2\pi(2g-2)}\left(\frac{2g-2}{e}\right)^{2g-2} e^{\frac{1}{12(2g-2)}-\frac{1}{360(2g-2)^3}}} \\
&= \sqrt{\frac{2g-2p-q}{2g-2}} \frac{(2g-2p-q)^{2g-2p-q}}{(2g-2)^{2g-2}} e^{2(p-1)+q} e^{\frac{1}{12(2g-2p-q)}-\frac{1}{12(2g-2)}+\frac{1}{360(2g-2)^3}} \\
&\leq \frac{1}{(2g-2)^{2(p-1)+q}} 4^{2(p-1)+q} e^{\frac{1}{12}+\frac{1}{360}} \leq 2\left(\frac{4}{g}\right)^{2(p-1)+q}.
\end{aligned}$$

For this case, using Theorem 7.1.10 on the volume terms, there exists some $D > 0$ for large enough g, such that

$$\frac{\prod_{i=1}^{p} \nu\left(\mathcal{H}_1\left(\kappa_i'\right)\right)}{\nu\left(\mathcal{H}_1\left(\kappa\right)\right)} \leq \frac{D \cdot 4^{p-1} \cdot (2g-1)}{\prod_{i=1}^{p} \chi_{a,i}\left(a_i+1\right) \cdot \prod_{k=1}^{p} \chi_{b,k}\left(b_k'+1\right)\left(b_k''+1\right)}$$

So, for $D > 0$ we obtain

$$\begin{aligned}
c &= \frac{1}{|\Gamma_-| \cdot |\Gamma_+|} \cdot \prod_{i=1}^{p} \chi_{a,i}\left(a_i+1\right) \cdot \prod_{k=1}^{p} \chi_{b,k}\left(b_k'+1\right)\left(b_k''+1\right) \\
&\quad \cdot \frac{1}{2^{p-1}} \cdot \frac{\prod_{i=1}^{p}\left(\frac{d_i}{2}-1\right)!}{\left(\frac{d}{2}-2\right)!} \cdot \frac{\prod_{i=1}^{p} \nu\left(\mathcal{H}_1\left(\kappa_i'\right)\right)}{\nu\left(\mathcal{H}_1\left(\kappa\right)\right)} \\
&\leq D \cdot (2g-1) \cdot 4^{p-1} \cdot \frac{1}{2^{p-1}} \cdot 2\left(\frac{4}{g}\right)^{2(p-1)+q} \\
&= D \cdot (2g-1) \frac{2^{2(p-1)} \cdot 2^{4(p-1)+2q} \cdot 2}{2^{p-1} \cdot g^{2(p-1)+q}} \\
&= D \cdot (2g-1) \frac{2^{5(p-1)+2q+1}}{g^{2(p-1)+q}}
\end{aligned}$$

Let us consider the surfaces with one cylinder first, so $q = 1$. We now need to estimate the number of configurations. For the multiplicity p, we can choose from one of the geodesic segments with fixed holonomy vector at σ of order $2g-2$, resulting in $2g-1$ possibilities. For the other p segments, we have at most $(2g-1-1)$ choices, so

$$N_{p,\text{cylinder}} \leq (2g-1)(2g-2)^p.$$

Next, we consider surfaces with one surface being of two hole type, so $q = 0$. For the multiplicity p, we can choose from one of the geodesic segments with fixed holonomy vector at σ of order $2g-2$, resulting in $2g-1$ possibilities. For the other $p-1$ segments, we have at most $(2g-2)$ choices, so

$$N_{p,\text{two-hole}} \leq (2g-1)(2g-2)^{p-1}.$$

In total, there exists some constant $D > 0$ for large enough g, such that

$$\begin{aligned}
c_{\text{loop}} &\leq \sum_{p=1}^{g-1} N_{p,\text{cylinder}} \cdot c_{p,\text{cylinder}} + \sum_{p=2}^{g-1} N_{p,\text{two-hole}} \cdot c_{p,\text{two-hole}} \\
&\leq \sum_{p=1}^{\infty} (2g-1)(2g-2)^p \cdot D \cdot (2g-1) \frac{2^{5(p-1)+3}}{g^{2(p-1)+1}} \\
&\quad + \sum_{p=2}^{\infty} (2g-1)(2g-2)^{p-1} \cdot D \cdot (2g-1) \frac{2^{5(p-1)+1}}{g^{2(p-1)}} \\
&\leq D \cdot (2g-1)^2 \cdot \sum_{p=1}^{\infty} \left((2g)^p \frac{2^{5(p-1)+3}}{g^{2(p-1)+1}} + (2g)^p \frac{2^{5p+1}}{g^{2p}}\right)
\end{aligned}$$

$$
\begin{aligned}
&= D \cdot (2g-1)^2 \cdot \sum_{p=1}^{\infty} \left(\frac{2^{6p-2}}{g^{p-1}} + \frac{2^{6p+1}}{g^p} \right) \\
&\leq D \cdot (2g-1)^2 \cdot \sum_{p=1}^{\infty} \frac{2^{6p+2}}{g^{p-1}} \\
&= 256 \cdot D \cdot (2g-1)^2 \cdot \frac{1}{1-\frac{64}{g}}.
\end{aligned}
$$

Therefore, there exists some constant $M > 0$ for large enough g, such that

$$
\begin{aligned}
\nu\left(\mathcal{H}_1^{\frac{2^{-n}}{\sqrt{\pi(g-1)}},\mathrm{thin}}(2g-2)\right) &\leq M \cdot (g-1)^2 \cdot \pi \cdot \left(\frac{2^{-n}}{\sqrt{\pi(g-1)}}\right)^2 \cdot \nu\left(\mathcal{H}_1(2g-2)\right) \\
&= 2^{-2n} \cdot M \cdot (g-1) \cdot \nu\left(\mathcal{H}_1(2g-2)\right). \qquad \square
\end{aligned}
$$

Proposition 8.2.6 (Small ε case)
For large enough genus g, there exists a constant M such that the expected value of the Cheeger constant h on $\tilde{\mathcal{H}} := \mathcal{H}_1^{\frac{1}{\sqrt{\pi(g-1)}},\mathrm{thin}}(2g-2)$ is bounded by

$$
\mathbb{E}_{\tilde{\mathcal{H}}}(h) \leq \frac{\nu\left(\mathcal{H}_1(2g-2)\right)}{\nu\left(\tilde{\mathcal{H}}\right)} \cdot 32 \cdot M \cdot (g-1)^{\frac{3}{2}}.
$$

Proof. The expected value is given by

$$
\mathbb{E}_{\tilde{\mathcal{H}}}(h) = \frac{1}{\nu\left(\tilde{\mathcal{H}}\right)} \int_{\tilde{\mathcal{H}}} h(X)\,\mathrm{d}\nu(X,\omega).
$$

This can be separated by Remark 8.2.3 into

$$
\mathbb{E}_{\tilde{\mathcal{H}}}(h) = \frac{1}{\nu\left(\tilde{\mathcal{H}}\right)} \sum_{n=0}^{\infty} \int_{U_n} h(X)\,\mathrm{d}\nu(X,\omega).
$$

A short calculation using Lemma 8.2.4 and Proposition 8.2.5 yields:

$$
\begin{aligned}
\mathbb{E}_{\tilde{\mathcal{H}}}(h) &= \frac{1}{\nu\left(\tilde{\mathcal{H}}\right)} \sum_{n=0}^{\infty} \int_{U_n} h(X)\,\mathrm{d}\nu(X,\omega) \\
&\leq \frac{1}{\nu\left(\tilde{\mathcal{H}}\right)} \sum_{n=0}^{\infty} \int_{U_n} 2^{n+3}\sqrt{\pi(g-1)}\,\mathrm{d}\nu(X,\omega) \\
&= \frac{1}{\nu\left(\tilde{\mathcal{H}}\right)} \sum_{n=0}^{\infty} 2^{n+3}\sqrt{\pi(g-1)} \cdot \nu\left(U_n\right) \\
&\leq \frac{1}{\nu\left(\tilde{\mathcal{H}}\right)} \sum_{n=0}^{\infty} 2^{n+3}\sqrt{\pi(g-1)} \cdot 2^{-2n} \cdot M \cdot (g-1) \cdot \nu\left(\mathcal{H}_1(2g-2)\right) \\
&= \frac{\nu\left(\mathcal{H}_1(2g-2)\right)}{\nu\left(\tilde{\mathcal{H}}\right)} \cdot \sum_{n=0}^{\infty} 2^{-n+3} \cdot \sqrt{\pi} \cdot M \cdot (g-1)^{\frac{3}{2}} \\
&\leq \frac{\nu\left(\mathcal{H}_1(2g-2)\right)}{\nu\left(\tilde{\mathcal{H}}\right)} \cdot 32 \cdot M \cdot (g-1)^{\frac{3}{2}}. \qquad \square
\end{aligned}
$$

Finally, we will show our bound on $\mathcal{H}_1^{\frac{1}{\sqrt{\pi(g-1)}},\text{thick}}$. For this, we first show that we can assume the restriction $\varepsilon < \frac{2}{\sqrt{\pi(2g-2)}}$.

Lemma 8.2.7 (Boundedness of ε)
In the large ε case, the thick part $\mathcal{H}_1^{\varepsilon,\text{thick}}(2g-2)$ is empty for $\varepsilon > \frac{2}{\sqrt{\pi(2g-2)}}$. So, in the thick part of our decomposition, $\varepsilon < \frac{2}{\sqrt{\pi(2g-2)}}$ holds.

Proof. Let $(X,\omega) \in \mathcal{H}(2g-2)$ be a translation surface from the large ε case, such that $\frac{1}{\sqrt{\pi(g-1)}} < \varepsilon$ and every saddle connection has at least length ε. Consider a Delaunay triangulation on the singularities of (X,ω). Each triangle has at least the area of an equilateral triangle of side length ε, so at least $\frac{\sqrt{3}}{4}\varepsilon^2$. For a genus g surface, a triangulation contains at least $4g-2$ triangles, therefore

$$1 = \operatorname{area}(X) \geq (4g-2)\frac{\sqrt{3}}{4}\varepsilon^2,$$

which implies

$$\varepsilon \leq \sqrt{\frac{2}{\sqrt{3}(2g-1)}} < \frac{2}{\sqrt{\pi(2g-2)}}. \qquad \square$$

This allows us to estimate h in the thick part.

Lemma 8.2.8 (Boundedness of h)
In the thick part of our decomposition $h \leq 24\pi\varepsilon(g-1)$ holds.

Proof. Let $(X,\omega) \in \mathcal{H}(2g-2)$ be a translation surface from the large ε case, such that $\frac{1}{\sqrt{\pi(g-1)}} < \varepsilon$ and every saddle connection has at least length ε. Using our bound for ε from the proof of Lemma 8.2.7 for a Delaunay triangulation on the singularities of (X,ω), we obtain

$$\begin{aligned}4-\pi\varepsilon^2(2g-2) &\geq 4-\pi\frac{2}{\sqrt{3}(2g-1)}(2g-2)\\ &= 4-\frac{2(2g-2)\pi}{\sqrt{3}(2g-1)}\\ &\geq 4-\frac{2\pi}{\sqrt{3}}\\ &\geq \frac{1}{3}.\end{aligned}$$

And therefore $h \leq \frac{4\pi\varepsilon(2g-2)}{4-\pi\varepsilon^2(2g-2)} \leq 24\pi\varepsilon(g-1)$. $\square$

Proposition 8.2.9 (Large ε case)
The expected value of the Cheeger constant h on $\tilde{\tilde{\mathcal{H}}} := \mathcal{H}_1^{\frac{1}{\sqrt{\pi(g-1)}},\text{thick}}(2g-2)$ is bounded by

$$\mathbb{E}_{\tilde{\tilde{\mathcal{H}}}}(h) \leq 24\sqrt{2\pi(g-1)}.$$

Proof. Let $(X, \omega) \in \tilde{\tilde{\mathcal{H}}}$. We can use Lemmas 8.2.7 and 8.2.8 to see that

$$h(X) \leq 24\pi\varepsilon(g-1) \leq 24\pi \frac{2}{\sqrt{\pi(2g-2)}}(g-1) = 24\sqrt{2\pi(g-1)}.$$

Hence

$$\mathbb{E}_{\tilde{\tilde{\mathcal{H}}}}(h) \leq 24\sqrt{2\pi(g-1)}. \qquad \square$$

Combining our estimates for the small and large ε case yields the following result.

Theorem 8.2.10 (Upper bound on the expected value of the geometric Cheeger constant in the minimal stratum)
There exists $\hat{g} \in \mathbb{N}^+$ and a constant $C > 0$, such that an upper bound for the expected value of the geometric Cheeger constant h in the minimal stratum for $g \geq \hat{g}$ is given by

$$\mathbb{E}_{\mathcal{H}_1(2g-2)}(h) \leq C g^{\frac{3}{2}}.$$

Proof. Let $\hat{g}$ be large enough, such that for $g > \hat{g}$ Propositions 8.2.6 and 8.2.9 holds. Then, we combine our result from Propositions 8.2.6 and 8.2.9, to obtain:

$$\begin{aligned}
\mathbb{E}_{\mathcal{H}_1(2g-2)}(h) &= \frac{\nu\left(\tilde{\mathcal{H}}\right)}{\nu\left(\mathcal{H}_1(2g-2)\right)} \mathbb{E}_{\tilde{\mathcal{H}}}(h) + \frac{\nu\left(\tilde{\tilde{\mathcal{H}}}\right)}{\nu\left(\mathcal{H}_1(2g-2)\right)} \mathbb{E}_{\tilde{\tilde{\mathcal{H}}}}(h) \\
&\leq 32 \cdot M \cdot (g-1)^{\frac{3}{2}} + 24\sqrt{2\pi(g-1)}.
\end{aligned} \qquad \square$$

This works exceptional well since on the translation surface, we have one single singularity giving us a lot of "space" around it to work with. To extend this result to the worst case of surfaces from the principal stratum is not straight forward. One approach to this problem is changing the Cheeger constant to be more adapted to the known results by [EMZ03].

9 Geotopological Cheeger constant

For the principal stratum, calculation of the geometric Cheeger constant is very hard. Since all strata can be obtained by collapsing singularities of the principal stratum, the principal stratum contains the most generic surfaces of any stratum. Since we fix the area to 1, the density of singularities increase arbitrarily high for growing genus. We therefore struggle to calculate the geometric Cheeger constant. However, the progress through Eskin–Masur–Zorich gives hope to tackle a slightly different problem, a topological variant of the geometric Cheeger constant.

To develop this variant of the geometric Cheeger constant, which we will call the geotopological Cheeger constant, we do not use the conventional approach of dividing by the minimum of surface areas on either side. Instead, we use the notion of separating complexity, which in our case involves splitting the surface based upon its genus. Then we minimize the length of separating curves for all possible genus separations. This geotopological approach is aptly named, as the denominator reflects topological properties while the numerator remains anchored in geometry.

Definition 9.0.1 (Geotopological Cheeger constant)
Let (X, ω) be a translation surface in $\mathcal{H}_1(\kappa)$ of genus g. For $m \in \{1, \ldots, g-1\}$, let $\mathcal{B}_m$ be the set of all closed curves connecting two distinct singularities consisting of two homologous saddle connections separating (X, ω) with genus m on one of the resulting surface and genus $g-m$ on the other surface. Encode this configuration by $\mathcal{C}_m$ for saddle connections of multiplicity 2.

After separating the surface as in Construction 7.3.11, we obtain $(X_1, \omega_1) \in \mathcal{H}(\kappa_1)$ and $(X_2, \omega_2) \in \mathcal{H}(\kappa_2)$, such that $\sum_{k_i \in \kappa_1} k_i = 2m - 2$ and $\sum_{k_i \in \kappa_2} k_i = 2g - 2m - 2$.

For $m \in \{1, \ldots, g-1\}$, let

$$h_m^\top(X) \coloneqq \inf_{\gamma \in \mathcal{B}_m} \frac{\operatorname{length}(\gamma)}{\frac{\min\{m, g-m\}}{g}}$$

denote the *genus m geotopological Cheeger constant*. Furthermore, we define

$$h^\top(X) \coloneqq \min_{m \in \{1, \ldots, g-1\}} h_m^\top(X) = \min_{m \in \left\{1, \ldots, \left\lfloor \frac{g}{2} \right\rfloor\right\}} h_m^\top(X)$$

as the *geotopological Cheeger constant*.

Remark 9.0.2 (Area approximation)
In selecting $\frac{m}{g}$ as the denominator for $h_m^\top$, we aim to mirror the role of area in the conventional geometric Cheeger constant, if we assume a uniform distribution of genus

across the surface. We divide by g to ensure that it is comparable to the classical Cheeger constant with unit area surfaces.

The infimum in the definition of the genus m geotopological Cheeger constant is a minimum since $\mathcal{B}_m$ is restricted to curves made of saddle connections.

We will control the geotopological Cheeger constant $h^\top$ on the thick and thin part separately. On the thick part, it is enough to consider geometric ideas like the Delaunay triangulation to yield an upper bound. We further must separate the thin part, such that its influence on the expected value of $h^\top$ can be controlled on each set separately.

We also want to give one short insight, that almost all saddle connections of a large-genus surface $(X, \omega) \in \mathcal{H}_1(\kappa)$ are longer than $\frac{1}{g}$ and we therefore have to choose our cutoff $\varepsilon(\kappa) > \frac{1}{g}$, this will be needed later to get the asymptotic of the geotopological Cheeger constant solely in terms of g. To show this, we need the following asymptotic formula:

Lemma 9.0.3 (Siegel–Veech constant for $p = 1$)
There exists a constant $D > 0$ such that for any integer $g > 2$, we get

$$\left| c\left((1^{2g-2}), \mathcal{C}'\right) - 4(2g-2)(2g-3) \right| \leq \frac{2D(2g-2)(2g-3)}{g},$$

where $\mathcal{C}'$ is the configuration $(1, 1, (1), (1))$ corresponding to a saddle connection connecting two singularities.

Proof. We get this formula by summing up all possible combinations of pairs of singularities connecting two different singularities of $\mathcal{H}_1(1^{2g-2})$ over the formula from Theorem 1.2 of [Agg19] and dividing by 2 since we ignore the orientation. □

Lemma 9.0.4 (On the average length of saddle connections)
For large genus g, on most translation surfaces $(X, \omega) \in \mathcal{H}_1(1^{2g-2})$, all saddle connections are longer than or equal to $\frac{1}{g}$.

Proof. Combining Corollary 7.2.11 and Lemma 9.0.3 yields some $D > 0$, such that:

$$\begin{aligned}\frac{1}{\nu\left(\mathcal{H}_1\left(1^{2g-2}\right)\right)} \int_{\mathcal{H}_1(1^{2g-2})} |V_{\mathcal{C}'}(X, \varepsilon)| \ \mathrm{d}\nu(X) &= c\left((1^{2g-2}), \mathcal{C}'\right) \pi\varepsilon^2 \\ &= \left[4(2g-2)(2g-3) \pm \frac{4D(2g-2)(2g-3)}{g}\right] \pi\varepsilon^2.\end{aligned}$$

By choosing $\varepsilon = g^{-1-\eta}$ for any $\eta > 0$, we get:

$$\frac{1}{\nu\left(\mathcal{H}_1\left(1^{2g-2}\right)\right)} \int_{\mathcal{H}_1(1^{2g-2})} |V_{\mathrm{sc}}(X, \varepsilon)| \ \mathrm{d}\nu(X) = \mathcal{O}\left(g^{-2\eta}\right) \xrightarrow{g \to \infty} 0.$$

The saddle connections without loops dominate those coming from loops. So, the average count of saddle connections $|V_{\mathrm{sc}}(X, \varepsilon)|$ converges to 0 on $\mathcal{H}_1(1^{2g-2})$ for $g \to \infty$. For $\eta \to 0$, we see that saddle connections of length smaller than $\frac{1}{g}$ are rare. □

Remark 9.0.5 (The length $\frac{1}{\sqrt{g}}$ is already common)
Saddle connections with length $\frac{1}{\sqrt{g}}$ in $\mathcal{H}_1(1^{2g-2})$ are already common. We can see this by reevaluating the right hand side in the proof of Lemma 9.0.4.

9.1 Thick part

In this section, we look at the thick part of our thin-thick decomposition and primarily utilize geometric reasoning to derive an upper bound for the expected value of the Cheeger constant in the thick part. This approach is enabled by the fact that all saddle connections between singularities possess a minimum length in the thick part.

Proposition 9.1.1 (Upper bound on the expected value of the geotopological Cheeger constant in the thick part)
For $\varepsilon > 0$, the expected value of the geotopological Cheeger constant on the thick part of the principal stratum has an upper bound

$$\mathbb{E}_{\mathcal{H}_1^{\varepsilon,\text{thick}}(1^{2g-2})}\left(h^\top\right) \leq \frac{1024}{3\sqrt{3}}\frac{g}{\varepsilon}.$$

Proof. Let $(X,\omega) \in \mathcal{H}_1^{\varepsilon,\text{thick}}(1^{2g-2})$. For $m \in \left\{1,\dots,\left\lfloor\frac{g}{2}\right\rfloor\right\}$, let $\tilde{\gamma}_m$ be the minimal curve as in Definition 9.0.1, so it consists of two saddle connections connecting two singularities. Now consider a Delaunay triangulation Δ with the singularities of (X,ω) as the vertices. We have $\tilde{\gamma}_m = \tilde{\gamma}_{m,1} \cup \tilde{\gamma}_{m,2}$ with $\tilde{\gamma}_{m,1}, \tilde{\gamma}_{m,2}$ being two saddle connections connecting the singularities p_1 with p_2 and p_2 with p_1. Define a chain of saddle connections γ_m starting in p_1 through p_2 and finishing in p_1 such that it only consists of edges of Δ. A Delaunay triangulation of a surface in $\mathcal{H}(1^{2g-2})$ has exactly $8g-8$ triangles. The curve γ_m separates $\overline{X}$ into two different subsurfaces X_1 and X_2, triangulated by also at most $8g-8$ triangles.

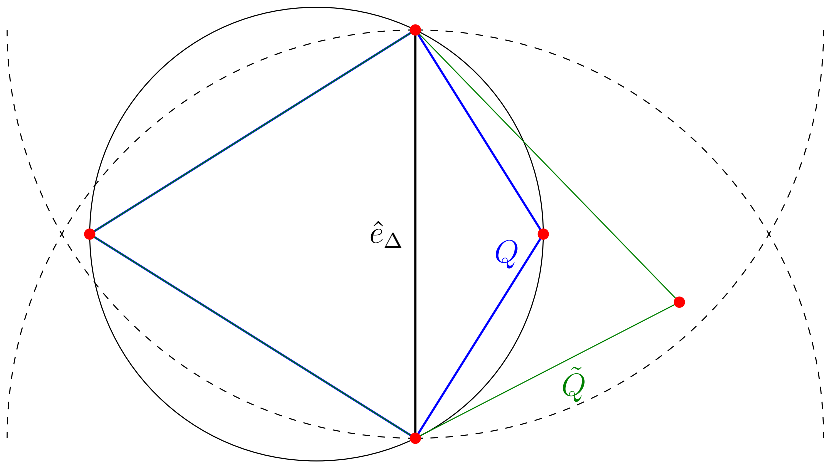

Figure 9.1: Construction of Q

Let $\hat{e}_\Delta$ be the longest edge in Δ. Consider the two triangles adjacent to $\hat{e}_\Delta$ and let $\tilde{Q}$ be the union of those two triangles. Since Δ is Delaunay, the circumscribed circle around an adjacent triangle T does not contain any other singularity. Choose a new quadrilateral Q inside of $\tilde{Q}$, such that it contains the corners of T as its corners and another corner on the circle that inscribes T on the opposite side of T according to $\hat{e}_\Delta$, such that $T \subseteq Q \subseteq \tilde{Q}$.

Choose it in such a way, that the new edge lengths in Q are at least half the length of the corresponding old edge lengths in $\tilde{Q}$. This is always possible since the old corner of $\tilde{Q}$ not in T has to be inside the intersection of the circles around the endpoints of $\hat{e}_\Delta$ with radius $\operatorname{length}(\hat{e}_\Delta)$ because Δ is Delaunay and every edge length is at most $\operatorname{length}(\hat{e}_\Delta)$. Since both triangles in Q with $\hat{e}_\Delta$ as one of their sides fulfill the triangle inequality, at least one other side in both triangles has to be of side length greater than or equal to $\frac{\operatorname{length}(\hat{e}_\Delta)}{2}$. Since (X,ω) is an element of the thick part, every side of $\tilde{Q}$ also has a length of at least ε and the two new edges in Q have at least side length $\frac{\varepsilon}{2}$.

The radius R of the circumscribed circle around Q fulfills the bound $R \leq \frac{\operatorname{length}(\hat{e}_\Delta)}{\sqrt{3}}$. This is because the sides adjacent to $\hat{e}_\Delta$ have at most a length of $\operatorname{length}(\hat{e}_\Delta)$.

We know the area of Q has an upper bound of 1 and therefore by the area formula for inscribed quadrilateral we get

$$1 \geq \operatorname{area}(Q) \geq \frac{\operatorname{length}(\hat{e}_\Delta) \cdot \left(\frac{\operatorname{length}(\hat{e}_\Delta)}{2} \cdot \varepsilon + \frac{\operatorname{length}(\hat{e}_\Delta)}{2} \cdot \frac{\varepsilon}{2}\right)}{4R} \geq \frac{3\sqrt{3}}{16} \cdot \operatorname{length}(\hat{e}_\Delta) \cdot \varepsilon,$$

if the sides with a length of at least $\frac{\operatorname{length}(\hat{e}_\Delta)}{2}$ are opposite to each other. If they are next to each other, we get:

$$1 \geq \operatorname{area}(Q) \geq \frac{\operatorname{length}(\hat{e}_\Delta) \cdot \left(\left(\frac{\operatorname{length}(\hat{e}_\Delta)}{2}\right)^2 + \frac{\varepsilon^2}{2}\right)}{4R},$$

so

$$\operatorname{length}(\hat{e}_\Delta) \leq \sqrt{\frac{16}{\sqrt{3}} - 2\varepsilon^2},$$

which is for small ε smaller than the first bound. So, without loss of generality, assume the worse situation, in which case $\operatorname{length}(\hat{e}_\Delta) \leq \frac{16}{3\sqrt{3}\varepsilon}$.

A connected surface consisting of n triangles has at most $n+2$ edges on its boundary. The length of γ_m is therefore bounded by

$$\begin{aligned}\operatorname{length}(\gamma_m) &\leq 2(8g-6)\operatorname{length}(\hat{e}_\Delta)\\ &\leq \frac{256}{3\sqrt{3}}\frac{g}{\varepsilon}.\end{aligned}$$

Therefore for $m = \left\lfloor \frac{g}{2} \right\rfloor \geq \frac{g}{4}$:

$$\begin{aligned}h^\top(X) \leq h_m^\top(X) &\leq \frac{\operatorname{length}(\gamma_m)g}{m}\\ &\leq \frac{1024}{3\sqrt{3}}\frac{g}{\varepsilon}.\end{aligned}$$

The proposition holds, since $h^\top$ is uniformly bounded for every $(X,\omega) \in \mathcal{H}_1^{\varepsilon,\text{thick}}(1^{2g-2})$. $\square$

9.2 Thin part

In this section, we subdivide the thin part into multiple parts in such a way, that we can use the results of the previous section.

Proposition 9.2.1 (Volume bounds)
Let $g \geq 3$ and $g > g_1 \in \mathbb{N}^+$. For the configuration $\mathcal{C}_{g_1}$ from Definition 9.0.1, which corresponds to the decomposition of a surface $(X, \omega) \in \mathcal{H}_1^{\varepsilon,\text{thin}}(1^{2g-2})$ into $(X_1, \omega_1) \in \mathcal{H}(1^{2g_1-2})$ and $(X_2, \omega_2) \in \mathcal{H}(1^{2g_2-2})$ with $g_1 + g_2 = g$ and $1 \leq g_1 \leq g_2$. Then for $\varepsilon > 0$:

$$\begin{aligned}
\nu\left(\mathcal{H}_1^{\varepsilon,\text{thin}}(1^{2g-2}, \mathcal{C}_{g_1})\right) &\leq \frac{64\,(2g-2)!\,(4g_1-4)!\,(4g_2-4)!}{(2g_1-2)!\,(2g_2-2)!\,(4g-4)! \cdot 4^g} \cdot \pi\varepsilon^2 \\
&\quad \cdot \left(1 + \frac{2^{2^{200}}}{g_1}\right)\left(1 + \frac{2^{2^{200}}}{g_2}\right) + o\left(\varepsilon^2\right), \\
\nu\left(\mathcal{H}_1^{\varepsilon,\text{thin}}(1^{2g-2}, \mathcal{C}_{g_1})\right) &\geq \frac{32\,(2g-2)!\,(4g_1-4)!\,(4g_2-4)!}{(2g_1-2)!\,(2g_2-2)!\,(4g-4)! \cdot 4^g} \cdot \pi\varepsilon^2 \\
&\quad \cdot \left(1 - \frac{2^{2^{200}}}{g_1}\right)\left(1 - \frac{2^{2^{200}}}{g_2}\right) + o\left(\varepsilon^2\right).
\end{aligned}$$

Proof. We are in the setting of Lemma 7.3.20. There is only a $\gamma \to -\gamma$ symmetry if $g_1 = g_2$, so $|\Gamma_-| \cdot |\Gamma_+| \in \{2, 4\}$.

Since this is only a constant factor, we will just use the worst case for $|\Gamma_-|$ in all calculations, so $|\Gamma_-| = 1$ for the upper and $|\Gamma_-| = 2$ for the lower bound.

We separate $\kappa = (1^{2g-2})$ in $p = 2$ components with $\kappa_1 = (1^{2g_1-2})$ and $\kappa_2 = (1^{2g_2-2})$ and therefore $\text{soo}(1) = 2g - 2$ and $\text{soo}_i(1) = 2g_i - 2$. The singularities of the configuration are only marked points z_1, z_2 after degeneration and therefore $a_1 = a_2 = 0$. The real dimension of $\mathcal{H}(1^{2g_i-2})$ is $8g_i - 6$. The real dimension of $\mathcal{H}_1(1^{2g-2})$ is $8g - 6$. Because of Lemma 7.3.20, we get:

$$\begin{aligned}
\nu\left(\mathcal{H}_1^{\varepsilon,\text{thin}}(1^{2g-2}, \mathcal{C}_{g_1})\right) &= \frac{\prod_{i=1}^p (a_i + 1)}{|\Gamma_-| \cdot |\Gamma_+|} \cdot \prod_{k \in \kappa} \left(\frac{\text{soo}(k)!}{\prod_{i=1}^p \text{soo}_i(k)!}\right) \cdot \prod_{\substack{i=1 \\ a_i \neq 0}}^p \text{soo}_i(a_i) \\
&\quad \cdot \frac{1}{2^{p-1}} \cdot \frac{\prod_{i=1}^p \left(\frac{d_i}{2} - 1\right)!}{\left(\frac{d}{2} - 1\right)!} \cdot \prod_{i=1}^p \nu\left(\mathcal{H}_1\left(\kappa_i\right)\right) \cdot \pi\varepsilon^2 + o\left(\varepsilon^2\right) \\
&\leq \frac{1}{2} \cdot \frac{(2g-2)!}{(2g_1-2)!\,(2g_2-2)!} \cdot 1 \cdot \frac{1}{2} \cdot \frac{(4g_1-4)!\,(4g_2-4)!}{(4g-4)!} \\
&\quad \cdot \nu\left(\mathcal{H}_1\left(1^{2g_1-2}\right)\right) \cdot \nu\left(\mathcal{H}_1\left(1^{2g_2-2}\right)\right) \cdot \pi\varepsilon^2 + o\left(\varepsilon^2\right) \\
&= \frac{(2g-2)!\,(4g_1-4)!\,(4g_2-4)!}{4\,(2g_1-2)!\,(2g_2-2)!\,(4g-4)!} \\
&\quad \cdot \nu\left(\mathcal{H}_1\left(1^{2g_1-2}\right)\right) \cdot \nu\left(\mathcal{H}_1\left(1^{2g_2-2}\right)\right) \cdot \pi\varepsilon^2 + o\left(\varepsilon^2\right).
\end{aligned}$$

And analogously

$$\nu\left(\mathcal{H}_1^{\varepsilon,\text{thin}}(1^{2g-2},\mathcal{C}_{g_1})\right) \geq \frac{(2g-2)!\,(4g_1-4)!\,(4g_2-4)!}{8\,(2g_1-2)!\,(2g_2-2)!\,(4g-4)!} \cdot \nu\left(\mathcal{H}_1\left(1^{2g_1-2}\right)\right)\cdot\nu\left(\mathcal{H}_1\left(1^{2g_2-2}\right)\right)\cdot \pi\varepsilon^2 + o\left(\varepsilon^2\right).$$

Using Theorem 7.1.10, we get this proposition. □

The problem with calculating the geotopological Cheeger constant now, is that the Cheeger constant can still explode if we have short saddle connections as seen in Proposition 8.1.7. Even after fixing the length for the first short saddle connection, we still encounter the same difficulties for the second, third, and so on short saddle connection. That is why we need to show the following proposition.

Proposition 9.2.2 (Thin-thick dominates)
Let $g \geq 3$ and $g > g_1 \in \mathbb{N}^+$. Let $\mathcal{C}$ be the configuration encoding any short saddle connection. For g big enough, for all $\delta > 0$, there exists $\varepsilon \leq \frac{1}{g^{1+\delta}}$, such that:

$$\frac{1}{2}\nu\left(\mathcal{H}_1^{\varepsilon,\text{thin-thick}}(1^{2g-2},\mathcal{C})\right) \leq \nu\left(\mathcal{H}_1^{\varepsilon,\text{thin}}(1^{2g-2},\mathcal{C})\right) \leq 2\nu\left(\mathcal{H}_1^{\varepsilon,\text{thin-thick}}(1^{2g-2},\mathcal{C})\right).$$

Proof. We want to show, that

$$\nu\left(\mathcal{H}_1^{\varepsilon,\text{thin-thin}}(1^{2g-2},\mathcal{C})\right) \leq \nu\left(\mathcal{H}_1^{\varepsilon,\text{thin-thick}}(1^{2g-2},\mathcal{C})\right).$$

Then the second inequality is true, since

$$\begin{aligned}\nu\left(\mathcal{H}_1^{\varepsilon,\text{thin}}(1^{2g-2},\mathcal{C})\right) &= \nu\left(\mathcal{H}_1^{\varepsilon,\text{thin-thick}}(1^{2g-2},\mathcal{C})\right) + \nu\left(\mathcal{H}_1^{\varepsilon,\text{thin-thin}}(1^{2g-2},\mathcal{C})\right)\\ &\leq 2\nu\left(\mathcal{H}_1^{\varepsilon,\text{thin-thick}}(1^{2g-2},\mathcal{C})\right)\end{aligned}$$

and the first inequality is trivially true. To show that the thin-thick part dominates the thin-thin part for $\varepsilon \leq \frac{1}{g^{1+\delta}}$ for all $\delta > 0$, let us compute a lower bound for the thin-thick and an upper bound for the thin-thin part.

We begin by calculating the lower bound. Let (X,ω) be a translation surface from the thin-thick part $\mathcal{H}_1^{\varepsilon,\text{thin-thick}}(1^{2g-2},\mathcal{C})$. We can collapse the two singularities from $\mathcal{C}$ and obtain a surface (X',ω') from $\mathcal{H}_1(2,1^{2g-4})$. Using Theorem 7.1.10, we see that there exists some $M' > 0$, such that for large enough g:

$$\nu\left(\mathcal{H}_1(2,1^{2g-4})\right) \geq M'\cdot\nu\left(\mathcal{H}_1(1^{2g-2})\right).$$

This can be done for example for $M' = \frac{4}{9}$ with $g \geq 2\cdot 2^{2^{200}}$. Since we do not want to fix the singularities in $\mathcal{C}$, using Lemma 7.3.20 we obtain some constant $M'' > 0$, independent of ε and g, such that

$$\nu\left(\mathcal{H}_1^{\varepsilon,\text{thin-thick}}(1^{2g-2},\mathcal{C})\right) = \frac{\prod_{i=1}^{p}(a_i+1)}{|\Gamma_-|\cdot|\Gamma_+|}\cdot\prod_{k\in\kappa}\left(\frac{\mathrm{soo}(k)!}{\prod_{i=1}^{p}\mathrm{soo}_i(k)!}\right)\cdot\prod_{\substack{i=1\\a_i\neq 0}}^{p}\mathrm{soo}_i(a_i)$$

$$
\begin{aligned}
&\cdot \frac{1}{2^{p-1}} \cdot \frac{\prod_{i=1}^{p}\left(\frac{d_i}{2}-1\right)!}{\left(\frac{d}{2}-1\right)!} \cdot \prod_{i=1}^{p} \nu\left(\mathcal{H}_1\left(\kappa_i\right)\right) \cdot \pi\varepsilon^2 + o\left(\varepsilon^2\right)\\
&\geq \frac{1}{2\cdot 2} \cdot \left(\frac{(2g-2)!}{(2g-4)!}\right) \cdot 1 \cdot 1 \cdot 1 \cdot \nu\left(\mathcal{H}_1\left(2, 1^{2g-4}\right)\right) \cdot \pi\varepsilon^2 + o\left(\varepsilon^2\right)\\
&= \frac{1}{4} \cdot (2g-2)(2g-3) \cdot \nu\left(\mathcal{H}_1\left(2, 1^{2g-4}\right)\right) \cdot \pi\varepsilon^2 + o\left(\varepsilon^2\right)\\
&\geq M'' \cdot g^2\varepsilon^2 \cdot \nu\left(\mathcal{H}_1(1^{2g-2})\right)
\end{aligned}
$$

for large enough g.

Let us now consider an upper bound for the thin-thin part. For the thin-thin part, there are multiple ways how these at least two families of short homologous saddle connections of different multiplicity can be arranged. In the principal stratum, saddle connections of multiplicity 3 cannot occur because the total angle around each singularity is at most 4π. So, each saddle connection can have at most multiplicity 2.

For multiplicity 2 we have a pair of homologous saddle connections joining a pair of distinct singularities. Let us denote the set of these surfaces by $\mathcal{H}_{\text{mult-2}} \subseteq \mathcal{H}_1^{\varepsilon,\text{thin-thin}}(1^{2g-2})$. Since all singularities have degree 1, they need to be distinct. If we fix the pair of singularities, we can use a Siegel–Veech type argument: Using Proposition 3.4 from the appendix of [Agg19], we get a constant A', such that the Siegel–Veech constant for this configuration $\mathcal{C}_{1,1}^2$ is bounded by

$$
c\left(\mathcal{H}_{\text{mult-2}}\right) = c\left(\mathcal{H}_1(1^{2g-2}), \mathcal{C}_{1,1}^2\right) \leq \frac{A'}{g^2}.
$$

So, for arbitrary singularities, we can choose $\frac{1}{2}(2g-2)(2g-3)$ pairs of singularities again and use the recursion formula from Proposition 7.3.19 to see, that there exists some constant $A'' > 0$, such that

$$
\nu\left(\mathcal{H}_{\text{mult-2}}\right) \leq \frac{A''}{g^2}(2g-2)(2g-3)\varepsilon^2 \cdot \nu\left(\mathcal{H}_1(2, 1^{2g-4})\right).
$$

Using Theorem 7.1.10, we can estimate $\nu\left(\mathcal{H}_1(2, 1^{2g-4})\right)$ with $\nu\left(\mathcal{H}_1(1^{2g-2})\right)$ and there exists some constant A, independent of ε and g, such that

$$
\nu\left(\mathcal{H}_{\text{mult-2}}\right) \leq A \cdot \varepsilon^2 \cdot \nu\left(\mathcal{H}_1(1^{2g-2})\right)
$$

for large enough g.

So, we now can only consider saddle connections of multiplicity 1. Consider the most generic case, where we have two saddle connections, where the collapsing procedures of Construction 7.3.4 do not interfere with each other. Let us denote the set of these surfaces by $\mathcal{H}_{\text{gen}} \subseteq \mathcal{H}_1^{\varepsilon,\text{thin-thin}}(1^{2g-2})$. We can collapse these two saddle connections one after another independently. After collapsing the two non-homologous short saddle connections, we obtain a surface (X', ω') from $\mathcal{H}_1(2, 2, 1^{2g-6})$. Using Theorem 7.1.10, there exists some constant $\tilde{M}$, such that

$$
\nu\left(\mathcal{H}_1(2, 2, 1^{2g-2})\right) \leq \tilde{M} \cdot \nu\left(\mathcal{H}_1(1^{2g-2})\right).
$$

Using Construction 7.3.13 we obtain maps

$$\mathcal{H}_{\text{gen}} \to \mathcal{H}_1^{\varepsilon,\text{thin}}\left(2, 1^{2g-4}\right) \times \overline{B}_\varepsilon(0) \to \mathcal{H}_1\left(2, 2, 1^{2g-6}\right) \times \overline{B}_\varepsilon(0) \times \overline{B}_\varepsilon(0)$$

being a volume preserving covering of degree $(2g-2)(2g-3)\frac{3}{2}$ for the first map and a volume preserving covering of degree $(2g-4)(2g-5)\cdot\frac{3}{2}$ for the second map. We therefore obtain some constant $B > 0$, independent of ε and g, such that

$$\nu\left(\mathcal{H}_{\text{gen}}\right) \leq B \cdot g^4 \varepsilon^4 \cdot \nu\left(\mathcal{H}_1(1^{2g-2})\right)$$

for large enough g. For $\varepsilon \leq \frac{1}{g^{1+\delta}}$, this will be just enough to show this statement, as we will see in the end of the proof.

However, we still have to control the other cases. If the two saddle connections share one singularity, then either the saddle connections and the extensions from Construction 7.3.7 never intersect and we can actually perform Construction 7.3.7 or not.

Let us first consider the case, where we can perform the collapsing and denote these surfaces by $\mathcal{H}_{\text{coll-3}}$. For $(X, \omega) \in \mathcal{H}_{\text{coll-3}}$, we can collapse both saddle connections simultaneously and obtain the covering

$$\mathcal{H}_{\text{coll-3}} \to \mathcal{H}_1\left(3, 1^{2g-5}\right) \times \overline{B}_\varepsilon(0) \times \overline{B}_\varepsilon(0)$$

of degree $(2g-2)(2g-3)(2g-4)\frac{4}{2}$. Therefore with Theorem 7.1.10, there exists some constant $C > 0$, independent of ε and g, such that

$$\nu\left(\mathcal{H}_{\text{coll-3}}\right) \leq C \cdot g^3 \varepsilon^4 \cdot \nu\left(\mathcal{H}_1(1^{2g-2})\right)$$

for large enough g.

However, sometimes the saddle connections and their one-sided extension will intersect. There are three types of intersections possible, see Figure 9.2. If they intersect like in Figure 9.2a, we know there exists some closed chain of saddle connections of length $\leq 2\varepsilon$. If they intersect like in Figure 9.2b, analogously we know there exists some closed chain of saddle connections of length $\leq 3\varepsilon$. For the last intersection pattern Figure 9.2c, we get a chain of saddle connections of length $\leq 4\varepsilon$.

In all of these cases, take the shortest saddle connection from the loop, all other saddle connections shall be longer. We can ignore the case, where there are multiple shortest saddle connections, since they will contribute a set of measure 0. Also the chain of saddle connections shall contain at least three saddle connections. We can ignore the case, where there are only two saddle connections, since these saddle connections, then will need to have the same direction and contribute a set of measure 0 again. If there is only one saddle connection in the chain, we have a loop connecting a singularity of degree 1 to itself.

Let us denote the set of surfaces with a saddle connection in a loop by $\mathcal{H}_{\text{loop}}$. Similar arguments as in Proposition 8.2.5 show that the growth of the corresponding Siegel–Veech constant with multiplicity $p = 1$ dominates. So we can use Corollary 5 from the appendix

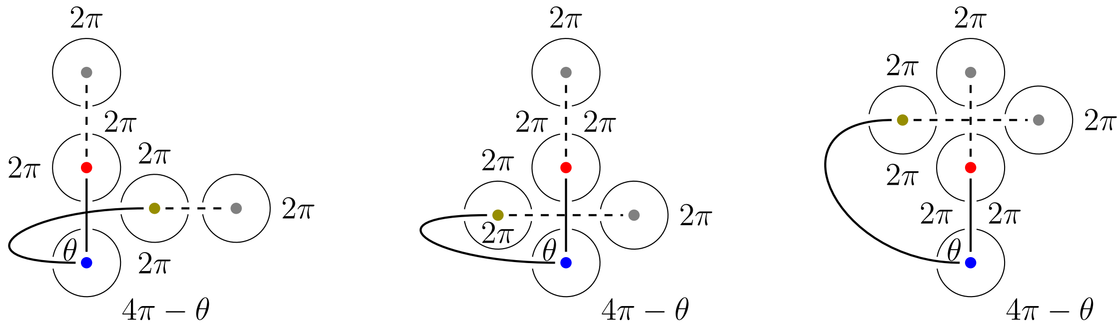

(a) Two saddle connections (b) A saddle connection and an extension (c) Two extensions

Figure 9.2: Construction 7.3.7 prohibited by different intersection patterns

of [Agg20] and get a Siegel–Veech constant in this kind of problem which is at most constant for each of the $2g-2$ singularities. Summing over these $2g-2$ singularities, there exists some constant $D > 0$, independent of ε and g, such that

$$\nu\left(\mathcal{H}_{\text{loop}}\right) \leq D \cdot g\varepsilon^2 \cdot \nu\left(\mathcal{H}_1(1^{2g-2})\right)$$

for large enough g.

Let us denote the set of surfaces with a chain of at least three saddle connections in a loop of which one saddle connection is the smallest one by $\mathcal{H}_{\text{chain}}$. We can now collapse the unique shortest saddle connection from our chain and obtain the covering

$$\mathcal{H}_{\text{chain}} \to \mathcal{H}_1^{\varepsilon,\text{thin}}\left(2, 1^{2g-4}\right) \times \overline{B}_\varepsilon(0)$$

of degree $(2g-2)(2g-3)\frac{3}{2}$. Furthermore, after collapsing, we have one saddle connection of length $\leq 4\varepsilon$ next to our singularity of order 2. Using Corollary 1 from the appendix of [Agg20] for the Siegel–Veech constant in Proposition 7.2.19 shows there exists some constant $E' > 0$, such that

$$\frac{\mathcal{H}_1^{\varepsilon,\text{thin}}\left(2, 1^{2g-4}\right)}{\mathcal{H}_1\left(2, 1^{2g-4}\right)} \leq E'(2g-4)\varepsilon^2,$$

since we can choose from $2g-4$ different singularities of order 1 in this construction. Therefore with Theorem 7.1.10, there exists some constant $E > 0$, independent of ε and g, such that

$$\nu\left(\mathcal{H}_{\text{chain}}\right) \leq E \cdot g^2\varepsilon^2 \cdot g\varepsilon^2 \cdot \nu\left(\mathcal{H}_1(1^{2g-2})\right) = E \cdot g^3\varepsilon^4 \cdot \nu\left(\mathcal{H}_1(1^{2g-2})\right)$$

for large enough g.

The last remaining case to consider is where we have two saddle connections that interfere with each other and do not share a singularity. Similar to the intersection types for Construction 7.3.7 from before, there are again three types of intersection possible, see Figure 9.3.

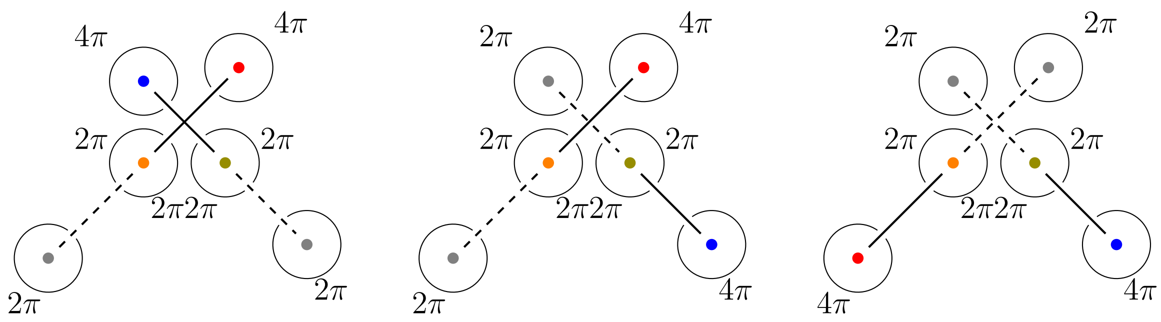

(a) Two saddle connections (b) A saddle connection and an extension (c) Two extensions

Figure 9.3: One-sided Construction 7.3.4 prohibited by different intersection patterns

We can consider a saddle connection of length $\leq 2\varepsilon$ connecting one singularity from the first saddle connection to a singularity of the other saddle connection. Therefore our surface will be from $\mathcal{H}_{\text{gen}}^{2\varepsilon}$ and we can use the same arguments from before with 2ε instead of ε.

The statement

$$\nu\left(\mathcal{H}_1^{\varepsilon,\text{thin-thin}}(1^{2g-2},\mathcal{C})\right) \leq \nu\left(\mathcal{H}_1^{\varepsilon,\text{thin-thick}}(1^{2g-2},\mathcal{C})\right)$$

is now true, if

$$A\cdot\varepsilon^2 \leq g^2\varepsilon^2,\; B\cdot g^4\varepsilon^4 \leq g^2\varepsilon^2,\; C\cdot g^3\varepsilon^4 \leq g^2\varepsilon^2,\; D\cdot g\varepsilon^2 \leq g^2\varepsilon^2 \text{ and } E\cdot g^3\varepsilon^4 \leq g^2\varepsilon^2.$$

This is the case for large enough g, for any $\delta > 0$, when $\varepsilon \leq \frac{1}{g^{1+\delta}}$. □

The proof of Proposition 9.2.2 was made possible by the invaluable ideas coming from the discussions with Kasra Rafi.

Corollary 9.2.3 (Upper and lower volume bound of the thin part)
There exists $c \in \mathbb{R}$, $\hat{g} \in \mathbb{N}^+$, such that for $g \geq \hat{g}$ and configuration $\mathcal{C}_{g_1}$ from Definition 9.0.1, which corresponds to the decomposition of a translation surface $(X,\omega) \in \mathcal{H}_1^{\varepsilon,\text{thin}}(1^{2g-2})$ into $(X_1,\omega_1) \in \mathcal{H}(1^{2g_1-2})$ and $(X_2,\omega_2) \in \mathcal{H}(1^{2g_2-2})$ with $g_1+g_2 = g$ and $g_1 = \left\lfloor \frac{g}{2} \right\rfloor$, the following holds for $\varepsilon \leq \frac{1}{g^{1+\delta}}$ for every $\delta > 0$:

$$\nu\left(\mathcal{H}_1^{\varepsilon,\text{thin}}(1^{2g-2},\mathcal{C}_{g_1})\right) \leq \frac{288\,(2g-2)!\,(4g_1-4)!\,(4g_2-4)!}{(2g_1-2)!\,(2g_2-2)!\,(4g-4)!\cdot 4^g}\cdot\pi\varepsilon^2,$$
$$\nu\left(\mathcal{H}_1^{\varepsilon,\text{thin}}(1^{2g-2},\mathcal{C}_{g_1})\right) \geq \frac{4\,(2g-2)!\,(4g_1-4)!\,(4g_2-4)!}{(2g_1-2)!\,(2g_2-2)!\,(4g-4)!\cdot 4^g}\cdot\pi\varepsilon^2.$$

Proof. With $\varepsilon = \frac{1}{g^{1+\delta}}$ and for large enough $g > \tilde{g}$, ε is small enough such that Proposition 9.2.2 holds. Therefore we can use Proposition 9.2.1 with an additional factor of 2 for the upper and $\frac{1}{2}$ for the lower bounds:

$$\begin{aligned}
\nu\left(\mathcal{H}_1^{\varepsilon,\text{thin}}(1^{2g-2},\mathcal{C}_{g_1})\right) &\leq \frac{128\,(2g-2)!\,(4g_1-4)!\,(4g_2-4)!}{(2g_1-2)!\,(2g_2-2)!\,(4g-4)!\cdot 4^g}\cdot \pi\varepsilon^2 \\
&\quad \cdot \left(1+\frac{2^{2^{200}}}{g_1}\right)\left(1+\frac{2^{2^{200}}}{g_2}\right), \\
\nu\left(\mathcal{H}_1^{\varepsilon,\text{thin}}(1^{2g-2},\mathcal{C}_{g_1})\right) &\geq \frac{16\,(2g-2)!\,(4g_1-4)!\,(4g_2-4)!}{(2g_1-2)!\,(2g_2-2)!\,(4g-4)!\cdot 4^g}\cdot \pi\varepsilon^2 \\
&\quad \cdot \left(1-\frac{2^{2^{200}}}{g_1}\right)\left(1-\frac{2^{2^{200}}}{g_2}\right).
\end{aligned}$$

The corollary follows by choosing

$$\hat{g} \coloneqq \max\left\{2\cdot 2^{2^{200}}, \tilde{g}\right\} \in \mathbb{N}^+.$$

The condition $g \geq 2\cdot 2^{2^{200}}$ is chosen, such that

$$\begin{aligned}
\left(1+\frac{2^{2^{200}}}{g_1}\right)\left(1+\frac{2^{2^{200}}}{g_2}\right) &\leq \frac{9}{4}, \\
\left(1-\frac{2^{2^{200}}}{g_1}\right)\left(1-\frac{2^{2^{200}}}{g_2}\right) &\geq \frac{1}{4},
\end{aligned}$$

if $g_1 = \left\lfloor \frac{g}{2} \right\rfloor$ and $g_2 = g - g_1$. $\square$

Remark 9.2.4 (Volume only)
It is important to note that in the preceding proof of Corollary 9.2.3, we exclusively focus on volumes. We approximate the volume of the thin part using solely the thin-thick part.

We can now establish an upper bound for the Cheeger constant in the thin part. A very large Cheeger constant is rare within the stratum, as it only occurs when there are short saddle connections, whose volume we can now control.

Proposition 9.2.5 (Upper bound on the expected value of the geotopological Cheeger constant in the thin part)
There exists a $\hat{g} \in \mathbb{N}^+$, such that an upper bound for the expected value of the geotopological Cheeger constant in the thin part of the principal stratum for $g \geq \hat{g}$ and $\varepsilon \leq \frac{1}{g^{1+\delta}}$ for any $\delta > 0$ is given by

$$\mathbb{E}_{\mathcal{H}_1^{\varepsilon,\text{thin}}(1^{2g-2})}(h^\top) \leq 2^{16}\cdot\frac{g}{\varepsilon}.$$

Proof. Separate $\mathcal{H}_1^{\varepsilon,\text{thin}}(1^{2g-2}) = \bigsqcup_{n\in\mathbb{N}_0} U_n$ into the sets

$$\begin{aligned}
U_n = \Big\{(X,\omega) \in \mathcal{H}_1^{\varepsilon,\text{thin}}(1^{2g-2}) \;\Big|\; &\text{smallest saddle connection } \sigma : \\
&2^{-n-1}\varepsilon < \text{length}(\sigma) \leq 2^{-n}\varepsilon\Big\}.
\end{aligned}$$

Let $(X, \omega) \in U_n$. Continue like in the proof of Proposition 9.1.1:

For $m \in \left\{1, \dots, \left\lfloor \frac{g}{2} \right\rfloor\right\}$, let $\tilde{\gamma}_m$ be the minimal curve like in Definition 9.0.1. Now consider a Delaunay triangulation Δ on the singularities of $\overline{X}$ and a representative γ_m for each $\tilde{\gamma}_m$ on the edge set of Δ. A Delaunay triangulation of a surface in $\mathcal{H}(1^{2g-2})$ has exactly $8g-8$ triangles. γ_m separates $\overline{X}$ in two different areas triangulated by at most $8g-8$ triangles.

Since every saddle connection of $(X, \omega) \in U_n$ has at least size $2^{-n-1}\varepsilon$, we get analogously to Proposition 9.1.1 an upper bound on the longest edge $\hat{e}_\Delta$:

$$\operatorname{length}(\hat{e}_\Delta) \leq \frac{2^{n+5}}{3\sqrt{3} \cdot \varepsilon}.$$

And again, analogously to Proposition 9.1.1, the length of γ_m is bounded by

$$\begin{aligned} \operatorname{length}(\gamma_m) &\leq 2(8g-6) \operatorname{length}(\hat{e}_\Delta) \\ &\leq \frac{2^{n+9}}{3\sqrt{3}} \cdot \frac{g}{\varepsilon}. \end{aligned}$$

Therefore

$$\begin{aligned} h^\top(X) \leq h^\top_m(X) &\leq \frac{\operatorname{length}(\gamma_m) g}{m} \\ &\leq \frac{2^{n+11}}{3\sqrt{3}} \cdot \frac{g}{\varepsilon} \end{aligned}$$

for $(X, \omega) \in U_n \subseteq \mathcal{H}_1^{2^{-n} \cdot \varepsilon, \mathrm{thin}}(1^{2g-2})$.

We can now estimate the expected value of $h^\top(\cdot) < h^\top_{\left\lfloor \frac{g(\cdot)}{2} \right\rfloor}(\cdot)$ on the thin part for small enough $\varepsilon \leq \frac{1}{g}$ and $g \geq \hat{g}$:

$$\begin{aligned} \mathbb{E}_{\mathcal{H}_1^{\varepsilon,\mathrm{thin}}(1^{2g-2})}(h^\top(X)) &\leq \mathbb{E}_{\mathcal{H}_1^{\varepsilon,\mathrm{thin}}\left(1^{2g-2}, \mathcal{C}_{\left\lfloor \frac{g}{2} \right\rfloor}\right)} \left(h^\top_{\left\lfloor \frac{g}{2} \right\rfloor}(X)\right) \\ &\leq \frac{1}{\nu\left(\mathcal{H}_1^{\varepsilon,\mathrm{thin}}\left(1^{2g-2}, \mathcal{C}_{\left\lfloor \frac{g}{2} \right\rfloor}\right)\right)} \sum_{n=0}^{\infty} \nu\left(U_n\right) \frac{2^{n+11}}{3\sqrt{3}} \cdot \frac{g}{\varepsilon} \\ &= \sum_{n=0}^{\infty} \frac{\nu\left(U_n\right)}{\nu\left(\mathcal{H}_1^{\varepsilon,\mathrm{thin}}\left(1^{2g-2}, \mathcal{C}_{\left\lfloor \frac{g}{2} \right\rfloor}\right)\right)} \frac{2^{n+11}}{3\sqrt{3}} \cdot \frac{g}{\varepsilon} \\ &\leq \sum_{n=0}^{\infty} \frac{\nu\left(\mathcal{H}_1^{2^{-n} \cdot \varepsilon,\mathrm{thin}}\left(1^{2g-2}, \mathcal{C}_{\left\lfloor \frac{g}{2} \right\rfloor}\right)\right)}{\nu\left(\mathcal{H}_1^{\varepsilon,\mathrm{thin}}\left(1^{2g-2}, \mathcal{C}_{\left\lfloor \frac{g}{2} \right\rfloor}\right)\right)} \frac{2^{n+11}}{3\sqrt{3}} \cdot \frac{g}{\varepsilon} \\ &\leq \sum_{n=0}^{\infty} \frac{288}{4 \cdot 2^{2n}} \frac{\cdot 2^{n+11}}{3\sqrt{3}} \cdot \frac{g}{\varepsilon} \\ &= \frac{294912}{3\sqrt{3}} \cdot \frac{g}{\varepsilon} < 2^{16} \cdot \frac{g}{\varepsilon}. \end{aligned}$$

□

9.3 Results

To optimize our bound for the geotopological Cheeger constant, ε should be as fast growing in g as possible. However, we are restricted by Proposition 9.2.2, such that ε must be growing asymptotically more slowly than or in the same way as $\frac{1}{g^{1+\delta}}$. Using $\varepsilon = \frac{1}{g^{1+\delta}}$ yields the best result for our proof.

Theorem 9.3.1 (Upper bound on the expected value of the geotopological Cheeger constant in the principal stratum)
For any $\delta > 0$, there exists $\hat{g} \in \mathbb{N}^+$, such that an upper bound for the expected value of the geotopological Cheeger constant $h^\top$ in the principal stratum for $g \geq \hat{g}$ is given by

$$\mathbb{E}_{\mathcal{H}_1(1^{2g-2})}(h^\top) \leq 2^{16} \cdot g^{2+\delta}.$$

Proof. The best cut-off for the thin-thick decomposition is given by $\varepsilon = \frac{1}{g^{1+\delta}}$. The Cheeger constant for the decomposition

$$\mathcal{H}_1(1^{2g-2}) = \mathcal{H}_1^{\frac{1}{g^{1+\delta}},\text{thick}}(1^{2g-2}) \sqcup \mathcal{H}_1^{\frac{1}{g^{1+\delta}},\text{thin}}(1^{2g-2})$$

can be analyzed on each part separately. The upper bound for the expected value of the Cheeger constant can be obtained by taking the maximum average Cheeger constant calculated for each individual part of the thin-thick decomposition. Specifically, we can rely on Propositions 9.1.1 and 9.2.5 to conclude that the thin part provides the highest bound for the Cheeger constant in our case. Thus, the upper bound we obtain for the expected Cheeger constant is given by the result of Proposition 9.2.5 with ε set to $\frac{1}{g^{1+\delta}}$. □

Our bound is not sharp, as we have used a worst-case scenario in our geometric approximation. In reality, we would expect a clustering behavior for our Delaunay triangulation, which would reduce the growth by $g^{\frac{1}{2}}$. Additionally, in the calculations for the quadrilateral Q, we would expect constant growth rather than linear growth in g. Thus, a total upper bound of $g^{\frac{1}{2}+\delta}$ may be feasible to achieve with the current methods.

We hope to obtain a lower bound for the Cheeger constant in the future and remain optimistic and motivated to continue this line of research. There is still a great deal of untapped potential in exploring the Cheeger constant for various other strata beyond the one we have focused on.

Bibliography

[Agg19] Amol Aggarwal. “Large genus asymptotics for Siegel-Veech constants.” In: *Geom. Funct. Anal.* 29.5 (2019), pp. 1295–1324. ISSN: 1016-443X,1420-8970. DOI: 10.1007/s00039-019-00509-0. URL: https://doi.org/10.1007/s00039-019-00509-0.

[Agg20] Amol Aggarwal. “Large genus asymptotics for volumes of strata of Abelian differentials.” In: *J. Amer. Math. Soc.* 33.4 (2020). With an appendix by Anton Zorich, pp. 941–989. ISSN: 0894-0347. DOI: 10.1090/jams/947. URL: https://doi.org/10.1090/jams/947.

[Art+23] Mauro Artigiani, Anja Randecker, Chandrika Sadanand, Ferrán Valdez, and Gabriela Weitze-Schmithüsen. *Realizing groups as symmetries of infinite translation surfaces.* 2023. arXiv: 2311.00158 [math.GT]. URL: https://arxiv.org/abs/2311.00158.

[AEZ16] Jayadev Siddhanta Athreya, Alex Eskin, and Anton Zorich. “Right-angled billiards and volumes of moduli spaces of quadratic differentials on $\mathbb{C}\mathrm{P}^1$.” In: *Ann. Sci. Éc. Norm. Supér. (4)* 49.6 (2016). With an appendix by Jon Chaika, pp. 1311–1386. ISSN: 0012-9593,1873-2151. DOI: 10.24033/asens.2310. URL: https://doi.org/10.24033/asens.2310.

[Bea95] Alan Frank Beardon. *The geometry of discrete groups.* Vol. 91. Graduate Texts in Mathematics. Corrected reprint of the 1983 original. Springer-Verlag, New York, 1995, pp. xii+337. ISBN: 0-387-90788-2. DOI: 10.1007/978-1-4612-1146-4. URL: https://doi.org/10.1007/978-1-4612-1146-4.

[Béd03] Nicolas Bédaride. “Billiard complexity in rational polyhedra.” In: *Regul. Chaotic Dyn.* 8.1 (2003), pp. 97–104. ISSN: 1560-3547,1468-4845. DOI: 10.1070/RD2003v008n01ABEH000228. URL: https://doi.org/10.1070/RD2003v008n01ABEH000228.

[BM10] Irene Ingeborg Bouw and Martin Möller. “Teichmüller curves, triangle groups, and Lyapunov exponents.” In: *Ann. of Math. (2)* 172.1 (2010), pp. 139–185. ISSN: 0003-486X,1939-8980. DOI: 10.4007/annals.2010.172.139. URL: https://doi.org/10.4007/annals.2010.172.139.

[Bow13] Joshua Paul Bowman. "The complete family of Arnoux-Yoccoz surfaces." In: *Geom. Dedicata* 164 (2013), pp. 113–130. ISSN: 0046-5755,1572-9168. DOI: 10.1007/s10711-012-9762-9. URL: https://doi.org/10.1007/s10711-012-9762-9.

[Bus82] Peter Buser. "A note on the isoperimetric constant." In: *Ann. Sci. École Norm. Sup. (4)* 15.2 (1982), pp. 213–230. ISSN: 0012-9593. DOI: 10.24033/asens.1426. URL: https://doi.org/10.24033/asens.1426.

[Car56] Constantin Carathéodory. *Gesammelte mathematische Schriften. Bd. 4.* Herausgegeben im Auftrag und mit Unterstützung der bayerischen Akademie der Wissenschaften. C. H. Beck'sche Verlagsbuchhandlung, Munich, 1956, ix+494 pp.+1 plate.

[CHT02] Julien Cassaigne, Pascal Hubert, and Serge Eugene Troubetzkoy. "Complexity and growth for polygonal billiards." In: *Ann. Inst. Fourier (Grenoble)* 52.3 (2002), pp. 835–847. ISSN: 0373-0956,1777-5310. DOI: 10.5802/aif.1903. URL: https://doi.org/10.5802/aif.1903.

[Cha04] Reza Chamanara. "Affine automorphism groups of surfaces of infinite type." In: *In the Tradition of Ahlfors and Bers, III (William Abikoff and Andrew Haas, eds.)* 355 (2004), pp. 123–145. DOI: 10.1090/conm/355. URL: http://dx.doi.org/10.1090/conm/355.

[Che+20] Dawei Chen, Martin Möller, Adrien Sauvaget, and Don Zagier. "Masur-Veech volumes and intersection theory on moduli spaces of Abelian differentials." In: *Invent. Math.* 222.1 (2020), pp. 283–373. ISSN: 0020-9910,1432-1297. DOI: 10.1007/s00222-020-00969-4. URL: https://doi.org/10.1007/s00222-020-00969-4.

[CMZ18] Dawei Chen, Martin Möller, and Don Zagier. "Quasimodularity and large genus limits of Siegel-Veech constants." In: *J. Amer. Math. Soc.* 31.4 (2018), pp. 1059–1163. ISSN: 0894-0347,1088-6834. DOI: 10.1090/jams/900. URL: https://doi.org/10.1090/jams/900.

[Chu97] Fan Rong King Chung Graham. *Spectral graph theory.* Vol. 92. CBMS Regional Conference Series in Mathematics. Published for the Conference Board of the Mathematical Sciences, Washington, DC; by the American Mathematical Society, Providence, RI, 1997, pp. xii+207. ISBN: 0-8218-0315-8. DOI: 10.1090/cbms/092. URL: https://doi.org/10.1090/cbms/092.

[DH07] Max Dehn and Poul Heegaard. "Analysis situs." German. In: *Encyklopädie der mathematischen Wissenschaften mit Einschluss ihrer Anwendungen* III.I (1907), pp. 153–220. URL: http://resolver.sub.uni-goettingen.de/purl?PPN360609635.

[Del+22] Vincent Delecroix, Élise Goujard, Peter Zograf, and Anton Zorich. "Large genus asymptotic geometry of random square-tiled surfaces and of random multicurves." In: *Invent. Math.* 230.1 (2022), pp. 123–224. ISSN: 0020-9910,1432-1297. DOI: 10.1007/s00222-022-01123-y. URL: https://doi.org/10.1007/s00222-022-01123-y.

[DHV24] Vincent Delecroix, Pascal Hubert, and Ferrán Valdez. *Infinite Translation Surfaces In The Wild*. 2024. arXiv: 2403.05424 [math.GT]. URL: https://arxiv.org/abs/2403.05424.

[EM01] Alex Eskin and Howard Masur. "Asymptotic formulas on flat surfaces." In: *Ergodic Theory Dynam. Systems* 21.2 (2001), pp. 443–478. ISSN: 0143-3857. DOI: 10.1017/S0143385701001225. URL: https://doi.org/10.1017/S0143385701001225.

[EMZ03] Alex Eskin, Howard Masur, and Anton Zorich. "Moduli spaces of abelian differentials: the principal boundary, counting problems, and the Siegel-Veech constants." In: *Publ. Math. Inst. Hautes Études Sci.* 97 (2003), pp. 61–179. ISSN: 0073-8301. DOI: 10.1007/s10240-003-0015-1. URL: https://doi.org/10.1007/s10240-003-0015-1.

[EO01] Alex Eskin and Andrei Okounkov. "Asymptotics of numbers of branched coverings of a torus and volumes of moduli spaces of holomorphic differentials." In: *Invent. Math.* 145.1 (2001), pp. 59–103. ISSN: 0020-9910,1432-1297. DOI: 10.1007/s002220100142. URL: https://doi.org/10.1007/s002220100142.

[EZ15] Alex Eskin and Anton Zorich. "Volumes of strata of Abelian differentials and Siegel-Veech constants in large genera." In: *Arnold Math. J.* 1.4 (2015), pp. 481–488. ISSN: 2199-6792,2199-6806. DOI: 10.1007/s40598-015-0028-0. URL: https://doi.org/10.1007/s40598-015-0028-0.

[Fog02] N. Pytheas Fogg. *Substitutions in dynamics, arithmetics and combinatorics*. Ed. by V. Berthé, S. Ferenczi, C. Mauduit, and A. Siegel. Vol. 1794. Lecture Notes in Mathematics. Springer-Verlag, Berlin, 2002, pp. xviii+402. ISBN: 3-540-44141-7. DOI: 10.1007/b13861. URL: https://doi.org/10.1007/b13861.

[FK36] Ralph Hartzler Fox and Richard Brandon Kershner. "Concerning the transitive properties of geodesics on a rational polyhedron." In: *Duke Math. J.* 2.1 (1936), pp. 147–150. ISSN: 0012-7094,1547-7398. DOI: 10.1215/S0012-7094-36-00213-2. URL: https://doi.org/10.1215/S0012-7094-36-00213-2.

[GX13] Jean Gallier and Dianna Xu. *A guide to the classification theorem for compact surfaces*. Vol. 9. Geometry and Computing. Springer, Heidelberg, 2013, pp. xii+178. ISBN: 978-3-642-34363-6. DOI:

10.1007/978-3-642-34364-3. URL: https://doi.org/10.1007/978-3-642-34364-3.

[GJ00] Eugene Gutkin and Chris Judge. "Affine mappings of translation surfaces: geometry and arithmetic." In: *Duke Math. J.* 103.2 (2000), pp. 191–213. ISSN: 0012-7094,1547-7398. DOI: 10.1215/S0012-7094-00-10321-3. URL: https://doi.org/10.1215/S0012-7094-00-10321-3.

[Hat02] Allen Hatcher. *Algebraic topology.* Cambridge University Press, Cambridge, 2002, pp. xii+544. ISBN: 0-521-79540-0. DOI: 10.1017/S0013091503214620. URL: https://doi.org/10.1017/S0013091503214620.

[Her21] Frank Herrlich. *Modulräume von Translationsflächen.* Lecture Notes, Karlsruhe Institue of Technology. 2021.

[Hoo13a] William Patrick Hooper. "Grid graphs and lattice surfaces." In: *Int. Math. Res. Not. IMRN* 12 (2013), pp. 2657–2698. ISSN: 1073-7928,1687-0247. DOI: 10.1093/imrn/rns124. URL: https://doi.org/10.1093/imrn/rns124.

[Hoo13b] William Patrick Hooper. *Immersions and the space of all translation structures.* 2013. arXiv: 1310.5193 [math.GT]. URL: https://arxiv.org/abs/1310.5193.

[Hoo15] William Patrick Hooper. "The invariant measures of some infinite interval exchange maps." In: *Geometry and Topology* 19.4 (2015), pp. 1895–2038. DOI: 10.2140/gt.2015.19.1895. URL: https://doi.org/10.2140/gt.2015.19.1895.

[Hoo18] William Patrick Hooper. "Immersions and translation structures I: The space of structures on the pointed disk." In: *Conform. Geom. Dyn.* 22 (2018), pp. 235–270. ISSN: 1088-4173. DOI: 10.1090/ecgd/326. URL: https://doi.org/10.1090/ecgd/326.

[HS06] Pascal Hubert and Thomas Andrew Schmidt. "An introduction to Veech surfaces." In: *Handbook of dynamical systems. Vol. 1B.* Elsevier B. V., Amsterdam, 2006, pp. 501–526. ISBN: 0-444-52055-4. DOI: 10.1016/S1874-575X(06)80031-7. URL: https://doi.org/10.1016/S1874-575X(06)80031-7.

[Joh80] Dennis Johnson. "Spin structures and quadratic forms on surfaces." In: *J. London Math. Soc. (2)* 22.2 (1980), pp. 365–373. ISSN: 0024-6107,1469-7750. DOI: 10.1112/jlms/s2-22.2.365. URL: https://doi.org/10.1112/jlms/s2-22.2.365.

[Kat87] Anatole Boris Katok. "The growth rate for the number of singular and periodic orbits for a polygonal billiard." In: *Comm. Math. Phys.* 111.1 (1987), pp. 151–160. ISSN: 0010-3616,1432-0916. DOI: 10.1007/BF01239021. URL: https://doi.org/10.1007/BF01239021.

[Ker23] Béla Kerékjártó. *Vorlesungen über Topologie. I, Flächentopologie.* Vol. 8. Die Grundlehren der mathematischen Wissenschaften in Einzeldarstellungen. Springer-Verlag, Berlin, 1923, pp. ix+272. ISBN: 978-3-642-50515-7. DOI: 10.1007/978-3-642-50825-7. URL: https://doi.org/10.1007/978-3-642-50825-7.

[KZ03] Maxim Kontsevich and Anton Zorich. "Connected components of the moduli spaces of Abelian differentials with prescribed singularities." In: *Invent. Math.* 153.3 (2003), pp. 631–678. ISSN: 0020-9910,1432-1297. DOI: 10.1007/s00222-003-0303-x. URL: https://doi.org/10.1007/s00222-003-0303-x.

[Mas82] Howard Masur. "Interval exchange transformations and measured foliations." In: *Ann. of Math. (2)* 115.1 (1982), pp. 169–200. ISSN: 0003-486X. DOI: 10.2307/1971341. URL: https://doi.org/10.2307/1971341.

[MRR22] Howard Masur, Kasra Rafi, and Anja Randecker. "Expected covering radius of a translation surface." In: *Int. Math. Res. Not. IMRN* 10 (2022), pp. 7967–8002. ISSN: 1073-7928. DOI: 10.1093/imrn/rnaa385. URL: https://doi.org/10.1093/imrn/rnaa385.

[MS91] Howard Masur and John Smillie. "Hausdorff Dimension of Sets of Nonergodic Measured Foliations." In: *Annals of Mathematics* 134.3 (1991), pp. 455–543. ISSN: 0003486X. DOI: 10.2307/2944356. URL: https://doi.org/10.2307/2944356 (visited on 07/07/2022).

[McM03] Curtis Tracy McMullen. "Teichmüller geodesics of infinite complexity." In: *Acta Mathematica* 191.2 (Sept. 2003), pp. 191–223. ISSN: 1871-2509. DOI: 10.1007/BF02392964. URL: https://doi.org/10.1007/BF02392964.

[Mir13] Maryam Mirzakhani. "Growth of Weil-Petersson volumes and random hyperbolic surfaces of large genus." In: *J. Differential Geom.* 94.2 (2013), pp. 267–300. ISSN: 0022-040X,1945-743X. DOI: 10.4310/jdg/1367438650. URL: https://doi.org/10.4310/jdg/1367438650.

[MZ15] Maryam Mirzakhani and Peter Zograf. "Towards large genus asymptotics of intersection numbers on moduli spaces of curves." In: *Geom. Funct. Anal.* 25.4 (2015), pp. 1258–1289. ISSN: 1016-443X,1420-8970. DOI: 10.1007/s00039-015-0336-5. URL: https://doi.org/10.1007/s00039-015-0336-5.

[Mor21] Harold Calvin Marston Morse. "Recurrent geodesics on a surface of negative curvature." In: *Trans. Amer. Math. Soc.* 22.1 (1921), pp. 84–100. ISSN: 0002-9947,1088-6850. DOI: 10.2307/1988844. URL: https://doi.org/10.2307/1988844.

[Pro51] Eugène Prouhet. "Mémoire sur quelques relations entre les puissances des nombres." French. In: *Comptes rendus hebdomadaires des séances de l'Académie des sciences* 33.1 (1851), p. 225.

[Rad25] Tibor Radó. “Über den Begriff der Riemannschen Fläche.” German. In: *Acta Litterarum ac Scientiarum Szeged* 2 (1925), pp. 101–121. URL: https://www.maths.ed.ac.uk/~v1ranick/papers/rado.pdf.

[Ran12] Anja Randecker. *Skript zur Vortragsreihe „Unendliche Translationsflächen“*. Lecture Notes, Karlsruhe Institue of Technology. 2012–2017. URL: https://www.math.kit.edu/iag3/~randecker/media/unendliche_translationsflaechen.pdf.

[Ran18] Anja Randecker. “Wild translation surfaces and infinite genus.” In: *Algebr. Geom. Topol.* 18.5 (2018), pp. 2661–2699. ISSN: 1472-2747,1472-2739. DOI: 10.2140/agt.2018.18.2661. URL: https://doi.org/10.2140/agt.2018.18.2661.

[Rei24a] Maurice Reichert. *Bakers map surface asymptotic.ipynb*. Aug. 2024. URL: https://cocalc.com/share/public_paths/07ce34aaca2cfa1865317c853badabee46016e6f.

[Rei24b] Maurice Reichert. *HTV cutting sequence for clover type surfaces.ipynb*. Aug. 2024. URL: https://cocalc.com/share/public_paths/adebea7f19f33d8da601737c49407fecddc6e1ff.

[Rei24c] Maurice Reichert. *octagon phase space.ipynb*. Aug. 2024. URL: https://cocalc.com/share/public_paths/7717bf86d73fcc1e144a2c55ec1fb395c098b0fd.

[Rei24d] Maurice Reichert. *staircase arm phase space.ipynb*. Aug. 2024. URL: https://cocalc.com/share/public_paths/44af608fcfe79aa460e3adbfa36435a28586eb12.

[Ric63] Ian Richards. “On the classification of noncompact surfaces.” In: *Trans. Amer. Math. Soc.* 106 (1963), pp. 259–269. ISSN: 0002-9947,1088-6850. DOI: 10.2307/1993768. URL: https://doi.org/10.2307/1993768.

[Sau18] Adrien Sauvaget. “Volumes and Siegel-Veech constants of $\mathcal{H}(2g-2)$ and Hodge integrals.” In: *Geom. Funct. Anal.* 28.6 (2018), pp. 1756–1779. ISSN: 1016-443X,1420-8970. DOI: 10.1007/s00039-018-0468-5. URL: https://doi.org/10.1007/s00039-018-0468-5.

[Sch04] Gabriela Schmithüsen. “An algorithm for finding the Veech group of an origami.” In: *Experiment. Math.* 13.4 (2004), pp. 459–472. ISSN: 1058-6458,1944-950X. URL: https://projecteuclid.org/euclid.em/1109106438.

[Ser85] Caroline Series. “The geometry of Markoff numbers.” In: *Math. Intelligencer* 7.3 (1985), pp. 20–29. ISSN: 0343-6993,1866-7414. DOI: 10.1007/BF03025802. URL: https://doi.org/10.1007/BF03025802.

[SU11] John Smillie and Corinna Ulcigrai. "Beyond Sturmian sequences: coding linear trajectories in the regular octagon." In: *Proc. Lond. Math. Soc. (3)* 102.2 (2011), pp. 291–340. ISSN: 0024-6115,1460-244X. DOI: 10.1112/plms/pdq018. URL: https://doi.org/10.1112/plms/pdq018.

[Thu78] William Paul Thurston. *The geometry and topology of three-manifolds.* Lecture Notes, Princeton University. 1978–1980. URL: https://archive.org/details/ThurstonTheGeometryAndTopologyOfThreeManifolds.

[Thu88] William Paul Thurston. "On the geometry and dynamics of diffeomorphisms of surfaces." In: *Bull. Amer. Math. Soc. (N.S.)* 19.2 (1988), pp. 417–431. ISSN: 0273-0979,1088-9485. DOI: 10.1090/S0273-0979-1988-15685-6. URL: https://doi.org/10.1090/S0273-0979-1988-15685-6.

[Tro98] Serge Eugene Troubetzkoy. "Complexity lower bounds for polygonal billiards." In: *Chaos* 8.1 (1998), pp. 242–244. ISSN: 1054-1500,1089-7682. DOI: 10.1063/1.166301. URL: https://doi.org/10.1063/1.166301.

[Vee82] William Austin Veech. "Gauss measures for transformations on the space of interval exchange maps." In: *Ann. of Math. (2)* 115.1 (1982), pp. 201–242. ISSN: 0003-486X. DOI: 10.2307/1971391. URL: https://doi.org/10.2307/1971391.

[Vee89] William Austin Veech. "Teichmüller curves in moduli space, Eisenstein series and an application to triangular billiards." In: *Invent. Math.* 97.3 (1989), pp. 553–583. ISSN: 0020-9910,1432-1297. DOI: 10.1007/BF01388890. URL: https://doi.org/10.1007/BF01388890.

[Vee98] William Austin Veech. "Siegel measures." In: *Ann. of Math. (2)* 148.3 (1998), pp. 895–944. ISSN: 0003-486X,1939-8980. DOI: 10.2307/121033. URL: https://doi.org/10.2307/121033.

[Via06] Marcelo Viana. "Ergodic theory of interval exchange maps." In: *Rev. Mat. Complut.* 19.1 (2006), pp. 7–100. ISSN: 1139-1138,1988-2807. DOI: 10.5209/rev_REMA.2006.v19.n1.16621. URL: https://doi.org/10.5209/rev_REMA.2006.v19.n1.16621.

[ZK75] Alexander Nikolaevic Zemljakov and Anatole Boris Katok. "Topological transitivity of billiards in polygons." In: *Mat. Zametki* 18.2 (1975), pp. 291–300. ISSN: 0025-567X. DOI: 10.1007/BF01818045. URL: https://doi.org/10.1007/BF01818045.

[Zor02] Anton Zorich. "Square tiled surfaces and Teichmüller volumes of the moduli spaces of abelian differentials." In: *Rigidity in dynamics and geometry (Cambridge, 2000).* Springer, Berlin, 2002, pp. 459–471. ISBN: 3-540-43243-4. DOI: 10.1007/978-3-662-04743-9_25. URL: https://doi.org/10.1007/978-3-662-04743-9_25.

Index